AWARD NUMBER: W81XWH-16-1-0621

TITLE: Cellular Plasticity in the Diabetic Myocardium

PRINCIPAL INVESTIGATOR: Nikolaos G Frangogiannis

RECIPIENT: Albert Einstein College of Medicine
Bronx, NY 10461

REPORT DATE: September 2017

TYPE OF REPORT: Annual

PREPARED FOR: U.S. Army Medical Research and Materiel Command
Fort Detrick, Maryland 21702-5012

REPORT DOCUMENTATION PAGE

Form Approved
OMB No. 0704-0188

1. REPORT DATE	2. REPORT TYPE	3. DATES COVERED
September 17	Annual	1 Sep 2016 - 31 Aug 2017

4. TITLE AND SUBTITLE

Cellular Plasticity in the Diabetic Myocardium

5a. CONTRACT NUMBER

5b. GRANT NUMBER

W81XWH-16-1-0621

5c. PROGRAM ELEMENT NUMBER

6. AUTHOR(S)

Dr. Nikolaos Frangogiannis

E-Mail: Nikolaos.Frangogiannis@einstein.yu.edu

5d. PROJECT NUMBER

5e. TASK NUMBER

5f. WORK UNIT NUMBER

7. PERFORMING ORGANIZATION NAME(S) AND ADDRESS(ES)

Albert Einstein College of Medicine
1300 Morris Park Avenue
Bronx, NY 10461

8. PERFORMING ORGANIZATION REPORT NUMBER

9. SPONSORING / MONITORING AGENCY NAME(S) AND ADDRESS(ES)

U.S. Army Medical Research and Materiel Command
Fort Detrick, Maryland 21702-5012

10. SPONSOR/MONITOR'S ACRONYM(S)

11. SPONSOR/MONITOR'S REPORT NUMBER(S)

12. DISTRIBUTION / AVAILABILITY STATEMENT

Approved for Public Release; Distribution Unlimited

13. SUPPLEMENTARY NOTES

14. ABSTRACT

Heart fibrosis and loss of blood vessels are prominent pathologic abnormalities in diabetics that lead to the development of heart failure. Moreover, reduced angiogenesis after a heart attack is responsible for defective myocardial repair in diabetic subjects. Although the negative impact of diabetes on the heart is widely appreciated, the cellular alterations and molecular signals involved in fibrosis and blood vessel loss in diabetes remain unknown. Applying genetic fate mapping tools, we have uncovered an unexpected plasticity and heterogeneity in reparative cells and identified common cellular links between angiogenesis and fibrosis. We investigate the role of these novel biological mechanisms in the pro-fibrotic and angiostatic effects of diabetes, focusing on the contribution of pericytes and endothelial cells in the cardiac tissue repair process.

15. SUBJECT TERMS Diabetes, cardiomyopathy, heart failure, fibrosis, angiogenesis, vascular rarefaction, pericytes, endothelial cells, endothelial-tomesenchymal transition, cellular plasticity, extracellular matrix, cell fate mapping, gene expression, signaling pathways

16. SECURITY CLASSIFICATION OF:			17. LIMITATION OF ABSTRACT	18. NUMBER OF PAGES	19a. NAME OF RESPONSIBLE PERSON
a. REPORT	b. ABSTRACT	c. THIS PAGE			19b. TELEPHONE NUMBER *(include area code)*
Unclassified	Unclassified	Unclassified	Unclassified	99	

Table of Contents

Page

USAMRMC Proposal Number PR151029P1
Title: "Cellular Plasticity in the Diabetic Myocardium"
DoD Award Number W81XWH-16-1-0622

First Annual Report from 09/01/2016 to 08/31/2017

1. Introduction

Heart tissue fibrosis and loss of blood vessels are prominent pathologic abnormalities in diabetics and lead to the development of heart failure. Moreover, reduced angiogenesis after a heart attack is responsible for defective myocardial repair in diabetic subjects. Although the negative impact of diabetes on heart function and repair is widely appreciated, the cellular alterations and molecular signals involved in fibrosis and blood vessel loss in diabetes remain unknown. Applying genetic fate mapping tools, we have uncovered an unexpected plasticity and heterogeneity in reparative cells and identified common cellular links between angiogenesis and fibrosis. We investigate the role of these novel biological mechanisms in the pro-fibrotic and angiostatic effects of diabetes, focusing on the contribution of pericytes and endothelial cells in the cardiac tissue repair process.

2. Keywords

Diabetes, cardiomyopathy, heart failure, fibrosis, angiogenesis, vascular rarefaction, pericytes, endothelial cells, endothelial-to-mesenchymal transition, cellular plasticity, extracellular matrix, lineage tracing, cell fate mapping, gene expression, signaling pathways

3. Accomplishments

Major Scientific Goals of the Project

The project has the following three major goals:

a) Determine the contribution of pericytes to the development of cardiac fibrosis in diabetic mice (**AECOM);**

b) Evaluate the role of endothelial cells in the development of cardiac fibrosis in diabetic mice (**VUMC)**;

c) Identify molecular pathways promoting fibrosis and causing blood vessel loss in diabetic hearts (**AECOM & VUMC**).

Scientific Accomplishments of the Project

a) Work performed at AECOM

We have characterized the db/db mouse as a model of cardiac fibrosis and diastolic dysfunction that recapitulates characteristics of human heart failure with preserved ejection fraction (HFpEF). Moreover, we have systematically studied gender-specific responses in this model. Our experiments demonstrated that obese diabetic db/db mice in a C57Bl6J background exhibit cardiac remodeling, associated with modest ventricular dilation, accompanied by marked left ventricular hypertrophy, in the absence of systolic dysfunction (Figure 1A-I). Elevated left ventricular end-diastolic pressure (LVEDP) in db/db mice suggests significant diastolic dysfunction (Figure 1J-L). Hypertrophic changes, chamber dilation and diastolic dysfunction are more prominent in female animals. Thus, the db/db mouse model recapitulates features of HFpEF observed in human patient populations and is particularly useful in understanding the pathogenesis of cardiac dysfunction associated with metabolic disease.

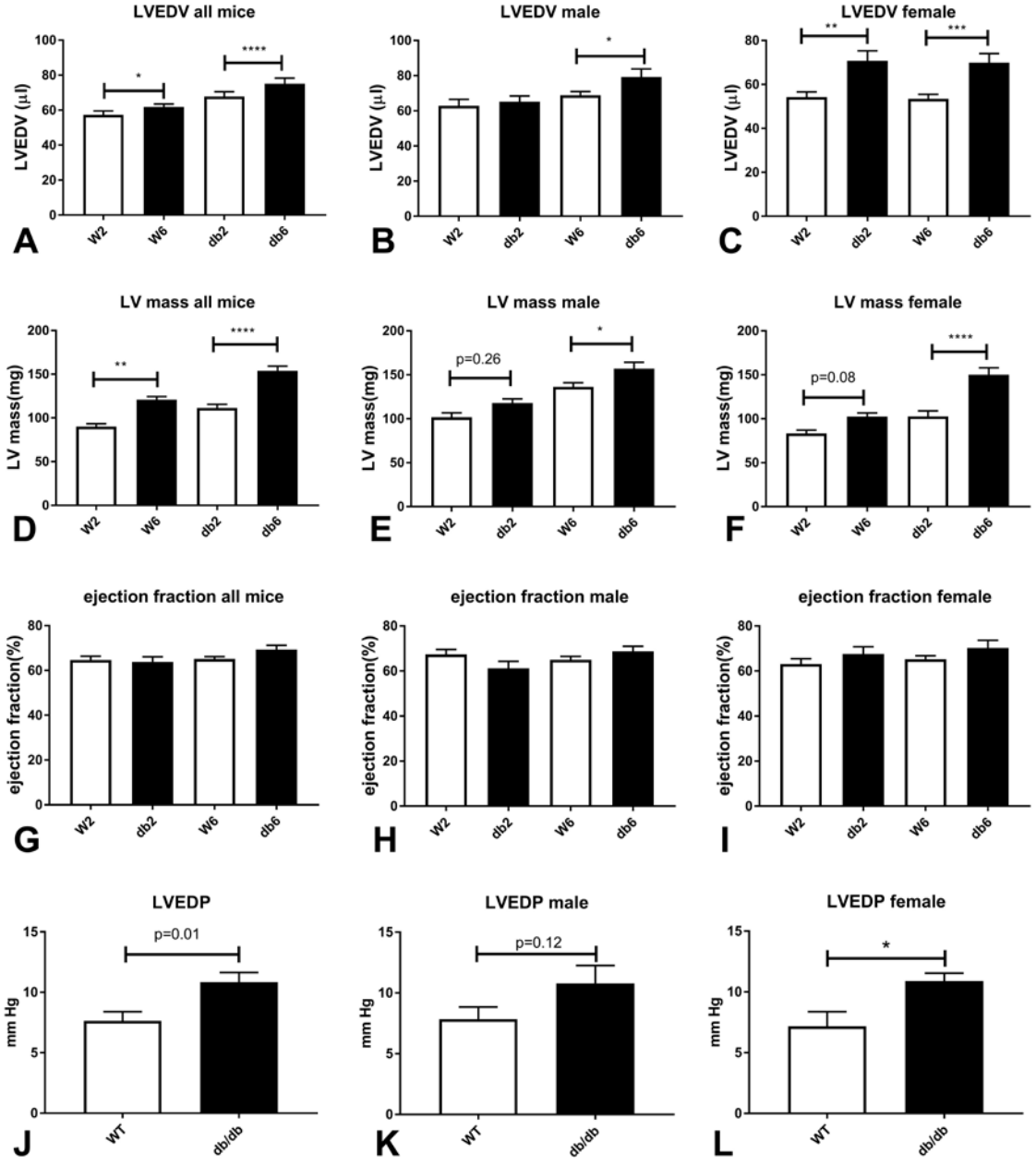

Fig. 1: The db/db mouse recapitulates features of human Heart failure with preserved ejection fraction (HFpEF). A-C: db/db mice exhibit modest dilative remodeling at 6 months of age, evidenced by an increase in left ventricular end-diastolic volume (LVEDV). D-F. LV mass is markedly increased in db/db mice. Cardiac hypertrophy is accentuated in female db/db mice. G-I: Ejection fraction is preserved in db/db mice documenting absence of systolic dysfunction. J-L: Left ventricular end-diastolic pressure (LVEDP) is increased, predominantly in female db/db mice, suggesting diastolic dysfunction (n=6-38/group).

We have documented fibroblast activation in db/db mice. In order to examine the mechanisms of fibroblast activation in diabetic mice, we have isolated fibroblasts from 4-6 month old WT and db/db hearts. db/db fibroblasts had increased baseline levels of collagen I and III transcription, but had blunted responses to TGF-β1 stimulation (Figure 2A-B). Fibroblast activation in db/db hearts is not associated with myofibroblast conversion. In contrast to infarct fibroblasts, diabetic fibroblasts do not exhibit expression of α-smooth muscle actin (α-SMA), periostin or fibroblast activation protein (FAP). These findings suggest that diabetes stimulates an alternative activation pathway that is not associated with myofibroblast conversion.

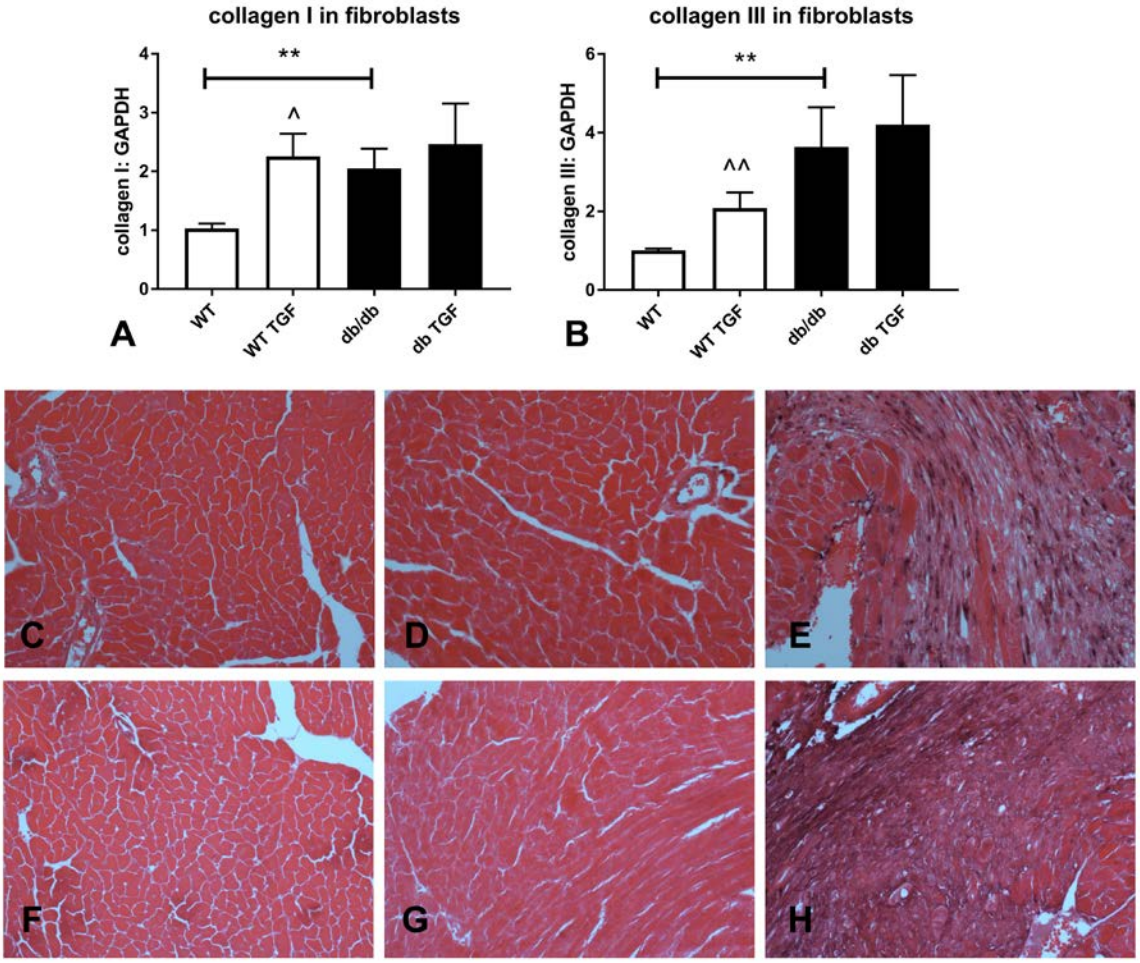

Fig 2: Activation of diabetic fibroblasts does not involve myofibroblast conversion. A-B: Cardiac fibroblasts harvested from db/db mice (at 4-6 months of age) exhibit increased baseline transcription of collagen I (A) and collagen III (B). However, the response of diabetic fibroblasts from 4-6 month old mice to TGF-β1 is blunted (n=6/group). C-H. Activation of fibroblasts in the diabetic heart does not involve myofibroblast conversion.

Immunohistochemical staining for fibroblast activation protein (FAP, panels C-E) and periostin (F-H) in hearts from lean WT mice (C, F) and db/db mice (D, G) and in lean mouse infarcts (after 7 days of coronary occlusion). Infarcted mouse hearts exhibit infiltration with activated FAP and periostin-expressing myofibroblasts. In contrast, periostin and FAP are not expressed in diabetic hearts.

We have assessed expression of TGF-β-related genes in db/db mouse hearts.

Because TGF-betas are critically involved in the fibrotic response and are activated in a high-glucose environment, we performed a comprehensive analysis of the effects of diabetes on TGF-β superfamily genes using a PCR array. We found that at the 6 month timepoint, TGF-β isoforms is not significantly upregulated in the diabetic myocardium; however expression of the TβRII receptor and the inhibitory pseudoreceptor BAMBI is markedly higher. Moreover, BMP4, BMP6 and Bmpr2 exhibit significant upregulation (Figure 3). The findings highlight the complex regulation of TGF-β cascades in vivo. Early induction of TGF-βs may be followed by activation of endogenous inhibitory pathways (such as the decoy receptor BAMBI), in order to restrain TGF-β-driven fibrosis.

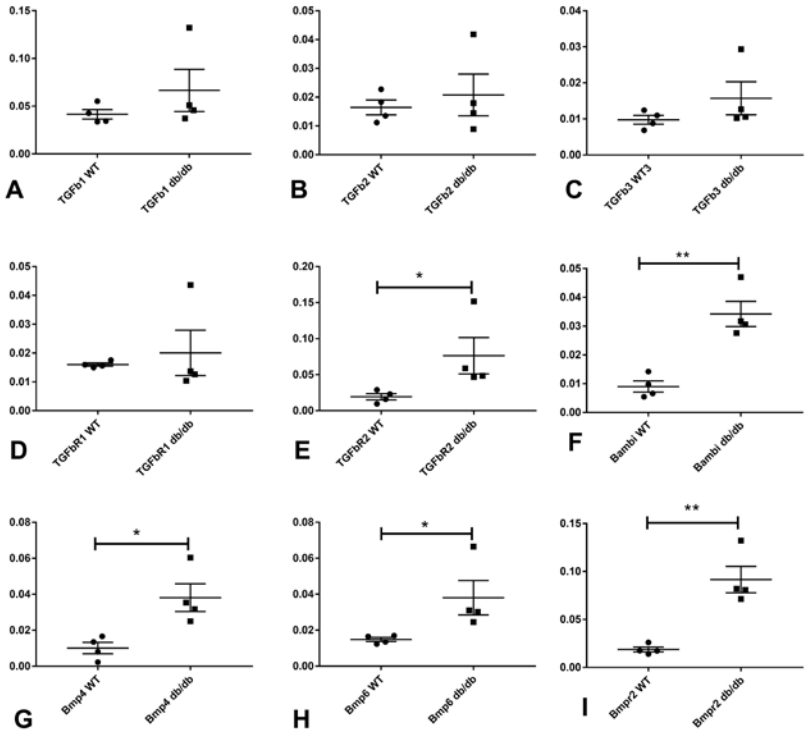

Fig 3: Induction of TGF-β superfamily genes in the diabetic heart. PCR array was used to assess gene expression in male mouse hearts at 6 months of age (n=4). TGF-β isoforms

were not significantly upregulated in db/db mice; however expression of the TβRII receptor and the inhibitory pseudoreceptor BAMBI were markedly elevated. There was also evidence for activation of the BMP cascade. BMP4, BMP6 and Bmpr2 expression levels were significantly higher in db/db hearts.

We are using lineage tracing strategies to test the hypothesis that cardiac pericytes generate fibroblasts in the diabetic myocardium. We have crossed db/+ mice with NG2-dsred pericyte reporter animals to generate diabetic pericyte reporter mice. db/+; NG2dsred animals are bred with db/+ controls, in order to generate db/db;NG2dsred mice (12.5% of the offspring). Unfortunately breeding of 2 NG2dsred animals appears to significantly decrease litter size; thus generation of adequate numbers of diabetic pericyte reporter mice will require expansion of our colonies. For lineage tracing, NG2-Cre mice were crossed with R26R*stopYFP* (Rosa-YFP) mice in order to generate double transgenic NG2-Cre-YFP mice to specifically label pericytes and their progeny. We currently have 12 breeding cages of db/+; NG2-Cre; Rosa-YFP to generate homozygote db/db mice that are also positive for NG2-Cre Rosa-YFP. We have already generated 6 diabetic mice, positive for NG-2Cre and Rosa-YFP that can be used for lineage tracing. The first experimental material from these animals will be available in 2 months.

b) Work performed at VUMC

We are using Cre/Lox-based cell lineage tracing strategies to evaluate the contribution of endothelial cells to the generation of extracellular matrix producing cells in diabetic mouse hearts, thereby contributing to interstitial fibrosis and myocardial dysfunction. To this end, we have crossed the Tie1-Cre mice to the R26R*stopYFP* (Rosa-YFP) mice in order to generate double transgenic Tie-1-Cre-YFP mice to specifically label endothelial cells and their progeny. These mice were then bred to each other and genotyped in order to generate Tie-1-Cre-YFP mice that are homozygote for both the Cre recombinase and R26RYFP loci. Double homozygote Tie-1-Cre-YFP mice were then bred to db/+ heterozygotes to generate db/+ Tie1-Cre Rosa-YFP mice and non-diabetic Tie1-Cre Rosa-YFP siblings as controls. We have obtained approximately 25 db/+ heterozygotes and 30 non-diabetic controls that are also heterozygote for both the Tie1-Cre Rosa-YFP loci. We are currently breeding db/+ Tie-1-Cre Rosa-YFP mice to generate homozygote db/db mice that are also positive for Tie-1-Cre Rosa-YFP. At

present, 5 breeding pairs are successfully breeding. Five newly added cages (total of 10 breeding pairs) are expected to expand the number of experimental animals with desired genotypes to 10-15 mice, which will be sufficient to perform the endothelial cell lineage tracing experiments.

c) Work performed collaboratively at VUMC and AECOM

To identify novel molecular pathways linked to pathological fibrosis and vascular rarefaction in diabetics, we compared total heart gene expression profiles between female control and diabetic mice at 6 months of age, where there is clear functional and histological evidence of diabetic cardiomyopathy. In brief, hearts from 3 normal and 3 db/db mice were isolated at **AECOM a**nd shipped to **VUMC** where total RNA was extracted using standard techniques. The 6 RNA samples were then sent to the Vanderbilt sequencing core (VANTAGE). 5 of 6 samples (3 db/db and 2 normal controls) passed the strict RNA quality control and processed for RNA sequencing. A portion of the purified and validated RNA samples that passed quality controls was shipped from **VUMC** back to **AECOM** for analysis using TGF-β superfamily gene PCR arrays (please see **section a** above)

Paired end sequencing was performed at 75X depth with 45 million reads per sample. Raw data (FASTQ files) were uploaded to Partek Flow for analysis and data quality assessment. Sequences were aligned to the mm10 platform of the *Mus musculus* genome using STAR, followed by total count normalization with minimum values set to a minimum of 0.0001. Data were annotated using Ensemble Release 83 and quantified at the gene level using the Partek E/M multimodel algorithm. Partek Genomics Suite 6.6 was used for principal components analysis and for hierarchical clustering with average linkage and Euclidian distance of normalized values (RPM) generated from BAM files (i.e., aligned sequences).

As shown in Figure 4, diabetic heart samples clustered separately from controls, with 2,269 transcripts showing significant differences between the two genotypes. In

total, 310 genes showed higher and 1,959 genes showed lower expression levels in diabetic hearts compared to normal controls.

Data were submitted to Gene Set Enrichment Analysis (GSEA) at the Broad Institute and to DAVID (Database for Annotation, Visualization and Integrated Discovery). Up and down-regulated processes were analyzed using DAVID and gene ontology. GSEA provided signaling pathways derived from the RNA sequencing data and associated genes.

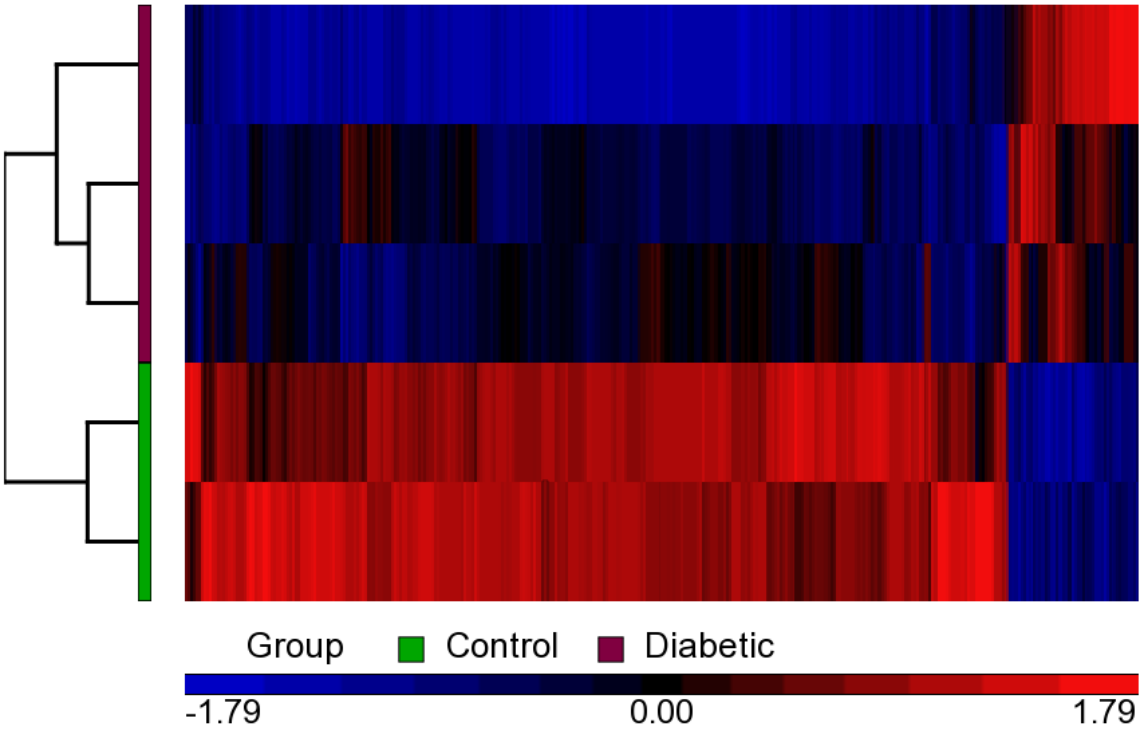

Fig 4: Hierarchical clustering of 2,269 RNA transcript reads per kilobase per million mapped reads for genes with significant differential expression (fold difference >1.5, p value <0.05) between 2 control and 3 diabetic samples using Partek Genomics Suite with average linkage and Euclidean distance measures. Bright red, bright blue, and black indicate the highest, lowest, and median normalized reads, respectively. Vertical dendrograms represent the individual tissue samples (green = control, purple = diabetic).

The results showed that many upregulated transcripts represent genes expressed during heart development (Figure 5), a finding that is consistent with previous reports indicating activation of the fetal gene expression program in failing diabetic hearts. Moreover, there is upregulation of extracellular matrix (ECM) proteins, indicative of fibrosis. Among key signaling pathways, we found activation of Wnt signaling

components, suggesting a role of the pathway in defective angiogenesis and fibrosis in diabetic hearts. In contrast, the majority of the downregulated pathways suggest abnormal immune system response and deregulation of catabolic pathways (Figure 6).

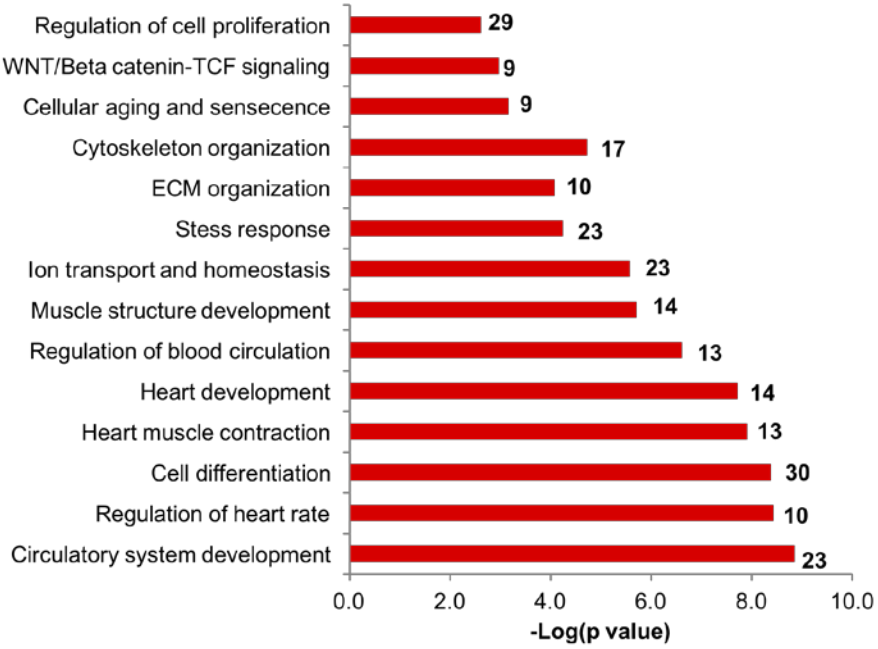

Fig 5: Chart showing key up-regulated pathways in diabetic hearts. The number of genes in each pathway is indicated to the right.

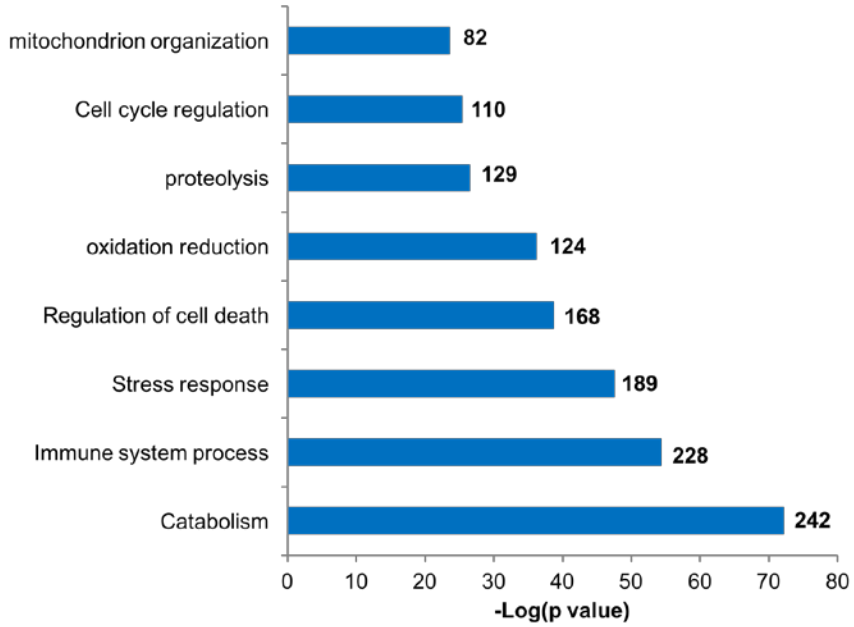

Fig 6: Chart showing key down-regulated pathways in diabetic hearts. The number of genes in each pathway is indicated to the right.

Training opportunities and professional development

Linda Alex, PhD has joined the project. Dr Alex is a post-doctoral fellow who completed her thesis work on the biology of cardiac fibroblasts. In our laboratory, Dr Alex has characterized the cardiomyopathic process in diabetic mice (Figures 1-3), had performed extensive in vitro work investigating the phenotype of diabetic fibroblasts and has developed diabetic mouse lines for identification and lineage tracing of cardiac pericytes. This project provides a unique training opportunity for Dr Alex, combining in vitro and in vivo studies to dissect the cell biological basis of diabetes-associated cardiac fibrosis.

How were the results disseminated to communities of interest?

A manuscript characterizing the fibrotic response in db/db mice is currently in preparation and will be submitted for publication within the next few months. Findings describing atrial remodeling in diabetic mice were recently published (Hanif et al., Cardiovasc. Pathol. 2017). Most of the findings presented in this report are preliminary; these were not yet disseminated to the general scientific community and public, except during informal presentations and discussions in internal work-in-progress meetings and regular teleconferences between the partnering institutions. The concepts explored in this proposal have significantly contributed to development of our paradigm on the pathogenesis of cardiac fibrosis and are discussed in a series of invited review manuscripts and editorials (please see “products”).

Plans for the next reporting period

During the next reporting period, we expect to perform a significant part of the planned cell lineage tracing experiments. The time consuming breeding period to achieve the desired triple genotypes is almost complete. Therefore, we expect to analyze hearts from 2 and 6 months old mice using primarily histological techniques to assess the extent of endothelial-to-mesenchymal transition contribution to vascular rarefaction and fibrosis. Furthermore, the contribution of pericytes in fibrosis and the pathophysiology of diabetic cardiomyopathy will be assessed using the corresponding Cre lines.

We will validate the primary RNAseq data using histological, molecular and cellular techniques. These analyses will likely yield new insights in the development of diabetic cardiomyopathy and may identify new targets to treat heart disease in diabetics. We are particularly excited about the potential involvement of TGF-beta signaling cascades in diabetes-associated fibrosis and the molecular links between the fundamental metabolic perturbations in diabetes, obesity and metabolic dysfunction (hyperglycemia, alterations in insulin signaling and adipokine expression, oxidative stress, generation of advanced glycation end-products, etc) and the TGF-beta response.

Our preliminary data also show significant differences in gene activity in diabetic hearts between female and male mice. Because women suffer more severe diabetic cardiomyopathy than men, we plan to systematic compare gender-specific gene expression profiles, expanding the RNAseq analysis to male hearts at comparable ages to females. We will also perform independent lineage tracing studies in male and female mice. We expect these original studies to provide novel information about gender-specific deficits in diabetes.

4. Impact

HFpEF is a major cause of morbidity and mortality worldwide. There is currently no effective treatment for patients with HFpEF. Although cardiac fibrosis has been implicated in the pathogenesis of HFpEF, the cellular basis for fibrotic remodeling of the ventricle is poorly understood. Metabolic diseases (such as obesity and diabetes) are associated with an increased incidence of HFpEF; however, the pathophysiological mechanisms responsible for this association remain unknown. Our experiments have established a model of HFpEF due to metabolic disease that can be used to dissect cellular mechanisms. This is of outstanding significance for pathophysiologic dissection in vivo. Our planned experiments will use lineage tracing strategies, in vivo and in vitro approaches to dissect the basis for activation of diabetic fibroblasts. The significance of the studies extends beyond the cardiovascular field, as diabetes-associated tissue fibrosis has an impact on other organs (such as the kidney and the liver).

5. Changes/Problems

No changes or problems to report

6. Products

Publications

1. NG Frangogiannis. The functional pluralism of fibroblasts in the infarcted myocardium. *Circ Res* 2016; 119: 1049-1051. Acknowledgment of DoD grant support: Yes.

2. AV Shinde, C Humeres, and NG Frangogiannis. The role of α-smooth muscle actin in fibroblast-mediated matrix contraction and remodeling. *BBA Mol Bas Dis* 2017; 1863: 298-309. Acknowledgment of DoD grant support: Yes.

3. NG Frangogiannis. The extracellular matrix in myocardial injury, repair and remodeling. *J Clin Invest* 2017; 127: 1600-1612. Acknowledgment of DoD grant support: Yes.

4. W Hanif, L Alex, Y Su, AV Shinde, I Russo, N Li, and NG Frangogiannis. Left atrial remodeling, hypertrophy and fibrosis in mouse models of heart failure. *Cardiovasc Pathol* 2017;30-27-37. Acknowledgment of DoD grant support: Yes.

5. AV Shinde, M Dobaczewski, JJ De Haan, A Saxena, KK Lee, Y Xia, W Chen, Y Su, W Hanif, IK Madahar, VM Paulino, G Melino and NG Frangogiannis. Tissue transglutaminase induction in the pressure-overloaded myocardium regulates cardiac remodeling. *Cardiovasc Res* 2017; 113:892-905. Acknowledgment of DoD grant support: Yes.

6. NG Frangogiannis. Activation of the innate immune system in the pathogenesis of acute heart failure. *Eur Heart J Acute Cardiovasc Care* 2017 Apr1 (epub ahead of print). Acknowledgment of DoD grant support: Yes.

7. NG Frangogiannis. Fibroblasts and the extracellular matrix in right ventricular disease. *Cardiovasc Res* 2017; 113: 12: 1453-1464. Acknowledgment of DoD grant support: Yes.

8. Shinde AV and NG Frangogiannis. Mechanisms of fibroblast activation in the remodeling myocardium. Curr Pathobiol Rep 2017; 5:145-152. Acknowledgment of DoD grant support: Yes.

5. PARTICIPANTS & OTHER COLLABORATING ORGANIZATIONS

What individuals have worked on the project?
Provide the following information for: (1) PDs/PIs; and (2) each person who has worked at least one person month per year on the project during the reporting period, regardless of the source of compensation (a person month equals approximately 160 hours of effort). If information is unchanged from a previous submission, provide the name only and indicate "no change".

Name	**Nikolaos Frangogiannis**	**"no change"**
Project Role	**PI**	
Research Identifier e.g ORCHID ID):		
Nearest person month worked	**2**	
Contribution to Project	**Dr Frangogiannis developed the proposed concepts, designed the experiments, and participated to the analysis.**	
Funding Support		
Name	**Ya Su**	**"no change"**
Project Role	**Associate**	
Research Identifier e.g ORCHID ID):		
Nearest person month worked	**6**	
Contribution to Project	**Dr Ya Su performs in vivo echocardiographic experiments and contributes to the development of mouse lines for lineage tracing and to the in vitro studies.**	

Funding Support		
Name	**Linda Alex**	**"no change"**
Project Role	**Research Associate**	
Research Identifier e.g ORCHID		
Nearest person month worked	**12**	
Contribution to Project	**Dr Linda Alex is breeding the colonies of diabetic pericyte reporter mice and the animals for lineage tracing. She performs genotypic and characterization of all genetic tools. She performs in vitro experiments for stimulation of cardiac pericytes and fibroblasts.**	
Funding Support		

Has there been a change in the active other support of the PD/PI(s) or senior/key personnel since the last reporting period?
If there is nothing significant to report during this reporting period, state "Nothing to Report."

If the active support has changed for the PD/PI(s) or senior/key personnel, then describe what the change has been. Changes may occur, for example, if a previously active grant has closed and/or if a previously pending grant is now active. Annotate this information so it is clear what has changed from the previous submission. Submission of other support information is not necessary for pending changes or for changes in the level of effort for active support reported previously. The awarding agency may require prior written approval if a change in active other support significantly impacts the effort on the project that is the subject of the project report.

No changes to report.

What other organizations were involved as partners?
If there is nothing significant to report during this reporting period, state "Nothing to Report."

Describe partner organizations – academic institutions, other nonprofits, industrial or commercial firms, state or local governments, schools or school systems, or other organizations (foreign or domestic) – that were involved with the project. Partner organizations may have provided financial or in-kind support, supplied facilities or equipment, collaborated in the research, exchanged personnel, or otherwise contributed.

Provide the following information for each partnership:
<u>Organization Name:</u>
<u>Location of Organization: (if foreign location list country)</u>
<u>Partner's contribution to the project</u> (identify one or more)

- *Financial support;*
- *In-kind support (e.g., partner makes software, computers, equipment, etc., available to project staff);*
- *Facilities (e.g., project staff use the partner's facilities for project activities);*
- *Collaboration (e.g., partner's staff work with project staff on the project);*

- *Personnel exchanges (e.g., project staff and/or partner's staff use each other's facilities, work at each other's site); and*
- *Other.*

Organization Name	Vanderbilt University	
Location of Organization	Vanderbilt Center for Stem Cell MRB IV - P425C Biology 2213 Garland Avenue Nashville, TN 37232-6300	Collaborating PI: Dr Antonis Hatzopoulos
Partner's Contribution	Dr. Antonis Hatzopoulos is an expert in the cell biology of the vascular cells and examines the involvement of endothelial cells in mediating diabetes-associated fibrosis	
Financial Support		
Facilities		
Collaboration	Collaboration between the PIs as outlined above	
Personal exchanges		
Other		

6. SPECIAL REPORTING REQUIREMENTS

COLLABORATIVE AWARDS: For collaborative awards, independent reports are required from BOTH the Initiating Principal Investigator (PI) and the Collaborating/Partnering PI. A duplicative report is acceptable; however, tasks shall be clearly marked with the responsible PI and research site. A report shall be submitted to **https://ers.amedd.army.mil** for each unique award. They must also submit a progress report.

Dr Hatzopoulos (Partnering PI) will submit his own progress report. Both reports contain the same description of the accomplishments; contributions of each laboratory to the reported accomplishments are clearly indicated.

QUAD CHARTS: If applicable, the Quad Chart (available on https://www.usamraa.army.mil) should be updated and submitted with attachments.

N/A

7. **APPENDICES:** Attach all appendices that contain information that supplements, clarifies or supports the text. Examples include original copies of journal articles, reprints of manuscripts and abstracts, a curriculum vitae, patent applications, study questionnaires, and surveys, etc.

Active other support of the PI (Nikolaos Frangogiannis)

ACTIVE:

Title of the project: Chemokines in healing myocardial infarcts
R01 HL076246
Funding agency: NIH/NHLBI
Investigator relationship:
Principal Investigator
Dates of funding: 6/2005-4/2019.
The project deals with cell-specific chemokine and cytokine actions in the infarcted myocardium. There is no overlap with the current DoD-funded project.

Title of the project: Resolution of inflammation in healing myocardial infarcts
R01 HL085440
Funding agency: NIH/NHLBI
Investigator relationship:
Principal Investigator
Dates of funding: 12/2007-5/2021
This project deals with the role of intracellular signals that inhibit innate immune responses in the infarcted heart. There is no overlap with the current DoD-funded project.

Title of the project: Fibroblast-Cardiomyocyte Interactions in
the Pressure Overloaded Myocardium
PR151134
Funding agency: Department of Defense office of the Congressionally Directed Medical Research Programs (CDMRP).
Investigator relationship:
Principal Investigator (Partnering PI award; co-PI: Dr. Richard Kitsis
Albert Einstein College of Medicine)
Dates of funding: 9/15/2016-9/14/2019.

Goals of the project: The project studies protective interactions between fibroblasts and cardiomyocytes in the pressure-overloaded heart. There is no overlap with the current DoD-funded project.

PENDING:
None

OVERLAP:
None

The Functional Pluralism of Fibroblasts in the Infarcted Myocardium

Nikolaos G. Frangogiannis

The mammalian heart contains a large population of interstitial fibroblast–like cells; in the adult mouse myocardium, 10% to 30% of myocardial cells were identified as fibroblasts.[1,2] These cells expand following injury and play an important role in cardiac repair[3] but may also participate in the pathogenesis of adverse postinfarction remodeling.[4] Traditional views consider cardiac fibroblasts as matrix-producing cells that simply serve to preserve the structural integrity of the ventricle after acute myocardial infarction by replacing dead cardiomyocytes with scar tissue and contribute to cardiac fibrosis in pathophysiologic conditions associated with chronic pressure overload or metabolic dysfunction.[5,6] However, this unidimensional view is not an accurate reflection of fibroblast function. A growing body of in vitro findings and in vivo observations suggests that fibroblasts exhibit a remarkable functional pluralism. In addition to their established role in matrix synthesis and metabolism, fibroblasts are also capable of secreting a wide range of immunoregulatory, cytoprotective, and angiogenic mediators in response to microenvironmental changes.

Article, see p 1116

In adult mammals, sudden death of myocardial cells overwhelms the negligible regenerative reserve of the myocardium; as a result, the infarcted heart heals through the formation of a collagen-based scar. Repair of the infarcted myocardium is dependent on timely activation and repression of an inflammatory reaction that serves to clear the infarct from dead cells and matrix debris. Inflammation after myocardial infarction is activated through the release of danger-associated molecular patterns from dying cells and degraded matrix.[7] These danger signals have been reported to activate all cell types involved in cardiac injury and repair. Cardiac fibroblasts respond to danger-associated molecular patterns and can produce large amounts of chemokines and cytokines that may play an important role in the activation of the postinfarction inflammatory response.[8] Moreover, it has been suggested that cardiac fibroblasts may modulate prosurvival signaling cascades in ischemic cardiomyocytes, affecting their susceptibility to apoptosis or necrosis. Unfortunately, these intriguing concepts on the role of fibroblasts in myocardial disease are currently supported almost exclusively by in vitro experiments and by associative evidence.[7,9,10] Considering the wide range of cell types capable of responding to danger signals triggering the inflammatory reaction after myocardial infarction, the relative significance of fibroblasts remains unclear. Dissection and documentation of the role of fibroblasts as cellular effectors of myocardial inflammation have been hampered by the challenges in the development of fibroblast-specific targeting approaches in vivo.[11]

In this issue of *Circulation Research*, Woodall et al[12] provide the first direct in vivo evidence supporting a crucial role for cardiac fibroblasts in regulating cardiomyocyte survival and in triggering the inflammatory response after myocardial infarction. The authors generated mice with fibroblast-specific loss of G protein–coupled receptor kinase 2 (GRK2), a ubiquitous member of the GRK family with a central role in signal transduction. In a model of reperfused myocardial infarction, fibroblast-specific GRK2 loss reduced the size of the infarct, decreasing secretion of proinflammatory cytokines, such as tumor necrosis factor-α, and attenuating cardiomyocyte apoptosis. In vitro, GRK2 loss attenuated nuclear translocation of nuclear factor-κB and subsequent tumor necrosis factor-α synthesis in isolated fibroblasts. Moreover, conditioned media from fibroblasts lacking GRK2 potentiated Akt signaling in cardiomyocytes, suggesting the activation of a cytoprotective pathway. Although the study provides the first direct documentation of a crucial role for cardiac fibroblasts in regulating cardiomyocyte injury and inflammation in the early stages after myocardial ischemia, the molecular mechanisms responsible for the observed effects remain unclear.

Do Cardiac Fibroblasts in the Ischemic Myocardium Function as Inflammatory Cells?

After myocardial infarction, release of danger-associated molecular patterns activates innate immune signaling pathways in several different cell types, triggering an intense inflammatory reaction. Endothelial cells, leukocytes, mast cells, and surviving cardiomyocytes have been suggested as likely cellular targets of danger-associated molecular patterns released by necrotic cells and may contribute to the activation of the postinfarction inflammatory response by secreting cytokines and chemokines.[13–15] Cardiac fibroblasts are also capable of secreting large amounts of proinflammatory mediators on stimulation with danger signals. Interleukin-1 is rapidly released in the infarcted myocardium and promotes a proinflammatory and matrix-degrading fibroblast phenotype, while suppressing

From the Department of Medicine (Cardiology), The Wilf Family Cardiovascular Research Institute, Albert Einstein College of Medicine, Bronx, NY.

Correspondence to Nikolaos G. Frangogiannis, MD, Department of Medicine (Cardiology), The Wilf Family Cardiovascular Research Institute, Albert Einstein College of Medicine, 1300 Morris Park Ave Forchheimer G46B, Bronx, NY 10461. E-mail nikolaos.frangogiannis@einstein.yu.edu

(*Circ Res*. 2016;119:1049-1051.
DOI: 10.1161/CIRCRESAHA.116.309926.)

***Circulation Research* is available at http://circres.ahajournals.org**
DOI: 10.1161/CIRCRESAHA.116.309926

α-smooth muscle actin synthesis and inhibiting myofibroblast conversion.[9] Thus, interleukin-1 stimulation may delay premature infiltration of the infarct with matrix-synthetic fibroblasts, until the wound is cleared from dead cells and matrix debris. Although the findings of this study are consistent with an important role of cardiac fibroblasts in promoting inflammation after myocardial infarction, the protective effects of GRK2 loss may not be caused by direct anti-inflammatory actions. Fibroblast-specific GRK2 loss decreased neutrophil infiltration in vivo and reduced tumor necrosis factor-α release in vitro. However, the in vivo attenuation of the inflammatory response may represent an epiphenomenon reflecting the significant reduction in infarct size, in the absence of a primary role of GRK2 in regulation of inflammation. The notion that GRK2 may be directly involved in the activation of a proinflammatory program is not supported by studies in immune cells. In vivo and in vitro investigations in T cells[16] and in myeloid cells[17] suggested that GRK2 not only does not stimulate inflammatory gene synthesis but may also be involved in negative regulation of inflammation.

Fibroblasts May Regulate Cardiomyocyte Survival

A growing body of evidence suggests that in injured and remodeling hearts, fibroblasts critically regulate cardiomyocyte responses. In the pressure-overloaded myocardium, activated fibroblasts transduce hypertrophic signals[18] mediated, at least in part, through secretion of miRNA-enriched exosomes.[19] In myocardial ischemia, administration of the secretome of neonatal cardiac fibroblasts before reperfusion significantly reduced the size of the infarct.[10] The current investigation suggests that endogenous fibroblast GRK2 signaling may extend ischemic injury, accentuating cardiomyocyte apoptosis. Several mechanisms may account for the proapoptotic effects of activated fibroblasts during the early postischemic phase (Figure). First, fibroblasts may secrete soluble proapoptotic mediators, such as proinflammatory cytokines, thus promoting cardiomyocyte death. Second, fibroblasts may indirectly reduce cardiomyocyte survival by modulating the composition of the extracellular matrix through the secretion of proteases. Protease-mediated degradation of the pericellular extracellular matrix may deprive ischemic cardiomyocytes from essential prosurvival signals. Third, ischemic fibroblasts may secrete exosomes that activate proapoptotic pathways in cardiomyocytes. Final, activation of GRK2 in ischemic fibroblasts may inhibit a yet unidentified prosurvival mechanism that may involve fibroblast-derived secretion of soluble mediators or deposition of matricellular proteins. Unfortunately, this study did not systematically pursue the mechanisms responsible for these intriguing interactions between fibroblasts and cardiomyocytes.

The Role of Activated Fibroblasts During the Proliferative Phase of Infarct Healing: Beyond Matrix Synthesis

Clearance of the infarcted heart from dead cells and matrix debris is associated with the activation of anti-inflammatory pathways, leading to the suppression and resolution of the inflammatory response.[20] Although cardiac fibroblasts are capable of producing large amounts of anti-inflammatory cytokines, such as interleukin-10 and transforming growth factor-β,[21] whether they actively participate in negative regulation of the inflammatory response remains unknown. Growth factor-mediated conversion of fibroblasts into myofibroblasts is associated with the activation of a matrix-synthetic program and secretion of collagens. Deposition of structural matrix proteins is the best-documented function of myofibroblasts in healing infarcts.[3] In addition to their role in scar formation, infarct myofibroblasts may also serve as an important source of growth factors and matricellular proteins, regulating the angiogenic response after myocardial infarction.[22] Whether the diverse functions of infarct fibroblasts in inflammation and repair reflect the activation of specific subpopulations remains unknown. Although several different developmental sources of cardiac fibroblasts have been identified in normal and injured hearts,[2] the functional properties of these cells have not been systematically investigated. The inducible collagen1α2-Cre driver used in this study should target all cardiac fibroblasts, thus precluding any conclusions on distinct effects of specific subsets.

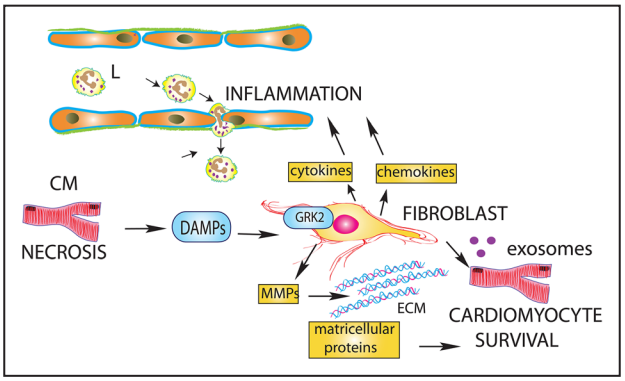

Figure. Cardiac fibroblasts are not unidimensional matrix-secreting cells but exhibit remarkable functional pluralism. After myocardial infarction, release of danger-associated molecular patterns (DAMPs) by necrotic cardiomyocytes (CM) activates a proinflammatory phenotype in fibroblasts, inducing secretion of cytokines and chemokines and stimulating leukocyte (L) infiltration. Moreover, during the early postischemic period, fibroblasts may modulate survival pathways in cardiomyocytes, affecting their susceptibility to ischemic death. These effects may be mediated through the secretion of soluble proapoptotic or antiapoptotic mediators by fibroblasts, via release of exosomes containing miRNAs or through modulation of the extracellular matrix (ECM) by fibroblast-derived matrix metalloproteinases (MMPs). MMP-mediated degradation of the matrix may deprive fibroblasts from essential prosurvival signals. Fibroblast G protein–coupled receptor kinase 2 (GRK2) signaling may extend ischemic injury after myocardial infarction through proinflammatory actions or by activating a proapoptotic pathway in cardiomyocytes.

Targeting the Cardiac Fibroblast in the Infarcted and Remodeling Myocardium

The consistent association between cardiac fibrosis and adverse outcome in a wide range of cardiac conditions has suggested that the fibroblast may be a promising therapeutic target in patients with myocardial infarction or heart failure. However, unlike primary fibrotic disorders in other systems (such as systemic sclerosis or idiopathic pulmonary fibrosis), in the myocardium, fibrotic remodeling often reflects

a reparative process that is activated in response to cardiomyocyte injury. In conditions associated with replacement fibrosis, such as myocardial infarction, targeting the reparative functions of fibroblasts may have catastrophic consequences. Implementation of therapeutic strategies targeting fibroblasts is further complicated by the wide range of modulatory functions of fibroblasts on cardiomyocyte hypertrophy and survival, on inflammatory activation, and on angiogenesis. In vivo dissection of the diverse actions of cardiac fibroblasts after injury is crucial to design therapeutic strategies that target detrimental actions, without interfering with protective effects. Moreover, identification and characterization of fibroblast subsets with distinct phenotypic characteristics and functional profiles may explain the functional pluralism of fibroblasts in injured and remodeling tissues.

Sources of Funding

Dr Frangogiannis's laboratory is supported by National Institutes of Health grants R01 HL76246 and R01 HL85440 and by grants from the Department of Defense Congressionally Directed Medical Research Programs (CDMRP).

Disclosures

None.

References

1. Pinto AR, Ilinykh A, Ivey MJ, Kuwabara JT, D'Antoni ML, Debuque R, Chandran A, Wang L, Arora K, Rosenthal NA, Tallquist MD. Revisiting cardiac cellular composition. *Circ Res*. 2016;118:400–409. doi: 10.1161/CIRCRESAHA.115.307778.
2. Ali SR, Ranjbarvaziri S, Talkhabi M, Zhao P, Subat A, Hojjat A, Kamran P, Müller AM, Volz KS, Tang Z, Red-Horse K, Ardehali R. Developmental heterogeneity of cardiac fibroblasts does not predict pathological proliferation and activation. *Circ Res*. 2014;115:625–635. doi: 10.1161/CIRCRESAHA.115.303794.
3. Shinde AV, Frangogiannis NG. Fibroblasts in myocardial infarction: a role in inflammation and repair. *J Mol Cell Cardiol*. 2014;70:74–82. doi: 10.1016/j.yjmcc.2013.11.015.
4. Kaur H, Takefuji M, Ngai CY, Carvalho J, Bayer J, Wietelmann A, Poetsch A, Hoelper S, Conway SJ, Möllmann H, Looso M, Troidl C, Offermanns S, Wettschureck N. Targeted ablation of periostin-expressing activated fibroblasts prevents adverse cardiac remodeling in mice. *Circ Res*. 2016;118:1906–1917. doi: 10.1161/CIRCRESAHA.116.308643.
5. Kong P, Christia P, Frangogiannis NG. The pathogenesis of cardiac fibrosis. *Cell Mol Life Sci*. 2014;71:549–574. doi: 10.1007/s00018-013-1349-6.
6. Travers JG, Kamal FA, Robbins J, Yutzey KE, Blaxall BC. Cardiac fibrosis: the fibroblast awakens. *Circ Res*. 2016;118:1021–1040. doi: 10.1161/CIRCRESAHA.115.306565.
7. Zhang W, Lavine KJ, Epelman S, Evans SA, Weinheimer CJ, Barger PM, Mann DL. Necrotic myocardial cells release damage-associated molecular patterns that provoke fibroblast activation in vitro and trigger myocardial inflammation and fibrosis in vivo. *J Am Heart Assoc*. 2015;4:e001993. doi: 10.1161/JAHA.115.001993.
8. Smith RS, Smith TJ, Blieden TM, Phipps RP. Fibroblasts as sentinel cells. Synthesis of chemokines and regulation of inflammation. *Am J Pathol*. 1997;151:317–322.
9. Saxena A, Chen W, Su Y, Rai V, Uche OU, Li N, Frangogiannis NG. IL-1 induces proinflammatory leukocyte infiltration and regulates fibroblast phenotype in the infarcted myocardium. *J Immunol*. 2013;191:4838–4848. doi: 10.4049/jimmunol.1300725.
10. Abrial M, Da Silva CC, Pillot B, Augeul L, Ivanes F, Teixeira G, Cartier R, Angoulvant D, Ovize M, Ferrera R. Cardiac fibroblasts protect cardiomyocytes against lethal ischemia-reperfusion injury. *J Mol Cell Cardiol*. 2014;68:56–65. doi: 10.1016/j.yjmcc.2014.01.005.
11. Kong P, Christia P, Saxena A, Su Y, Frangogiannis NG. Lack of specificity of fibroblast-specific protein 1 in cardiac remodeling and fibrosis. *Am J Physiol Heart Circ Physiol*. 2013;305:H1363–H1372. doi: 10.1152/ajpheart.00395.2013.
12. Woodall MC, Woodall BP, Ghao E, Yuan A, Koch WJ. Cardiac fibroblast GRK2 deletion enhances contractility and remodeling following ischemia/reperfusion injury. *Circ Res*. 2016:119:1116–1127. doi: 10.1161/CIRCRESAHA.116.309538.
13. Arslan F, Smeets MB, O'Neill LA, Keogh B, McGuirk P, Timmers L, Tersteeg C, Hoefer IE, Doevendans PA, Pasterkamp G, de Kleijn DP. Myocardial ischemia/reperfusion injury is mediated by leukocytic toll-like receptor-2 and reduced by systemic administration of a novel anti-toll-like receptor-2 antibody. *Circulation*. 2010;121:80–90. doi: 10.1161/CIRCULATIONAHA.109.880187.
14. Frangogiannis NG, Lindsey ML, Michael LH, Youker KA, Bressler RB, Mendoza LH, Spengler RN, Smith CW, Entman ML. Resident cardiac mast cells degranulate and release preformed TNF-alpha, initiating the cytokine cascade in experimental canine myocardial ischemia/reperfusion. *Circulation*. 1998;98:699–710.
15. Zhu M, Goetsch SC, Wang Z, Luo R, Hill JA, Schneider J, Morris SM Jr, Liu ZP. FoxO4 promotes early inflammatory response upon myocardial infarction via endothelial Arg1. *Circ Res*. 2015;117:967–977. doi: 10.1161/CIRCRESAHA.115.306919.
16. Vroon A, Heijnen CJ, Lombardi MS, Cobelens PM, Mayor F Jr, Caron MG, Kavelaars A. Reduced GRK2 level in T cells potentiates chemotaxis and signaling in response to CCL4. *J Leukoc Biol*. 2004;75:901–909. doi: 10.1189/jlb.0403136.
17. Patial S, Saini Y, Parvataneni S, Appledorn DM, Dorn GW II, Lapres JJ, Amalfitano A, Senagore P, Parameswaran N. Myeloid-specific GPCR kinase-2 negatively regulates NF-κB1p105-ERK pathway and limits endotoxemic shock in mice. *J Cell Physiol*. 2011;226:627–637. doi: 10.1002/jcp.22384.
18. Takeda N, Manabe I, Uchino Y, Eguchi K, Matsumoto S, Nishimura S, Shindo T, Sano M, Otsu K, Snider P, Conway SJ, Nagai R. Cardiac fibroblasts are essential for the adaptive response of the murine heart to pressure overload. *J Clin Invest*. 2010;120:254–265. doi: 10.1172/JCI40295.
19. Bang C, Batkai S, Dangwal S, et al. Cardiac fibroblast-derived microRNA passenger strand-enriched exosomes mediate cardiomyocyte hypertrophy. *J Clin Invest*. 2014;124:2136–2146. doi: 10.1172/JCI70577.
20. Prabhu SD, Frangogiannis NG. The biological basis for cardiac repair after myocardial infarction: from inflammation to fibrosis. *Circ Res*. 2016;119:91–112. doi: 10.1161/CIRCRESAHA.116.303577.
21. Driesen RB, Nagaraju CK, Abi-Char J, Coenen T, Lijnen PJ, Fagard RH, Sipido KR, Petrov VV. Reversible and irreversible differentiation of cardiac fibroblasts. *Cardiovasc Res*. 2014;101:411–422. doi: 10.1093/cvr/cvt338.
22. Dostal D, Glaser S, Baudino TA. Cardiac fibroblast physiology and pathology. *Compr Physiol*. 2015;5:887–909. doi: 10.1002/cphy.c140053.

Key Words: Editorials ■ fibroblasts ■ inflammation ■ mice ■ myocardial infarction ■ myocardium

Circulation Research
JOURNAL OF THE AMERICAN HEART ASSOCIATION

The Functional Pluralism of Fibroblasts in the Infarcted Myocardium

Nikolaos G. Frangogiannis

Circ Res. 2016;119:1049-1051
doi: 10.1161/CIRCRESAHA.116.309926
Circulation Research is published by the American Heart Association, 7272 Greenville Avenue, Dallas, TX 75231

Print ISSN: 0009-7330. Online ISSN: 1524-4571

Biochimica et Biophysica Acta 1863 (2017) 298–309

Contents lists available at ScienceDirect

Biochimica et Biophysica Acta

journal homepage: www.elsevier.com/locate/bbadis

The role of α-smooth muscle actin in fibroblast-mediated matrix contraction and remodeling

Arti V. Shinde, Claudio Humeres, Nikolaos G. Frangogiannis *

The Wilf Family Cardiovascular Research Institute, Department of Medicine (Cardiology), Albert Einstein College of Medicine, Bronx, NY, United States

ARTICLE INFO

Article history:
Received 21 June 2016
Received in revised form 9 October 2016
Accepted 2 November 2016
Available online 4 November 2016

Keywords:
Myofibroblast
α-Smooth muscle actin
Myocardial infarction
Extracellular matrix
Transforming growth factor-β

ABSTRACT

Cardiac myofibroblasts play an important role in myocardial remodeling. Although α-smooth muscle actin (α-SMA) expression is the hallmark of mature myofibroblasts, its role in regulating fibroblast function remains poorly understood. We explore the effects of the matrix environment in modulating cardiac fibroblast phenotype, and we investigate the role of α-SMA in fibroblast function using loss- and gain-of-function approaches. In murine myocardial infarction, infiltration of the infarct border zone with abundant α-SMA-positive myofibroblasts was associated with scar contraction. Isolated cardiac fibroblasts cultured in plates showed high α-SMA expression localized in stress fibers, exhibited activation of focal adhesion kinase (FAK), and synthesized large amounts of extracellular matrix proteins. In contrast, when these cells were cultured in collagen lattices, they exhibited marked reduction of α-SMA expression, negligible FAK activation, attenuated collagen synthesis, and increased transcription of genes associated with matrix metabolism. Transforming Growth Factor-β1-mediated contraction of fibroblast-populated collagen pads was associated with accentuated α-SMA synthesis. In contrast, serum- and basic Fibroblast Growth Factor-induced collagen pad contraction was associated with reduced α-SMA expression. α-SMA siRNA knockdown attenuated contraction of collagen pads populated with serum-stimulated cells. Surprisingly, α-SMA overexpression also reduced collagen pad contraction, suggesting that α-SMA is not sufficient to promote contraction of the matrix. Reduced contraction by α-SMA-overexpressing cells was associated with attenuated proliferative activity, in the absence of any effects on apoptosis. α-SMA may be implicated in contraction and remodeling of the extracellular matrix, but is not sufficient to induce contraction. α-SMA expression may modulate cellular functions, beyond its effects on contractility.

1. Introduction

In healing tissues, fibroblasts acquire a contractile phenotype, characterized by formation of microfilament bundles, and by de novo expression of α-smooth muscle actin (α-SMA). These activated cells, termed "myofibroblasts" [1–7] participate in the reparative response, by secreting large amounts of extracellular matrix proteins [8,9] and may be responsible for contraction of healing wounds [10]. Repair of injured tissues is dependent on timely activation and deactivation of myofibroblasts; prolonged or excessive myofibroblast activity may result in fibrosis and organ dysfunction [11–13].

The normal mammalian myocardium contains a large number of fibroblast-like cells [14–16]. In the absence of injury, these interstitial cells remain quiescent; however, a wide range of injurious processes can induce cardiac fibroblast activation. Conversion of cardiac fibroblasts into activated α-SMA-positive myofibroblasts is consistently noted following myocardial infarction, both in human patients [17] and in experimental models [18,19]. Because the adult mammalian heart has negligible regenerative capacity, activated myofibroblasts play a crucial role in post-infarction cardiac repair, by secreting extracellular matrix proteins, thus protecting the heart from catastrophic rupture. Moreover, the capacity of infarct myofibroblasts to contract the scar may play an important role in protecting the chamber from adverse remodeling [20]. On the other hand, excessive activation of fibroblasts in the infarcted heart may contribute to fibrosis, increase stiffness, and promote both systolic and diastolic dysfunction [21,12].

Our group and other investigators have used experimental animal models and in vitro approaches to study the role of fibroblasts in the infarcted and remodeling myocardium [22–29]. In vitro studies investigating myocardial fibrotic responses, have used either cardiac fibroblasts cultured and stimulated in plates, or cells enmeshed in collagen lattices [25,30–32]. Assessment of fibroblast-mediated contraction in collagen pads provides a robust and pathophysiologically relevant model of fibroblast function. Although α-SMA expression is a hallmark

* Corresponding author at: The Wilf Family Cardiovascular Research Institute, Albert Einstein College of Medicine, 1300 Morris Park Avenue Forchheimer G46B, Bronx, NY 10461, United States.
E-mail address: nikolaos.frangogiannis@einstein.yu.edu (N.G. Frangogiannis).

http://dx.doi.org/10.1016/j.bbadis.2016.11.006
0925-4439/

of the mature myofibroblast, its role in regulation of fibroblast behavior and function remains poorly understood. Studies using fibroblast-populated collagen lattices suggested that α-SMA expression increases fibroblast contractile activity [33], and plays a crucial role in focal adhesion maturation [34]. However, other investigations showed that, at a single cell level, fibroblasts and myofibroblasts were found to exert comparable contractile forces [35]. Because fibroblasts are highly dynamic cells [36], interpretation of the findings derived from different in vitro models requires understanding of the distinct characteristics of fibroblasts in each model. Our study compares cardiac fibroblast phenotype between the two models, and explores the role of α-SMA in fibroblast-mediated matrix contraction.

We report that, in both reperfused and non-reperfused mouse infarcts, scar contraction is associated with marked infiltration of the infarct border zone with myofibroblasts. In vitro, culture of cardiac fibroblasts in collagen pads markedly suppressed α-SMA expression and reduced extracellular matrix synthesis, while promoting synthesis of genes associated with matrix metabolism. Contraction of fibroblast-populated pads in response to serum, or specific growth factors was not consistently associated with upregulation of α-SMA. siRNA knockdown and overexpression experiments demonstrated that α-SMA is involved in collagen pad contraction, but is not sufficient to induce contraction of the matrix. Surprisingly α-SMA expression modulated proliferative activity in cardiac fibroblasts. Our findings highlight the dynamic phenotype of fibroblasts under different conditions and suggest that α-SMA may exert actions independent of its effects on cell contraction.

2. Materials and methods

2.1. Mouse models of reperfused and non-reperfused myocardial infarction

Both male and female, 3–4 month old C57/BL6J mice underwent coronary occlusion/reperfusion protocols as previously described [37]. Mice were anesthetized by isoflurane inhalation (isoflurane 2–3% vol/vol). Non-reperfused myocardial infarction was induced using an open chest model of permanent left coronary artery ligation [38]. Reperfused infarction was induced using a well-characterized closed-chest model of coronary occlusion and reperfusion [39]. Infarcted hearts (after 7 or 28 days of permanent coronary occlusion and after 1 h ischemia/7–28 days of reperfusion) were fixed in formalin and embedded in paraffin.

2.2. Immunohistochemistry and histology

Infarcted hearts were sectioned systematically from based to apex in 250 μm partitions as previously described [39]. One section from each partition was stained for sirius red to identify the healing scar. Scar size was morphometrically assessed using ImagePro software by dividing the total scar area to the total area of the left ventricle (from all partitions). Myofibroblasts in infarcted hearts were identified, as spindle-shaped cells located outside the vascular media with α-SMA immunofluorescence using the anti-α-SMA antibody (1A4, Santa Cruz Biotech) and an Alexa-Fluor 594-labeled secondary antibody (Molecular Probes). Sections were counterstained with DAPI.

2.3. Isolation and stimulation of mouse cardiac fibroblasts

Cardiac fibroblasts were isolated from C57/BL6J animals using enzymatic digestion as previously described [40,41] and were cultured in DMEM/F12 (GIBCO Invitrogen Corporation, Carlsbad, CA) with 10% Fetal Calf Serum (FCS). Cells were serum-starved at passage 2 for 16 h and subsequently stimulated with either 10 ng/ml or 50 ng/ml of recombinant TGF-β1 (R&D Systems, Minneapolis MN) for 4–24 h. Total RNA was isolated from the stimulated cells using GeneJET RNA Purification Kit (ThermoFisher Scientific) and was reverse transcribed to cDNA using the iScript™ cDNA synthesis kit (Bio-Rad) following the manufacturer's guidelines. Quantitative PCR was performed using SsoFast™ EvaGreen® Supermix (Bio-Rad) on the CFX384™ Real-Time PCR Detection System (Bio-Rad). Primers were synthesized by Integrated DNA Technologies. The following genes were assessed: α-SMA, type I collagen, type III collagen, matrix metalloproteinase (MMP)2, MMP3, MMP8, tissue inhibitor of metalloproteinases (TIMP)1, fibronectin and GAPDH. Each sample was run in triplicate. For experiments with collagen pads, RNA was isolated from the stimulated collagen pads using GeneJET RNA Purification Kit and the RNA obtained was used for quantitative PCR as mentioned above.

2.4. Collagen pad contraction assay

Cardiac fibroblasts isolated from adult C57/BL6J mice were cultured to passage 2 and serum-starved overnight (16 h). Collagen matrix was prepared on ice by diluting a stock solution of rat collagen I (3.0 mg/ml) (GIBCO Invitrogen Corporation, Carlsbad, CA) with 2X MEM and distilled water for a final concentration of 1 mg/ml collagen. Cell suspensions in 2X MEM were mixed with collagen solution to achieve the final $3*10^5$ cells/ml concentration. Subsequently, 500 μl of this suspension was aliquoted to a 24-well culture plate (BD Falcon, San Jose, CA) and allowed to polymerize at 37 °C for 30 min. Following polymerization, pads were released from wells, transferred to 6-well culture plate (BD Falcon, San Jose, CA) and cultured in 0% FCS DMEM/F12 for 24 h. After 24 h, the pictures of the plates were taken in Bio-Rad ChemiDoc Imager, and the area of each pad was measured using Image Pro software. After incubation, the pads were fixed in formalin and processed in paraffin for subsequent histological analysis. For growth factor stimulation experiments, the collagen pads were suspended in either serum free DMEM/F12 or with 10% fetal bovine serum, or TGF-β1 (1–50 ng/ml), or bFGF (50 ng/ml) for 24 h.

2.5. α-SMA siRNA knockdown and overexpression experiments

For siRNA knockdown, mouse cardiac fibroblasts at passage 1 were seeded at 80% confluence (10 cm dishes) in complete medium and were either transfected with 50 nM ON-TARGET plus siRNA to α-SMA or transfected with a non-silencing control siRNA (Dharmacon) using Lipofectamine® 3000 Reagent (ThermoFisher Scientific). The ONTARGET modification is shown to dramatically decrease the off-target effects of the siRNA. In a pilot experiment we tested the effectiveness of 4 different siRNAs in reducing α-SMA protein levels in unstimulated HT cardiac fibroblasts. We found that although three of the four siRNAs reduced the expression of α-SMA, only one of the duplexes (#4, J-061937-12) reduced α-SMA protein expression by ~70%. We used this siRNA for all following in vitro experiments to achieve targeted knockdown of α-SMA.

The cells were returned to a 5% CO_2 incubator and allowed to recover for 24 h. After 24 h, the cells were harvested using TrypLE ™ Express reagent, counted and populated on collagen pads ($3*10^5$ cells/ml concentration). The pads were either suspended in serum free DMEM/F12 or stimulated with media containing 10% serum or 10 ng/ml TGF-β for 72 h after which the pads were Imaged using Bio-Rad ChemiDoc Imager and contraction was assessed using Image J software. Cells were plated in parallel dishes to verify knockdown either by Western blots or by fluorescence microscopy.

For α-SMA overexpression experiments, mouse cardiac fibroblasts at passage 1 were seeded at 80% confluence (10 cm dishes) in complete medium and were either transfected with 2.5 ng of αSMA cDNA (Origene ™ Technologies) or transfected with a control entry vector using Lipofectamine®3000 Reagent (ThermoFisher Scientific). The cells were then processed as above.

2.6. Immunofluorescence

In order to assess focal adhesion kinase (FAK) activation, cardiac fibroblasts ($1*10^5$ cells per well) from wild type mice were seeded on four-well glass culture slides (BD Falcon). Two days later, cells were serum-starved for 16 h before adding different doses of TGF-β for 65 min. The cells were fixed for 30 min with 4% paraformaldehyde and processed for immunofluorescence with antibodies recognizing phosphorylated FAK (Anti-phospho Y397 FAK, #ab39967, Abcam) and α-SMA (1A4, Santa Cruz Biotech), followed by Alexa Fluor 488– or Alexa Fluor 594–conjugated secondary antibodies respectively. The slides were mounted using VECTASHIELD Antifade Mounting Medium with DAPI (#H-1200). Images were obtained with a Zeiss Axio Imager.M2 microscope and Zeiss AxioVision software.

For the α-SMA knockdown, cardiac fibroblasts from wild type mice were transfected with 50 nM ONTARGETplus siRNA to α-SMA or transfected with a non-silencing control siRNA (Dharmacon) and for overexpression experiments, cells were transfected with 2.5 ng of α-SMA cDNA (Origene TM Technologies) or transfected with a control entry vector using Lipofectamine®3000 Reagent. The cells were returned to a 5% CO_2 incubator, allowed to recover for 72 h, then fixed for 30 min with 4% paraformaldehyde and processed for immunofluorescence with the anti-α-SMA antibody.

2.7. Assessment of cell density and size in collagen pads

Fibroblast-populated collagen pads were fixed in formalin and embedded in paraffin for histologic analysis. Histological sections from fibroblast-populated pads were stained with sirius red, and counterstained with hematoxylin, as previously described [25], to identify the fibroblasts and to quantitate their density and cell area. For assessment of cell density 4 random low power (50×) fields were used for each pad; cell density was expressed as the number of fibroblast profiles per unit area. For quantitation of cell area, we traced and measured the area of 30 fibroblasts from each pad using AxioVision software (Zeiss).

2.8. Assessment of fibroblast proliferation in collagen pads

Histological sections from fibroblast-populated pads were deparaffinized in xylene, rehydrated through graded alcohols, and permeabilized using Triton-X (0.1%) at room temperature for 8 min, followed by several washes in PBS. Nonspecific antibody binding was blocked by incubation for 1 h with 10% goat serum in PBS. Immunohistochemical staining was performed with the monoclonal Rat Anti-Mouse Ki-67 Antibody (Clone TEC-3, DAKO) using the Vectastain ABC kit (Vector laboratories). Sections were developed with the Vector Blue Alkaline Phosphatase Substrate (Vector laboratories) and counterstained with the nuclear Fast Red (Sigma, N 8002) to identify nuclei. After two washes in distilled water, the pads were mounted using an aqueous mounting medium (Vecta Mount AQ; Vector laboratories). Quantitative analysis was performed by scanning 30 random fields at 400× magnification. Ki-67 positive cells density was calculated as the number of Ki-67 positive cells per unit area.

2.9. Assessment of fibroblast apoptosis

Histological sections from fibroblast-populated pads were deparaffinized, rehydrated, then permeabilized using Triton-X. Apoptotic cells were detected using the fluorescent TUNEL cell death detection kit (in situ cell death Detection Kit-TMR Red; Roche). Sections were mounted with mounting medium that contained DAPI, to counterstain nuclei (VECTASHIELD Mounting Medium with DAPI, Vector Laboratories). 4 random fields at 400× magnification were imaged from each pad, and the number of positive and negative TUNEL+ cells was counted. The density of apoptotic cells was expressed as the number of TUNEL+ cells divided per unit area.

2.10. RNA extraction and qPCR

Isolated total RNA from isolated cardiac fibroblasts was reverse transcribed to cDNA using the iScript™ cDNA synthesis kit (Bio-Rad) following the manufacturer's guidelines. Quantitative PCR was performed using SsoFast™ EvaGreen® Supermix (Bio-Rad) on the CFX384™ Real-Time PCR Detection System (Bio-Rad). Primers were synthesized by Integrated DNA Technologies. The following sets of primers were used in the study: TIMP1 forward GCCTGAACACTGTCTA CTT reverse TTGCTGCTGTCTGATAGTT; MMP2 forward TCCGCTGCATC CAGACTT, reverse GGTCCTGGCAATCCCTTTGTATA; MMP3 forward ATTTGGGTTTCTCTACTT, reverse GAAGAACTATAAGCATCAG; MMP8 forward TTAGGATGAGCCATAAGT, reverse TTGCTTGGTCTCTTCTAT; collagen I forward GATACTTGAAGAATATGAAC, reverse AATGCTGAATC TAATGAA; collagen III forward TACTCATTCACCAGCATA, reverse GTAT AGTCTTCAGGTCTCA; fibronectin forward AGACTTCTCTCCTCAATG, reverse ACCAAACCATAAGAACTTT; GAPDH forward AACGACCCCTTCAT TGACCT, reverse CACCAGTAGACTCCACGACA.

2.11. Protein extraction and western blotting

Mouse cardiac fibroblasts were transfected with either control non-targeting siRNA or α-SMA siRNA. 96 h after transfection, cells were rinsed and lysed on ice in standard radioimmunoprecipitation assay (RIPA) lysis buffer [50mMtris-HCl (pH 8), 150 mM NaCl, 1%Triton X-100, 0.2 mM EDTA, 0.1% SDS, 0.5% sodium deoxycholate, 2 mM phenylmethylsulfonyl fluoride, 10% protease inhibitor cocktail (Roche), 10% phosphatase inhibitor cocktail (Roche)], and protein concentrations were determined with the BCA Assay Reagent (Pierce). Lysates (30 μg–50 μg) were subjected to SDS–polyacrylamide gel electrophoresis and transferred onto Immuno-Blot polyvinylidene difluoride membranes (Bio-Rad). The membranes were blocked [5% BSA in tris-buffered saline (TBS)–Tween], incubated with antibodies to α-SMA (1A4, Santa Cruz Biotech), or phosphorylated FAK (Anti-phospho Y397 FAK, #ab39967, Abcam), washed, and then incubated with horseradish peroxidase (HRP)–linked secondary antibody (1% nonfat milk in TBS-Tween for 1 h). Bound antibodies were detected by enhanced chemiluminescence with SuperSignal West Pico or Femto reagents (Pierce). Signal intensity was measured with ChemiDoc™ MP System (Bio Rad) and analyzed by Image Lab 3.0 software (Bio Rad). Membranes were then stripped and reprobed with an antibody against GAPDH (Santa Cruz Biotechnology) to verify equal loading.

2.12. Statistical analysis

Data are expressed as mean ± SEM. For comparisons of two groups unpaired, 2-tailed Student's *t*-test using (when appropriate) Welch's correction for unequal variances was performed. The Mann-Whitney test was used for comparisons between 2 groups that did not show Gaussian distribution. For comparison of multiple groups 1-way ANOVA was performed, followed by *t*-test corrected for multiple comparisons (Student-Newman-Keuls). The Kruskal-Wallis test, followed by Dunn's multiple comparison post-test was used when one or more groups did not show Gaussian distribution.

3. Results

3.1. Infiltration of the healing infarct with α-SMA-expressing myofibroblasts is associated with scar contraction

Repair of the adult mammalian heart is associated with replacement of dead cardiomyocytes with a collagen-based scar. We used quantitative morphometric analysis of sirius red-stained sections to study remodeling of the scar in mouse models of reperfused and non-reperfused myocardial infarction. Reperfused myocardial infarction heals through formation of a mid-myocardial scar after 7 days of

reperfusion, that spares subendocardial and subepicardial regions (Fig. 1A). After 28 days of reperfusion, scar size is significantly decreased (Fig. 1B–C), reflecting scar contraction. Permanent coronary occlusion results in transmural infarction of the same territory (Fig. 1D). Scar size expressed as a percentage of the left ventricular area is markedly reduced after 28 days of permanent coronary occlusion, reflecting contraction and thinning of the scar and progressive hypertrophy of the non-infarcted segments (Fig. 1E–F). Immunofluorescent staining for α-SMA labels abundant myofibroblasts in the infarct border zone after 7 days of coronary occlusion, as spindle-shaped immunoreactive cells, located outside the vascular media (Fig. 1G). The number of α-SMA + myofibroblasts is reduced after 28 days of coronary occlusion (Fig. 1H). In contrast, in remote myocardial segments, α-SMA immunoreactivity is predominantly localized in vascular mural cells (Fig. 1I–J).

3.2. Fibroblasts populating free-floating collagen pads induce contraction upon stimulation with serum or TGF-β1

α-SMA + myofibroblasts infiltrating the infarct may be responsible for contraction of healing myocardial scars. In order to investigate mediators responsible for fibroblast-mediated scar contraction, we used an in vitro model, in which isolated mouse cardiac fibroblasts are enmeshed in free-floating collagen pads. Stimulation with 10% serum induced marked contraction of the fibroblast-populated pads (Supplemental Fig. 1A, B). TGF-β1 stimulation (1 ng/ml) also induced pad contraction; higher concentrations of TGF-β1 (10–50 ng.ml) did not further increase pad contraction (Supplemental Fig. 1C–D).

3.3. When enmeshed into free-floating collagen pads, cardiac fibroblasts exhibit markedly reduced baseline synthesis of collagens and α-SMA and decreased FAK activation

Next, we examined the effects of culture in the collagen pad on cardiac fibroblast morphology and gene expression. Fibroblasts cultured in the high-tension (HT) environment of the plate exhibited a flat, spread out morphology. Immunofluorescent staining showed that fibroblasts cultured in plates exhibited α-SMA incorporation in cytoskeletal filaments (Fig. 2A). In contrast, fibroblasts cultured in the low-tension (LT) environment of the collagen pad were elongated, had dendritic projections and had low levels of α-SMA immunofluorescence with punctate cytoplasmic localization (Fig. 2B–C). Comparison of gene expression showed that pad fibroblasts had a markedly lower expression of α-SMA, collagen I, and III, when compared with HT fibroblasts. In contrast, fibronectin mRNA expression was comparable between LT and HT fibroblasts. LT fibroblasts exhibited markedly accentuated synthesis of genes associated with matrix metabolism, showing increased MMP2, MMP3, MMP8 and TIMP1 levels (Fig. 2).

Because FAK signaling is implicated in myofibroblast transdifferentiation and activation [42,43], we compared FAK activity between HT and LT cells. Western blotting for p-FAK and immunofluorescence demonstrated that HT cells had abundant expression of

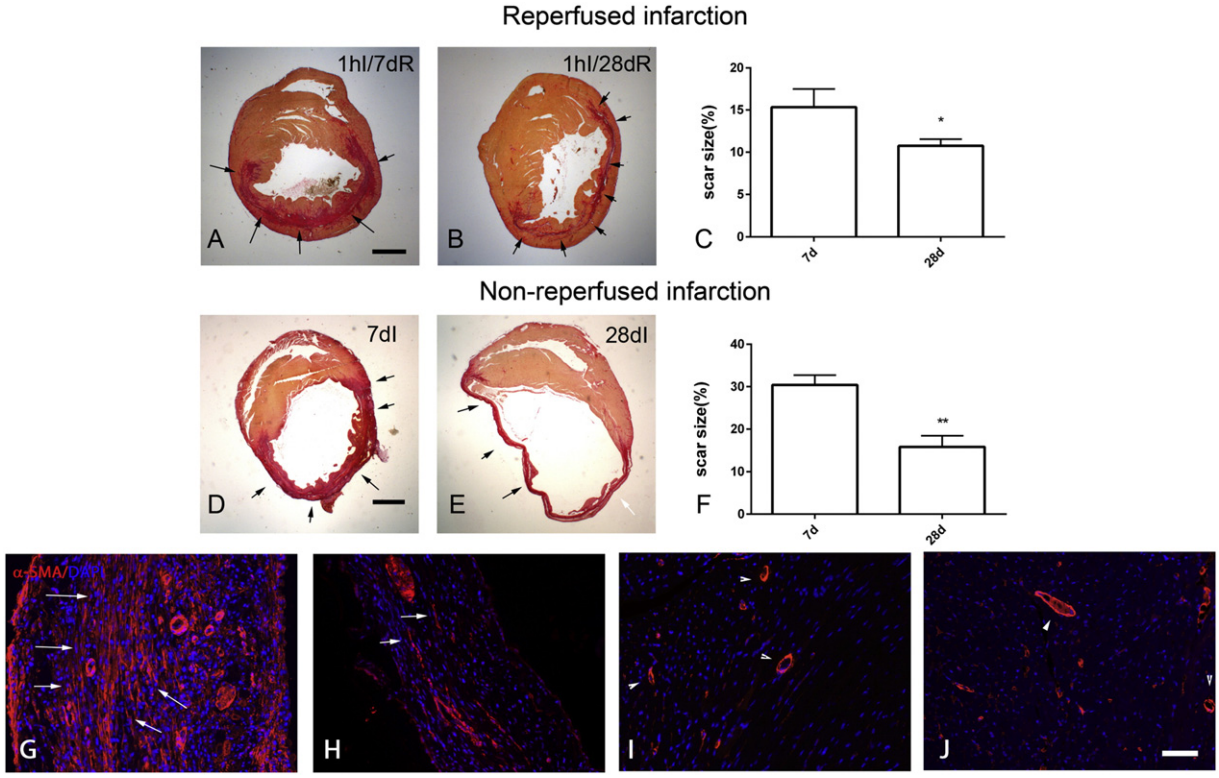

Fig. 1. In healing mouse infarcts, myofibroblast infiltration is associated with scar contraction. A–F: Sirius red staining was performed to label the area of the infarct in mice undergoing reperfused (A–C) and non-reperfused infarction protocols (D–F) (scalebar = 1 mm). Mouse hearts were sectioned at 250 μm partitions and the scar size was assessed by measuring the sirius red-stained area at each level. A. The representative image shows a midmyocardial scar (arrows) after 1 h of ischemia and 7 days of reperfusion, sparing the subendocardial and subepicardial region. B. After 1 h of ischemia and 28 days of reperfusion, there is marked thinning of the infarcted area (arrows). C. Quantitative analysis shows a marked reduction of scar size after 28 days of reperfusion, reflecting contraction of the scar (*$p < 0.05$, n = 15–23/group). D. Permanent coronary occlusion caused a transmural infarct, leading to replacement of dead cardiomyocytes with scar (arrows) in the entire area at risk. E. Marked thinning of the scar was noted after 28 days of permanent occlusion (arrows). F. Quantitative analysis showed a 50% reduction in scar size at the 28-day timepoint, reflecting scar contraction (**$p < 0.01$, n = 14/group). G–J. α-SMA staining identifies abundant myofibroblasts in healing myocardial infarcts after 7 days of coronary ischemia (arrows). H. Myofibroblast density is markedly reduced after 28 days of ischemia, as the scar matures (arrows). I–J. In contrast, in the remodeling non-infarcted myocardium, α-SMA immunoreactivity is predominantly localized in the arteriolar media (arrowheads - I, 7 days of ischemia; J, 28 days of ischemia) (scalebar = 50 μm).

p-FAK in the presence or absence of TGF-b1. In contrast, LT cells showed negligible FAK activity (Supplemental Fig. 2).

3.4. Distinct effects of TGF-β on collagen and α-SMA synthesis in HT and LT fibroblasts

Next, we examined the effects of TGF-β1 stimulation on α-SMA and collagen mRNA synthesis in HT fibroblasts. TGF-β1 stimulation (10 ng/ml) induced a 1.7-fold upregulation of α-SMA levels after 4 h of stimulation and a 3-fold increase after 24 h of stimulation (Fig. 3A). Moreover, in HT cells, TGF-β1 induced a transient upregulation of collagen I and III mRNA synthesis after 4 h of stimulation (Fig. 3B, C). In low-tension cardiac fibroblasts both low (10 ng/ml) and high (50 ng/ml) concentrations of TGF-β induced a modest (1.5–2.0-fold) upregulation of α-SMA (Fig. 3D, G), but did not affect collagen I and collagen III synthesis (Fig. 3E–F, H–I).

3.5. In LT fibroblasts, TGF-β1 stimulation promotes a matrix-preserving fibroblast phenotype

In LT fibroblasts, both low (10 ng/ml – Supplemental Fig. 3A–D) and high (50 ng/ml – Supplemental Fig. 3E–H) TGF-β1 concentrations induced a matrix-preserving program, markedly attenuating MMP2 (Supplemental Fig. 3A, E), MMP3 (Supplemental Fig. 3B, F) and MMP8 synthesis (Supplemental Fig. 3C, G), and upregulating TIMP1 expression (Supplemental Fig. 3D, H).

3.6. Serum-induced pad contraction is associated with reduced α-SMA mRNA synthesis

Stimulation with 10% serum markedly increased contraction of fibroblast-populated collagen pads (Supplemental Fig. 1). Surprisingly, increased pad contraction upon serum stimulation was associated with reduced α-SMA expression (Supplemental Fig. 4A), suggesting that serum-induced pad contraction was not due to enhanced myofibroblast transdifferentiation. Moreover, serum stimulation did not significantly affect collagen I and III synthesis (Supplemental Fig. 4B–C), but reduced MMP2 mRNA expression (Supplemental Fig. 4D) and enhanced TIMP1 expression levels (Supplemental Fig. 4G). Serum had no significant effects on transcription of the collagenases MMP3 and MMP8 (Supplemental Fig. 4E, F).

3.7. Basic fibroblast growth factor (bFGF)-mediated pad contraction is associated with attenuated α-SMA synthesis

Stimulation with bFGF (50 ng/ml) also significantly increased contraction in fibroblast-populated collagen pads (Fig. 4A, B). bFGF stimulation markedly reduced α-SMA synthesis in pad fibroblasts (Fig. 4C), suggesting that enhanced myofibroblast transdifferentiation is not responsible for bFGF-induced pad contraction. bFGF reduced matrix protein expression in pad fibroblasts, significantly attenuating collagen I and collagen III mRNA synthesis (Fig. 4D, E). Moreover, bFGF stimulation reduced MMP2 (Fig. 4F) and MMP8 expression (Fig. 4H) and increased TIMP1 levels (Fig. 4I), changes consistent with activation of a matrix-preserving fibroblast phenotype. bFGF had no effect on MMP3 mRNA expression (Fig. 4G).

3.8. α-SMA overexpression does not significantly affect contraction of fibroblast-populated pads upon serum stimulation

α-SMA expression has been implicated in scar contraction both in vivo, and in fibroblast-populated collagen pads. Our experiments showed that, although contraction of the healing infarct is associated with infiltration of the scar with α-SMA-expressing myofibroblasts (Fig. 1), pad fibroblasts express low levels of α-SMA, and accentuated contraction of pads populated with serum or bFGF-stimulated fibroblasts cannot be attributed to increased α-SMA levels (Supplemental Fig. 4, Fig. 4). In order to directly investigate the potential role of α-SMA in mediating collagen pad contraction, we performed α-SMA overexpression experiments. α-SMA-overexpressing cells, cultured in the high-tension environment of the plate exhibited increased α-SMA expression, incorporated into the cytoskeletal stress fibers (Fig. 5A–B). Surprisingly, α-SMA overexpression attenuated contraction in pads populated by unstimulated cells, and did not affect contraction by serum-stimulated fibroblasts (Fig. 5C). Immunofluorescent staining demonstrated that α-SMA-overexpressing fibroblasts in collagen pads exhibited increased cytoplasmic and sub-membrane α-SMA staining, in the absence of localization in stress fibers (Fig. 5D, E).

3.9. In fibroblast-populated collagen pads, α-SMA overexpression attenuates the serum-mediated increase in fibroblast density

In order to examine the basis for the surprising attenuation of pad contraction upon α-SMA overexpression, we studied the morphometric characteristics of α-SMA-overexpressing fibroblasts in pads. Serum stimulation induced a marked increase in cell density; α-SMA overexpression attenuated the serum-mediated increase in fibroblast density (Supplemental Fig. 5A, C). Quantitative morphometric analysis showed that serum stimulation increased mean cell area; α-SMA overexpression attenuated the serum-induced increase in cell size (Supplemental Fig. 5B, D).

3.10. α-SMA overexpression reduces fibroblast proliferative activity, but does not affect apoptosis

Reduced cell density in collagen pads populated with α-SMA overexpressing fibroblasts may be due to attenuated proliferation or increased cell death. In order to investigate the effects of α-SMA overexpression on fibroblast proliferation, we identified proliferating cells using staining for Ki-67. Sections from mouse bowel were used as a positive control (Fig. 6A). Serum stimulation markedly increased the number of proliferating fibroblasts; α-SMA overexpression attenuated serum-mediated fibroblast proliferation (Fig. 6B–C). In order to examine whether α-SMA overexpression affects fibroblast apoptosis we performed TUNEL staining (Fig. 6D). Serum stimulation reduced the number of apoptotic cells in both α-SMA overexpressing and control cells. α-SMA overexpression did not affect the number of apoptotic cells (Fig. 6E–F).

3.11. α-SMA knockdown attenuates contraction in fibroblast-populated collagen pads upon serum stimulation

Next, we examined whether α-SMA knockdown affects contraction of fibroblast-populated collagen pads. siRNA knockdown markedly attenuated expression of α-SMA in fibroblasts (Fig. 7A–C). α-SMA knockdown markedly reduced contraction of pads populated with serum-stimulated cells, suggesting that α-SMA is implicated in serum-induced pad contraction (Fig. 7D).

3.12. α-SMA knockdown increases cell density in serum-stimulated collagen pads

Attenuated serum-mediated contraction in pads populated with α-SMA KD cells occurred despite a significantly increased cell density (Supplemental Fig. 6A, C). α-SMA KD did not affect cell size in unstimulated and serum-stimulated cells (Supplemental Fig. 6B, D).

3.13. α-SMA knockdown accentuates serum-mediated fibroblast proliferation without affecting fibroblast apoptosis

Ki-67 staining showed that α-SMA knockdown increases baseline proliferative activity and accentuates serum-induced proliferation in

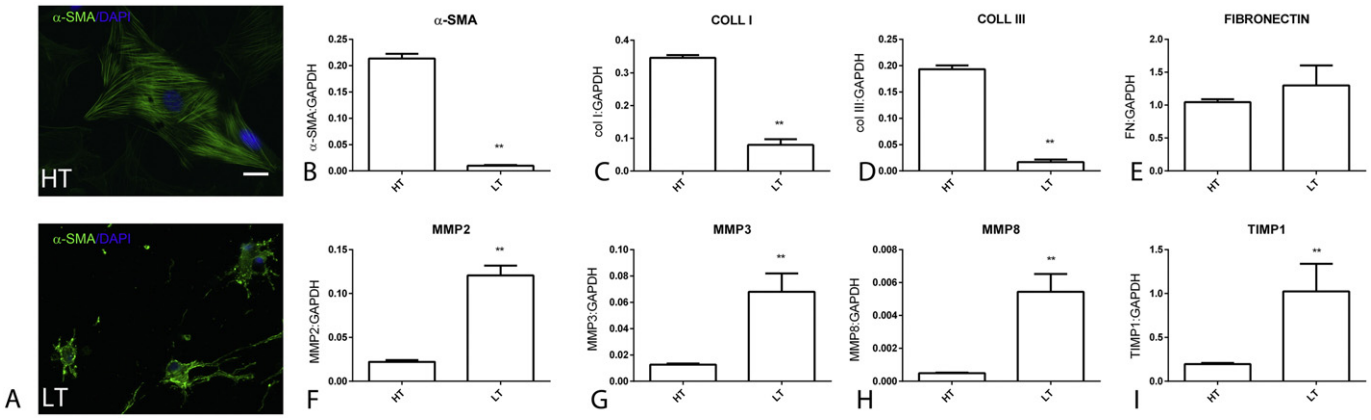

Fig. 2. Comparison of phenotypic characteristics between high-tension (HT) fibroblasts, cultured in plates, and low-tension (LT) fibroblasts after 24 h in collagen pads. A. HT and LT cells were stained for α-SMA. Immunofluorescence shows that HT fibroblasts are large cells with incorporation of α-SMA in the cytoskeleton (scalebar = 10 μm). In contrast, LT cells in collagen pads exhibit low level punctate α-SMA staining (arrows). qPCR analysis shows that HT fibroblasts exhibit markedly higher α-SMA (B), collagen I (C) and III (D) mRNA synthesis. Fibronectin synthesis was comparable between HT and LT cells (E). LT cells in collagen pads exhibited much higher expression of genes associated with matrix metabolism, such as MMP2 (F), MMP3 (G), MMP8 (H) and TIMP1 (I) ($^{**}p < 0.01$, n = 6/group).

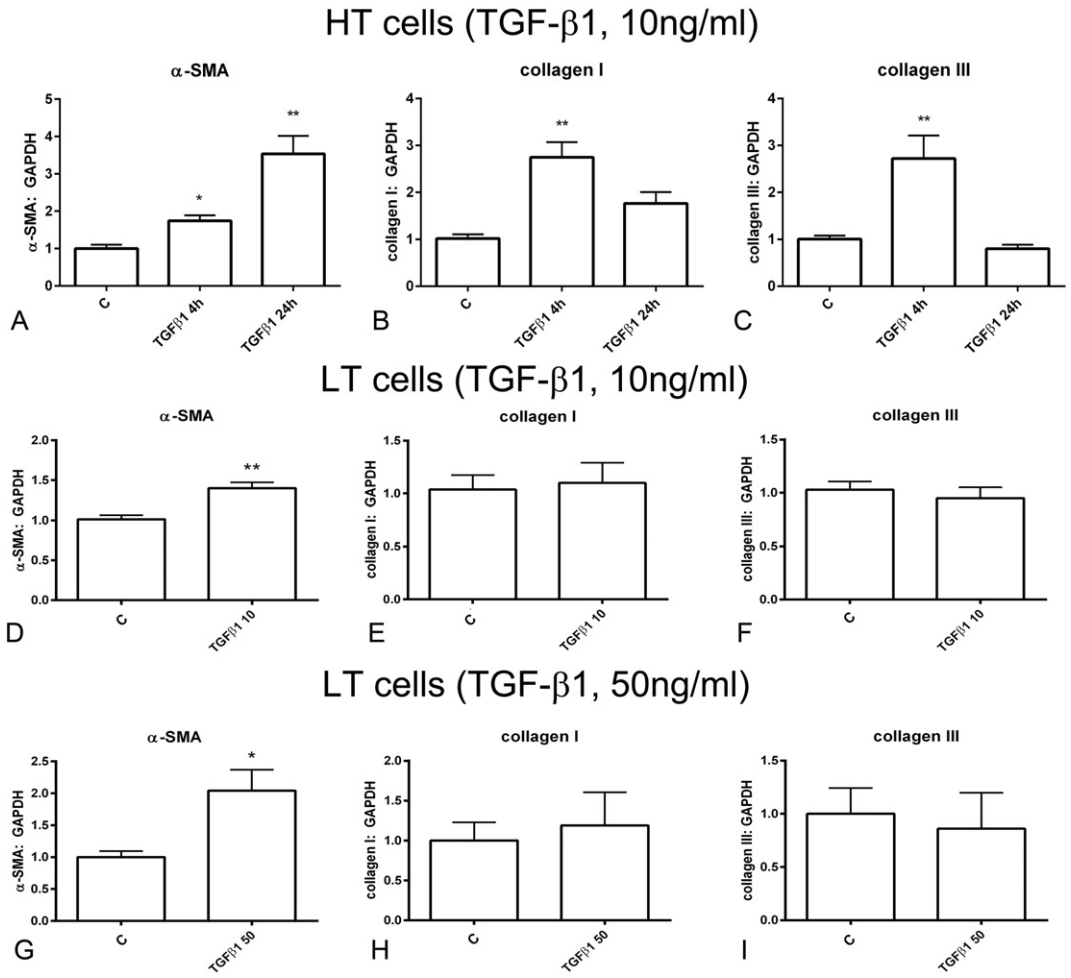

Fig. 3. Effects of TGF-β1 stimulation on α-SMA and collagen synthesis in high-tension fibroblasts (cultured in plates) and in low-tension cardiac fibroblasts (stimulated in collagen pads). A. In high-tension cells, TGF-β1 (10 ng/ml) stimulation for 4–24 h markedly upregulated α-SMA mRNA synthesis. B–C. TGF-β1 also induced a transient upregulation of collagen I (B) and III (C). D–F. In low tension cells, stimulation with low concentration TGF-β1 (10 ng/ml) modestly, but significantly increased α-SMA expression (D), without affecting collagen I (E) and III (F) synthesis. G–I. High concentration TGF-β1 (50 ng/ml) also upregulated α-SMA synthesis (G) in low tension cells without affecting collagen I (H) and III (I) levels ($^{*}p < 0.05$, $^{**}p < 0.01$ vs. C, n = 6–12/group).

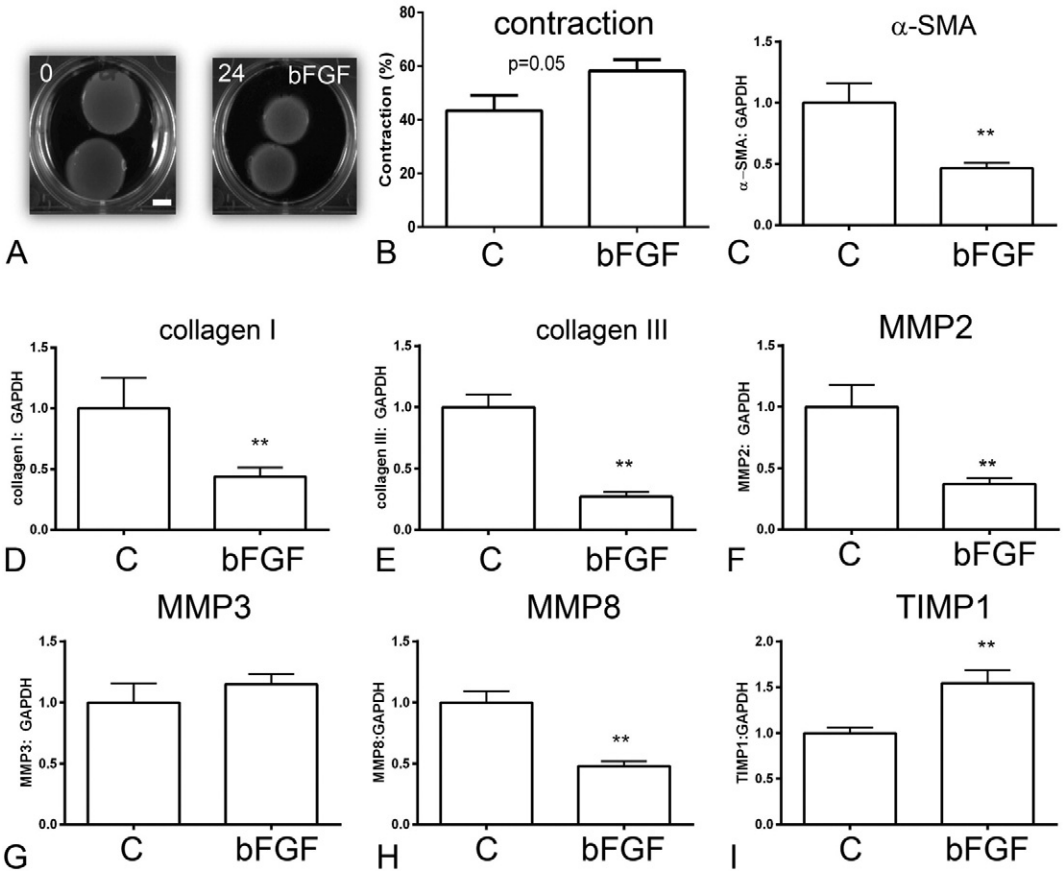

Fig. 4. Effects of bFGF on collagen pad contraction and fibroblast gene expression. A–B. bFGF enhanced contraction of fibroblast-populated collagen pads (scalebar = 5 mm). C. bFGF stimulation reduced α-SMA expression by cardiac fibroblasts. bFGF attenuated collagen I (D) and III (E) synthesis. F. bFGF reduced fibroblast MMP2 expression. G. bFGF did not affect MMP3 synthesis (G), but significantly decreased MMP8 expression by cardiac fibroblasts. I. bFGF accentuated TIMP1 expression (**$p < 0.01$, n = 8–14/group).

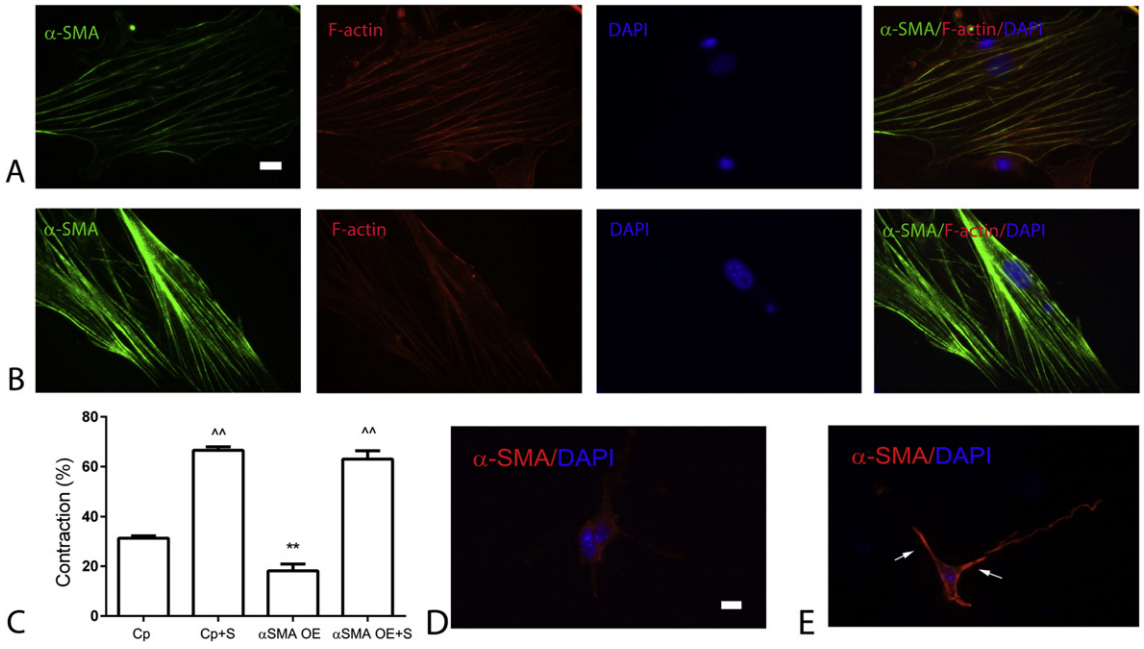

Fig. 5. α-SMA overexpression in cardiac fibroblasts attenuates baseline pad contraction and does not affect serum-stimulated contraction. A. Isolated high-tension fibroblasts were stained for α-SMA, phalloidin (to identify F-actin filaments) and DAPI. B. α-SMA overexpression markedly increased α-SMA expression and incorporation in cytoskeletal stress fibers. C. α-SMA overexpression (OE) attenuated baseline pad contraction, without affecting serum (S)-induced contraction (**$p < 0.01$ vs. control-plasmid (Cp), n = 8–10/group; ^^$p < 0.01$ vs. unstimulated cells). D. In collagen pads, cardiac fibroblasts exhibit low levels of α-SMA immunoreactivity. E. α-SMA-overexpressing cells in collagen pads show high expression of α-SMA with cytoplasmic and sub-membrane localization (arrows) (scalebar = 10 μm).

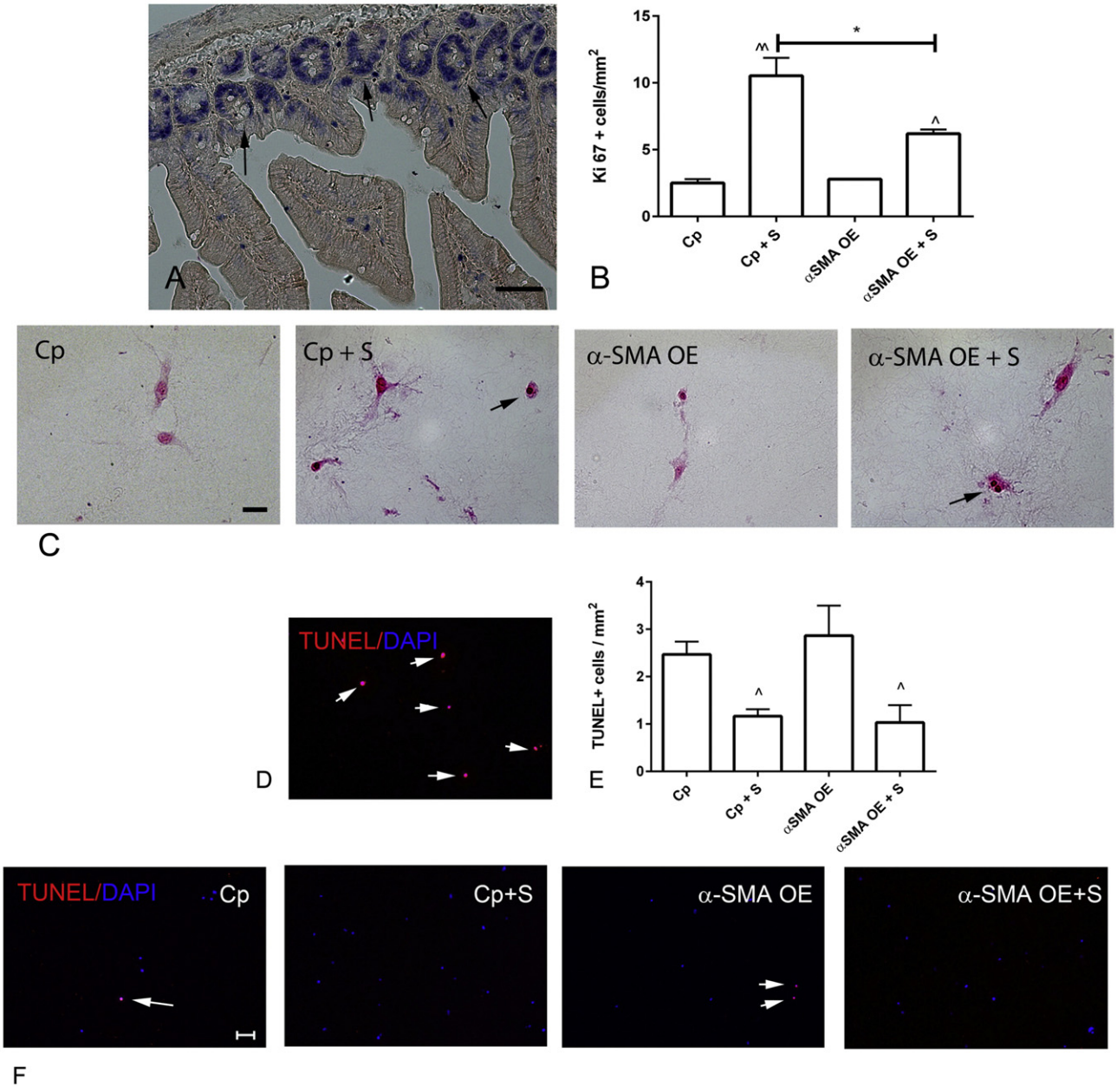

Fig. 6. α-SMA overexpression attenuates fibroblast proliferation, but does not affect apoptosis. A–C. Ki-67 immunohistochemistry was used to identify proliferating cells. A. Sections from the mouse bowel were used as a positive control, identifying proliferating epithelial cells in the base of intestinal crypts (arrows) (scalebar = 50 μm). B–C. Quantitative analysis of the density of Ki-67 + cells in pads showed that serum (S) increased the density of proliferating cells (C-arrows) (^$p < 0.05$, ^^$p < 0.01$ vs. control, *$p < 0.05$; n = 3/group). α-SMA overexpression (OE) did not affect the baseline density of proliferating cells (when compared with control-plasmid (Cp) cells), but attenuated serum-mediated proliferative activity (B- scalebar = 20 μm). D–F. TUNEL staining was used to identify apoptotic cells (scalebar = 50 μm). D. DNAse-treated sections served as a positive control (arrows). Small numbers of apoptotic cells were noted in control collagen pads (E, F - arrows). The density of apoptotic cells was reduced in serum-stimulated pads (^$p < 0.05$ vs. corresponding unstimulated cells, n = 3/group); however, α-SMA overexpression did not affect fibroblast apoptosis.

cardiac fibroblasts (Fig. 8A–B). TUNEL staining showed that α-SMA knockdown does not affect fibroblast apoptosis in control and serum-stimulated fibroblasts (Fig. 8C–D).

4. Discussion

Our study demonstrates that cardiac fibroblasts exhibit dynamic phenotypic alterations in response to their microenvironment. Culture of cardiac myofibroblasts in collagen pads causes disassembly of stress fibers and markedly reduces α-SMA and collagen synthesis, while inducing expression of genes associated with matrix metabolism. Although α-SMA expression in infarct myofibroblasts has been implicated in scar contraction, in free-floating collagen pads, serum and bFGF induce contraction, despite a reduction of α-SMA levels. We also report that α-SMA expression in fibroblasts is not sufficient to induce contraction of free-floating collagen pads, but may modulate proliferative activity. Our findings illustrate the remarkable phenotypic plasticity of cardiac fibroblasts and suggest that α-SMA expression in myofibroblasts may have effects beyond scar contraction.

4.1. The dynamic changes of the fibroblasts in healing infarcts

Following myocardial infarction, alarmins released by dying cardiomyocytes trigger an intense inflammatory reaction that clears the wound from dead cells, while setting the stage for repair [44]. Secretion of inflammatory mediators and growth factors induces

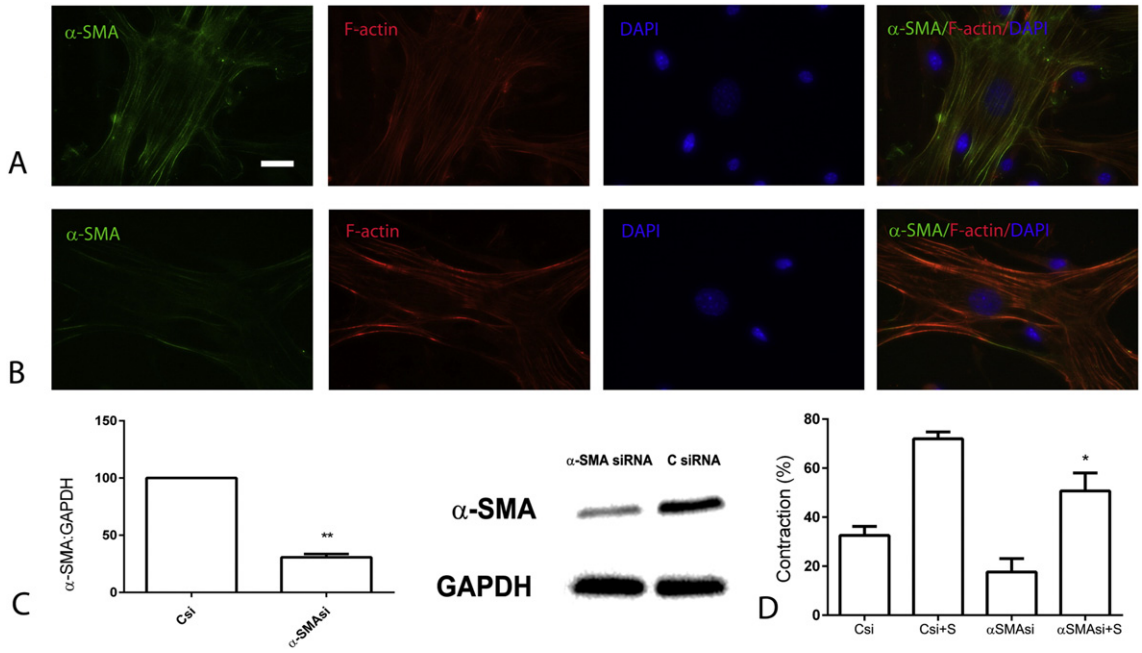

Fig. 7. α-SMA knockdown attenuates serum-mediated collagen pad contraction. siRNA knockdown experiments were performed to examine the role of α-SMA in contraction of fibroblast-populated collagen pads. A–B. α-SMA staining showed that siRNA knockdown markedly reduced α-SMA content in high-tension cardiac fibroblasts (scalebar = 10 μm). C. Western blotting confirmed the reduction of α-SMA expression (**$p < 0.01$ vs., control siRNA, n = 3/group). D. α-SMA knockdown attenuated serum (S)-induced contraction of collagen pads (*$p < 0.05$ vs. Csi + S, n = 3–6/group).

sequential phenotypic alterations in cardiac fibroblasts that contribute to the inflammatory and reparative response. During the early hours after infarction, cardiac fibroblasts may acquire a pro-inflammatory and matrix-degrading phenotype, serving as an important source of cytokines, chemokines and proteases, and mediating leukocyte infiltration [41]. In the inflammatory environment of the infarct, Interleukin (IL)-1 induces MMP expression and reduces fibroblast α-SMA synthesis, delaying myofibroblast transdifferentiation until the wound is cleared from dead cells and matrix debris [41]. Clearance of apoptotic cells and matrix fragments by professional phagocytes is associated with release of anti-inflammatory mediators (such as TGF-β), and with suppression of pro-inflammatory cytokine synthesis. In the infarct border zone, release of bioactive TGF-β co-operates with specialized matrix proteins, triggering conversion of fibroblasts into myofibroblasts [40,45]. Activated myofibroblasts, the main matrix-producing cells in the healing infarct [46], express large amounts of α-SMA (Fig. 1). Because of its abundant expression in infarct myofibroblasts and its known contractile properties, α-SMA has been suggested as a crucial mediator in contraction and remodeling of the healing scar [33].

4.2. Culture in a collagen lattice alters the phenotypic characteristics of cardiac fibroblasts

Mechanical tension and changes in the composition of the surrounding extracellular matrix play important roles in modulating the phenotypic and functional characteristics of fibroblasts [47,48]. Our findings highlight the pronounced effects of the matrix environment on fibroblast phenotype. In culture plates, a large number of cardiac fibroblasts undergo myofibroblast transdifferentiation, forming stress fibers decorated by α-SMA. In contrast, when cardiac fibroblasts are cultured in collagen pads, they acquire a round, or dendritic morphology and express low levels of α-SMA (<5% of the levels in high-tension fibroblasts), exhibiting disassembly of the stress fibers (Fig. 2A–B). Activation of FAK signaling may be implicated in acquisition of a myofibroblast phenotype in cells cultured in plates [49] (Supplemental Fig. 2). In contrast, in the low tension environment of the collagen pad FAK activity is markedly suppressed.

Moreover, pad fibroblasts synthesize much lower amounts of collagen I and III, but exhibit high level synthesis of genes involved in matrix metabolism, such as MMPs and TIMPs (Fig. 2C–I). Thus, high tension fibroblasts resemble activated myofibroblasts in healing infarcts, whereas pad fibroblasts have characteristics similar to the quiescent interstitial populations residing in normal myocardium. The two distinct models of cardiac fibroblast culture provide complementary information regarding the properties of fibroblasts in homeostasis and disease.

4.3. Contraction of fibroblast-populated pads is not associated with increased a-SMA expression

When populated with fibroblasts, collagen pads contract recapitulating scar contraction following myocardial infarction. Collagen pad contraction is accentuated when the cells are stimulated with serum, or with the growth factors TGF-β1 and bFGF (Supplemental Fig. 1, Fig. 4). Known associations between myofibroblast phenotype and contractile activity suggest that increased expression of α-SMA, the predominant contractile protein expressed by myofibroblasts, may be involved in pad contraction [33]. Surprisingly, our findings do not support this notion. Increased pad contraction is not consistently associated with higher levels of α-SMA expression by fibroblasts. Although in TGF-β-stimulated cells, increased α-SMA levels were associated with accentuated pad contraction (Supplemental Fig. 1, Fig. 3), serum and bFGF stimulation induced collagen contraction, despite a significant reduction in α-SMA synthesis (Supplemental Fig. 1, Supplemental Fig. 4, Fig. 4).

4.4. Effects of a-SMA knockdown on contraction of fibroblast-populated pads

In order to directly examine whether α-SMA expression mediates contraction of fibroblast-populated collagen pads, we performed siRNA knockdown experiments. α-SMA knockdown attenuated contraction of serum-stimulated collagen pads (Fig. 7). The finding may reflect loss of early myofibroblast-induced contraction upon α-SMA downmodulation. Before placement in the pads, cardiac myofibroblasts

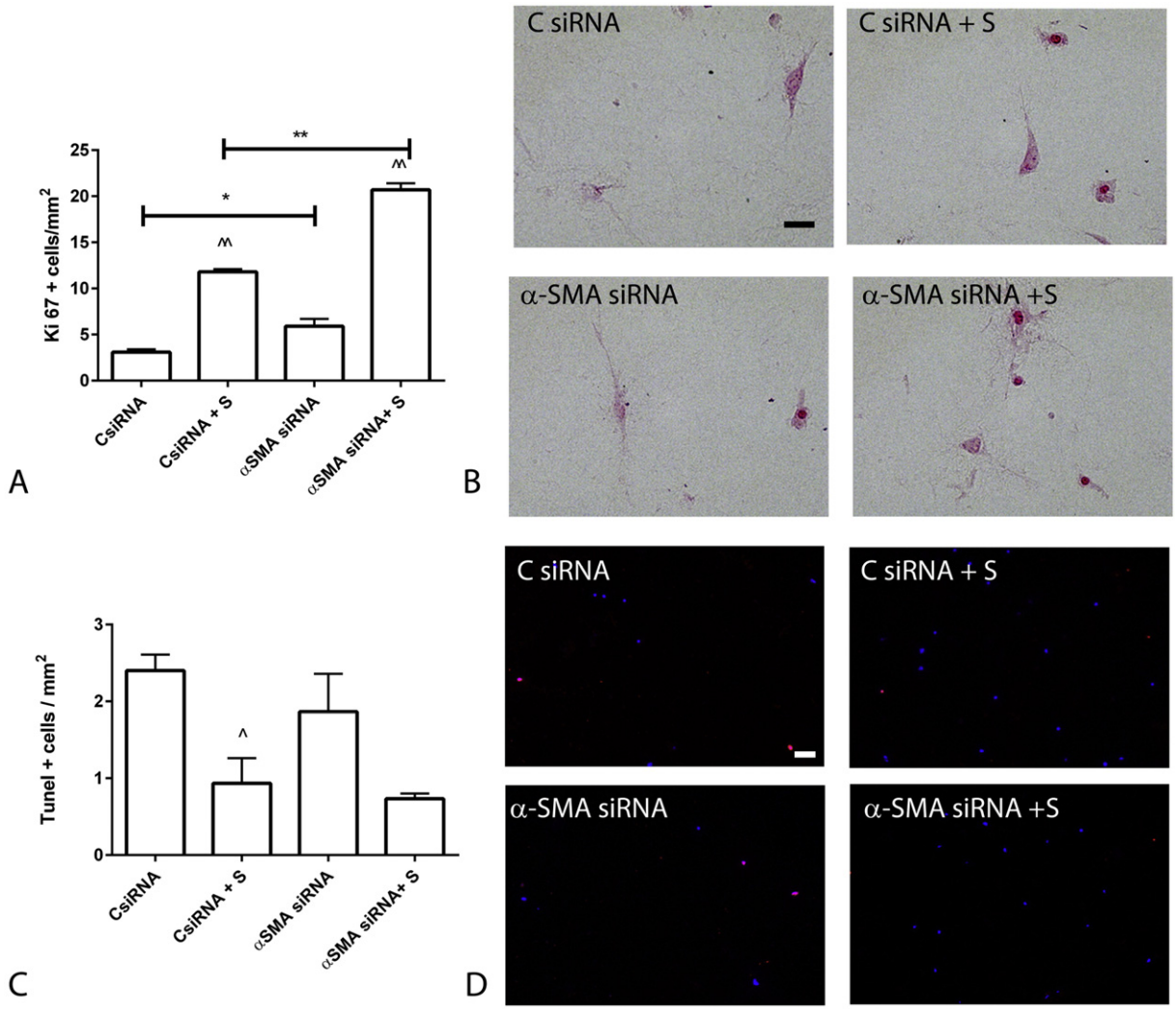

Fig. 8. α-SMA knockdown increased fibroblast proliferation, but had no effects on apoptosis. A–B. Ki-67 staining was used to identify proliferating cells (scalebar = 20 μm). Serum stimulation (S) markedly increased cell proliferation (^^$p < 0.01$ vs. corresponding controls); α-SMA siRNA knockdown accentuated proliferative activity (*$p < 0.05$, **$p < 0.01$ vs. corresponding controls). C–D. TUNEL staining was used to assess apoptosis (scalebar = 50 μm). Serum stimulation decreased the density of apoptotic cells (^$p < 0.05$ vs. control); however α-SMA SiRNA knockdown did not affect fibroblast apoptosis (n = 3–6/group).

exhibit high levels of α-SMA expression that may be responsible for early contraction of the pad, until levels are suppressed in the low tension environment of the collagen lattice. Surprisingly, α-SMA knockdown accentuated proliferative activity, without affecting apoptosis (Fig. 8). Thus, reduced contraction upon α-SMA knockdown occurred despite an increase in the number of cells populating the pad.

4.5. a-SMA overexpression is not sufficient to induce collagen pad contraction, but reduces proliferative activity

We reasoned that, although α-SMA may not be the only factor mediating collagen contraction in fibroblast-populated pads, forced overexpression of α-SMA in fibroblasts may be sufficient to promote contraction. Surprisingly, increased α-SMA expression in cardiac fibroblasts attenuated contraction of collagen pads populated with unstimulated cells, and had no effects on pads containing serum-stimulated fibroblasts (Fig. 5). The failure of α-SMA overexpression to induce contraction may be explained by the absence of α-SMA incorporation into stress fibers in cells populating the pads. In the low tension environment of the collagen pad, fibroblasts do not exhibit stress fibers; overexpressing cells exhibit punctate cytoplasmic and sub-membrane α-SMA localization (Fig. 5D–E) that would not be expected to accentuate contractile force. Our findings suggest that α-SMA overexpression is not sufficient to increase fibroblast-mediated matrix contraction; this process may require expression of other contractile proteins, or activation of signaling pathways necessary for preservation of stress fibers and for incorporation of α-SMA into the stress fibers [50,51]. Moreover, the observed inhibitory effects of α-SMA overexpression on pad contraction may reflect changes in proliferative activity of the cells. Reduced serum-induced fibroblast proliferation in α-SMA-overexpressing cells (Fig. 6) may be responsible, at least in part, for attenuated pad contraction.

4.6. a-SMA as a modulator of fibroblast phenotype

In addition to its known role as a regulator of contractile activity, α-SMA may exert additional actions, modulating pathways critical for cellular responses. Associative studies have suggested that high α-SMA expression may mark a fibroblast subtype with a higher capacity to remodel the extracellular matrix [52]. Whether this is due to direct actions of α-SMA, or represents an epiphenomenon is unclear. Experiments investigating the effects of α-SMA expression on fibroblast migration have produced conflicting results. Lung fibroblasts expressing large amounts of α-SMA exhibited increased migratory activity towards fibronectin [53]. However, other studies demonstrated that fibroblast strains with increased α-SMA expression had reduced migratory

capacity and that α-SMA knockdown increased cell motility [54]. α-SMA has been implicated in activation of mechanosensitive signaling pathways. Filamentous α-SMA activates Mitogen Activated Protein Kinase (MAPK) signaling, and cells overexpressing α-SMA exhibit accentuated tensile force-induced activation of p38 [55]. In embryonic stem cells, α-SMA expression may regulate cell fate [56]. In mesenchymal stromal cells, α-SMA overexpression reduced adipogenic potential by inducing Yes-associated protein (YAP)/transcriptional coactivator with PDZ-binding motif (TAZ) nuclear localization [57]. Because overactive YAP/TAZ signaling is associated with a proliferative phenotype [58], activation of this pathway may not explain our observed effects of α-SMA overexpression on cardiac fibroblast proliferation. The potential significance of cytoplasmic α-SMA expression in the absence of stress fiber localization remains unclear.

4.7. In vivo actions of α-SMA

Information on the role of α-SMA expression by activated myofibroblasts in vivo remains limited. In a model of cutaneous injury, mice with global loss of α-SMA had delayed contraction and immature organization of cutaneous wounds [59]. Whether these defects result from impaired myofibroblast transdifferentiation, or reflect actions of α-SMA in vascular cells and wound angiogenesis or vascular maturation remains unknown. In vivo approaches specifically targeting α-SMA expression in myofibroblasts are needed to dissect the potential role of α-SMA expression in fibroblast activation and function.

Funding sources

Supported by NIH grants R01 HL76246 and R01 HL85440, grants from the Department of Defense Congressionally-directed medical research programs (CDMRP grants PR151134 and PR151029) (Dr Frangogiannis), and by an American Heart Association (AHA) Founders' affiliate post-doctoral award (Dr Shinde) (Award #14POST20140028).

Disclosures

None.

Transparency document

The Transparency document associated with this article can be found, in the online version.

Appendix A. Supplementary data

Supplementary data to this article can be found online at http://dx.doi.org/10.1016/j.bbadis.2016.11.006.

References

[1] G. Gabbiani, G. Majno, Dupuytren's contracture: fibroblast contraction? An ultrastructural study, Am. J. Pathol. 66 (1972) 131–146.
[2] G. Gabbiani, M. Le Lous, A.J. Bailey, S. Bazin, A. Delaunay, Collagen and myofibroblasts of granulation tissue. A chemical, ultrastructural and immunologic study, Virchows Arch. B Cell Pathol. 21 (1976) 133–145.
[3] G. Gabbiani, The myofibroblast in wound healing and fibrocontractive diseases, J. Pathol. 200 (2003) 500–503.
[4] B. Hinz, Formation and function of the myofibroblast during tissue repair, J. Invest. Dermatol. 127 (2007) 526–537.
[5] J. Davis, J.D. Molkentin, Myofibroblasts: trust your heart and let fate decide, J. Mol. Cell. Cardiol. 70 (2014) 9–18.
[6] J.J. Tomasek, G. Gabbiani, B. Hinz, C. Chaponnier, R.A. Brown, Myofibroblasts and mechano-regulation of connective tissue remodelling, Nat. Rev. Mol. Cell Biol. 3 (2002) 349–363.
[7] B. Hinz, Myofibroblasts, Exp. Eye Res. 142 (2016) 56–70.
[8] I.A. Darby, N. Zakuan, F. Billet, A. Desmouliere, The myofibroblast, a key cell in normal and pathological tissue repair, Cell. Mol. Life Sci. 73 (2016) 1145–1157.
[9] A. Deb, E. Ubil, Cardiac fibroblast in development and wound healing, J. Mol. Cell. Cardiol. 70 (2014) 47–55.
[10] F. Grinnell, Fibroblasts, myofibroblasts, and wound contraction, J. Cell Biol. 124 (1994) 401–404.
[11] J.G. Travers, F.A. Kamal, J. Robbins, K.E. Yutzey, B.C. Blaxall, Cardiac fibrosis: the fibroblast awakens, Circ. Res. 118 (2016) 1021–1040.
[12] P. Kong, P. Christia, N.G. Frangogiannis, The pathogenesis of cardiac fibrosis, Cell. Mol. Life Sci. 71 (2014) 549–574.
[13] N.A. Turner, K.E. Porter, Function and fate of myofibroblasts after myocardial infarction, Fibrogenesis Tissue Repair 6 (2013) 5.
[14] C.A. Souders, S.L. Bowers, T.A. Baudino, Cardiac fibroblast: the renaissance cell, Circ. Res. 105 (2009) 1164–1176.
[15] R. Zak, Development and proliferative capacity of cardiac muscle cells, Circ. Res. 35 (Suppl. II) (1974) 17–26.
[16] A.R. Pinto, A. Ilinykh, M.J. Ivey, J.T. Kuwabara, M.L. D'Antoni, R. Debuque, A. Chandran, L. Wang, K. Arora, N.A. Rosenthal, M.D. Tallquist, Revisiting cardiac cellular composition, Circ. Res. 118 (2016) 400–409.
[17] I.E. Willems, M.G. Havenith, J.G. De Mey, M.J. Daemen, The alpha-smooth muscle actin-positive cells in healing human myocardial scars, Am. J. Pathol. 145 (1994) 868–875.
[18] N.G. Frangogiannis, L.H. Michael, M.L. Entman, Myofibroblasts in reperfused myocardial infarcts express the embryonic form of smooth muscle myosin heavy chain (SMemb), Cardiovasc. Res. 48 (2000) 89–100.
[19] R. Vracko, D. Thorning, Contractile cells in rat myocardial scar tissue, Lab. Investig. 65 (1991) 214–227.
[20] A.V. Shinde, N.G. Frangogiannis, Fibroblasts in myocardial infarction: a role in inflammation and repair, J. Mol. Cell. Cardiol. 70C (2014) 74–82.
[21] N.G. Frangogiannis, The inflammatory response in myocardial injury, repair, and remodelling, Nat. Rev. Cardiol. 11 (2014) 255–265.
[22] R.H. Cunnington, J.M. Northcott, S. Ghavami, K.L. Filomeno, F. Jahan, M.S. Kavosh, J.J. Davies, J.T. Wigle, I.M. Dixon, The Ski-Zeb2-Meox2 pathway provides a novel mechanism for regulation of the cardiac myofibroblast phenotype, J. Cell Sci. 127 (2014) 40–49.
[23] E.C. Flack, M.L. Lindsey, C.E. Squires, B.S. Kaplan, R.E. Stroud, L.L. Clark, P.G. Escobar, W.M. Yarbrough, F.G. Spinale, Alterations in cultured myocardial fibroblast function following the development of left ventricular failure, J. Mol. Cell. Cardiol. 40 (2006) 474–483.
[24] C.E. Squires, G.P. Escobar, J.F. Payne, R.A. Leonardi, D.K. Goshorn, N.J. Sheats, I.M. Mains, J.T. Mingoia, E.C. Flack, M.L. Lindsey, Altered fibroblast function following myocardial infarction, J. Mol. Cell. Cardiol. 39 (2005) 699–707.
[25] M. Bujak, M. Dobaczewski, C. Gonzalez-Quesada, Y. Xia, T. Leucker, P. Zymek, V. Veeranna, A.M. Tager, A.D. Luster, N.G. Frangogiannis, Induction of the CXC chemokine interferon-gamma-inducible protein 10 regulates the reparative response following myocardial infarction, Circ. Res. 105 (2009) 973–983.
[26] H. Lal, F. Ahmad, J. Zhou, J.E. Yu, R.J. Vagnozzi, Y. Guo, D. Yu, E.J. Tsai, J. Woodgett, E. Gao, T. Force, Cardiac fibroblast GSK-3beta regulates ventricular remodeling and dysfunction in ischemic heart, Circulation. (2014).
[27] M.R. Zeglinski, J.J. Davies, S. Ghavami, S.G. Rattan, A.J. Halayko, I.M. Dixon, Chronic expression of ski induces apoptosis and represses autophagy in cardiac myofibroblasts, Biochim. Biophys. Acta 1863 (2016) 1261–1268.
[28] R. Vivar, C. Humeres, C. Munoz, P. Boza, S. Bolivar, F. Tapia, S. Lavandero, M. Chiong, G. Diaz-Araya, FoxO1 mediates TGF-beta1-dependent cardiac myofibroblast differentiation, Biochim. Biophys. Acta 1863 (2016) 128–138.
[29] E. Ubil, J. Duan, I.C. Pillai, M. Rosa-Garrido, Y. Wu, F. Bargiacchi, Y. Lu, S. Stanbouly, J. Huang, M. Rojas, T.M. Vondriska, E. Stefani, A. Deb, Mesenchymal-endothelial transition contributes to cardiac neovascularization, Nature 514 (2014) 585–590.
[30] P. Lijnen, V. Petrov, R. Fagard, Transforming growth factor-beta 1-mediated collagen gel contraction by cardiac fibroblasts, J. Renin-Angiotensin-Aldosterone Syst. 4 (2003) 113–118.
[31] J.M. Carthy, F.S. Garmaroudi, Z. Luo, B.M. McManus, Wnt3a induces myofibroblast differentiation by upregulating TGF-beta signaling through SMAD2 in a beta-catenin-dependent manner, PLoS One 6 (2011), e19809.
[32] O. Frunza, I. Russo, A. Saxena, A.V. Shinde, C. Humeres, W. Hanif, V. Rai, Y. Su, N.G. Frangogiannis, Myocardial Galectin-3 expression is associated with remodeling of the pressure-overloaded heart and may delay the hypertrophic response without affecting survival, dysfunction, and cardiac fibrosis, Am. J. Pathol. 186 (2016) 1114–1127.
[33] B. Hinz, G. Celetta, J.J. Tomasek, G. Gabbiani, C. Chaponnier, Alpha-smooth muscle actin expression upregulates fibroblast contractile activity, Mol. Biol. Cell 12 (2001) 2730–2741.
[34] B. Hinz, V. Dugina, C. Ballestrem, B. Wehrle-Haller, C. Chaponnier, Alpha-smooth muscle actin is crucial for focal adhesion maturation in myofibroblasts, Mol. Biol. Cell 14 (2003) 2508–2519.
[35] L.K. Wrobel, T.R. Fray, J.E. Molloy, J.J. Adams, M.P. Armitage, J.C. Sparrow, Contractility of single human dermal myofibroblasts and fibroblasts, Cell Motil. Cytoskeleton 52 (2002) 82–90.
[36] W. Chen, N.G. Frangogiannis, Fibroblasts in post-infarction inflammation and cardiac repair, Biochim. Biophys. Acta 1833 (2013) 945–953.
[37] W. Chen, A. Saxena, N. Li, J. Sun, A. Gupta, D.W. Lee, Q. Tian, M. Dobaczewski, N.G. Frangogiannis, Endogenous IRAK-M attenuates postinfarction remodeling through effects on macrophages and fibroblasts, Arterioscler. Thromb. Vasc. Biol. 32 (2012) 2598–2608.
[38] A. Saxena, A.V. Shinde, Z. Haque, Y.J. Wu, W. Chen, Y. Su, N.G. Frangogiannis, The role of Interleukin Receptor Associated Kinase (IRAK)-M in regulation of myofibroblast phenotype in vitro, and in an experimental model of non-reperfused myocardial infarction, J. Mol. Cell. Cardiol. 89 (2015) 223–231.

[39] P. Christia, M. Bujak, C. Gonzalez-Quesada, W. Chen, M. Dobaczewski, A. Reddy, N.G. Frangogiannis, Systematic characterization of myocardial inflammation, repair, and remodeling in a mouse model of reperfused myocardial infarction, J. Histochem. Cytochem. 61 (2013) 555–570.
[40] M. Dobaczewski, M. Bujak, N. Li, C. Gonzalez-Quesada, L.H. Mendoza, X.F. Wang, N.G. Frangogiannis, Smad3 signaling critically regulates fibroblast phenotype and function in healing myocardial infarction, Circ. Res. 107 (2010) 418–428.
[41] A. Saxena, W. Chen, Y. Su, V. Rai, O.U. Uche, N. Li, N.G. Frangogiannis, IL-1 induces proinflammatory leukocyte infiltration and regulates fibroblast phenotype in the infarcted myocardium, J. Immunol. 191 (2013) 4838–4848.
[42] A. Leask, Focal adhesion kinase: a key mediator of transforming growth factor beta signaling in fibroblasts, Adv. Wound Care (New Rochelle) 2 (2013) 247–249.
[43] D. Lagares, O. Busnadiego, R.A. Garcia-Fernandez, M. Kapoor, S. Liu, D.E. Carter, D. Abraham, X. Shi-Wen, P. Carreira, B.A. Fontaine, B.S. Shea, A.M. Tager, A. Leask, S. Lamas, F. Rodriguez-Pascual, Inhibition of focal adhesion kinase prevents experimental lung fibrosis and myofibroblast formation, Arthritis Rheum. 64 (2012) 1653–1664.
[44] J. Lugrin, R. Parapanov, N. Rosenblatt-Velin, S. Rignault-Clerc, F. Feihl, B. Waeber, O. Muller, C. Vergely, M. Zeller, A. Tardivel, P. Schneider, P. Pacher, L. Liaudet, Cutting edge: IL-1alpha is a crucial danger signal triggering acute myocardial inflammation during myocardial infarction, J. Immunol. 194 (2015) 499–503.
[45] F. Arslan, M.B. Smeets, P.W. Riem Vis, J.C. Karper, P.H. Quax, L.G. Bongartz, J.H. Peters, I.E. Hoefer, P.A. Doevendans, G. Pasterkamp, D.P. de Kleijn, Lack of fibronectin-EDA promotes survival and prevents adverse remodeling and heart function deterioration after myocardial infarction, Circ. Res. 108 (2011) 582–592.
[46] J.P. Cleutjens, M.J. Verluyten, J.F. Smiths, M.J. Daemen, Collagen remodeling after myocardial infarction in the rat heart, Am. J. Pathol. 147 (1995) 325–338.
[47] M. Dobaczewski, J.J. de Haan, N.G. Frangogiannis, The extracellular matrix modulates fibroblast phenotype and function in the infarcted myocardium, J. Cardiovasc. Transl. Res. 5 (2012) 837–847.
[48] Y. Xia, M. Dobaczewski, C. Gonzalez-Quesada, W. Chen, A. Biernacka, N. Li, D.W. Lee, N.G. Frangogiannis, Endogenous thrombospondin 1 protects the pressure-overloaded myocardium by modulating fibroblast phenotype and matrix metabolism, Hypertension 58 (2011) 902–911.
[49] V.J. Thannickal, D.Y. Lee, E.S. White, Z. Cui, J.M. Larios, R. Chacon, J.C. Horowitz, R.M. Day, P.E. Thomas, Myofibroblast differentiation by transforming growth factor-beta1 is dependent on cell adhesion and integrin signaling via focal adhesion kinase, J. Biol. Chem. 278 (2003) 12384–12389.
[50] S.D. Varney, C.B. Betts, R. Zheng, L. Wu, B. Hinz, J. Zhou, L. Van De Water, Hic-5 is required for myofibroblast differentiation by regulating mechanically dependent MRTF-A nuclear accumulation, J. Cell Sci. 129 (2016) 774–787.
[51] S. Anderson, L. DiCesare, I. Tan, T. Leung, N. SundarRaj, Rho-mediated assembly of stress fibers is differentially regulated in corneal fibroblasts and myofibroblasts, Exp. Cell Res. 298 (2004) 574–583.
[52] P.D. Arora, C.A. McCulloch, Dependence of collagen remodelling on alpha-smooth muscle actin expression by fibroblasts, J. Cell. Physiol. 159 (1994) 161–175.
[53] M. Kawamoto, T. Matsunami, R.F. Ertl, Y. Fukuda, M. Ogawa, J.R. Spurzem, N. Yamanaka, S.I. Rennard, Selective migration of alpha-smooth muscle actin-positive myofibroblasts toward fibronectin in the Boyden's blindwell chamber, Clin. Sci. (Lond.) 93 (1997) 355–362.
[54] L. Ronnov-Jessen, O.W. Petersen, A function for filamentous alpha-smooth muscle actin: retardation of motility in fibroblasts, J. Cell Biol. 134 (1996) 67–80.
[55] J. Wang, J. Fan, C. Laschinger, P.D. Arora, A. Kapus, A. Seth, C.A. McCulloch, Smooth muscle actin determines mechanical force-induced p38 activation, J. Biol. Chem. 280 (2005) 7273–7284.
[56] S. Clement, M. Stouffs, E. Bettiol, S. Kampf, K.H. Krause, C. Chaponnier, M. Jaconi, Expression and function of alpha-smooth muscle actin during embryonic-stem-cell-derived cardiomyocyte differentiation, J. Cell Sci. 120 (2007) 229–238.
[57] N.P. Talele, J. Fradette, J.E. Davies, A. Kapus, B. Hinz, Expression of alpha-smooth muscle actin determines the fate of mesenchymal stromal cells, Stem Cell Rep. 4 (2015) 1016–1030.
[58] F. Liu, D. Lagares, K.M. Choi, L. Stopfer, A. Marinkovic, V. Vrbanac, C.K. Probst, S.E. Hiemer, T.H. Sisson, J.C. Horowitz, I.O. Rosas, L.E. Fredenburgh, C. Feghali-Bostwick, X. Varelas, A.M. Tager, D.J. Tschumperlin, Mechanosignaling through YAP and TAZ drives fibroblast activation and fibrosis, Am. J. Phys. Lung Cell. Mol. Phys. 308 (2015) L344–L357.
[59] M.M. Ibrahim, L. Chen, J.E. Bond, M.A. Medina, L. Ren, G. Kokosis, A.M. Selim, H. Levinson, Myofibroblasts contribute to but are not necessary for wound contraction, Lab. Investig. 95 (2015) 1429–1438.

The extracellular matrix in myocardial injury, repair, and remodeling

Nikolaos G. Frangogiannis

Wilf Family Cardiovascular Research Institute, Department of Medicine (Cardiology), Albert Einstein College of Medicine, New York, New York, USA.

The cardiac extracellular matrix (ECM) not only provides mechanical support, but also transduces essential molecular signals in health and disease. Following myocardial infarction, dynamic ECM changes drive inflammation and repair. Early generation of bioactive matrix fragments activates proinflammatory signaling. The formation of a highly plastic provisional matrix facilitates leukocyte infiltration and activates infarct myofibroblasts. Deposition of matricellular proteins modulates growth factor signaling and contributes to the spatial and temporal regulation of the reparative response. Mechanical stress due to pressure and volume overload and metabolic dysfunction also induce profound changes in ECM composition that contribute to the pathogenesis of heart failure. This manuscript reviews the role of the ECM in cardiac repair and remodeling and discusses matrix-based therapies that may attenuate remodeling while promoting repair and regeneration.

Introduction

The mammalian myocardium comprises cardiomyocytes and large populations of interstitial noncardiomyocytes (1) enmeshed within an intricate network of extracellular matrix (ECM) proteins. In health, the cardiac ECM does not simply serve as a mechanical scaffold, but may also transduce signals that are important for cell survival and function. Most cardiac pathologic conditions are associated with expansion of the cardiac interstitial matrix and with marked alterations in its composition (2, 3); these changes perturb cardiac systolic and diastolic function. In myocardial infarction, sudden death of up to a billion cardiomyocytes overwhelms the extremely limited regenerative capacity of the adult mammalian heart. As a result, the infarcted ventricle heals through activation of a superbly orchestrated cellular response that clears the wound of dead cells and matrix debris, ultimately leading to formation of a collagen-based scar (4). In conditions associated with pressure or volume overload, dynamic alterations in the ECM network may affect cardiomyocyte survival and may regulate the response of interstitial cells to mechanical stress. Metabolic diseases are also associated with profound alterations in the composition of the cardiac ECM that contribute to the pathogenesis of diastolic dysfunction and may suppress the myocardial reparative reserve. Despite increased recognition of its role in mediating cell biological responses, the contribution of the ECM in cardiac pathophysiology remains underappreciated. This Review discusses the dynamic alterations of the ECM following cardiac injury and their contribution to cardiac remodeling and function.

The ECM network in the normal mammalian heart

The myocardial matrix network comprises primarily fibrillary collagen that is organized on three interconnected levels: the endomysium surrounds individual cardiomyocytes, the perimysium defines major bundles, and the epimysium encases the entire cardiac muscle (5, 6). In all mammalian species studied to date, type I collagen is the major structural component of the cardiac interstitium, accounting for approximately 85% to 90% of the collagenous matrix (7), and is predominantly localized in the epimysium and perimysium. In contrast, type III collagen represents 5% to 11% of total myocardial collagen and is more prominent in the endomysium (7–9). In addition to collagens, the cardiac ECM also contains fibronectin, glycosaminoglycans, and proteoglycans, and it serves as a reservoir for growth factors and proteases, which are stored in the normal matrix and can be activated following injury. Although the role of the matrix network in providing structural support, preserving ventricular geometry, and facilitating force transmission is intuitive, the collagen-based cardiac matrix also transduces key signals necessary for survival and function of both cardiomyocytes and noncardiomyocytes. The molecular pathways responsible for the interactions between matrix proteins and the cellular elements in normal hearts remain poorly understood.

Alterations of the ECM network following myocardial infarction

Repair of the infarcted myocardium can be divided into three distinct but overlapping phases: the inflammatory phase, the proliferative phase, and the maturation phase (10). In all three phases of infarct healing, the dynamic changes in the composition of the ECM play a critical role in regulation of the cellular responses that mediate cardiac repair (11). During the inflammatory phase, early degradation of matrix proteins generates bioactive fragments (termed matrikines) that may contribute to activation of inflammatory and reparative cascades (Figure 1). Moreover, formation of a provisional matrix network derived from extravasated plasma proteins serves as a highly plastic conduit for infiltrating inflammatory cells. Removal of dead cells and matrix debris by professional phagocytes induces release of antiinflammatory mediators, marking the transition to the proliferative phase of cardiac repair. At this stage, the ECM is enriched through induction and deposition of matricellular

Conflict of interest: The author has declared that no conflict of interest exists.
Reference information: *J Clin Invest.* 2017;127(5):1600–1612.
https://doi.org/10.1172/JCI87491.

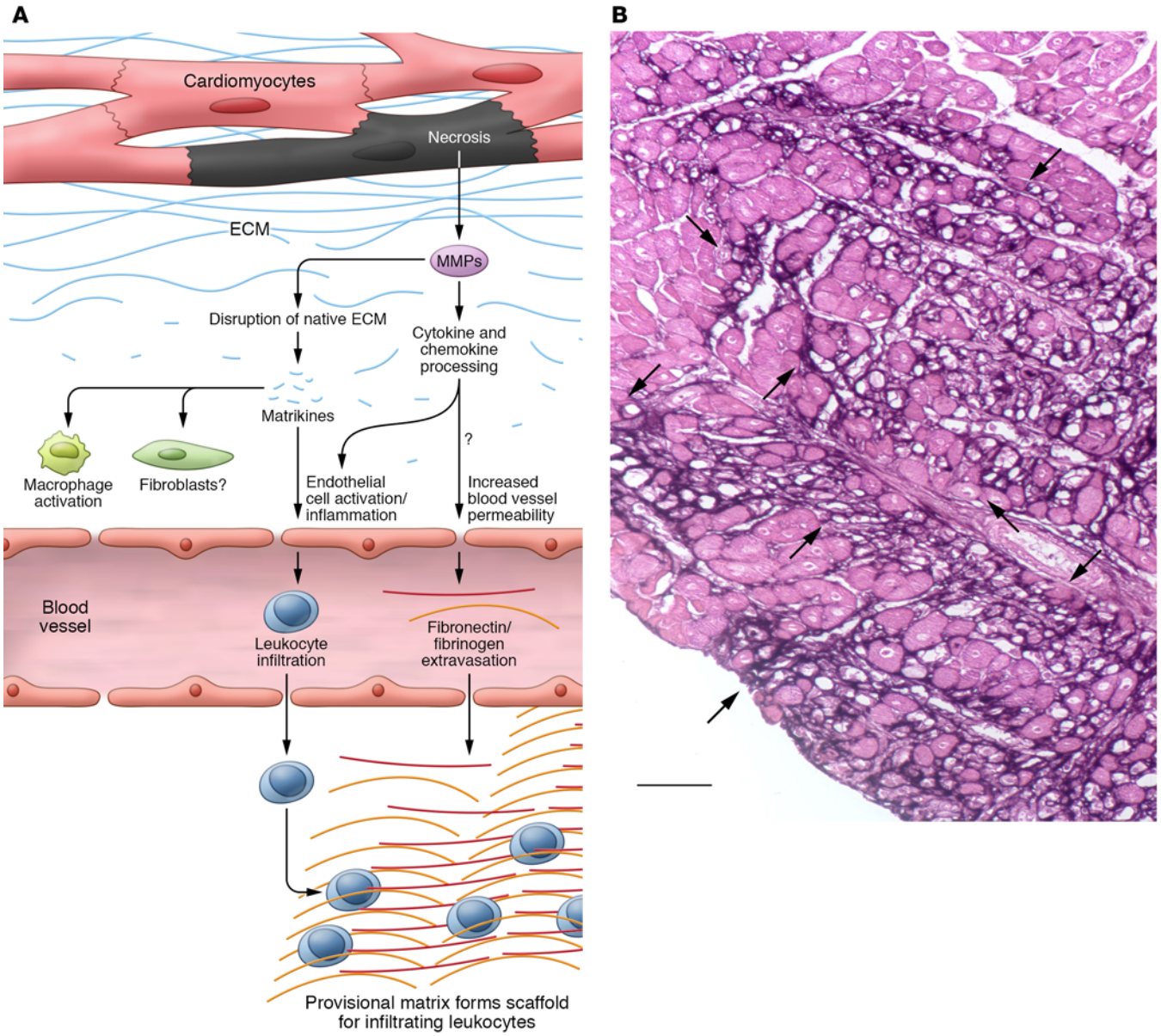

Figure 1. The ECM during the inflammatory phase of cardiac repair. (**A**) Cardiomyocyte necrosis is associated with induction and activation of proteases in the infarcted region. Activated proteases cause fragmentation of the native ECM, resulting in release of matrikines, bioactive peptides that activate an inflammatory macrophage phenotype and may also modulate responses of fibroblasts and vascular endothelial cells. The effects of MMPs in the ischemic and infarcted myocardium are not limited to the ECM. MMPs may modulate inflammatory and reparative responses by processing cytokines and chemokines. They may also inhibit chemokine actions by degrading glycosaminoglycan-binding sites and mediate dysfunction by targeting intracellular proteins. Increased vessel permeability in the infarcted region results in extravasation of plasma proteins, such as fibrinogen and fibronectin. Accumulation of these proteins in the infarcted region forms a provisional matrix that serves as a scaffold for infiltrating leukocytes. Fibrin and fibronectin modulate the phenotype of immune and reparative cells through integrin-mediated actions. (**B**) Fibrinogen/fibrin staining using a peroxidase-based technique (black) illustrates the formation of the provisional fibrin-based matrix network (indicated by arrows) in the infarcted canine myocardium (one hour ischemia followed by seven days reperfusion). Counterstained with eosin. Scale bar: 50 μm. Reproduced with permission from the *FASEB Journal* (155).

proteins, defined as extracellular macromolecules that do not serve a primary structural role, but modulate cellular phenotype, activate proteases and growth factors, and transduce signaling cascades (12, 13). Activated myofibroblasts are the dominant cells during the proliferative phase of cardiac repair and deposit large amounts of structural ECM proteins. Finally, during the maturation phase, crosslinking of the ECM, fibroblast quiescence, and vascular maturation lead to formation of a stable collagen-based scar.

ECM during the inflammatory phase of cardiac repair

Activation of matrix metalloproteinases. Myocardial ischemia causes rapid activation of latent matrix metalloproteinases (MMPs) and subsequent generation of matrix fragments (14, 15). MMP activation is detected in the cardiac interstitium as early as ten minutes after coronary occlusion (16), before any evidence of irreversible cardiomyocyte injury, and may be driven by ischemia-

mediated ROS generation (17). Cardiomyocyte necrosis accentuates the matrix-degrading response. Large amounts of MMPs are synthesized de novo by ischemic cardiomyocytes, fibroblasts, endothelial cells, and inflammatory leukocytes that infiltrate the infarct (18). Both collagenases (e.g., MMP1) and gelatinases (MMP2 and MMP9) are upregulated in the infarcted myocardium (19).

It should be emphasized that the actions of MMPs are not limited to effects on the ECM. MMPs regulate inflammatory responses through proteolytic processing of cytokines, chemokines, and growth factors (20–24) or by degrading glycosaminoglycan binding sites, thus interfering with a molecular step that is critical for chemokine immobilization on the endothelial cell surface and subsequent interaction with leukocytes (25). MMPs also have intracellular targets, degrading cardiomyocyte proteins, such as myosin, α-actinin, and titin (26–28). The relative significance of the matrix-independent actions of MMPs in the pathogenesis of ischemic dysfunction and postinfarction remodeling remains unknown.

Generation of matrikines. In injured and remodeling tissues, protease-mediated fragmentation of matrix proteins results in generation of matrikines (29–32). Elastin fragments and collagen-derived peptides are the best-studied matrikines and have been implicated in activation of immune cells and fibroblasts (29, 33). The collagen-derived tripeptide proline-glycine-proline (PGP) and its acetylated form have been demonstrated as acting as neutrophil chemoattractants in models of pulmonary inflammation, signaling through activation of the chemokine receptor CXCR2 (34). PGP generation requires activation of a multistep cascade that involves MMP8, MMP9, and prolyl endopeptidase (35). Proteolytic processing of laminins by MMP2 and MMP14 has also been demonstrated as yielding fragments with potent neutrophil chemoattractant properties (36).

Although the rapid activation of MMPs in the infarct is associated with matrix fragmentation, the role of these fragments as bioactive proinflammatory matrikines has not been documented. In experimental models, release of type I collagen fragments in the serum has been documented within 30 minutes after coronary occlusion (37). Fragmentation of components of the basement membrane, such as collagen IV, and of noncollagenous matrix constituents has also been demonstrated in the infarcted myocardium (38–41). Low–molecular weight hyaluronan fragments exert potent proinflammatory actions in the infarcted region; impaired clearance of these fragments has been shown to prolong and accentuate proinflammatory signaling in leukocytes and vascular cells (42, 43). Matrix fragments may also modulate fibroblast and vascular cell phenotype (44). Endostatin, a 20-kDa fragment of collagen XVIII, exerts potent angiostatic actions (45) and stimulates fibroblast proliferation (46). MMP9-mediated cleavage of collagen IV also generates fragments with angiostatic properties, such as tumstatin (47). The role of endogenous matrix fragments in regulation of fibrogenic and angiogenic responses following myocardial infarction remains poorly understood.

The plasma-derived provisional matrix regulates the inflammatory response. Degradation of the original cardiac matrix network in the infarcted myocardium is accompanied by formation of a provisional matrix (39). Rapid induction of VEGF in the infarcted heart increases vascular permeability (48), leading to extravasation of plasma fibrinogen and fibronectin and generating a complex and dynamic fibrin-based matrix network (39, 49). The role of the provisional matrix in regulating cardiac repair remains poorly understood; current concepts are predominantly based on extrapolation of findings from studies that investigate reparative responses in other systems. In addition to its hemostatic role, the provisional matrix may serve as a scaffold for migrating inflammatory cells and support proliferating endothelial cells and fibroblasts (50). Components of the provisional matrix interact with migrating cells through cell surface integrins (51) and may also transduce signaling cascades that modulate immune cell phenotype and gene expression (52). In vitro, fibrinogen stimulates macrophage-derived chemokine secretion through TLR4 activation (53).

In a mouse model of reperfused myocardial infarction, fibrin-mediated interactions contributed to early injury by accentuating the inflammatory response (54). Treatment with a naturally occurring peptide that competes with the fibrin fragment N-terminal disulfide knot-II (an analog of the fibrin E1 fragment) for binding to vascular endothelial cadherin reduced infarct size, attenuating leukocyte infiltration in the ischemic myocardium in both rodent and large animal models (54, 55). Unfortunately, the effects of the peptide in a small clinical trial were much less impressive. Peptide administration in patients with ST-elevation myocardial infarction (STEMI) did not affect the size of the infarct assessed through magnetic resonance imaging and did not reduce serum troponin I levels (56).

The provisional matrix may also play an important role in the transition to the proliferative phase of cardiac repair by serving as a reservoir for cytokines and growth factors. The heparin-binding domain of fibrin binds to a wide range of growth factors, including members of the PDGF, FGF, VEGF, and TGF families (57), that may activate reparative fibroblasts and vascular cells.

ECM during the proliferative phase of infarct healing

Dynamic changes in the composition of the ECM may contribute to the reparative cellular responses during the proliferative phase of cardiac repair (Figure 2). Clearance of matrix fragments by phagocytes may activate antiinflammatory signals, suppressing recruitment of proinflammatory leukocytes. Lysis of the plasma-derived provisional matrix is followed by organization of a cell-derived matrix network, comprising cellular fibronectin, hyaluronan, proteoglycans, and a wide range of matricellular macromolecules (39) that transduce growth factor signals to reparative cells (58). The dynamic alterations of the ECM during the proliferative phase provide essential signals for conversion of fibroblasts into myofibroblasts and may activate angiogenic pathways necessary for neovessel formation, thus supplying the metabolically active wound with oxygen and nutrients (11).

Fibrin network clearance and cell-derived provisional matrix formation. In healing wounds, the plasma-derived ECM is cleared through extracellular proteolysis by fibrinolytic enzymes (59) and through endocytosis by $CCR2^+$ macrophages (60). In the healing infarct, clearance of the fibrin-based provisional matrix by the plasminogen/plasmin system is an important part of the reparative response. Mice lacking plasminogen exhibited markedly attenuated recruitment of inflammatory leukocytes in the infarct and impaired granulation tissue formation (61). Lysis of the fibrin-based

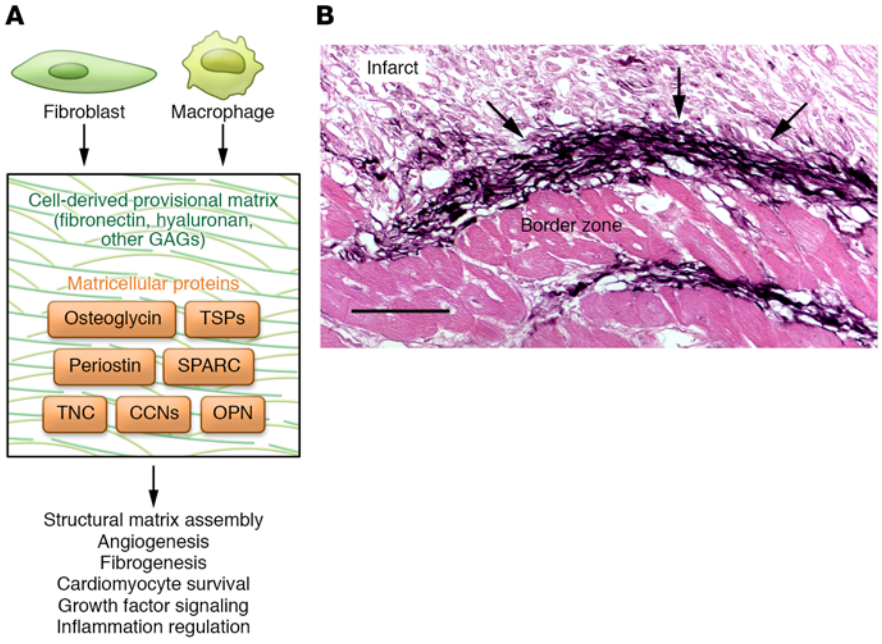

Figure 2. The role of the cell-derived provisional matrix in cardiac repair. (**A**) During the proliferative phase of cardiac repair, fibroblasts and macrophages contribute to the formation of a cell-derived provisional matrix, enriched with a wide range of matricellular macromolecules that do not serve a primary structural role, but modulate cellular phenotype and function. Specialized matrix proteins (such as ED-A domain fibronectin) and matricellular proteins, such as TSPs, tenascin-C (TNC), osteopontin (OPN), SPARC, periostin, osteoglycin, and members of the CCN family, bind to the matrix and modulate growth factor and protease activity. Specific matricellular proteins have been reported as regulating inflammation, participating in fibrogenic and angiogenic responses, modulating cardiomyocyte survival, and contributing to assembly of the structural matrix. (**B**) Matricellular proteins may be critical in spatial and temporal regulation of growth factor signaling. Immunohistochemical staining using a peroxidase-based technique (black) shows the strikingly selective localization of the prototypical matricellular protein TSP1 (arrows), a critical activator of TGF-β, in the border zone of a healing canine myocardial infarction (one hour ischemia followed by seven days reperfusion). Spatially and temporally restricted induction of matricellular proteins regulates growth factor signaling, preventing expansion of profibrotic responses beyond the infarcted area, despite possible diffusion of the soluble mediators in viable segments. Counterstained with eosin. Reproduced with permission from *Circulation* (75). Scale bar: 50 μm. GAGs, glycosaminoglycosans.

matrix is followed by secretion of cellular fibronectin by fibroblasts and macrophages (62, 63) and by deposition of hyaluronan and versican, forming a network of cell-derived provisional matrix that is later enriched with a wide range of matricellular macromolecules (12). During the proliferative phase of healing, the highly dynamic matrix becomes a regulatory center that transduces essential signals to activate reparative fibroblasts and vascular cells.

Components of the provisional matrix regulate fibroblast activation. Repair of the infarcted heart is dependent on recruiting and activating resident fibroblast populations (64) to acquire a myofibroblast phenotype that expresses contractile proteins such as α-smooth muscle actin (α-SMA) and secretes large amounts of collagens. Myofibroblast transdifferentiation requires cooperation between soluble growth factors, such as TGF-β1, and components of the provisional matrix. In vitro, the ED-A domain splice variant of fibronectin is critical for TGF-β1–mediated α-SMA upregulation (65). In vivo, ED-A fibronectin loss attenuates myofibroblast transdifferentiation in healing myocardial infarction (66). The specific interactions between the ED-A segment and the TGF-β–signaling cascade remain unknown. Hyaluronan and versican have also been implicated in myofibroblast conversion. In vitro, pericellular hyaluronan was required to maintain a myofibroblast phenotype in TGF-β–stimulated cells (67). In vivo, loss of CD44, the main receptor for haluronan, impaired collagen synthesis in infarct fibroblasts (40). Versican loss in dermal fibroblasts attenuated myofibroblast conversion (68). Although versican is upregulated in healing myocardial infarcts (69), its in vivo role in transdifferentiation of injury-site cardiac myofibroblasts has not been directly documented.

Induction of matricellular proteins. During the proliferative phase of infarct healing, the cardiac ECM is enriched through the deposition of a wide range of structurally diverse matricellular proteins that do not serve a direct structural role, but act contextually by regulating cytokine and growth factor responses and modulating cell phenotype and function (70, 71). The family includes the thrombospondins TSP-1, -2, and -4, tenascin-C and -X, secreted protein, acidic and cysteine-rich (SPARC), osteopontin, periostin, and members of the CCN family (72). Several other proteins (including members of the galectin and syndecan family, fibulins, osteoglycin, and other small leucine-rich proteoglycans) have been found to exert matricellular actions as part of their broader spectrum of functional properties. Most members of the matricellular family show low expression in the normal myocardium, but are markedly upregulated following myocardial injury. In healing infarctions, angiotensin and growth factors stimulate de novo synthesis and secretion of matricellular proteins in fibroblasts or immune or vascular cells (39, 73, 74). Once secreted into the interstitium, matricellular macromolecules bind to the structural matrix and transduce signaling cascades through ligation of cell surface receptors or contribute to activation of cytokines, growth factors, and proteases in the pericellular space. An overview of the pattern of regulation, function, targets, and mechanisms of action of the matricellular proteins discussed below is given in Table 1.

Several prototypical members of the matricellular family are markedly upregulated following myocardial infarction and protect the myocardium from adverse remodeling (75–78). Localized induction of TSP-1 in the infarct border zone may form a barrier that prevents expansion of inflammation in viable myocardial areas through local activation of antiinflammatory signals (75). Osteopontin may protect from left ventricular dilation by promoting matrix deposition in the infarcted region (79). SPARC has been shown to protect from cardiac rupture and postinfarction heart failure by contributing to collagen maturation through activation of growth factor signaling (80). Periostin serves as a crucial regulator of fibroblast

recruitment and activity (81) and prevents cardiac rupture (81, 82), promoting formation of an organized collagen-based scar.

Although each matricellular protein has a unique functional profile, several unifying themes have emerged regarding their actions in the infarcted heart. First, the strikingly selective localization of prototypical members of the family in the infarct border zone and their regulatory effects on the activity of soluble mediators highlight their role in spatial regulation of cellular responses. Secreted growth factors and cytokines can diffuse beyond the infarct zone; the requirement for matricellular proteins in activating growth factor–mediated responses may serve to localize inflammatory and fibrotic responses within areas of injury. Second, transient expression of matricellular proteins during the proliferative phase of healing ensures temporal regulation of growth factor responses. Clearance of matricellular proteins from the infarcted area may serve as an important STOP signal, preventing uncontrolled fibrosis following injury. In vitro studies have demonstrated that alternatively activated macrophages internalize SPARC through the scavenger receptor stabilin 1 (83). However, the potential role of immune cell subsets in endocytosis and degradation of matricellular proteins in vivo has not been tested. Third, repair of the infarcted myocardium is dependent on a highly dynamic microenvironment that promotes cellular plasticity. In response to microenvironmental cues, interstitial cells exhibit phenotypic changes (84–86), leading to transitions from inflammatory to reparative phenotypes (87). Through their transient induction and incorporation into the matrix, matricellular proteins may play a critical role in regulating cell differentiation, contributing to the cellular plasticity observed in healing tissues through direct actions and via modulation of growth factor–mediated pathways.

ECM in the maturation phase of infarct healing

Scar maturation is associated with ECM crosslinking in the infarct zone and with a marked reduction in myofibroblast density (88). Descriptive studies have suggested that apoptosis may be involved in elimination of granulation tissue cells from the infarct (89, 90); however, the mechanisms responsible for cell-specific activation of a proapoptotic program in the late phase of infarct healing have not been investigated. Acquisition of a quiescent phenotype may precede apoptosis of infarct myofibroblasts. Formation of a mature crosslinked matrix and clearance of matricellular proteins may play an important role in regulating fibroblast deactivation in the healing infarct (91–93). It is tempting to hypothesize that endogenous mechanisms that restrain matricellular actions protect the infarcted heart from progressive fibrosis, depriving fibroblasts of the prolonged actions of growth factor–mediated signals. Vascular cells may also

Table 1. Matricellular proteins in myocardial infarction

Matricellular protein	Pattern of regulation	Function	Possible cellular targets	Possible mechanisms of action	References
TSP-1	Transient upregulation and deposition in the infarct border zone during the proliferative phase of healing	Protects the infarcted heart from adverse remodeling, limiting expansion of inflammation and extension of fibrosis	Fibroblasts, macrophages, vascular endothelial cells, T cells, cardiomyocytes	Activates TGF-β Inhibits MMPs Exerts angiostatic actions Exerts antiinflammatory actions Modulates nitric oxide signaling	12
Tenascin-C	Transient upregulation in infarcted area, border zone, and remodeling myocardium	May contribute to myocardial regeneration in fish and amphibians Promotes fibrosis and adverse remodeling in mammals	Fibroblasts, cardiomyocytes, macrophages, vascular cells	Exerts proinflammatory actions Triggers fibrogenic actions though accentuation of growth factor signaling Promotes angiogenic effects	145, 156, 157
SPARC	Abundant, but transient upregulation in infarcted myocardium, predominantly localized in macrophages and myofibroblasts	Protects from cardiac rupture May promote systolic dysfunction during the early postischemic phase	Fibroblasts, macrophages, vascular cells	Regulates matrix assembly and metabolism Accentuates growth factor signaling, promoting fibroblast activation and angiogenesis	80, 158
OPN	Markedly and transiently upregulated following infarction, primarily localized in macrophages	Protects from adverse remodeling	Fibroblasts, macrophages, T cells, vascular cells, cardiomyocytes	Regulates matrix assembly Activates growth factor signaling, promoting fibroblast activation and angiogenesis	79
Periostin	Marked, but transient upregulation in activated myofibroblasts in the infarct, border zone, and remodeling area	Protects from cardiac rupture, while promoting late fibrosis in remodeling segments	Fibroblasts	Regulates matrix assembly Activates a fibrogenic program	81, 82
CCN2	Marked, but transient upregulation in infarcted hearts through activation of TGF-β and angiotensin II	Cardiomyocyte-specific CCN2 overexpression studies suggested that CCN2 reduces infarct size following ischemia/reperfusion and attenuates adverse remodeling in nonreperfused infarction	Cardiomyocytes, fibroblasts, macrophages	Activates prosurvival pathways in cardiomyocytes Attenuates inflammation	159, 160
Osteoglycin	Marked upregulation in infarcted myocardium, associated with collagen deposition	Protects from cardiac rupture and prevents adverse remodeling	Fibroblasts	Regulates maturation of collagen fibers	161

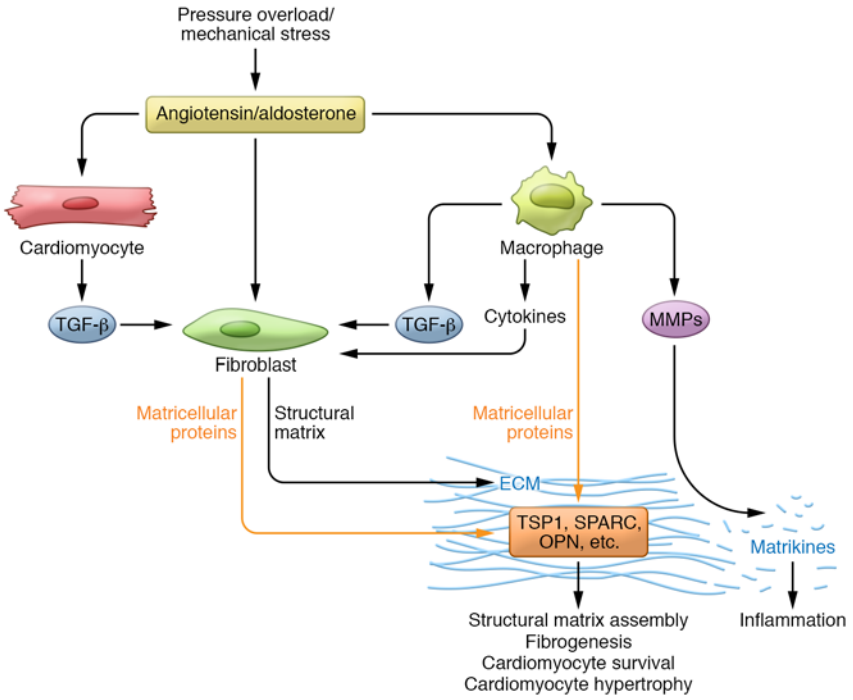

Figure 3. Matricellular proteins regulate cellular responses in the pressure-overloaded myocardium. In the pressure-overloaded heart, mechanical stress activates neurohumoral pathways and induces synthesis and release of matricellular macromolecules, including TSP1, -2, and -4, tenascin-C, OPN, SPARC, and periostin. Matricellular proteins have been implicated in regulation of matrix assembly, in transduction of mechanosensitive signaling, and in the pathogenesis of fibrosis and cardiac hypertrophy, and may also modulate survival of cardiomyocytes under conditions of stress. The effects of the matricellular proteins are exerted through direct activation of cell surface receptors or through modulation of growth factor– and protease-mediated responses.

respond to the mature ECM environment. During scar maturation, infarct microvessels acquire a coat of mural cells through activation of PDGFR-β signaling (88, 94); uncoated vessels regress. ECM proteins have been implicated in modulation of endothelial-pericyte interactions in vitro and in vivo (95, 96), but whether such effects play a role in maturation of infarct microvessels remains unknown.

It should be emphasized that in the presence of a large infarction with significant hemodynamic consequences, viable noninfarcted myocardium also exhibits slowly progressive interstitial fibrosis related to the pathophysiologic effects of pressure and volume loads. Inflammation and fibrosis are suppressed in the healing infarct, leading to formation of a mature collagen-based scar, but in the viable noninfarcted zone, increased wall stress may locally activate macrophages and fibroblasts, triggering chronic progressive expansion of the cardiac interstitial matrix (97, 98).

ECM in cardiac pressure and volume overload

Pressure and volume overload are critically implicated in the pathogenesis of heart failure in a wide variety of cardiac conditions. Left ventricular pressure overload is the critical pathophysiologic companion of the cardiomyopathy induced by systemic hypertension and aortic stenosis. On the other hand, valvular regurgitant lesions (such as aortic and mitral insufficiency) cause cardiac remodeling and heart failure by subjecting the heart to volume overload. Moreover, both pressure and volume loads contribute to the pathophysiology of postinfarction remodeling. Pressure and volume overload have distinct effects on the cardiac ECM that may account for their consequences on ventricular geometry and function.

ECM in the pressure-overloaded myocardium. In both experimental models and in human patients, cardiac pressure overload causes early hypertrophic remodeling and diastolic dysfunction, followed by decompensation, chamber dilation, and development of systolic heart failure. Pressure overload is associated with profound and dynamic changes in the composition of the ECM; these changes regulate geometry and function, not only by affecting the mechanical properties of the ventricle, but also by modulating cellular responses. In animal models, activation of cardiac fibroblasts is one of the earliest effects of pressure overload in the myocardium, ultimately leading to deposition of collagenous matrix and expansion of the interstitium (99–101). In human patients, hypertensive heart disease is associated with development of interstitial and periarteriolar fibrosis even in the absence of significant coronary atherosclerosis (102).

Fibrotic changes that develop in the pressure-overloaded myocardium may involve activation of cardiomyocytes, fibroblasts, and immune and vascular cells. Mechanical stress due to pressure overload activates the renin-angiotensin-aldosterone system (RAAS), triggering inflammatory signaling and leading to downstream stimulation of TGF-β cascades. Neurohumoral mediators, cytokines, and growth factors directly stimulate a fibrogenic program, triggering myofibroblast conversion and stimulating synthesis of large amounts of structural matrix proteins (103–106). Stress-induced fibroblast activation in the pressure-overloaded myocardium may also be indirect, at least in part, requiring stimulation of fibrogenic cascades in cardiomyocytes and immune cells. Mechanical stretch has been suggested as triggering purinergic signaling in cardiomyocytes, leading to release of fibrogenic growth factors (107). Moreover, T lymphocytes and macrophages have been implicated in activation of resident cardiac fibroblasts following pressure overload (108, 109).

Even in the absence of cardiomyocyte necrosis, mechanically activated myofibroblasts and immune cells secrete specialized matrix proteins (such as fibronectin) and enrich the interstitial matrix with a wide range of matricellular macromolecules (Figure 3 and refs. 110, 111). Fibronectin deposition in the pressure-overloaded heart may be involved in myofibroblast transdifferentiation and has been implicated as an important mediator in cardiomyocyte hypertrophy (112), possibly through activation of growth factor signaling. Deposition of matricellular proteins in the pressure-overloaded heart generates a highly dynamic matrix microenvironment and modulates fibrogenic and hypertrophic responses. Table 2 provides an overview of the regulation, functional role, and mechanisms of action of the matricellular proteins in the pressure-overloaded myocardium.

ECM in cardiac volume overload. Volume overload is associated with a distinct profile of changes in the composition of the ECM that ultimately lead to chamber dilation and contribute to systolic dysfunction. In contrast to the marked accentuation in collagen deposition triggered by a pressure load, volume overload is associated with a reduction in interstitial collagen content due to increased MMP expression (113–115) and augmented autophagic degradation of procollagen in cardiac fibroblasts (116). Pharmacologic inhibition studies suggested that MMP activation is directly implicated in dilative remodeling of the volume-overloaded ventricle (117), but the mechanisms responsible for the distinct cell biological changes and matrix alterations in volume overload remain poorly understood. Bradykinin receptor signaling has been implicated in matrix loss associated with volume overload (118), but the links between specific mechanical stimuli and myocardial cell activation are understudied. The limited data on the matricellular protein profile in volume-overloaded hearts are not accompanied by systematic investigations of the potential role of these proteins. Although marked increases in synthesis of fibronectin and periostin have been reported in experimental volume overload (114, 119), deposition of these fibrogenic matricellular proteins was not associated with increased secretion of structural matrix proteins.

The cardiac ECM in metabolic disease

Diabetics exhibit a high incidence of heart failure with preserved ejection fraction, associated with expansion of the cardiac ECM network (120). Fibrotic changes in diabetic hearts are, at least in part, independent of coronary artery disease or hypertension (121), reflecting direct effects of metabolic dysregulation on the ECM. Diabetes, obesity, and metabolic dysfunction are associated with activation of cardiac fibroblasts (122) and are accompanied by deposition of matricellular macromolecules (123) and progressive accumulation of fibrillary collagens in the cardiac interstitium (124, 125). The molecular basis for activation of the so-called diabetic fibroblast remains unknown. The role of hyperglycemia in mediating fibrogenic activation remains poorly defined. Whether stimulation of a fibrogenic program in diabetic fibroblasts requires diabetes-associated activation of fibrogenic signaling in cardiomyocytes, vascular, or immune cells is unclear. Expansion of the cardiac interstitium in diabetes involves activation of several distinct but overlapping pathways, including neurohumoral mediators (such as the RAAS), ROS, inflammatory cytokines and growth factors (such as TGF-β), adipokines, and the advanced glycation endproduct (AGE)/receptor for AGE (RAGE) axis. Moreover, hyperglycemia induces matricellular protein synthesis in several cell types (126). Diabetes-associated induction of matricellular proteins, such as

Table 2. Matricellular proteins in the pressure-overloaded myocardium

Matricellular protein	Pattern of regulation in models of pressure overload	Function	Possible mechanisms of action	References
TSP-1	Transient upregulation and deposition in interstitial and perivascular areas in models of TAC and systemic hypertension and in a combined model of hyperglycemia/abdominal aortic constriction	Activates fibroblasts in the pressure-overloaded heart, promoting a matrix-synthetic phenotype	Activates TGF-β Inhibits MMP activity	111, 162–164
TSP-2	High expression in myocardium of renin-overexpressing hypertensive rats that developed heart failure High expression in human patients with cardiac hypertrophy	Protects the angiotensin II–stimulated myocardium from rupture Protects the aging heart from dilation	Inhibition of MMP synthesis and activity Activation of prosurvival pathways in cardiomyocytes	165, 166
TSP-4	Rapid upregulation in the myocardium in response to angiotensin II treatment or TAC	Protects the pressure-overloaded heart from functional decompensation, systolic dysfunction, and death Downmodulates the fibrotic response in the pressure-overloaded heart	Suppresses expression of ECM proteins in fibroblasts and endothelial cells Activates mechanosensitive Erk and Akt signaling in cardiomyocytes, increasing contractility following pressure overload Has been suggested as also acting intracellularly, augmenting ER function and protecting from injury-related ER stress	167–171
Tenascin-C	Deposition in the cardiac interstitium following pressure overload Upregulation in cardiomyocytes subjected to mechanical strain	Accelerates cardiac fibrosis in response to angiotensin II infusion	May act in part through activation of integrin-mediated cytokine secretion in macrophages	99, 172–174
SPARC	Upregulation in models of TAC	Mediates fibrosis and promotes diastolic dysfunction in models of TAC	Contributes to postsynthetic procollagen processing	175, 176
OPN	Upregulation in models of TAC and angiotensin II infusion Increased expression in human hypertensive heart disease	Mediates fibrosis in models of TAC, angiotensin, and aldosterone infusion Prohypertrophic effects are less consistently observed in various models	Promotes fibroblast proliferation Activates fibroblasts through an miR-21–mediated pathway 177–183	
Periostin	Upregulated in activated fibroblasts and deposited in the cardiac interstitium in models of TAC	Promotes hypertrophy and fibrosis	Activates cardiac fibroblasts, promoting their migration and transdifferentiation Regulates collagen fibrillogenesis	82, 184

TAC, transverse aortic constriction

TSP-1, may drive the fate of cardiac interstitial cells toward a fibroblast phenotype promoting fibrotic remodeling.

Therapeutic ECM targeting in injured and remodeling myocardium

Matrix-based strategies to preserve structure, geometry, and function. Because of its importance in preserving structural integrity and function of the heart (127) and its crucial involvement in regulation of cellular responses in cardiac injury, repair, and remodeling (12), the cardiac ECM provides unique opportunities for therapeutic interventions in patients with myocardial infarction and heart failure. Several therapeutic approaches with established beneficial effects in patients with myocardial infarction and heart failure, such as ACE inhibition, angiotensin type 1 receptor blockade, β-adrenergic receptor antagonism, and mechanical unloading, may exert some of their protective actions through modulation of ECM deposition and metabolism (128).

Following myocardial infarction, catastrophic mechanical complications, such as cardiac rupture (129), are associated with accentuated matrix degradation or perturbed deposition of new structural matrix (130). These can be treated through application of a patch containing ECM proteins to restore the structural integrity of the ventricle (131). In the remodeling heart, approaches to tightly regulating matrix deposition and crosslinking may protect from adverse remodeling and development of heart failure. A large body of experimental evidence suggests that excessive accumulation of crosslinked structural matrix proteins increases myocardial stiffness and promotes diastolic dysfunction; in contrast, overactive matrix-degrading pathways may promote dilative remodeling, causing systolic dysfunction. In patients with myocardial infarction, therapeutic interventions directly targeting ECM metabolism through MMP inhibition have produced mixed results. Administration of a selective oral MMP inhibitor in patients with STEMI and reduced ejection fraction showed no significant protection from adverse remodeling (132), despite significant antiremodeling effects in animal models. In contrast, early nonselective MMP inhibition with doxycycline attenuated progression to dilative remodeling in patients with STEMI and left ventricular dysfunction (133). The conflicting findings may reflect the pathophysiological heterogeneity of human myocardial infarction; successful implementation of matrix modulation strategies may require development of biomarkers or imaging approaches to identify patients with specific alterations in matrix metabolism (134). Moreover, interpretation of the effects of therapies targeting MMPs are complicated by their wide range of actions beyond matrix metabolism involving processing and modulation of bioactive cytokines and growth factors.

Matrix-based interventions to modulate cellular cardiac repair responses. Specialized matrix proteins and matricellular macromolecules critically modulate the cellular responses in the infarcted and remodeling heart and may hold the key for development of new effective strategies to optimize repair and to reduce adverse remodeling following cardiac injury. Animal model studies have suggested that several members of the matricellular family protect the infarcted heart from adverse remodeling (12). Therapeutic approaches based on matricellular proteins are particularly attractive because of the capacity of matricellular macromolecules to modulate growth factor and cytokine signaling, thus localizing therapeutic effects in the area of interest. Unfortunately, the daunting complexity of the biology of matricellular proteins hampers therapeutic implementation. Matricellular proteins have multiple functional domains and act contextually depending on microenvironmental factors, such as the local composition of the matrix and the profile of cytokine and growth factor expression. Distinct actions of matricellular protein fragments further complicate therapeutic implementation. Identification of the functional domains responsible for specific protective or detrimental matricellular actions is needed in order to design peptide-based strategies that simulate these effects (12, 135).

Targeting the ECM to promote cardiac regeneration. In contrast with fish and amphibians, adult mammals have very limited capacity for myocardial regeneration (136), which is overwhelmed by the massive sudden loss of cardiomyocytes following infarction. Over the last 15 years, a wide range of cell therapy approaches has been tested in attempts to regenerate the injured human myocardium, with little success (137–139). Although beneficial actions have been reported with several different types of cell therapy, in many cases, protection of the infarcted myocardium was attributed to paracrine effects and to the modulation of inflammatory and fibrogenic signals rather than to activation of a regenerative program.

Several lines of evidence suggest that modulation of the ECM may be a crucial component of a regenerative response. First, in vitro, the composition of the ECM has a profound effect in regulation of cell cycle entry in cardiomyocyte progenitors and in neonatal cardiac myocytes (140, 141). Compliant matrices containing elastin promote dedifferentiation, proliferation, and clonal expansion of rat and mouse neonatal cardiomyocytes (140). Second, in fish and amphibians, myocardial regenerative responses seem to be dependent on deposition of a specialized ECM (142). A recent study reported that intramyocardial administration of ECM from healing zebrafish hearts may stimulate regeneration in mouse infarcts (143). Loss-of-function approaches suggested that fibronectin deposition may be critical for regeneration of the zebrafish heart (144). In newts, cardiac regeneration following injury was preceded by formation of a matrix network comprising tenascin-C, fibronectin, and hyaluronan. This specialized matrix network may serve as a path for progenitor cells as well as play an active role in activation of a regenerative program (145). Considering that, much like in fish and amphibians, myocardial infarction in mammals also induces a marked upregulation of tenascin-C and fibronectin without stimulating remuscularization, it is unlikely that matrix-dependent actions are sufficient to activate a regenerative program. Myocardial regeneration likely requires not only a "regenerative" matrix profile, but also local secretion of a yet-undefined combination of cytokines and growth factors, and activation of pathways that enhance plasticity of progenitor cell populations (146). Third, in several cell therapy studies in mammalian models of cardiac injury, application of matrix-based patches containing progenitor cells showed enhanced effectiveness (147, 148). It has been suggested that application of matrix patches that recapitulate the regenerative environment of the embryonic myocardium may increase

remuscularization following injury (149). Whether such effects may be due to direct actions of specific matrix proteins on cardiac progenitors or reflect matrix-dependent activation of other cell types (such as immune or vascular cells) remains unknown. Fourth, some experimental studies in mammals have suggested that matricellular macromolecules may induce proliferation of differentiated cardiomyocytes. Kühn and coworkers showed that recombinant periostin administered as an epicardial Gelfoam patch following infarction improved cardiac function and attenuated cardiac remodeling, triggering cell cycle reentry in differentiated cardiomyocytes in an integrin-dependent manner (150). Unfortunately, genetic manipulation of periostin expression in mice did not support the proposed proliferative actions of periostin on cardiomyocytes (151). Whether modulation of the matricellular protein profile following myocardial injury could facilitate activation of a regenerative program in adult infarcted hearts remains unknown.

A growing body of experimental work attempts to exploit technological advances in perfusion-decellularization strategies (152) to generate scaffolds comprising human cardiac ECM that may serve as tools for manufacture of cardiac grafts (153, 154). The acellular matrix obtained through decellularization could subsequently be used for recellularization with cardiomyocytes derived from induced pluripotent stem cells (iPSCs) in order to generate myocardial-like structures. Early studies have generated tissue constructs with definitive sarcomeric structure that exhibit contractile function and electrical conduction (153). Clearly, the current technology has significant limitations, and major advances are needed in order to pursue clinical translation. Complete reendothelialization is necessary to prevent activation of the coagulation system, generation of functional valvular structures is critical for ventricular function, and a conduction system is needed for transmission of electrical activity. Despite these problems, such matrix-driven strategies may represent the first step toward the generation of functional human cardiac grafts.

Conclusions

All myocardial cells are enmeshed within a dynamic network of ECM that not only serves a structural role and facilitates mechanical force transmission, but also regulates cell phenotype and function. Following cardiac injury, changes in composition of the cardiac ECM critically regulate inflammatory, reparative, fibrotic, and regenerative responses. Over the last two decades, understanding of the biology of the cardiac matrix has expanded well beyond the early concepts focusing on the role of matrix proteins in cardiac mechanics. We now view the matrix as a dynamic entity that responds to injury by undergoing dramatic transformations. Release of bioactive fragments and incorporation of matricellular proteins expands the functional repertoire of the matrix and drives repair by transducing key signals to many different cell types. Expansion of our knowledge on the structure, proteomic profile, and functional properties of matrix constituents will enrich our understanding of the pathobiology of heart disease, suggesting new therapeutic opportunities.

Acknowledgments

NGF's laboratory is supported by NIH grants R01 HL76246 and R01 HL85440 and by grants PR151134 and PR151029 from the Department of Defense Congressionally Directed Medical Research Programs (CDMRP).

Address correspondence to: Nikolaos G. Frangogiannis, The Wilf Family Cardiovascular Research Institute, Albert Einstein College of Medicine, 1300 Morris Park Avenue, Forchheimer G46B, Bronx, New York 10461, USA. Phone: 718.430.3546; E-mail: nikolaos.frangogiannis@einstein.yu.edu.

1. Pinto AR, et al. Revisiting cardiac cellular composition. *Circ Res*. 2016;118(3):400–409.
2. Kong P, Christia P, Frangogiannis NG. The pathogenesis of cardiac fibrosis. *Cell Mol Life Sci*. 2014;71(4):549–574.
3. Berk BC, Fujiwara K, Lehoux S. ECM remodeling in hypertensive heart disease. *J Clin Invest*. 2007;117(3):568–575.
4. Prabhu SD, Frangogiannis NG. The biological basis for cardiac repair after myocardial infarction: from inflammation to fibrosis. *Circ Res*. 2016;119(1):91–112.
5. Medugorac I, Jacob R. Characterisation of left ventricular collagen in the rat. *Cardiovasc Res*. 1983;17(1):15–21.
6. Leonard BL, Smaill BH, LeGrice IJ. Structural remodeling and mechanical function in heart failure. *Microsc Microanal*. 2012;18(1):50–67.
7. Bashey RI, Martinez-Hernandez A, Jimenez SA. Isolation, characterization, and localization of cardiac collagen type VI. Associations with other extracellular matrix components. *Circ Res*. 1992;70(5):1006–1017.
8. Jugdutt BI. Ventricular remodeling after infarction and the extracellular collagen matrix: when is enough enough? *Circulation*. 2003;108(11):1395–1403.
9. Weber KT. Cardiac interstitium in health and disease: the fibrillar collagen network. *J Am Coll Cardiol*. 1989;13(7):1637–1652.
10. Frangogiannis NG. Pathophysiology of myocardial infarction. *Compr Physiol*. 2015;5(4):1841–1875.
11. Dobaczewski M, Gonzalez-Quesada C, Frangogiannis NG. The extracellular matrix as a modulator of the inflammatory and reparative response following myocardial infarction. *J Mol Cell Cardiol*. 2010;48(3):504–511.
12. Frangogiannis NG. Matricellular proteins in cardiac adaptation and disease. *Physiol Rev*. 2012;92(2):635–688.
13. Murphy-Ullrich JE, Sage EH. Revisiting the matricellular concept. *Matrix Biol*. 2014;37:1–14.
14. Cannon RO, et al. Early degradation of collagen after acute myocardial infarction in the rat. *Am J Cardiol*. 1983;52(3):390–395.
15. Whittaker P, Boughner DR, Kloner RA. Role of collagen in acute myocardial infarct expansion. *Circulation*. 1991;84(5):2123–2134.
16. Etoh T, et al. Myocardial and interstitial matrix metalloproteinase activity after acute myocardial infarction in pigs. *Am J Physiol Heart Circ Physiol*. 2001;281(3):H987–H994.
17. Wang W, Sawicki G, Schulz R. Peroxynitrite-induced myocardial injury is mediated through matrix metalloproteinase-2. *Cardiovasc Res*. 2002;53(1):165–174.
18. Alfonso-Jaume MA, et al. Cardiac ischemia-reperfusion injury induces matrix metalloproteinase-2 expression through the AP-1 components FosB and JunB. *Am J Physiol Heart Circ Physiol*. 2006;291(4):H1838–H1846.
19. Danielsen CC, Wiggers H, Andersen HR. Increased amounts of collagenase and gelatinase in porcine myocardium following ischemia and reperfusion. *J Mol Cell Cardiol*. 1998;30(7):1431–1442.
20. Gearing AJ, et al. Matrix metalloproteinases and processing of pro-TNF-α. *J Leukoc Biol*. 1995;57(5):774–777.
21. Van Lint P, Libert C. Chemokine and cytokine processing by matrix metalloproteinases and its effect on leukocyte migration and inflammation. *J Leukoc Biol*. 2007;82(6):1375–1381.
22. Feng G, Hao D, Chai J. Processing of CXCL12 impedes the recruitment of endothelial progenitor cells in diabetic wound healing. *FEBS J*. 2014;281(22):5054–5062.
23. Peng H, Wu Y, Duan Z, Ciborowski P, Zheng JC. Proteolytic processing of SDF-1α by matrix

metalloproteinase-2 impairs CXCR4 signaling and reduces neural progenitor cell migration. *Protein Cell*. 2012;3(11):875–882.
24. Denney H, Clench MR, Woodroofe MN. Cleavage of chemokines CCL2 and CXCL10 by matrix metalloproteinases-2 and -9: implications for chemotaxis. *Biochem Biophys Res Commun*. 2009;382(2):341–347.
25. Cox JH, Dean RA, Roberts CR, Overall CM. Matrix metalloproteinase processing of CXCL11/I-TAC results in loss of chemoattractant activity and altered glycosaminoglycan binding. *J Biol Chem*. 2008;283(28):19389–19399.
26. Cauwe B, Opdenakker G. Intracellular substrate cleavage: a novel dimension in the biochemistry, biology and pathology of matrix metalloproteinases. *Crit Rev Biochem Mol Biol*. 2010;45(5):351–423.
27. Schulz R. Intracellular targets of matrix metalloproteinase-2 in cardiac disease: rationale and therapeutic approaches. *Annu Rev Pharmacol Toxicol*. 2007;47:211–242.
28. Ali MA, Cho WJ, Hudson B, Kassiri Z, Granzier H, Schulz R. Titin is a target of matrix metalloproteinase-2: implications in myocardial ischemia/reperfusion injury. *Circulation*. 2010;122(20):2039–2047.
29. Wells JM, Gaggar A, Blalock JE. MMP generated matrikines. *Matrix Biol*. 2015;44–46:122–129.
30. Gaggar A, Weathington N. Bioactive extracellular matrix fragments in lung health and disease. *J Clin Invest*. 2016;126(9):3176–3184.
31. Akthar S, et al. Matrikines are key regulators in modulating the amplitude of lung inflammation in acute pulmonary infection. *Nat Commun*. 2015;6:8423.
32. Adair-Kirk TL, Senior RM. Fragments of extracellular matrix as mediators of inflammation. *Int J Biochem Cell Biol*. 2008;40(6–7):1101–1110.
33. Senior RM, Griffin GL, Mecham RP. Chemotactic activity of elastin-derived peptides. *J Clin Invest*. 1980;66(4):859–862.
34. Weathington NM, et al. A novel peptide CXCR ligand derived from extracellular matrix degradation during airway inflammation. *Nat Med*. 2006;12(3):317–323.
35. Gaggar A, et al. A novel proteolytic cascade generates an extracellular matrix-derived chemoattractant in chronic neutrophilic inflammation. *J Immunol*. 2008;180(8):5662–5669.
36. Mydel P, et al. Neutrophil elastase cleaves laminin-332 (laminin-5) generating peptides that are chemotactic for neutrophils. *J Biol Chem*. 2008;283(15):9513–9522.
37. Villarreal F, Omens J, Dillmann W, Risteli J, Nguyen J, Covell J. Early degradation and serum appearance of type I collagen fragments after myocardial infarction. *J Mol Cell Cardiol*. 2004;36(4):597–601.
38. Lauten A, Gerhard-Garcia A, Suhr F, Fischer JH, Figulla HR, Bloch W. Impact of ischemia-reperfusion on extracellular matrix processing and structure of the basement membrane of the heart. *PLoS One*. 2014;9(3):e92833.
39. Dobaczewski M, Bujak M, Zymek P, Ren G, Entman ML, Frangogiannis NG. Extracellular matrix remodeling in canine and mouse myocardial infarcts. *Cell Tissue Res*. 2006;324(3):475–488.
40. Huebener P, et al. CD44 is critically involved in infarct healing by regulating the inflammatory and fibrotic response. *J Immunol*. 2008;180(4):2625–2633.
41. Trial J, et al. Fibronectin fragments modulate monocyte VLA-5 expression and monocyte migration. *J Clin Invest*. 1999;104(4):419–430.
42. Taylor KR, Trowbridge JM, Rudisill JA, Termeer CC, Simon JC, Gallo RL. Hyaluronan fragments stimulate endothelial recognition of injury through TLR4. *J Biol Chem*. 2004;279(17):17079–17084.
43. Teder P, et al. Resolution of lung inflammation by CD44. *Science*. 2002;296(5565):155–158.
44. Lindsey ML, et al. A novel collagen matricryptin reduces left ventricular dilation post-myocardial infarction by promoting scar formation and angiogenesis. *J Am Coll Cardiol*. 2015;66(12):1364–1374.
45. O'Reilly MS, et al. Endostatin: an endogenous inhibitor of angiogenesis and tumor growth. *Cell*. 1997;88(2):277–285.
46. Okada M, Oba Y, Yamawaki H. Endostatin stimulates proliferation and migration of adult rat cardiac fibroblasts through PI3K/Akt pathway. *Eur J Pharmacol*. 2015;750:20–26.
47. Hamano Y, et al. Physiological levels of tumstatin, a fragment of collagen IV α3 chain, are generated by MMP-9 proteolysis and suppress angiogenesis via αVβ3 integrin. *Cancer Cell*. 2003;3(6):589–601.
48. Andersson L, et al. Rip2 modifies VEGF-induced signalling and vascular permeability in myocardial ischaemia. *Cardiovasc Res*. 2015;107(4):478–486.
49. Brown LF, et al. Expression of vascular permeability factor (vascular endothelial growth factor) by epidermal keratinocytes during wound healing. *J Exp Med*. 1992;176(5):1375–1379.
50. Clark RA. Overview and general considerations of wound repair. In: Clark RA, Henson PM, eds. *The Molecular and Cellular Biology of Wound Repair*. New York, New York, USA: Plenum Press; 1988:3–33.
51. Flick MJ, et al. Leukocyte engagement of fibrin (ogen) via the integrin receptor αMβ2/Mac-1 is critical for host inflammatory response in vivo. *J Clin Invest*. 2004;113(11):1596–1606.
52. Corbett SA, Schwarzbauer JE. Fibronectin-fibrin cross-linking: a regulator of cell behavior. *Trends Cardiovasc Med*. 1998;8(8):357–362.
53. Smiley ST, King JA, Hancock WW. Fibrinogen stimulates macrophage chemokine secretion through toll-like receptor 4. *J Immunol*. 2001;167(5):2887–2894.
54. Petzelbauer P, et al. The fibrin-derived peptide Bbeta15-42 protects the myocardium against ischemia-reperfusion injury. *Nat Med*. 2005;11(3):298–304.
55. Roesner JP, et al. The fibrin-derived peptide Bbeta15-42 is cardioprotective in a pig model of myocardial ischemia-reperfusion injury. *Crit Care Med*. 2007;35(7):1730–1735.
56. Atar D, et al. Effect of intravenous FX06 as an adjunct to primary percutaneous coronary intervention for acute ST-segment elevation myocardial infarction results of the F.I.R.E. (Efficacy of FX06 in the Prevention of Myocardial Reperfusion Injury) trial. *J Am Coll Cardiol*. 2009;53(8):720–729.
57. Martino MM, Briquez PS, Ranga A, Lutolf MP, Hubbell JA. Heparin-binding domain of fibrin(ogen) binds growth factors and promotes tissue repair when incorporated within a synthetic matrix. *Proc Natl Acad Sci U S A*. 2013;110(12):4563–4568.
58. Rienks M, Papageorgiou AP, Frangogiannis NG, Heymans S. Myocardial extracellular matrix: an ever-changing and diverse entity. *Circ Res*. 2014;114(5):872–888.
59. Schäfer BM, Maier K, Eickhoff U, Todd RF, Kramer MD. Plasminogen activation in healing human wounds. *Am J Pathol*. 1994;144(6):1269–1280.
60. Motley MP, et al. A CCR2 macrophage endocytic pathway mediates extravascular fibrin clearance in vivo. *Blood*. 2016;127(9):1085–1096.
61. Creemers E, et al. Disruption of the plasminogen gene in mice abolishes wound healing after myocardial infarction. *Am J Pathol*. 2000;156(6):1865–1873.
62. Brown LF, Dubin D, Lavigne L, Logan B, Dvorak HF, Van de Water L. Macrophages and fibroblasts express embryonic fibronectins during cutaneous wound healing. *Am J Pathol*. 1993;142(3):793–801.
63. Ulrich MM, et al. Increased expression of fibronectin isoforms after myocardial infarction in rats. *J Mol Cell Cardiol*. 1997;29(9):2533–2543.
64. Kanisicak O, et al. Genetic lineage tracing defines myofibroblast origin and function in the injured heart. *Nat Commun*. 2016;7:12260.
65. Serini G, et al. The fibronectin domain ED-A is crucial for myofibroblastic phenotype induction by transforming growth factor-beta1. *J Cell Biol*. 1998;142(3):873–881.
66. Arslan F, et al. Lack of fibronectin-EDA promotes survival and prevents adverse remodeling and heart function deterioration after myocardial infarction. *Circ Res*. 2011;108(5):582–592.
67. Webber J, Meran S, Steadman R, Phillips A. Hyaluronan orchestrates transforming growth factor-β1-dependent maintenance of myofibroblast phenotype. *J Biol Chem*. 2009;284(14):9083–9092.
68. Hattori N, et al. Pericellular versican regulates the fibroblast-myofibroblast transition: a role for ADAMTS5 protease-mediated proteolysis. *J Biol Chem*. 2011;286(39):34298–34310.
69. Toeda K, et al. Versican is induced in infiltrating monocytes in myocardial infarction. *Mol Cell Biochem*. 2005;280(1-2):47–56.
70. Bornstein P. Matricellular proteins: an overview. *J Cell Commun Signal*. 2009;3(3–4):163–165.
71. Murphy-Ullrich JE. The de-adhesive activity of matricellular proteins: is intermediate cell adhesion an adaptive state? *J Clin Invest*. 2001;107(7):785–790.
72. Bornstein P, Sage EH. Matricellular proteins: extracellular modulators of cell function. *Curr Opin Cell Biol*. 2002;14(5):608–616.
73. Mackie EJ, et al. Expression of tenascin by vascular smooth muscle cells. Alterations in hypertensive rats and stimulation by angiotensin II. *Am J Pathol*. 1992;141(2):377–388.
74. Hashimoto S, Suzuki T, Dong HY, Yamazaki N, Matsushima K. Serial analysis of gene expression in human monocytes and macrophages. *Blood*. 1999;94(3):837–844.
75. Frangogiannis NG, et al. The critical role of endogenous Thrombospondin (TSP)-1 in preventing expansion of healing myocardial infarcts.

Circulation. 2005;111(22):2935–2942.
76. Willems IE, Arends JW, Daemen MJ. Tenascin and fibronectin expression in healing human myocardial scars. *J Pathol*. 1996;179(3):321–325.
77. Murry CE, Giachelli CM, Schwartz SM, Vracko R. Macrophages express osteopontin during repair of myocardial necrosis. *Am J Pathol*. 1994;145(6):1450–1462.
78. Dewald O, et al. Of mice and dogs: species-specific differences in the inflammatory response following myocardial infarction. *Am J Pathol*. 2004;164(2):665–677.
79. Trueblood NA, et al. Exaggerated left ventricular dilation and reduced collagen deposition after myocardial infarction in mice lacking osteopontin. *Circ Res*. 2001;88(10):1080–1087.
80. Schellings MW, et al. Absence of SPARC results in increased cardiac rupture and dysfunction after acute myocardial infarction. *J Exp Med*. 2009;206(1):113–123.
81. Shimazaki M, et al. Periostin is essential for cardiac healing after acute myocardial infarction. *J Exp Med*. 2008;205(2):295–303.
82. Oka T, et al. Genetic manipulation of periostin expression reveals a role in cardiac hypertrophy and ventricular remodeling. *Circ Res*. 2007;101(3):313–321.
83. Kzhyshkowska J, et al. Novel function of alternatively activated macrophages: stabilin-1-mediated clearance of SPARC. *J Immunol*. 2006;176(10):5825–5832.
84. Aisagbonhi O, Rai M, Ryzhov S, Atria N, Feoktistov I, Hatzopoulos AK. Experimental myocardial infarction triggers canonical Wnt signaling and endothelial-to-mesenchymal transition. *Dis Model Mech*. 2011;4(4):469–483.
85. Ubil E, et al. Mesenchymal-endothelial transition contributes to cardiac neovascularization. *Nature*. 2014;514(7524):585–590.
86. Zeisberg EM, et al. Endothelial-to-mesenchymal transition contributes to cardiac fibrosis. *Nat Med*. 2007;13(8):952–961.
87. Saxena A, et al. IL-1 induces proinflammatory leukocyte infiltration and regulates fibroblast phenotype in the infarcted myocardium. *J Immunol*. 2013;191(9):4838–4848.
88. Ren G, Michael LH, Entman ML, Frangogiannis NG. Morphological characteristics of the microvasculature in healing myocardial infarcts. *J Histochem Cytochem*. 2002;50(1):71–79.
89. Zhao W, Lu L, Chen SS, Sun Y. Temporal and spatial characteristics of apoptosis in the infarcted rat heart. *Biochem Biophys Res Commun*. 2004;325(2):605–611.
90. Takemura G, et al. Role of apoptosis in the disappearance of infiltrated and proliferated interstitial cells after myocardial infarction. *Circ Res*. 1998;82(11):1130–1138.
91. Tomasek JJ, Gabbiani G, Hinz B, Chaponnier C, Brown RA. Myofibroblasts and mechano-regulation of connective tissue remodelling. *Nat Rev Mol Cell Biol*. 2002;3(5):349–363.
92. Hinz B. Formation and function of the myofibroblast during tissue repair. *J Invest Dermatol*. 2007;127(3):526–537.
93. Bhattacharyya S, et al. Tenascin-C drives persistence of organ fibrosis. *Nat Commun*. 2016;7:11703.
94. Zymek P, et al. The role of platelet-derived growth factor signaling in healing myocardial infarcts. *J Am Coll Cardiol*. 2006;48(11):2315–2323.
95. Davis GE, Norden PR, Bowers SL. Molecular control of capillary morphogenesis and maturation by recognition and remodeling of the extracellular matrix: functional roles of endothelial cells and pericytes in health and disease. *Connect Tissue Res*. 2015;56(5):392–402.
96. Rivera LB, Brekken RA. SPARC promotes pericyte recruitment via inhibition of endoglin-dependent TGF-β1 activity. *J Cell Biol*. 2011;193(7):1305–1319.
97. Sager HB, et al. Proliferation and recruitment contribute to myocardial macrophage expansion in chronic heart failure. *Circ Res*. 2016;119(7):853–864.
98. Chen B, Frangogiannis NG. Macrophages in the remodeling failing heart. *Circ Res*. 2016;119(7):776–778.
99. Xia Y, Lee K, Li N, Corbett D, Mendoza L, Frangogiannis NG. Characterization of the inflammatory and fibrotic response in a mouse model of cardiac pressure overload. *Histochem Cell Biol*. 2009;131(4):471–481.
100. Abrahams C, Janicki JS, Weber KT. Myocardial hypertrophy in Macaca fascicularis. Structural remodeling of the collagen matrix. *Lab Invest*. 1987;56(6):676–683.
101. Herum KM, et al. Syndecan-4 is a key determinant of collagen cross-linking and passive myocardial stiffness in the pressure-overloaded heart. *Cardiovasc Res*. 2015;106(2):217–226.
102. Schwartzkopff B, Mundhenke M, Strauer BE. Remodelling of intramyocardial arterioles and extracellular matrix in patients with arterial hypertension and impaired coronary reserve. *Eur Heart J*. 1995;16(suppl I):82–86.
103. Moore-Morris T, et al. Resident fibroblast lineages mediate pressure overload-induced cardiac fibrosis. *J Clin Invest*. 2014;124(7):2921–2934.
104. Ali SR, et al. Developmental heterogeneity of cardiac fibroblasts does not predict pathological proliferation and activation. *Circ Res*. 2014;115(7):625–635.
105. Kuster GM, et al. Mineralocorticoid receptor inhibition ameliorates the transition to myocardial failure and decreases oxidative stress and inflammation in mice with chronic pressure overload. *Circulation*. 2005;111(4):420–427.
106. Grimm D, et al. Regulation of extracellular matrix proteins in pressure-overload cardiac hypertrophy: effects of angiotensin converting enzyme inhibition. *J Hypertens*. 1998;16(9):1345–1355.
107. Nishida M, et al. P2Y6 receptor-Galpha12/13 signalling in cardiomyocytes triggers pressure overload-induced cardiac fibrosis. *EMBO J*. 2008;27(23):3104–3115.
108. Yu Q, Horak K, Larson DF. Role of T lymphocytes in hypertension-induced cardiac extracellular matrix remodeling. *Hypertension*. 2006;48(1):98–104.
109. Laroumanie F, et al. $CD4^+$ T cells promote the transition from hypertrophy to heart failure during chronic pressure overload. *Circulation*. 2014;129(21):2111–2124.
110. Samuel JL, et al. Accumulation of fetal fibronectin mRNAs during the development of rat cardiac hypertrophy induced by pressure overload. *J Clin Invest*. 1991;88(5):1737–1746.
111. Xia Y, et al. Endogenous thrombospondin 1 protects the pressure-overloaded myocardium by modulating fibroblast phenotype and matrix metabolism. *Hypertension*. 2011;58(5):902–911.
112. Konstandin MH, et al. Fibronectin contributes to pathological cardiac hypertrophy but not physiological growth. *Basic Res Cardiol*. 2013;108(5):375.
113. Ulasova E, et al. Loss of interstitial collagen causes structural and functional alterations of cardiomyocyte subsarcolemmal mitochondria in acute volume overload. *J Mol Cell Cardiol*. 2011;50(1):147–156.
114. Chen YW, et al. Dynamic molecular and histopathological changes in the extracellular matrix and inflammation in the transition to heart failure in isolated volume overload. *Am J Physiol Heart Circ Physiol*. 2011;300(6):H2251–H2260.
115. Hutchinson KR, Stewart JA Jr, Lucchesi PA. Extracellular matrix remodeling during the progression of volume overload-induced heart failure. *J Mol Cell Cardiol*. 2010;48(3):564–569.
116. Fu L, Wei CC, Powell PC, Bradley WE, Collawn JF, Dell'Italia LJ. Volume overload induces autophagic degradation of procollagen in cardiac fibroblasts. *J Mol Cell Cardiol*. 2015;89(Pt B):241–250.
117. Chancey AL, Brower GL, Peterson JT, Janicki JS. Effects of matrix metalloproteinase inhibition on ventricular remodeling due to volume overload. *Circulation*. 2002;105(16):1983–1988.
118. Ryan TD, et al. Left ventricular eccentric remodeling and matrix loss are mediated by bradykinin and precede cardiomyocyte elongation in rats with volume overload. *J Am Coll Cardiol*. 2007;49(7):811–821.
119. Borer JS, et al. Myocardial fibrosis in chronic aortic regurgitation: molecular and cellular responses to volume overload. *Circulation*. 2002;105(15):1837–1842.
120. Russo I, Frangogiannis NG. Diabetes-associated cardiac fibrosis: Cellular effectors, molecular mechanisms and therapeutic opportunities. *J Mol Cell Cardiol*. 2016;90:84–93.
121. Regan TJ, et al. Evidence for cardiomyopathy in familial diabetes mellitus. *J Clin Invest*. 1977;60(4):884–899.
122. Hutchinson KR, Lord CK, West TA, Stewart JA. Cardiac fibroblast-dependent extracellular matrix accumulation is associated with diastolic stiffness in type 2 diabetes. *PLoS One*. 2013;8(8):e72080.
123. Gonzalez-Quesada C, et al. Thrombospondin-1 induction in the diabetic myocardium stabilizes the cardiac matrix in addition to promoting vascular rarefaction through angiopoietin-2 upregulation. *Circ Res*. 2013;113(12):1331–1344.
124. Fischer VW, Barner HB, Larose LS. Pathomorphologic aspects of muscular tissue in diabetes mellitus. *Hum Pathol*. 1984;15(12):1127–1136.
125. van Hoeven KH, Factor SM. A comparison of the pathological spectrum of hypertensive, diabetic, and hypertensive-diabetic heart disease. *Circulation*. 1990;82(3):848–855.
126. Raman P, Krukovets I, Marinic TE, Bornstein P, Stenina OI. Glycosylation mediates up-regulation of a potent antiangiogenic and proathero-

genic protein, thrombospondin-1, by glucose in vascular smooth muscle cells. *J Biol Chem*. 2007;282(8):5704–5714.
127. Clarke SA, Richardson WJ, Holmes JW. Modifying the mechanics of healing infarcts: Is better the enemy of good? *J Mol Cell Cardiol*. 2016;93:115–124.
128. Silvestre JS, et al. Activation of cardiac aldosterone production in rat myocardial infarction: effect of angiotensin II receptor blockade and role in cardiac fibrosis. *Circulation*. 1999;99(20):2694–2701.
129. Honda S, et al. Trends in the clinical and pathological characteristics of cardiac rupture in patients with acute myocardial infarction over 35 years. *J Am Heart Assoc*. 2014;3(5):e000984.
130. Hayashidani S, et al. Targeted deletion of MMP-2 attenuates early LV rupture and late remodeling after experimental myocardial infarction. *Am J Physiol Heart Circ Physiol*. 2003;285(3):H1229–H1235.
131. Holubec T, Caliskan E, Bettex D, Maisano F. Repair of post-infarction left ventricular free wall rupture using an extracellular matrix patch. *Eur J Cardiothorac Surg*. 2015;48(5):800–803.
132. Hudson MP, et al. Effects of selective matrix metalloproteinase inhibitor (PG-116800) to prevent ventricular remodeling after myocardial infarction: results of the PREMIER (Prevention of Myocardial Infarction Early Remodeling) trial. *J Am Coll Cardiol*. 2006;48(1):15–20.
133. Cerisano G, et al. Early short-term doxycycline therapy in patients with acute myocardial infarction and left ventricular dysfunction to prevent the ominous progression to adverse remodelling: the TIPTOP trial. *Eur Heart J*. 2014;35(3):184–191.
134. Frangogiannis NG. The inflammatory response in myocardial injury, repair, and remodelling. *Nat Rev Cardiol*. 2014;11(5):255–265.
135. Sawyer AJ, Kyriakides TR. Matricellular proteins in drug delivery: Therapeutic targets, active agents, and therapeutic localization. *Adv Drug Deliv Rev*. 2016;97:56–68.
136. Bergman O, et al. Evidence for cardiomyocyte renewal in humans. *Science*. 2009;324(5923):98–102.
137. Laflamme MA, Murray CE. Heart regeneration. *Nature*. 2011;473(7347):326–335.
138. Matsa E, Sallum K, Wu JC. Cardiac stem cell biology: glimpse of the past, present, and future. *Circ Res*. 2014;114(1):21–27.
139. Karantalis V, Hare JM. Use of mesenchymal stem cells for therapy of cardiac disease. *Circ Res*. 2015;116(8):1413–1430.
140. Yahalom-Ronen Y, Rajchman D, Sarig R, Geiger B, Tzahor E. Reduced matrix rigidity promotes neonatal cardiomyocyte dedifferentiation, proliferation and clonal expansion. *Elife*. 2015;4:e07455.
141. Qiu Y, et al. A role for matrix stiffness in the regulation of cardiac side population cell function. *Am J Physiol Heart Circ Physiol*. 2015;308(9):H990–H997.
142. Chablais F, Veit J, Rainer G, Jaźwińska A. The zebrafish heart regenerates after cryoinjury-induced myocardial infarction. *BMC Dev Biol*. 2011;11:21.
143. Chen WC, et al. Decellularized zebrafish cardiac extracellular matrix induces mammalian heart regeneration. *Sci Adv*. 2016;2(11):e1600844.
144. Wang J, Karra R, Dickson AL, Poss KD. Fibronectin is deposited by injury-activated epicardial cells and is necessary for zebrafish heart regeneration. *Dev Biol*. 2013;382(2):427–435.
145. Mercer SE, Odelberg SJ, Simon HG. A dynamic spatiotemporal extracellular matrix facilitates epicardial-mediated vertebrate heart regeneration. *Dev Biol*. 2013;382(2):457–469.
146. Uygur A, Lee RT. Mechanisms of cardiac regeneration. *Dev Cell*. 2016;36(4):362–374.
147. Gaetani R, et al. Epicardial application of cardiac progenitor cells in a 3D-printed gelatin/hyaluronic acid patch preserves cardiac function after myocardial infarction. *Biomaterials*. 2015;61:339–348.
148. Jang J, et al. 3D printed complex tissue construct using stem cell-laden decellularized extracellular matrix bioinks for cardiac repair. *Biomaterials*. 2017;112:264–274.
149. Serpooshan V, et al. Use of bio-mimetic three-dimensional technology in therapeutics for heart disease. *Bioengineered*. 2014;5(3):193–197.
150. Kühn B, et al. Periostin induces proliferation of differentiated cardiomyocytes and promotes cardiac repair. *Nat Med*. 2007;13(8):962–969.
151. Lorts A, Schwanekamp JA, Elrod JW, Sargent MA, Molkentin JD. Genetic manipulation of periostin expression in the heart does not affect myocyte content, cell cycle activity, or cardiac repair. *Circ Res*. 2009;104(1):e1–7.
152. Ott HC, et al. Perfusion-decellularized matrix: using nature's platform to engineer a bioartificial heart. *Nat Med*. 2008;14(2):213–221.
153. Guyette JP, et al. Bioengineering human myocardium on native extracellular matrix. *Circ Res*. 2016;118(1):56–72.
154. Sánchez PL, et al. Acellular human heart matrix: A critical step toward whole heart grafts. *Biomaterials*. 2015;61:279–289.
155. Frangogiannis NG, Mendoza LH, Lewallen M, Michael LH, Smith SW, Entman ML. Induction and suppression of interferon-inducible protein-10 (IP-10) following experimental canine myocardial infarction may regulate angiogenesis. *FASEB J*. 2001;15(8):1428–30.
156. Chablais F, Jazwinska A. The regenerative capacity of the zebrafish heart is dependent on TGFβ signaling. *Development*. 2012;139(11):1921–1930.
157. Tamaoki M, et al. Tenascin-C regulates recruitment of myofibroblasts during tissue repair after myocardial injury. *Am J Pathol*. 2005;167(1):71–80.
158. McCurdy SM, et al. SPARC mediates early extracellular matrix remodeling following myocardial infarction. *Am J Physiol Heart Circ Physiol*. 2011;301(2):H497–H505.
159. Ahmed MS, et al. Mechanisms of novel cardioprotective functions of CCN2/CTGF in myocardial ischemia-reperfusion injury. *Am J Physiol Heart Circ Physiol*. 2011;300(4):H1291–H1302.
160. Gravning J, et al. Myocardial connective tissue growth factor (CCN2/CTGF) attenuates left ventricular remodeling after myocardial infarction. *PLoS One*. 2012;7(12):e52120.
161. Van Aelst LN, et al. Osteoglycin prevents cardiac dilatation and dysfunction after myocardial infarction through infarct collagen strengthening. *Circ Res*. 2015;116(3):425–436.
162. Zhou Y, Poczatek MH, Berecek KH, Murphy-Ullrich JE. Thrombospondin 1 mediates angiotensin II induction of TGF-β activation by cardiac and renal cells under both high and low glucose conditions. *Biochem Biophys Res Commun*. 2006;339(2):633–641.
163. Muñoz-Pacheco P, et al. Eplerenone enhances cardioprotective effects of standard heart failure therapy through matricellular proteins in hypertensive heart failure. *J Hypertens*. 2013;31(11):2309–2319.
164. Belmadani S, et al. A thrombospondin-1 antagonist of transforming growth factor-β activation blocks cardiomyopathy in rats with diabetes and elevated angiotensin II. *Am J Pathol*. 2007;171(3):777–789.
165. Schroen B, et al. Thrombospondin-2 is essential for myocardial matrix integrity: increased expression identifies failure-prone cardiac hypertrophy. *Circ Res*. 2004;95(5):515–522.
166. Swinnen M, et al. Absence of thrombospondin-2 causes age-related dilated cardiomyopathy. *Circulation*. 2009;120(16):1585–1597.
167. Frolova EG, et al. Thrombospondin-4 regulates fibrosis and remodeling of the myocardium in response to pressure overload. *FASEB J*. 2012;26(6):2363–2373.
168. Mustonen E, et al. Thrombospondin-4 expression is rapidly upregulated by cardiac overload. *Biochem Biophys Res Commun*. 2008;373(2):186–191.
169. Lynch JM, et al. A thrombospondin-dependent pathway for a protective ER stress response. *Cell*. 2012;149(6):1257–1268.
170. Palao T, Rippe C, van Veen H, VanBavel E, Swärd K, Bakker EN. Thrombospondin-4 knockout in hypertension protects small-artery endothelial function but induces aortic aneurysms. *Am J Physiol Heart Circ Physiol*. 2016;310(11):H1486–H1493.
171. Cingolani OH, et al. Thrombospondin-4 is required for stretch-mediated contractility augmentation in cardiac muscle. *Circ Res*. 2011;109(12):1410–1414.
172. Yamamoto K, Dang QN, Kennedy SP, Osathanondh R, Kelly RA, Lee RT. Induction of tenascin-C in cardiac myocytes by mechanical deformation. Role of reactive oxygen species. *J Biol Chem*. 1999;274(31):21840–21846.
173. Hessel M, Steendijk P, den Adel B, Schutte C, van der Laarse A. Pressure overload-induced right ventricular failure is associated with re-expression of myocardial tenascin-C and elevated plasma tenascin-C levels. *Cell Physiol Biochem*. 2009;24(3–4):201–210.
174. Shimojo N, et al. Tenascin-C may accelerate cardiac fibrosis by activating macrophages via the integrin αVβ3/nuclear factor-κB/interleukin-6 axis. *Hypertension*. 2015;66(4):757–766.
175. Bradshaw AD, et al. Pressure overload-induced alterations in fibrillar collagen content and myocardial diastolic function: role of secreted protein acidic and rich in cysteine (SPARC) in post-synthetic procollagen processing. *Circulation*. 2009;119(2):269–280.
176. Harris BS, Zhang Y, Card L, Rivera LB, Brek-

ken RA, Bradshaw AD. SPARC regulates collagen interaction with cardiac fibroblast cell surfaces. *Am J Physiol Heart Circ Physiol*. 2011;301(3):H841–H847.
177. Matsui Y, et al. Role of osteopontin in cardiac fibrosis and remodeling in angiotensin II-induced cardiac hypertrophy. *Hypertension*. 2004;43(6):1195–1201.
178. Xie Z, Singh M, Singh K. Osteopontin modulates myocardial hypertrophy in response to chronic pressure overload in mice. *Hypertension*. 2004;44(6):826–831.
179. Singh K, et al. Myocardial osteopontin expression coincides with the development of heart failure. *Hypertension*. 1999;33(2):663–670.
180. Collins AR, et al. Osteopontin modulates angiotensin II-induced fibrosis in the intact murine heart. *J Am Coll Cardiol*. 2004;43(9):1698–1705.
181. Lorenzen JM, et al. Osteopontin is indispensible for AP1-mediated angiotensin II-related miR-21 transcription during cardiac fibrosis. *Eur Heart J*. 2015;36(32):2184–2196.
182. López B, et al. Osteopontin-mediated myocardial fibrosis in heart failure: a role for lysyl oxidase? *Cardiovasc Res*. 2013;99(1):111–120.
183. Sam F, et al. Mice lacking osteopontin exhibit increased left ventricular dilation and reduced fibrosis after aldosterone infusion. *Am J Hypertens*. 2004;17(2):188–193.
184. Wang D, et al. Effects of pressure overload on extracellular matrix expression in the heart of the atrial natriuretic peptide-null mouse. *Hypertension*. 2003;42(1):88–95.

Cardiovascular Pathology 30 (2017) 27–37

Contents lists available at ScienceDirect

Cardiovascular Pathology

Original Article

Left atrial remodeling, hypertrophy, and fibrosis in mouse models of heart failure

Waqas Hanif, Linda Alex, Ya Su, Arti V Shinde, Ilaria Russo, Na Li, Nikolaos G Frangogiannis *

The Wilf Family Cardiovascular Research Institute, Department of Medicine, Division of Cardiology, Albert Einstein College of Medicine, Bronx, NY

ARTICLE INFO

Article history:
Received 16 February 2017
Received in revised form 15 June 2017
Accepted 16 June 2017
Available online xxxx

Keywords:
Myocardial infarction
Heart failure
Atrial remodeling
Fibrosis
Hypertrophy
Diabetes

ABSTRACT

Left ventricular dysfunction increases left atrial pressures and causes atrial remodeling. In human subjects, increased left atrial size is a powerful predictor of mortality and adverse events in a broad range of cardiac pathologic conditions. Moreover, structural remodeling of the atrium plays an important role in the pathogenesis of atrial tachyarrhythmias. Despite the potential value of the atrium in assessment of functional endpoints in myocardial disease, atrial pathologic alterations in mouse models of left ventricular disease have not been systematically investigated. Our study describes the geometric, morphologic, and structural changes in experimental mouse models of cardiac pressure overload (induced through transverse aortic constriction), myocardial infarction, and diabetes. Morphometric and histological analysis showed that pressure overload was associated with left atrial dilation, increased left atrial mass, loss of myofibrillar content in a subset of atrial cardiomyocytes, atrial cardiomyocyte hypertrophy, and atrial fibrosis. In mice undergoing nonreperfused myocardial infarction protocols, marked left ventricular systolic dysfunction was associated with left atrial enlargement, atrial cardiomyocyte hypertrophy, and atrial fibrosis. Both infarcted animals and pressure overloaded mice exhibited attenuation and perturbed localization of atrial connexin-43 immunoreactivity, suggesting gap junctional remodeling. In the absence of injury, obese diabetic db/db mice had diastolic dysfunction associated with atrial dilation, atrial cardiomyocyte hypertrophy, and mild atrial fibrosis. Considering the challenges in assessment of clinically relevant functional endpoints in mouse models of heart disease, study of atrial geometry and morphology may serve as an important new tool for evaluation of ventricular function.

1. Introduction

Perturbations in left ventricular function have profound effects on the geometry and structural properties of the left atrium. Both systolic and diastolic heart failures result in elevation of left atrial pressures, leading to atrial dilation and hypertrophy. In human subjects, adverse left atrial remodeling predicts mortality and adverse outcome in a wide range of cardiac pathologic conditions. In a cross-sectional sample of a population >45 years of age, increased atrial volume was a marker of severity and duration of diastolic dysfunction [1]. In patients surviving acute myocardial infarction, left atrial volume was found to be a powerful predictor of mortality [2] and provided incremental prognostic information over clinical and echocardiographic data [3]. Left atrial volume independently predicted adverse outcome in patients with hypertrophic cardiomyopathy [4], ischemic cardiomyopathy [5], and chronic heart failure [6]. The prognostic value of atrial size is not limited to patients with established myocardial disease but has been extended to individuals free of cardiovascular conditions. In subjects with type 2 diabetes but without any known cardiovascular disease, left atrial volume was found to be an independent predictor of morbidity and mortality [7]. In a population of middle-aged and elderly individuals free of clinical cardiovascular disease, left atrial diameter was an independent predictor of incident first cardiovascular events [8]. Thus, in human patients, assessment of left atrial size and geometry is a valuable tool in evaluation of ventricular function and provides important prognostic information.

In addition to its prognostic significance, remodeling of the left atrium plays an important direct role in the pathogenesis of atrial tachyarrhythmias [9]. Atrial fibrosis disrupts electrical conduction and predisposes to initiation and maintenance of atrial fibrillation [10–12]. Moreover, structural and geometric atrial remodeling generates a thrombogenic substrate that predisposes to ischemic stroke and systemic embolic events [13].

Sources of funding: Supported by grants from the National Institutes of Health (R01 HL76246 and R01 HL85440 to N.G.F.), the Department of Defense (PR151134 and PR151029 to N.G.F.), and the American Heart Association Founders' Affiliate (to A.V.S.).
Disclosures: none.
Conflicts of interest: none.

* Corresponding author at: Division of Cardiology, The Wilf Cardiovascular Research Institute, 1300 Morris Park Avenue Forchheimer G46B, Albert Einstein College of Medicine, Bronx, NY 10461. Tel.: +1 718 430 3546; fax: +1 718 430 8989.
E-mail address: nikolaos.frangogiannis@einstein.yu.edu (N.G. Frangogiannis).

http://dx.doi.org/10.1016/j.carpath.2017.06.003
1054-8807/

Mouse models of myocardial disease have been extensively used to study the pathophysiology of myocardial infarction and heart failure [14–20]. Although sophisticated imaging modalities, histopathologic studies, and molecular approaches are used to study remodeling of the left ventricle, atrial pathology is often ignored. Few studies have documented atrial dilation in experimental mouse models of pressure overload [21] and permanent coronary ligation [22]; however, systematic characterization of atrial remodeling in experimental mouse models of heart disease has not been performed. The current study provides the first analysis of atrial remodeling, hypertrophy, and fibrosis in mouse models of postinfarctive cardiac remodeling, pressure-overload-induced cardiomyopathy, and diabetic heart disease.

2. Materials and methods

2.1. Animal protocols

Animal experiments were conducted in accordance with the National Institutes of Health Guide for the Care and Use of Laboratory Animals and were approved by the Albert Einstein College of Medicine Institutional Review Board.

2.2. Mouse model of cardiac pressure overload induced through transverse aortic constriction (TAC)

Male and female 4-month-old wild-type C57BL/6J mice (20.0–30.0 g body weight) were anesthetized with inhaled isoflurane and underwent TAC protocols for 7 days (n=11) or 28 days (n=8). Aortic banding was achieved by creating a constriction between the right innominate and left carotid arteries, as previously described [23–26]. The degree of pressure overload was assessed by measuring the right-to-left carotid artery flow velocity ratio after constricting the transverse aorta. Mice had echocardiographic analysis at baseline and after 7 and 28 days of TAC. At the end of the experiment, the animals were sacrificed, and the hearts were excised, fixed in zinc-formalin, and embedded in paraffin for histological studies. Comparisons with a group of control mice (n=7) was performed.

2.3. Mouse model of nonreperfused myocardial infarction

Male and female mice 3–4 months of age (20.0–30.0 g body weight) were anesthetized using inhaled isoflurane and underwent permanent proximal left coronary artery occlusion protocols. Mortality was 55%, observed during the first 6 days, primarily due to cardiac rupture. Surviving mice were followed for 7 days (n=6) or 28 days (n=10), as previously described [27]. Briefly, anesthetized mice underwent thoracotomy, and an 8.0 polypropylene suture with a U-shaped tapered needle was passed under the left anterior descending (LAD) coronary artery. Occlusion of the LAD was accomplished by ligating LAD until an ST-elevation appears on the electrocardiogram. Mice enrolled in the 28-day permanent occlusion group underwent echocardiography at baseline and prior to sacrifice. At the end of the experiment, the animals were sacrificed, and the hearts were excised, fixed in zinc-formalin, and embedded in paraffin for histological studies. Findings were compared to a group of control mice (n=7).

2.4. Mouse model of diabetes-associated heart disease

Lepr^{db}/+ mice on a C57BL/6J background (db/+) were purchased from Jackson Laboratories (Bar Harbor, ME, USA). Heterozygous db/+ mice were crossed in order to obtain db/db mice and corresponding lean controls [18,28]. Genotyping was performed through established polymerase chain reaction protocols. At 6 months of age, db/db mice (n=9) and corresponding control lean mice (n=7) underwent echocardiography and then were sacrificed, and the hearts were excised, fixed in zinc-formalin, and embedded in paraffin for histological studies.

2.5. Echocardiography

Short-axis M-mode and long-axis B-mode echocardiography was performed in anesthetized mice using the Vevo 2100 system (VisualSonics, Toronto, ON, Canada). The following parameters were measured as indicators of function and ventricular remodeling: left ventricular end-diastolic volume (LVEDV), ejection fraction, end-diastolic left ventricular anterior wall thickness (LVAWTd), end-diastolic left ventricular posterior wall thickness (LVPWTd), and left ventricular mass (LV mass). Lean and diabetic mice underwent Doppler echocardiography and tissue Doppler imaging at 6 months of age to assess diastolic function using the Vevo 2100 system (VisualSonics). Transmitral LV inflow velocities were measured from apical four-chamber view by pulsed-wave Doppler. Peak early E (E-wave) and late A (A-wave) filling velocities and E/A ratio were measured according to the guidelines of the American Society of Echocardiography [29]. Tissue Doppler imaging of the mitral annulus was obtained from the apical four-chamber view. A 1.0-mm sample volume was placed sequentially at the medial mitral annulus. Analysis was performed for assessment of early (E') diastolic velocity, and the E/E' ratio was calculated. Views and data were exported for offline calculation using Vevo 2100 quantification software (Vevo 2100 v.1.6.0). The offline analysis was performed by a sonographer blinded to study groups.

2.6. Histological analysis and quantitative morphometry

Formalin-fixed, paraffin-embedded hearts were sectioned from base to apex at 250-μm intervals as previously described [30]. Ten serial 5-μm sections were obtained at each interval, corresponding to an additional 50-μm segment. The first section from each interval was stained with hematoxylin/eosin (H&E). Each section was scanned at ×10 magnification, the left atrium was identified, and the left atrial wall area (LAWA), left atrial chamber area (LACA), and short and long axis of the atrium were measured using Axiovision LE 4.8 software (Zeiss). Assessment of left atrial volume and mass was performed by calculating the sum of the volumes of all 300-μm partitions. Because histological processing results in shrinkage of the processed tissue [31], the values were corrected by a linear factor of 1.3. The following formulas were used, adapted from our published work describing morphometric strategies used for assessment of ventricular remodeling following reperfused murine myocardial infarction [30]:

$$\text{LA volume} = (\text{LACA1} + \text{LACA2} + \ldots\ldots\ldots + \text{LACAn})^{*}h, \text{where } h = 0.3 \text{ mm},$$
$$\text{LA wall volume} = (\text{LAWA1} + \text{LAWA2} + \ldots + \text{LAWAn})^{*}h\ (h = 0.3\text{mm}),$$
$$\text{and LA mass} = \text{LA wall volume}^{*}1.065\text{mg}/\mu\text{l}\ (\text{specific gravity of myocardium}).$$

2.7. Wheat germ agglutinin (WGA) lectin histochemistry and quantitative assessment of cardiomyocyte size, interstitial fibrosis, and interstitial cellularity

In order to assess atrial cardiomyocyte hypertrophy in mouse models of heart disease, cardiomyocytes were outlined using WGA lectin histochemistry using a WGA Alexa Fluor 594 Conjugate (Life Technologies) (dilution 1:100). Sections were counterstained with DAPI. Cardiomyocyte size was quantitatively assessed using Axiovision LE 4.8 software (Zeiss). Fifty cardiomyocytes cut at cross section were assessed from each mouse. Mean cardiomyocyte area was expressed in μm^2. Interstitial fibrosis was assessed through quantitation of the WGA-stained interstitial area using Image Pro Plus software. Quantitative assessment of the WGA-stained area has been validated as a reliable technique for evaluation of cardiac fibrosis [32]. Quantitative assessment of interstitial cellularity in the left atrium was performed by counting the number of DAPI-positive interstitial nuclei per area of myocardium. Cell density was expressed as cells/mm^2. Six fields

scanned at 400× magnification from two different stained sections were used for analysis of each mouse.

2.8. Sirius red staining

Light microscopy and polarized light microscopy were used to label collagen fibers in the atrium, as previously described [19,33]. Briefly, paraffin sections (5 μ thick) were stained using picrosirius red. Circularly polarized images were obtained using Axio Imager M2 for polarized light microscopy (Zeiss). When the collagen fibers are stained with picrosirius red and viewed with polarized light, depending on the thickness of the collagen fibers, the hues range from green to yellow to orange to red.

2.9. Immunohistochemistry

In order to study connexin-43 localization in remodeling atria, histological sections from four mice per group were stained immunohistochemically with rabbit anti-connexin-43/GJA1 polyclonal antibody (Abcam, ab11370, dilution 1:1000). Staining was performed using a peroxidase-based technique with the Vectastain ELITE kit (Vector Labs). Following antigen retrieval with citrate buffer, sections were treated with 3% hydrogen peroxide to inhibit endogenous peroxidase activity and blocked with 10% goat serum to block nonspecific protein binding. Peroxidase activity was detected using diaminobenzidine with nickel. Negative controls were performed with incubation with rabbit IgG at the same concentration.

2.10. Statistical analysis

Statistical comparisons between more than two groups was performed using analysis of variance followed by *t* test corrected for multiple comparisons (Sidak's test). Comparisons between two groups were performed using *t* test. Non-Gaussian distributions were compared using the Mann–Whitney test. Data were expressed as mean ± S.E.M. Statistical significance was set at .05.

3. Results

3.1. Cardiac pressure overload causes left atrial hypertrophy and dilation

TAC protocols induced comparable increases in R:L carotid velocity ratio in the 7- (7.5±0.94) and 28-day group (9.0±1.04), suggesting similar pressure loads. The effects of pressure overload protocols on left ventricular geometry and function are shown in Table 1. After 7 days of TAC, mice exhibited early concentric left ventricular hypertrophy, followed by modest dilation and systolic dysfunction after 28 days. Pressure overload induced through TAC caused left atrial dilation and hypertrophy (Fig. 1A), evidenced by marked and progressive increases in left atrial volume and left atrial mass after 7–28 days (Fig. 1B–C). TAC reduced sphericity of the atrium, causing a marked increase in the long-axis dimension accompanied by a less impressive increase in the short axis (Fig. 1D and E).

Table 1
Left ventricular remodeling in the TAC model of cardiac pressure overload

	Pre	7 days (n=11)	Pre	28 days (n=8)
LVEDD (mm)	3.63±0.07	3.13±0.18*	3.01±0.26	3.86±0.17*
Ejection fraction (%)	61.32±3.77	59.08±7.34	78.54±3.87	49.89±4.91**
LVEDV (μl)	55.75±2.64	40.64±5.39*	37.87±7.01	65.62±7.29*
AWTd (mm)	0.90±0.07	1.37±0.10**	0.85±0.09	1.21±0.11**
PWTd (mm)	0.70±0.03	0.96±0.05**	0.85±0.07	0.98±0.08
LV mass (mg)	97.10±8.30	135.50±13.71*	84.56±17.45	161.20±19.01*

Two distinct groups of animals underwent 7-day (n=11) and 28-day (n=8) TAC protocols.
* P<.05.
** P<.01 vs. corresponding baseline.

3.2. Alterations of atrial geometry following nonreperfused myocardial infarction

Permanent left coronary artery occlusion caused transmural left ventricular myocardial infarction in all mice studied, accompanied by severe systolic dysfunction and dilative ventricular remodeling (Table 2). Postinfarctive LV remodeling was associated with marked left atrial hypertrophy and dilation (Fig. 2A). Left atrial volume and left atrial mass markedly increased in infarcted animals 7–28 days after coronary occlusion (Fig. 2B–C). Infarction was associated with a marked increase in long-axis dimensions (Fig. 2D); in contrast, the increase in short axis did not reach statistical significance (Fig. 2E), suggesting eccentric dilation of the atrium.

3.3. Diabetic hearts exhibit atrial remodeling

At 6 months of age, db/db mice exhibited marked obesity (body weight: db/db mice 59.7±6.42 g vs. WT mice 22.8±0.8 g, P<.01). Echocardiographic analysis showed that db/db mice had a significant increase in LVPWTd and a trend toward an increase in LV mass (Table 3). Doppler echocardiography showed that db/db mice had significantly higher E/E' ratio; this finding is consistent with worse diastolic function (Table 3). db/db mice developed atrial dilation and hypertrophy evidenced by markedly increased LA volume and LA mass (Fig. 3A–C). db/db mice had significantly increased long-axis, but not short-axis, dimensions, suggesting eccentric remodeling of the atrium (Fig. 3D–E).

3.4. Atrial cardiomyocyte hypertrophy and interstitial fibrosis in mouse models of left ventricular remodeling

Histologic analysis showed progressive loss of contractile elements in atrial cardiomyocytes of pressure-overloaded or infarcted animals but not in obese diabetic mice (Figs. 4-6). Evidence of left atrial cardiomyocyte hypertrophy was noted in all three models of left ventricular remodeling. In the model of cardiac pressure overload, the atrial myocardium showed loss of contractile elements in a subset of cardiomyocytes after 7–28 days of TAC (Fig. 4A–D). Sirius red staining visualized with light (Fig. 4E–G) and polarized (Fig. 4H–J) microscopy showed significant atrial interstitial fibrosis after 7–28 days of TAC. Quantitative analysis showed that left atrial cardiomyocytes exhibited a marked and progressive increase in size after 7–28 days of TAC (Fig. 4K–N).

Following myocardial infarction, some atrial cardiomyocytes exhibited marked loss of contractile elements and significant myocytolysis (Fig. 5A–D). Sirius red staining visualized with light and polarized microscopy showed significant fibrosis in the atrial myocardium 7–28 days after myocardial infarction (Fig. 5E–J). Quantitative analysis showed that atrial cardiomyocyte area was markedly increased after 7 days and remained increased after 28 days of coronary occlusion (Fig. 5K–N). In 6-month-old obese diabetic db/db mice, atrial cardiomyocyte morphology was relatively preserved (Fig. 6A–C). Sirius red staining showed that db/db mice exhibit mild atrial fibrosis. Atrial cardiomyocyte size was significantly increased in db/db mice when compared with age-matched lean animals (Fig. 6H–L).

Remodeling hearts also exhibited significant atrial fibrosis, evidenced by a marked expansion of the atrial interstitium, identified through sirius red and WGA lectin histochemical staining. Cardiac pressure overload was associated with a marked fivefold expansion of the atrial interstitium after 7–28 days of TAC (Fig. 4O). Nonreperfused myocardial infarction was associated with a sixfold increase in atrial interstitial area after 7–28 days of permanent coronary occlusion (Fig. 5O). db/

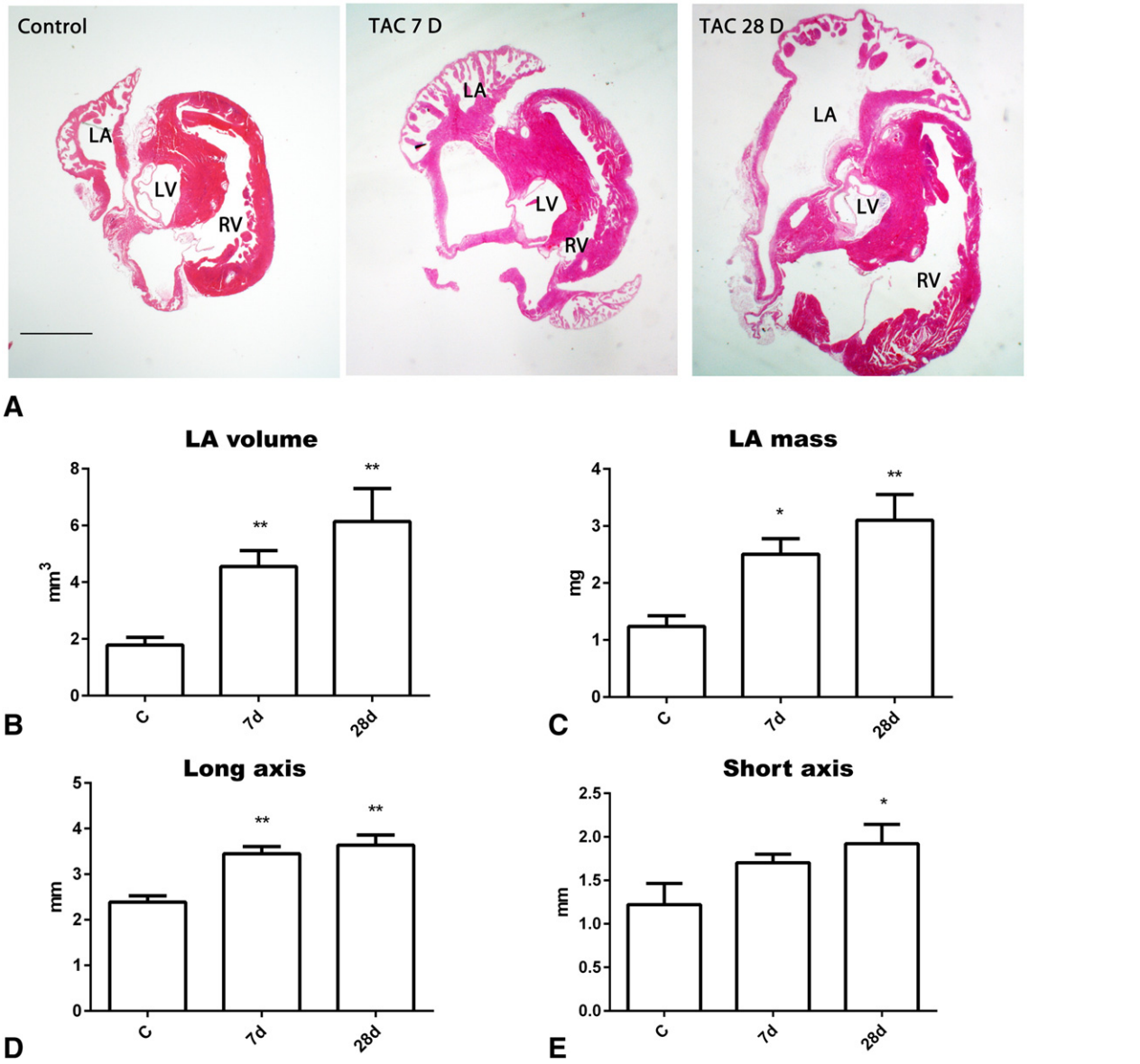

Fig. 1. Cardiac pressure overload induces left atrial remodeling. Following TAC, adult mice developed marked concentric left ventricular hypertrophy, followed by late depression of left ventricular systolic function and chamber dilation (Table 1). (A) Hearts were sectioned from base to apex; left atrial volumes and mass were assessed using quantitative morphometric analysis. TAC was associated with a marked increase in left atrial (LA) size. Representative images show H&E-stained sections from a control mouse and from animals sacrificed after 7 and 28 days of TAC. Quantitative analysis showed that pressure overload induced a marked increase in LA volume (B) and LA mass (C). TAC was associated with a marked increase in the long-axis dimension (D) of the LA and a much less impressive increase in the short-axis dimension (E), suggesting eccentric remodeling (*P<.05, **P<.01 vs. control, n=7–11/group). Additional symbols: LV, left ventricle; RV, right ventricle (scalebar=1 mm).

db mice had a twofold increase in atrial WGA-stained area, reflecting significant widening of the atrial interstitium in obese diabetic animals (Fig. 6M).

Atrial fibrosis was associated with increased interstitial cellular content in all three models of left ventricular disease. Cardiac pressure overload was associated with a fourfold increase in interstitial cellularity after 7–28 days of TAC (Fig. 4P). Following nonreperfused myocardial infarction, atrial interstitial density exhibited a threefold increase after 7 and 28 days of coronary occlusion (Fig. 5P). db/db hearts exhibited a 50% increase in interstitial cellularity when compared with lean mouse hearts (Fig. 6N).

Table 2
Left ventricular remodeling in the mouse model of myocardial infarction

	Pre	28 days (n=9)
LVEDD (mm)	3.77±0.10	6.70±0.28**
Ejection fraction (%)	61.32±3.96	9.81±2.35**
LVEDV (μl)	62.31±4.25	245.20±23.92**
AWTd (mm)	0.74±0.04	0.36±0.05**
PWTd (mm)	0.59±0.02	0.35±0.05**
LV mass (mg)	85.54±7.52	121.10±21.30

** P<.01 vs. pre.

3.5. Localization of connexin-43 in remodeling atria

Because changes in connexin expression have been linked with atrial arrhythmias, we examined connexin-43 localization in remodeling atria. In normal left atrium, connexin-43 was localized in intercalated discs (Fig. 7A). Following myocardial infarction, atrial connexin-43 immunoreactivity was markedly reduced and exhibited heterogeneous distribution and lateralization (Fig. 7B–C). Pressure-overloaded hearts also exhibited attenuated atrial connexin-43 expression, accompanied by lateralization (Fig. 7D–E). In contrast, db/db mice did not have significant changes in atrial connexin-43 expression (Fig. 7F).

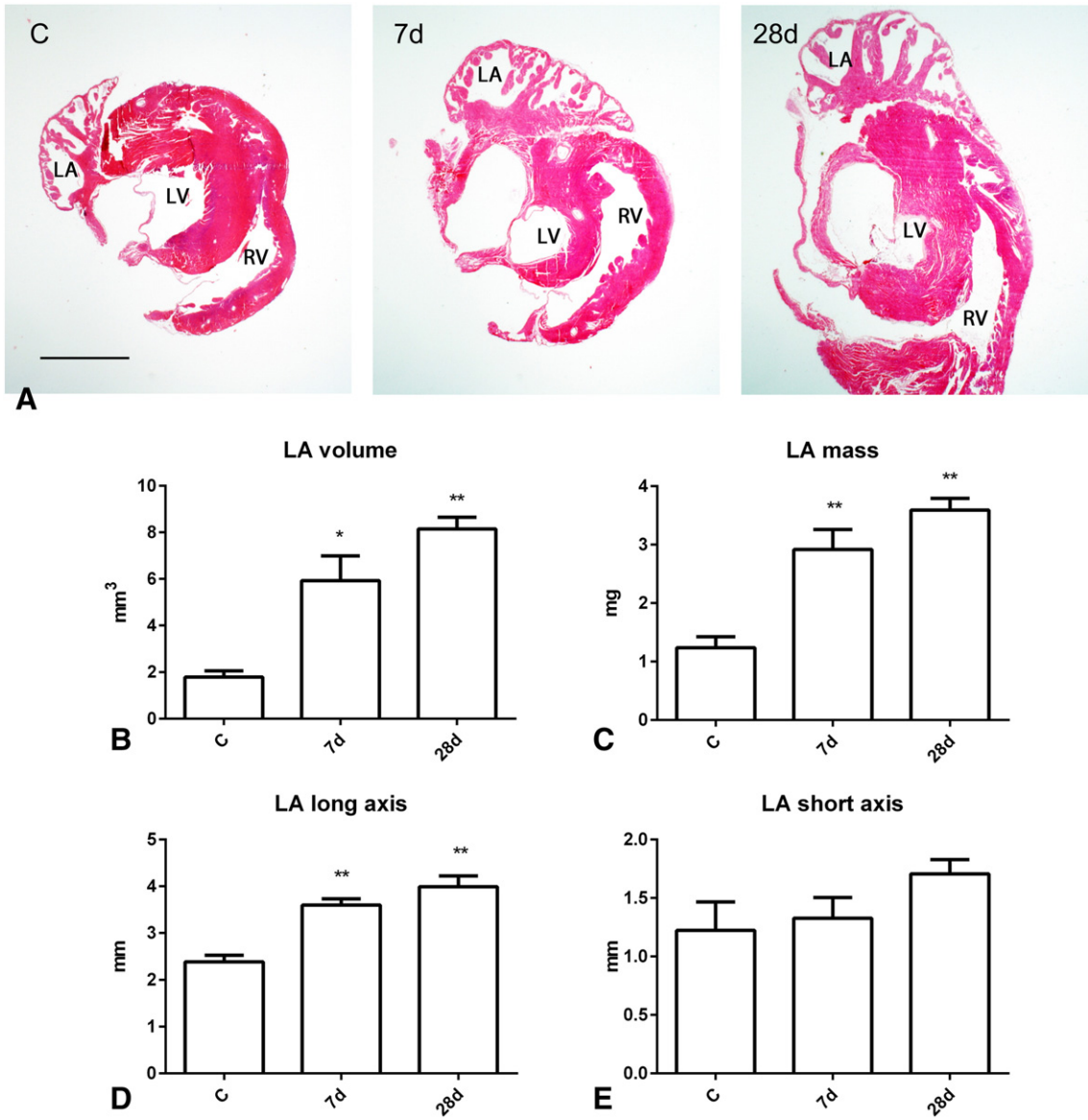

Fig. 2. Left atrial remodeling following nonreperfused myocardial infarction. Nonreperfused myocardial infarction is associated with marked left ventricular dilation and systolic dysfunction (Table 2). (A) Infarcted mouse hearts exhibit marked increases in LA size. Morphometric analysis showed that LA volume (B) and LA mass (C) are markedly increased 7–28 days after myocardial infarction. Atrial remodeling is characterized by marked increase in the long-axis dimension (D) but no significant effect on the short-axis dimension (E), suggesting eccentric remodeling (*P<.05, **P<.01 vs. control, n=6–10/group) (scalebar=1 mm).

4. Discussion

In human patients, assessment of atrial size and geometry serves as a window to cardiac hemodynamics and diastolic function. In contrast to Doppler indices of diastolic function, which are sensitive to changes in preload and afterload [34], left atrial size may be a more stable indicator that reflects the duration and severity of diastolic dysfunction [35]. Although left atrial volume has been extensively used as a relevant functional endpoint in assessment of diastolic function in large animal models of cardiac injury [36], changes in atrial geometry and structure are seldom studied in mouse models of left ventricular disease. This is due in part to technical challenges in evaluation of the left atrium in mice and in part to the absence of evidence characterizing the structural and geometric changes of the left atrium following murine cardiac injury. Our study provides a systematic descriptive analysis of atrial remodeling in three clinically relevant mouse models of left ventricular disease.

Table 3
Left ventricular remodeling in diabetic hearts

	Lean (n=6)	db/db (n=8)
BW (g)	22.81±0.81	59.66±6.42
TL (mm)	18.66±0.76	20.25±0.91
LVEDD (mm)	3.55±0.21	3.85±0.20
Ejection fraction (%)	67.28±2.71	65.41±1.86
LVEDV (μl)	55.98±4.57	73.68±6.73 (P=.07)
AWTd (mm)	0.91±0.01	0.91±0.04
PWTd (mm)	0.73±0.04	0.98±0.06**
LV mass (mg)	109.38±13.95	137.27±10.16 (P=.12)
E:A	1.5±0.15	1.54±0.18
E:E'	18.6±1.12	37.19±3.72**

** P<.01 vs. lean.

4.1. Atrial cardiomyopathy in mouse models of left ventricular disease

In the clinical context, the term *atrial cardiomyopathy* is used to describe a wide range of structural, functional, and electrophysiological alterations of the atria, capable of producing clinical manifestations [37]. A recent histopathological classification defined four classes of atrial

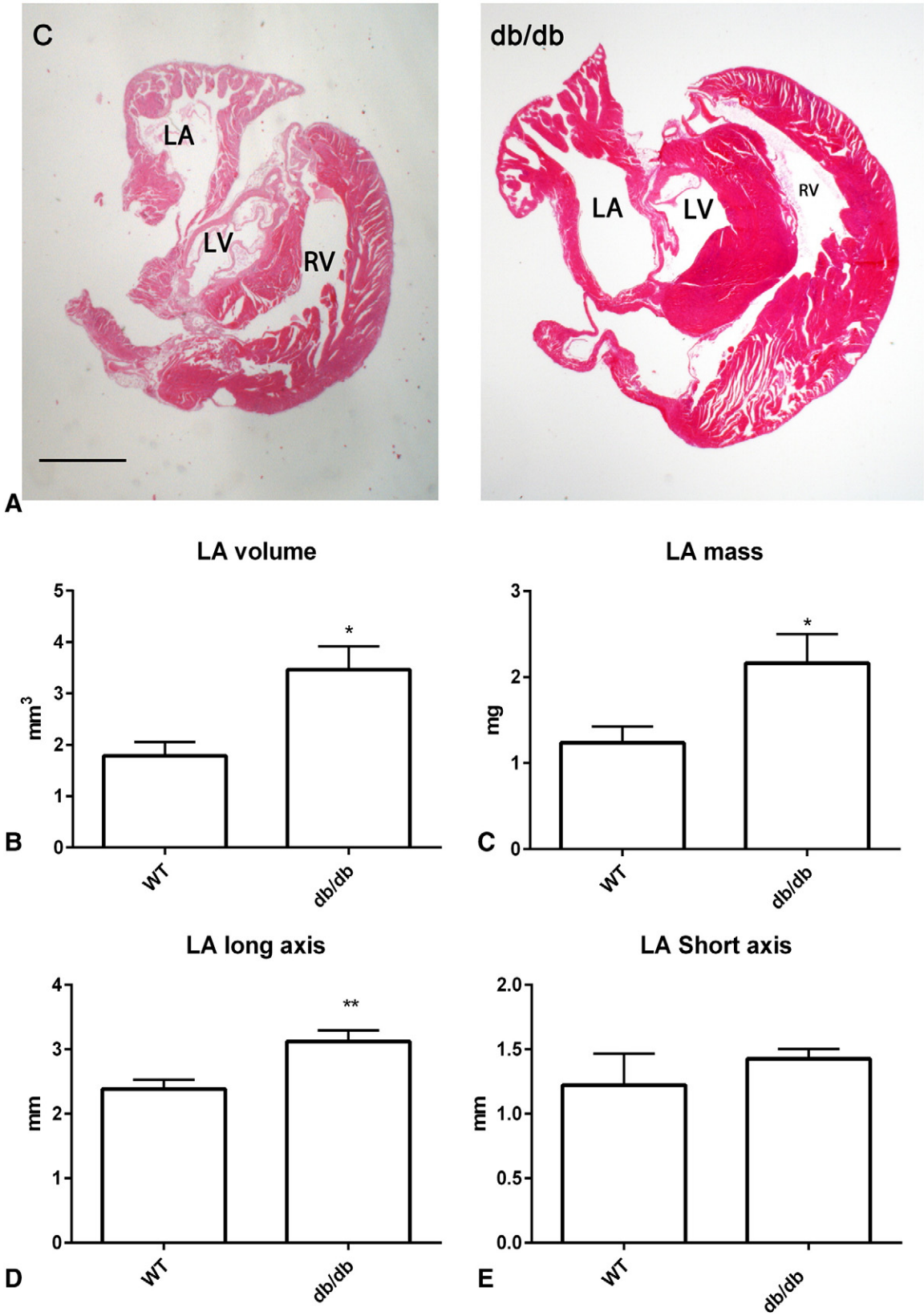

Fig. 3. Left atrial remodeling in diabetic mice. At 6 months of age, db/db mice exhibited a trend toward increased LV mass and evidence of diastolic dysfunction (Table 3). (A) These changes were associated with significantly increased LA size. Morphometric analysis showed that LA volume (B) and LA mass (C) were significantly higher in db/db mice when compared with lean controls. There was a significant increase in the long-axis LA dimension (D) without a significant difference in the LA short-axis dimension (E), suggesting eccentric atrial remodeling (scalebar=1 mm).

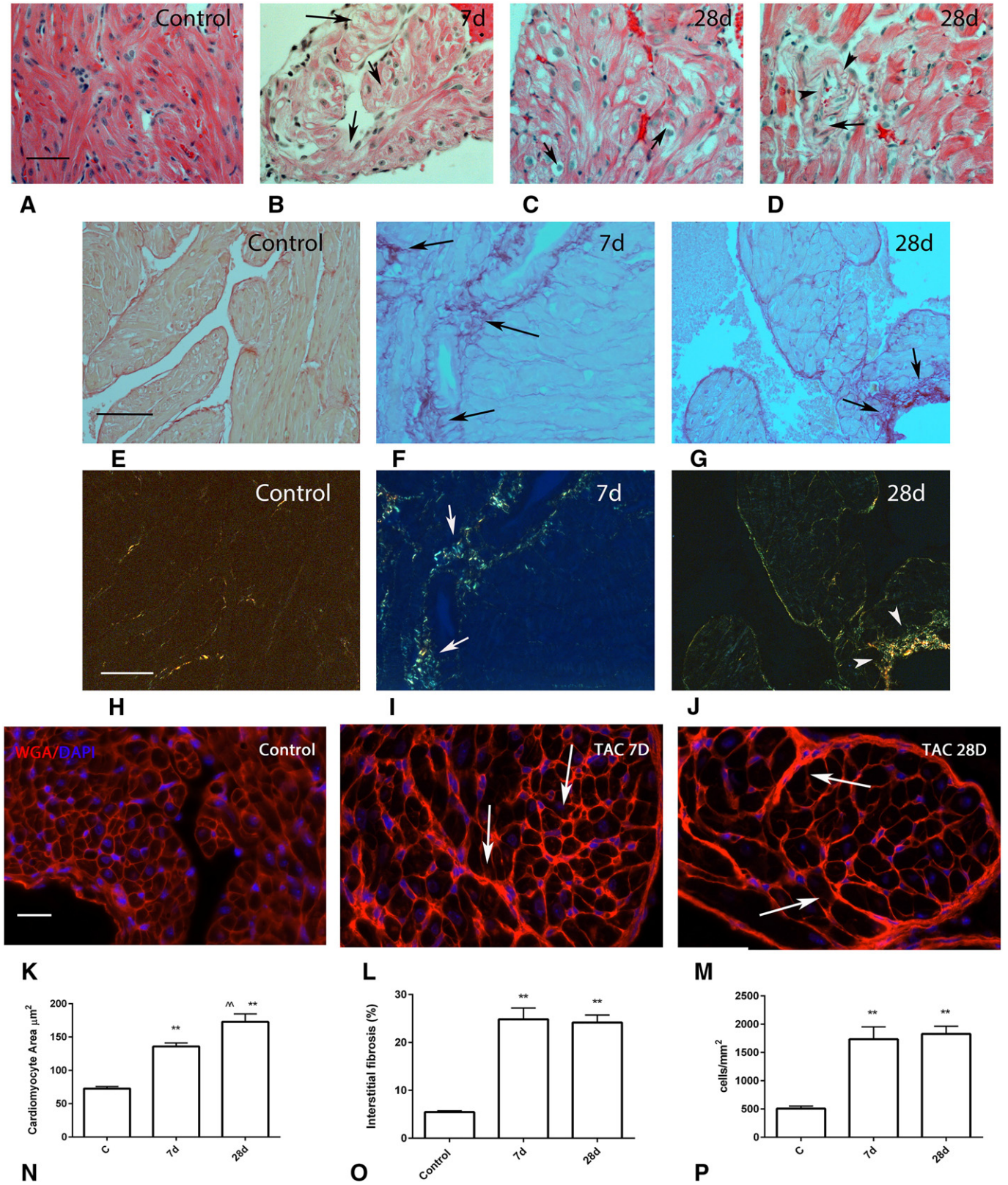

Fig. 4. Left ventricular pressure overload induces progressive loss of contractile elements in atrial cardiomyocytes and causes atrial cardiomyocyte hypertrophy and interstitial fibrosis. (A–D) H&E staining shows representative left atrial sections from a control mouse (A) and from pressure-overloaded animals after 7 (B) and 28 days (C–D) of TAC (scalebar=40 µm). Pressure-overloaded animals exhibited extensive loss of the myofibrillar component in a subset of atrial cardiomyocytes (arrows). (E–J) Sirius red staining visualized with light (E–G) and polarized microscopy (H–J) demonstrated significant atrial interstitial fibrosis (arrows) after 7–28 days of TAC. Thicker fibers exhibit orange/red birefringence when visualized with polarized light (J, arrowheads). Scalebar=75 µm. (K–M) WGA lectin histochemistry was used to outline cardiomyocytes and to quantitatively assess the atrial interstitial space. DAPI fluorescent staining was used to assess interstitial cellularity. Representative images show WGA/DAPI fluorescence in left atrial sections from control hearts (K) and from pressure-overloaded animals after 7 (L) and 28 (M) days of TAC (scalebar=25 µm). (N) Quantitative analysis showed that atrial cardiomyocyte size significantly increased after 7–28 days of TAC (**P<.01 vs. control; ^^P<.01 vs. 7 days, n=6/group). (O) The WGA-stained area in the left atrium was significantly increased after 7–28 days of TAC (**P<.01 vs. control, n=6/group), suggesting significant atrial interstitial fibrosis. (P) Left atrial interstitial cellularity was significantly increased after 7–28 days of TAC (**P<.01 vs. control, n=6/group).

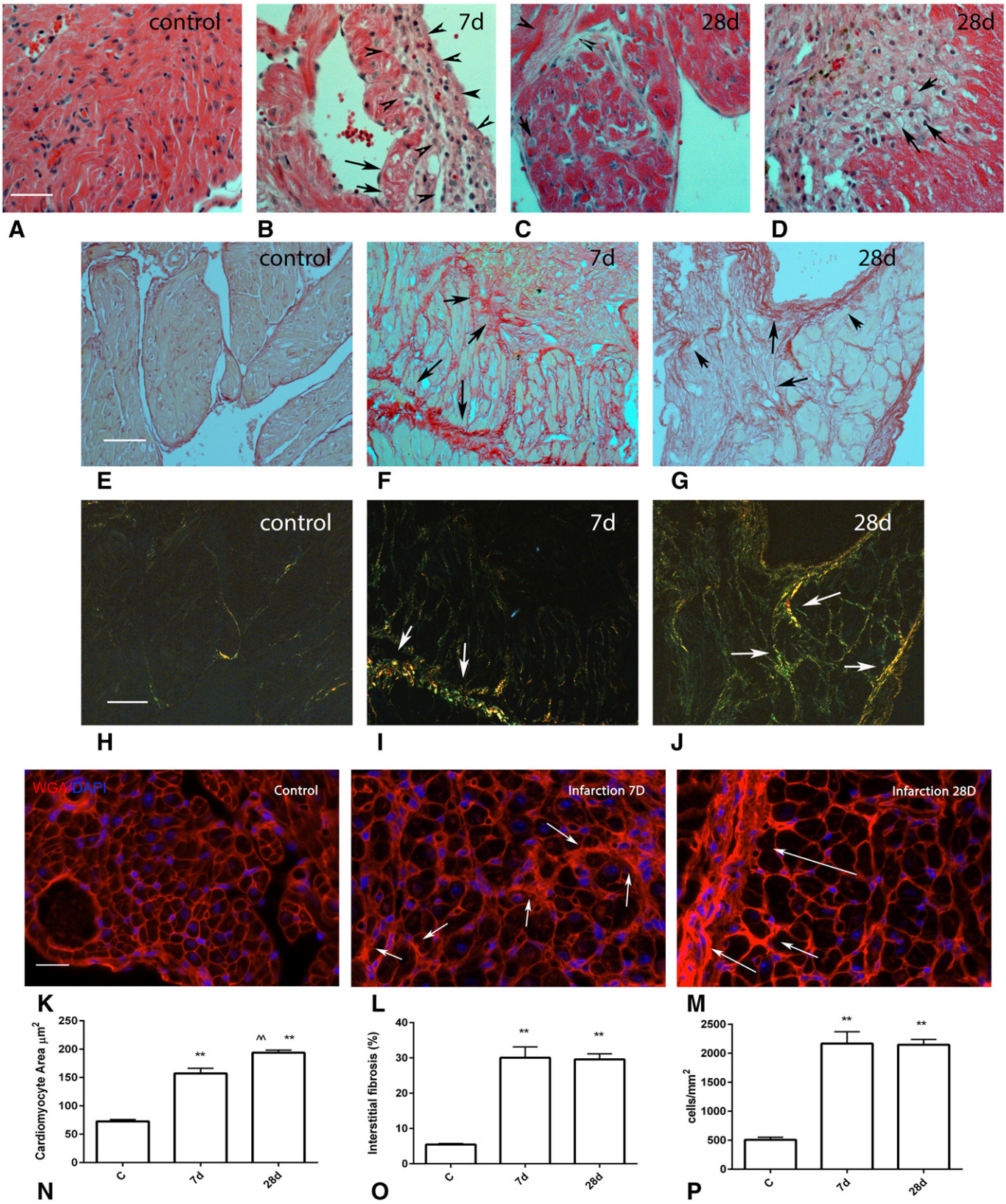

Fig. 5. Myocardial infarction is associated with atrial cardiomyocyte hypertrophy and interstitial fibrosis. (A–D) Representative H&E-stained atrial sections from control (A) and infarcted mouse hearts after 7 (B) and 28 days (C–D) of permanent coronary occlusion (scalebar=40 µm). Infarcted mice showed fibrosis (arrowheads). A significant number of cardiomyocytes exhibited loss of contractile material (arrows). (E–J) Sirius-red-stained sections visualized with light (E–G) and polarized (H–J) microscopy show fibrotic remodeling of the atrium following myocardial infarction (arrows, scalebar=60 µm). Thicker collagen fibers exhibit orange/red birefringence under polarized light (arrows). (K–M) WGA/DAPI fluorescence in representative atrial sections from control animals (K) and from infarcted animals after 7 (L) and 28 days of permanent coronary occlusion (M). Scalebar=25 µm. Quantitative analysis showed that left atrial cardiomyocyte size (N), the WGA-stained atrial interstitial area (O), and atrial interstitial cell density (P) were markedly increased 7–28 days after coronary occlusion (**P<.01 vs. control, ^^P<.01 vs. 7-days, n=6/group).

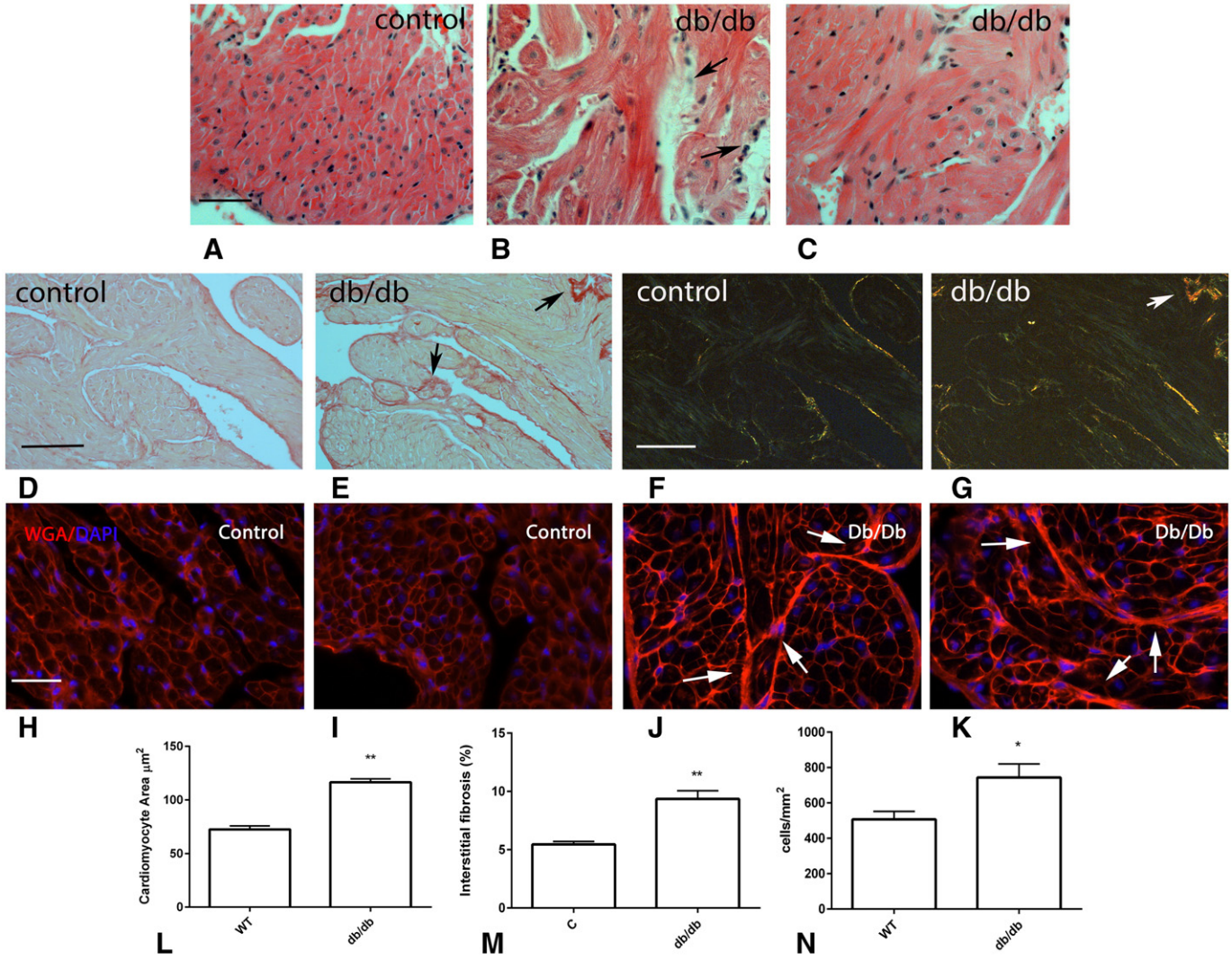

Fig. 6. Diabetic hearts exhibit atrial cardiomyocyte hypertrophy and expansion of the atrial interstitium. (A–C) Representative H&E-stained left atrial sections show that atria from db/db mice have hypertrophic changes and mild fibrosis (arrows) at 6 months of age (scalebar=40 µm). (D–G) Sirius-red-stained sections visualized with light (D–E) and polarized (F–G) microscopy show mild fibrotic remodeling of the atrium in db/db mice (arrows, scalebar=75 µm). Thicker collagen fibers exhibit orange/red birefringence under polarized light (G, arrow). (H–K) Representative images show WGA/DAPI fluorescence in left atrial sections from lean control mice (H, I) and db/db animals (J, K). Scalebar=30 µm. db/db animals exhibited increased left atrial cardiomyocyte size (L), an increase in WGA-stained interstitial area (M), and higher interstitial cell density (N) when compared to lean control animals (*P<.05, **P<.01 vs control, n=6/group).

cardiomyopathies on the basis of the predominant underlying pathology: class I shows primarily cardiomyocyte changes, class II exhibits principally fibrotic remodeling, class III shows a combination of cardiomyocyte and fibrotic alterations, and class IV is characterized by deposition of noncollagenous material or inflammatory infiltration in the presence or absence of cardiomyocyte alterations [37]. Our findings in three different mouse models of left ventricular disease suggest the presence of an atrial cardiomyopathy with class III characteristics. Mice undergoing TAC protocols and animals with nonreperfused myocardial infarction exhibited loss of contractile material in a subset of cardiomyocytes associated with progressive hypertrophy and fibrosis (Figs. 4 and 5). Obese diabetic mice had less severe atrial pathology, exhibiting mild atrial cardiomyocyte hypertrophy and atrial fibrosis (Fig. 6). The morphological and histopathological changes in the mouse models of left ventricular disease are summarized in Table 4.

4.2. Atrial remodeling and fibrosis in response to cardiac pressure overload

Using quantitative morphometry, we demonstrated that pressure overload causes marked increases in left atrial volume and left atrial mass, and reduced sphericity of the chamber, as early as 7 days after TAC (Fig. 1). These changes were associated with evidence of atrial fibrosis and atrial cardiomyocyte hypertrophy (Fig. 4). Published studies have documented dilative atrial remodeling in mouse models of pressure overload. Using echocardiographic analysis, Zile and coworkers [38] showed a late increase in left atrial dimensions 4 weeks after TAC. Late detection of atrial remodeling may reflect the challenges in echocardiographic visualization of the mouse atria and the eccentric pattern of remodeling. Moreover, in male mice undergoing TAC protocols, De Jong and colleagues noted a progressive atrial hypertrophy accompanied by increases in atrial expression of extracellular matrix proteins such as collagen I, III, and fibronectin [21]. The authors did not document histological evidence of atrial fibrosis; however, the limited sensitivity of the trichrome stain used to assess the atrial interstitial matrix [22] may explain these negative findings.

4.3. Atrial remodeling following myocardial infarction

Our findings documented eccentric left atrial dilation, hypertrophy, and left atrial fibrosis in mice with large nonreperfused left coronary artery territory infarcts (Figs. 2 and 5). The findings are consistent with similar observations by Colazzo and coworkers [22] that demonstrated

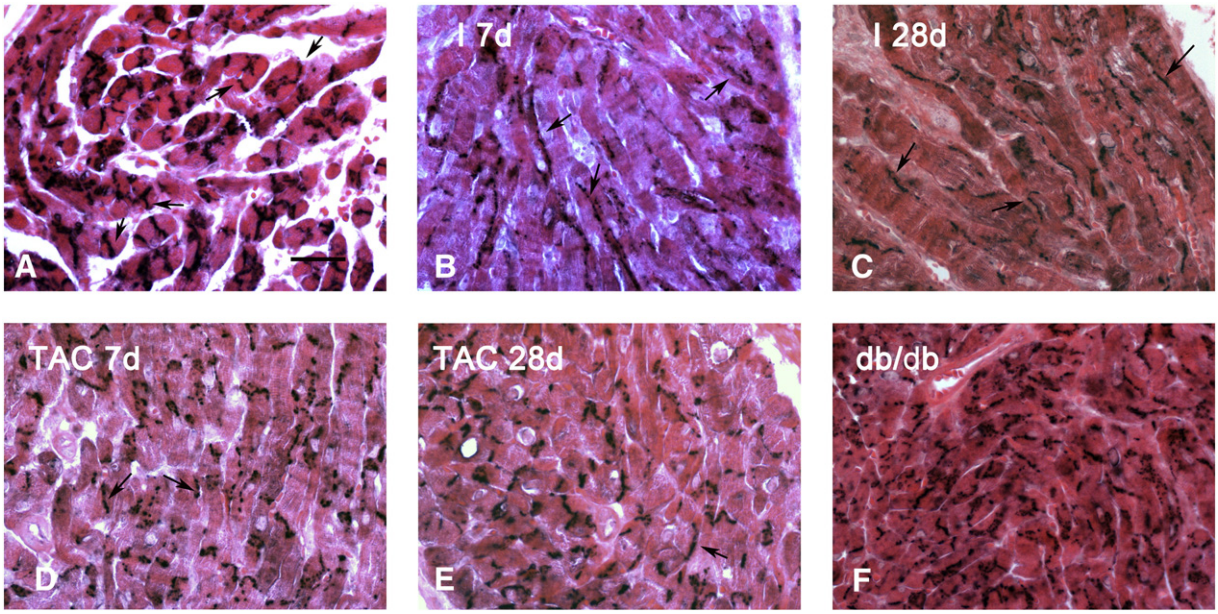

Fig. 7. Connexin-43 localization in remodeling atria. (A) Immunohistochemical staining shows that, in normal mouse left atrium, connexin-43 is localized in intercalated discs (arrows). (B–C) Representative left atrial sections from infarcted mice after 7 (B) and 28 days (C) of coronary occlusion show marked reduction of connexin-43 immunoreactivity associated with loss of the normal pattern and lateralization (arrows). (D–E) Attenuated connexin-43 expression and lateralization (arrows) were also noted in pressure-overloaded hearts after 7 (D) and 28 days (E) of TAC. (F) In contrast, db/db mice did not have significant changes in connexin-43 immunoreactivity. Representative sections show findings from four different animals for each group. Scalebar=25 μm.

echocardiographic evidence of increased left atrial dimensions 4 weeks after coronary occlusion. Although increased filling pressures due to the extensive left ventricular dysfunction likely account for the alterations in atrial geometry and architecture observed in infarcted animals, a subset of mice exhibited small areas of left atrial infarction that may contribute to atrial remodeling.

4.4. Atrial remodeling in diabetes, obesity, and metabolic dysfunction

Obese and diabetic subjects exhibit increases in left atrial volumes even in the absence of hypertension or overt cardiovascular disease [39]; these changes are accompanied by an increased incidence of atrial tachyarrhythmias [40]. Our findings show that mice with obesity and diabetes due to genetic central leptin resistance have significant atrial dilation and increased left atrial mass associated with atrial cardiomyocyte hypertrophy, fibrosis, and a 50% increase in interstitial cellularity (Fig. 6). Consistent with our findings, published studies have demonstrated significant atrial fibrosis in rats with type1 or type 2 diabetes [41,42]. In contrast, in mouse models of diabetes, atrial fibrosis has not been consistently documented. In adult male mice, a high-fat diet for 2 months increased the vulnerability to atrial arrhythmias without causing atrial fibrosis [43].

Atrial remodeling in obese diabetic subjects may reflect elevations in left ventricular filling pressures due to diastolic dysfunction but may also result from direct effects of metabolic dysregulation on atrial cardiomyocytes and fibroblasts [44]. Diabetes-associated generation of reactive oxygen species, activation of advanced glycation end-products (AGE)–receptor for AGE signaling, and stimulation of angiotensin II or growth factor pathways may activate atrial fibroblasts, triggering left atrial fibrosis [45]. In patients with coronary disease, diabetes was associated with an activated atrial fibroblast phenotype, showing a twofold increase in collagen transcription [46].

4.5. Connexin remodeling: a potential link between structural alterations and atrial tachyarrhythmias

Atrial remodeling is often associated with atrial tachyarrhythmias; however, the molecular links between structural changes and arrhythmia generation remain poorly understood. Gap junctions are specialized intercellular connections that enable propagation of the electrical impulse and consist of four transmembrane proteins, members of the connexin family [47]. In both experimental models and human patients, atrial fibrillation is associated with alterations in the levels of expression and in localization of the connexins [48,49]. However, the patterns of these changes are often inconsistent in various models [47]. Our findings demonstrate a marked attenuation in connexin-43 immunoreactivity in the left atrium of mice undergoing pressure overload or myocardial infarction protocols (Fig. 7). Reduced expression of connexin-43 in remodeling atria was associated with “lateralization,” ectopic expression of connexin-43 along the major axis of the

Table 4
Overview of the geometric and histopathological alterations of the left atrium in models of left ventricular disease

Mouse model	Geometric changes	Cardiomyocyte alterations	Interstitial changes
Nonreperfused myocardial infarction	1. Severe, progressive, eccentric left atrial dilation. 2. Markedly increased left atrial mass.	1. Myofibrillar loss in a subset of cardiomyocytes. 2. Progressive and severe atrial cardiomyocyte hypertrophy. 3. Connexin-43 loss and lateralization.	1. Severe atrial fibrosis. 2. Marked infiltration with interstitial cells
TAC	1. Severe, progressive eccentric left atrial dilation. 2. Markedly increased left atrial mass.	1. Myofibrillar loss in a subset of cardiomyocytes. 2. Progressive and severe atrial cardiomyocyte hypertrophy. 3. Connexin-43 loss and lateralization.	1. Severe atrial fibrosis. 2. Marked infiltration with interstitial cells
db/db mouse	1. Left atrial dilation. 2. Increased left atrial mass.	1. Atrial cardiomyocyte hypertrophy. 2. No significant degenerative changes in atrial cardiomyocytes. 3. Minimal changes in connexin-43 localization.	1. Mild atrial fibrosis. 2. Increased interstitial cell content.

cardiomyocytes, instead of the typical localization in intercalated discs. Whether gap junctional remodeling may trigger atrial fibrillation in mouse models of left ventricular disease remains unknown.

4.6. Conclusions

Much like in human patients, mouse models of left ventricular disease exhibit left atrial remodeling. Considering the prognostic value of atrial size parameters in patients with cardiovascular disease, assessment of left atrial mass, volume, and geometric remodeling may represent an important tool for functional evaluation, in particular in studies investigating the chronic consequences of diastolic dysfunction. Moreover, dissection of the cell biological mechanisms responsible for atrial fibrosis may contribute to our understanding of the pathogenesis of atrial tachyarrhythmias.

References

[1] Pritchett AM, Mahoney DW, Jacobsen SJ, Rodeheffer RJ, Karon BL, Redfield MM. Diastolic dysfunction and left atrial volume: a population-based study. J Am Coll Cardiol 2005;45(1):87–92.
[2] Moller JE, Hillis GS, Oh JK, Seward JB, Reeder GS, Wright RS, et al. Left atrial volume: a powerful predictor of survival after acute myocardial infarction. Circulation 2003; 107(17):2207–12.
[3] Beinart R, Boyko V, Schwammenthal E, Kuperstein R, Sagie A, Hod H, et al. Long-term prognostic significance of left atrial volume in acute myocardial infarction. J Am Coll Cardiol 2004;44(2):327–34.
[4] Yang WI, Shim CY, Kim YJ, Kim SA, Rhee SJ, Choi EY, et al. Left atrial volume index: a predictor of adverse outcome in patients with hypertrophic cardiomyopathy. J Am Soc Echocardiogr 2009;22(12):1338–43.
[5] Sabharwal N, Cemin R, Rajan K, Hickman M, Lahiri A, Senior R. Usefulness of left atrial volume as a predictor of mortality in patients with ischemic cardiomyopathy. Am J Cardiol 2004;94(6):760–3.
[6] Rossi A, Cicoira M, Bonapace S, Golia G, Zanolla L, Franceschini L, et al. Left atrial volume provides independent and incremental information compared with exercise tolerance parameters in patients with heart failure and left ventricular systolic dysfunction. Heart 2007;93(11):1420–5.
[7] Poulsen MK, Dahl JS, Henriksen JE, Hey TM, Hoilund-Carlsen PF, Beck-Nielsen H, et al. Left atrial volume index: relation to long-term clinical outcome in type 2 diabetes. J Am Coll Cardiol 2013;62(25):2416–21.
[8] Kizer JR, Bella JN, Palmieri V, Liu JE, Best LG, Lee ET, et al. Left atrial diameter as an independent predictor of first clinical cardiovascular events in middle-aged and elderly adults: the Strong Heart Study (SHS). Am Heart J 2006;151(2):412–8.
[9] Corradi D. Atrial fibrillation from the pathologist's perspective. Cardiovasc Pathol 2014;23(2):71–84.
[10] Thomas L, Abhayaratna WP. Left atrial reverse remodeling: mechanisms, evaluation, and clinical significance. JACC Cardiovasc Imaging 2017;10(1):65–77.
[11] Tanaka K, Zlochiver S, Vikstrom KL, Yamazaki M, Moreno J, Klos M, et al. Spatial distribution of fibrosis governs fibrillation wave dynamics in the posterior left atrium during heart failure. Circ Res 2007;101(8):839–47.
[12] Nattel S. How does fibrosis promote atrial fibrillation persistence: in silico findings, clinical observations, and experimental data. Cardiovasc Res 2016;110(3):295–7.
[13] Hirsh BJ, Copeland-Halperin RS, Halperin JL. Fibrotic atrial cardiomyopathy, atrial fibrillation, and thromboembolism: mechanistic links and clinical inferences. J Am Coll Cardiol 2015;65(20):2239–51.
[14] Frangogiannis NG. Pathophysiology of myocardial infarction. Compr Physiol 2015; 5(4):1841–75.
[15] Rai V, Sharma P, Agrawal S, Agrawal DK. Relevance of mouse models of cardiac fibrosis and hypertrophy in cardiac research. Mol Cell Biochem 2017;424(1–2):123–45.
[16] Kong P, Christia P, Frangogiannis NG. The pathogenesis of cardiac fibrosis. Cell Mol Life Sci 2014;71(4):549–74.
[17] Kemp CD, Conte JV. The pathophysiology of heart failure. Cardiovasc Pathol 2012; 21(5):365–71.
[18] Gonzalez-Quesada C, Cavalera M, Biernacka A, Kong P, Lee DW, Saxena A, et al. Thrombospondin-1 induction in the diabetic myocardium stabilizes the cardiac matrix in addition to promoting vascular rarefaction through angiopoietin-2 upregulation. Circ Res 2013;113(12):1331–44.
[19] Shinde AV, Dobaczewski M, de Haan JJ, Saxena A, Lee KK, Xia Y, et al. Tissue transglutaminase induction in the pressure-overloaded myocardium regulates matrix remodeling. Cardiovasc Res 2017. http://dx.doi.org/10.1093/cvr/cvx053 [epub ahead of print].
[20] Frangogiannis NG. The extracellular matrix in myocardial injury, repair, and remodeling. J Clin Invest 2017;127(5):1600–12.
[21] De Jong AM, Van Gelder IC, Vreeswijk-Baudoin I, Cannon MV, Van Gilst WH, Maass AH. Atrial remodeling is directly related to end-diastolic left ventricular pressure in a mouse model of ventricular pressure overload. PLoS One 2013;8(9):e72651.
[22] Colazzo F, Castiglioni L, Sironi L, Fontana L, Nobili E, Franzosi M, et al. Murine left atrium and left atrial appendage structure and function: echocardiographic and morphologic evaluation. PLoS One 2015;10(4):e0125541.
[23] Rockman HA, Ross RS, Harris AN, Knowlton KU, Steinhelper ME, Field LJ, et al. Segregation of atrial-specific and inducible expression of an atrial natriuretic factor transgene in an in vivo murine model of cardiac hypertrophy. Proc Natl Acad Sci U S A 1991;88(18):8277–81.
[24] Xia Y, Lee K, Li N, Corbett D, Mendoza L, Frangogiannis NG. Characterization of the inflammatory and fibrotic response in a mouse model of cardiac pressure overload. Histochem Cell Biol 2009;131(4):471–81.
[25] Frunza O, Russo I, Saxena A, Shinde AV, Humeres C, Hanif W, et al. Myocardial galectin-3 expression is associated with remodeling of the pressure-overloaded heart and may delay the hypertrophic response without affecting survival, dysfunction, and cardiac fibrosis. Am J Pathol 2016;186(5):1114–27.
[26] Xia Y, Dobaczewski M, Gonzalez-Quesada C, Chen W, Biernacka A, Li N, et al. Endogenous thrombospondin 1 protects the pressure-overloaded myocardium by modulating fibroblast phenotype and matrix metabolism. Hypertension 2011;58(5):902–11.
[27] Saxena A, Shinde AV, Haque Z, Wu YJ, Chen W, Su Y, et al. The role of interleukin receptor associated kinase (IRAK)-M in regulation of myofibroblast phenotype in vitro, and in an experimental model of non-reperfused myocardial infarction. J Mol Cell Cardiol 2015;89(Pt B):223–31.
[28] Biernacka A, Cavalera M, Wang J, Russo I, Shinde A, Kong P, et al. Smad3 signaling promotes fibrosis while preserving cardiac and aortic geometry in obese diabetic mice. Circ Heart Fail 2015;8(4):788–98.
[29] Nagueh SF, Appleton CP, Gillebert TC, Marino PN, Oh JK, Smiseth OA, et al. Recommendations for the evaluation of left ventricular diastolic function by echocardiography. J Am Soc Echocardiogr 2009;22(2):107–33.
[30] Christia P, Bujak M, Gonzalez-Quesada C, Chen W, Dobaczewski M, Reddy A, et al. Systematic characterization of myocardial inflammation, repair, and remodeling in a mouse model of reperfused myocardial infarction. J Histochem Cytochem 2013; 61(8):555–70.
[31] Kerns MJ, Darst MA, Olsen TG, Fenster M, Hall P, Grevey S. Shrinkage of cutaneous specimens: formalin or other factors involved? J Cutan Pathol 2008;35(12):1093–6.
[32] Emde B, Heinen A, Godecke A, Bottermann K. Wheat germ agglutinin staining as a suitable method for detection and quantification of fibrosis in cardiac tissue after myocardial infarction. Eur J Histochem 2014;58(4):2448.
[33] Whittaker P, Kloner RA, Boughner DR, Pickering JG. Quantitative assessment of myocardial collagen with picrosirius red staining and circularly polarized light. Basic Res Cardiol 1994;89(5):397–410.
[34] Hurrell DG, Nishimura RA, Ilstrup DM, Appleton CP. Utility of preload alteration in assessment of left ventricular filling pressure by Doppler echocardiography: a simultaneous catheterization and Doppler echocardiographic study. J Am Coll Cardiol 1997;30(2):459–67.
[35] Simek CL, Feldman MD, Haber HL, Wu CC, Jayaweera AR, Kaul S. Relationship between left ventricular wall thickness and left atrial size: comparison with other measures of diastolic function. J Am Soc Echocardiogr 1995;8(1):37–47.
[36] Ishikawa K, Aguero J, Oh JG, Hammoudi N, Fish LA, Leonardson L, et al. Increased stiffness is the major early abnormality in a pig model of severe aortic stenosis and predisposes to congestive heart failure in the absence of systolic dysfunction. J Am Heart Assoc 2015;4(5). http://dx.doi.org/10.1161/JAHA.115.001925.
[37] Goette A, Kalman JM, Aguinaga L, Akar J, Cabrera JA, Chen SA, et al. EHRA/HRS/APHRS/SOLAECE expert consensus on atrial cardiomyopathies: definition, characterization, and clinical implication. Europace 2016;18(10):1455–90.
[38] Zile MR, Baicu CF, Stroud RE, Van Laer A, Arroyo J, Mukherjee R, et al. Pressure overload-dependent membrane type 1-matrix metalloproteinase induction: relationship to LV remodeling and fibrosis. Am J Physiol Heart Circ Physiol 2012; 302(7):H1429–37.
[39] Atas H, Kepez A, Atas DB, Kanar BG, Dervisova R, Kivrak T, et al. Effects of diabetes mellitus on left atrial volume and functions in normotensive patients without symptomatic cardiovascular disease. J Diabetes Complications 2014;28(6):858–62.
[40] Goudis CA, Korantzopoulos P, Ntalas IV, Kallergis EM, Ketikoglou DG. Obesity and atrial fibrillation: a comprehensive review of the pathophysiological mechanisms and links. J Cardiol 2015;66(5):361–9.
[41] Saito S, Teshima Y, Fukui A, Kondo H, Nishio S, Nakagawa M, et al. Glucose fluctuations increase the incidence of atrial fibrillation in diabetic rats. Cardiovasc Res 2014; 104(1):5–14.
[42] Linz D, Hohl M, Dhein S, Ruf S, Reil JC, Kabiri M, et al. Cathepsin a mediates susceptibility to atrial tachyarrhythmia and impairment of atrial emptying function in Zucker diabetic fatty rats. Cardiovasc Res 2016;110(3):371–80.
[43] Takahashi K, Sasano T, Sugiyama K, Kurokawa J, Tamura N, Soejima Y, et al. High-fat diet increases vulnerability to atrial arrhythmia by conduction disturbance via miR-27b. J Mol Cell Cardiol 2016;90:38–46.
[44] Cavalera M, Wang J, Frangogiannis NG. Obesity, metabolic dysfunction, and cardiac fibrosis: pathophysiological pathways, molecular mechanisms, and therapeutic opportunities. Transl Res 2014;164(4):323–35.
[45] Russo I, Frangogiannis NG. Diabetes-associated cardiac fibrosis: cellular effectors, molecular mechanisms and therapeutic opportunities. J Mol Cell Cardiol 2016;90:84–93.
[46] Sedgwick B, Riches K, Bageghni SA, O'Regan DJ, Porter KE, Turner NA. Investigating inherent functional differences between human cardiac fibroblasts cultured from nondiabetic and type 2 diabetic donors. Cardiovasc Pathol 2014;23(4):204–10.
[47] Corradi D, Callegari S, Maestri R, Benussi S, Alfieri O. Structural remodeling in atrial fibrillation. Nat Clin Pract Cardiovasc Med 2008;5(12):782–96.
[48] Polontchouk L, Haefliger JA, Ebelt B, Schaefer T, Stuhlmann D, Mehlhorn U, et al. Effects of chronic atrial fibrillation on gap junction distribution in human and rat atria. J Am Coll Cardiol 2001;38(3):883–91.
[49] Kostin S, Klein G, Szalay Z, Hein S, Bauer EP, Schaper J. Structural correlate of atrial fibrillation in human patients. Cardiovasc Res 2002;54(2):361–79.

Cardiovascular Research (2017) **0**, 1–14
doi:10.1093/cvr/cvx053

Tissue transglutaminase induction in the pressure-overloaded myocardium regulates matrix remodelling

Arti V. Shinde[1], Marcin Dobaczewski[1], Judith J. de Haan[1], Amit Saxena[1], Kang-Kon Lee[1], Ying Xia[2], Wei Chen[1], Ya Su[1], Waqas Hanif[1], Inderpreet Kaur Madahar[1], Victor M. Paulino[1], Gerry Melino[3], and Nikolaos G. Frangogiannis[1,2]*

[1]Department of Medicine (Cardiology), Albert Einstein College of Medicine, The Wilf Family Cardiovascular Research Institute, Bronx, NY 10021, USA; [2]Department of Medicine, Baylor College of Medicine, Houston, TX 77030, USA; and [3]Biochemistry IDI-IRCCS Laboratory, Department of Experimental Medicine and Surgery, University of Rome Tor Vergata, 00133 Rome, Italy

Received 2 August 2016; revised 2 February 2017; editorial decision 3 March 2017; accepted 16 March 2017

Time for primary review: 37 days

Aims Tissue transglutaminase (tTG) is induced in injured and remodelling tissues, and modulates cellular phenotype, while contributing to matrix cross-linking. Our study tested the hypothesis that tTG may be expressed in the pressure-overloaded myocardium, and may regulate cardiac function, myocardial fibrosis and chamber remodelling.

Methods and results In order to test the hypothesis, wild-type and tTG null mice were subjected to pressure overload induced through transverse aortic constriction. Moreover, we used isolated cardiac fibroblasts and macrophages to dissect the mechanisms of tTG-mediated actions. tTG expression was upregulated in the pressure-overloaded mouse heart and was localized in cardiomyocytes, interstitial cells, and in the extracellular matrix. In contrast, expression of transglutaminases 1, 3, 4, 5, 6, 7 and FXIII was not induced in the remodelling myocardium. *In vitro*, transforming growth factor (TGF)-β1 stimulated tTG synthesis in cardiac fibroblasts and in macrophages through distinct signalling pathways. tTG null mice had increased mortality and enhanced ventricular dilation following pressure overload, but were protected from diastolic dysfunction. tTG loss was associated with a hypercellular cardiac interstitium, reduced collagen cross-linking, and with accentuated matrix metalloproteinase (MMP)2 activity in the pressure-overloaded myocardium. *In vitro*, tTG did not modulate TGF-β-mediated responses in cardiac fibroblasts; however, tTG loss was associated with accentuated proliferative activity. Moreover, when bound to the matrix, recombinant tTG induced synthesis of tissue inhibitor of metalloproteinases (TIMP)-1 through transamidase-independent actions.

Conclusions Following pressure overload, endogenous tTG mediates matrix cross-linking, while protecting the remodelling myocardium from dilation by exerting matrix-preserving actions.

Keywords Transglutaminase • Cardiac fibrosis • Collagen cross-linking • Fibroblast • Matrix metalloproteinase

1. Introduction

The extracellular matrix plays a critical role in regulating cardiac geometry and function, not only by providing structural support and by determining the mechanical properties of the ventricle, but also by modulating cellular phenotype and behaviour.[1–4] In the normal heart, the cardiac matrix shields interstitial cells from mechanical stress preventing their activation; matrix components may also transduce important homeostatic signals in cardiomyocytes, promoting their survival and regulating their function. In the pressure-overloaded myocardium, the cardiac extracellular matrix undergoes profound changes that critically regulate phenotype and function of both cardiomyocytes and interstitial cells. As the ventricle remodels, newly-synthesized matricellular macromolecules are incorporated into the matrix, serving as molecular bridges that transduce, or modulate growth factor- and cytokine-mediated signals, conferring plasticity to the cardiac interstitium.[5–7] Because all myocardial cells are enmeshed in the matrix network, matricellular actions drive the dynamic cellular changes that occur in the remodelling pressure-overloaded heart.

Tissue transglutaminase (tTG, transglutaminase 2/TG2), a member of the transglutaminase family, is a ubiquitously expressed 80 kDa protein

* Corresponding author. Tel: +718 430 3546; fax: +718 430 8989, E-mail: nikolaos.frangogiannis@einstein.yu.edu

that exerts a wide range of effects on the extracellular matrix and on cellular elements.[8,9] tTG may be secreted into the extracellular space, where it may influence cell behaviour through both enzymatic and non-enzymatic actions. As a typical transglutaminase, tTG catalyses protein deamidation, transamidation and cross-linking;[10] some of its enzymatic substrates have been identified in extracellular compartments, on the cell surface, and in the matrix.[8,11] tTG-mediated cross-linking of matrix proteins such as fibrinogen, fibronectin, collagen and laminin–nidogen basement membrane complexes[12,13] may contribute to the generation of a mechanically stable, stiff and protease-resistant matrix network. More recently, non-enzymatic actions of tTG have been documented, including adapter/scaffolding functions that may directly regulate cell adhesion, migration and differentiation.[8,9,14] Because activation of tTG in the extracellular environment appears to be transient due to its oxidation,[15] the non-enzymatic functions of the molecule may be particularly important *in vivo*. tTG is a stress-inducible gene in most mammalian tissues.[16] In failing hearts, tTG is one of the most upregulated proteins, exhibiting marked induction in experimental models of cardiac volume and pressure overload.[17,18] Although transgenic cardiac-specific overexpression of tTG in mice causes mild hypertrophy and diffuse interstitial fibrosis,[19] the role of endogenous tTG in cardiac remodelling has not been studied. We hypothesized that tTG induction in the pressure-overloaded myocardium may play an important role in fibrosis, dysfunction and geometric remodelling of the ventricle. We demonstrate for the first time that tTG exerts potent matrix-preserving effects on the pressure-overloaded myocardium, promoting fibrosis, matrix cross-linking, and diastolic dysfunction, while protecting from dilative remodelling and systolic dysfunction. Our *in vivo* and *in vitro* findings suggest that in addition to its actions on matrix cross-linking, tTG inhibits fibroblast proliferation and promotes a matrix-preserving phenotype in cardiac fibroblasts. When bound to the extracellular matrix, tTG stimulates TIMP1 synthesis through non-enzymatic effects, acting as a matricellular protein.

2. Methods (detailed description of the methodology is provided in the online supplement)

2.1 Animal protocols

Animal experiments were conducted in accordance with the National Institutes of Health Guide for the Care and Use of Laboratory Animals and were approved by the Baylor College of Medicine and Albert Einstein College of Medicine institutional review committees. Male and female, 2- to 4-month-old wild-type (WT) and tTG knockout (KO)[20] mice in a C57BL/6J background were genotyped using established protocols. Animals were anesthetized with inhaled isoflurane (4% for induction, 2% for maintenance). Aortic banding was achieved by creating a constriction between the right innominate and left carotid arteries, as previously described.[21] The degree of pressure overload was assessed by measuring right-to-left carotid artery flow velocity ratio after constricting the transverse aorta. For analgesia, buprenorphine (0.05–0.2 mg/kg s.c.) was administered at the time of surgery and q12h thereafter for 2 days. Intraoperatively, heart rate, respiratory rate and electrocardiogram were monitored and the depth of anaesthesia was assessed using the toe pinch method. At the end of the experiment, euthanasia was performed using 2% inhaled isoflurane followed by cervical dislocation. Early euthanasia was performed following criteria indicating suffering of the animal: weight loss > 20%, vocalization, dehiscent wound, hypothermia, signs of heart failure (cyanosis, dyspnoea, and tachypnea), lack of movement, hunched back, lack of food or water ingestion.

2.2 Echocardiography

Echocardiography was performed prior to instrumentation and before the end of each experiment using the Vevo 2100 system (VisualSonics, Toronto ON).

2.3 Pressure:volume loop analysis

Left ventricular pressure–volume analysis was performed using progressive isovolumic Langendorff retrograde perfusion of isolated murine hearts, as previously described.[22,23]

2.4 Immunohistochemistry, dual fluorescence and quantitative histology

Formalin-fixed, paraffin-embedded tissue samples were used for immunohistochemical staining. Collagen was labelled using picrosirius red. Quantitative assessment of myofibroblast and macrophage density was performed by counting the number of cells/myocardial area. Cardiomyocytes were outlined using wheat germ agglutinin (WGA) histochemistry.

2.5 Assessment of apoptosis using TUNEL staining and WGA lectin fluorescence

Apoptotic cardiomyocytes and interstitial cells were identified using fluorescent *In situ* Cell Death Detection Kit (Roche) and WGA staining.

2.6 RNA extraction and qPCR

RNA extraction and quantitative PCR were performed using established protocols.

2.7 Hydroxyproline biochemical assay

To assess cross-linking of collagen in pressure overloaded hearts we adopted established methods.[24]

2.8 Zymography

MMP activity in the pressure overloaded myocardium was examined by gelatin zymography.[23]

2.9 Flow cytometry

Suspensions of interstitial cells were prepared from WT and tTG KO hearts after 7 days of TAC. Cell suspensions were analysed with a Cell Lab Quanta SC flow cytometer (Beckman Coulter).

2.10 Cardiac fibroblast isolation and stimulation

Cardiac fibroblasts were isolated from WT, Smad3 KO and tTG KO animals as previously described.[25]

2.11 Western blotting

Protein was isolated from stimulated cells and western blotting was performed using standard protocols.

2.12 Studies on cardiac fibroblasts populating collagen pads

Cardiac fibroblasts isolated from WT and tTG KO animals were cultured to passage 2 and serum-starved overnight (16 h), then cultured in

collagen pads as previously described.[26,27] After incubation, the pads were used for RNA extraction and subsequent analyses. For experiments examining the effects of tTG on fibroblast phenotype, enzymatically active recombinant mouse tTG, or inactive tTG with a point mutation in the catalytic site (Zedira GmbH) was incorporated into collagen pads at a concentration of 50 μg/mL.

2.13 Macrophage isolation and stimulation

CD11b+ macrophages were isolated from the mouse spleen using immunomagnetic sorting.

2.14 Statistical analysis

For comparisons between more than two groups, parametric or non-parametric one-way ANOVA was used followed by *t*-test corrected for multiple comparisons. Comparisons between two groups were performed using unpaired *t*-test, or the Mann–Whitney test. Mortality was compared using the log rank test. Data were expressed as mean ± SEM. Statistical significance was set at 0.05.

3. Results

3.1 tTG is upregulated in the pressure-overloaded myocardium and is deposited in the extracellular matrix

qPCR analysis showed that tTG expression is markedly upregulated in the pressure-overloaded myocardium after 7 days of transverse aortic constriction (TAC) (*Figure 1A*). In contrast, myocardial expression of other transglutaminases (TG1, TG3, TG4, TG5, TG6, TG7 and factor XIIIA) was not upregulated following pressure overload (see Supplementary material online, *Figure S1*). We confirmed the specificity of the anti-tTG antibody using tissues from WT and tTG KO mice (see Supplementary material online, *Figure S2*). Immunohistochemical staining demonstrated that after 7–28 days of TAC, tTG was expressed in cardiomyocytes and interstitial cells in the remodelling myocardium, and was deposited in the fibrotic extracellular matrix (*Figure 1B–I*). Sections from tTG KO mice were used as negative controls, showing minimal tTG immunofluorescence (*Figure 1D*). Dual immunofluorescence localized intracellular tTG in cardiomyocytes (*Figure 1H and I*), α-SMA+ myofibroblasts (*Figure 1J*) and Mac2+ macrophages (*Figure 1K*).

3.2 Transforming growth factor (TGF)-β induces tTG synthesis in cardiac fibroblasts in a Smad3-dependent manner

TGF-β1 is induced and activated in the remodelling pressure-overloaded myocardium and may exert potent fibrogenic actions, inducing myofibroblast transdifferentiation and expression of matrix proteins.[28] Because cardiac myofibroblasts were identified as a major cellular source of tTG in the remodelling myocardium, we examined whether TGF-β stimulation upregulates tTG synthesis in isolated cardiac fibroblasts. TGF-β1 (25 ng/mL) induced a 2.0-fold increase in tTG mRNA expression by cardiac fibroblasts after 4 h of stimulation (*Figure 1L*). The effects of TGF-β were abrogated in Smad3 null cardiac fibroblasts, suggesting that TGF-β-induced tTG upregulation is Smad-dependent (*Figure 1L*). Although tTG was the TG showing the highest level of expression in cardiac fibroblasts, TG4 was also expressed. Expression levels of TG1, TG3, TG5, TG6, TG7 and FXIIIA were very low and were not upregulated upon stimulation with TGF-β1 (see Supplementary material online, *Figure S3A–H*). Dual staining combining pan-cadherin fluorescence to label the cytoplasmic membrane and tTG staining also showed tTG expression in cardiac fibroblasts and documented release into the extracellular matrix upon stimulation. Stimulation with serum, or TGF-β1 increased the intensity of tTG immunofluorescence and induced release of immunoreactive tTG into the surrounding matrix (see Supplementary material online, *Figure S4*). Cells from tTG KO hearts were used as a negative control and showed negligible immunofluorescence (see Supplementary material online, *Figure S4*).

3.3 TGF-β1 induces tTG upregulation in mouse macrophages through a Smad-independent pathway

Because tTG was localized in a subset of macrophages in the pressure-overloaded heart (*Figure 1K*), we examined whether cytokine stimulation upregulates tTG expression in mouse macrophages. TGF-β1, but not IL-1β stimulation induced tTG synthesis is mouse splenic macrophages harvested from WT or Smad3 KO animals (*Figure 1M*), suggesting that TGF-β1-induced tTG upregulation is mediated through a Smad3-independent pathway. Macrophages harvested from the pressure overloaded heart after 7 days of TAC showed significantly higher levels of tTG expression in comparison to mouse splenic macrophages (*Figure 1M*). tTG was the highest expressed TG in splenic macrophages (see Supplementary material online, *Figure S3I*). Macrophages also expressed lower levels of TG4 and FXIIIA; other TGs were not detected (see Supplementary material online, *Figure S3J and K*). TGF-β1 and IL-1β stimulation did not significantly modulate macrophage TG4 and FXIII expression (see Supplementary material online, *Figure S3J and K*).

3.4 tTG loss does not significantly affect baseline cardiac morphology and function

Although both WT and tTG KO mice were normoglycemic, tTG KOs had lower fasting blood glucose levels (see Supplementary material online, *Figure S5A*). Systolic and diastolic blood pressure was comparable between groups (see Supplementary material online, *Figure S5B*). tTG absence had no effects on baseline cardiac morphology and did not affect cardiac geometry and systolic function. Mitral inflow Doppler and tissue Doppler imaging showed no significant effects of tTG loss on baseline diastolic function (see Supplementary material online, *Figure S5*).

3.5 tTG null mice exhibit increased mortality following pressure overload

tTG-/- ($n = 129$) and WT mice ($n = 128$) underwent TAC protocols. Carotid flow ratio after TAC was comparable between groups (WT, $7.14 + 0.23$; KO, $7.16 + 0.3$; P = NS) indicating comparable pressure load. Sham WT and KO mice had comparable carotid flow ratios before and after the procedure (WT sham: pre, $0.96 + 0.05$ and post, $1.05 + 0.30$; KO sham: pre, $1.2 + 0.26$ and post, $1.08 + 0.04$, P = NS). When compared with WT animals, tTG KO mice had significantly increased mortality following pressure overload ($P < 0.01$, *Figure 2A*). There were no deaths in sham animals (WT, $n = 31$; KO, $n = 39$).

3.6 tTG absence is associated with accentuated dilative remodelling of the pressure-overloaded heart

After 28 days of pressure overload, tTG null mice exhibited marked ventricular dilation, evidenced by markedly higher LVEDD, LVESD, LVEDV

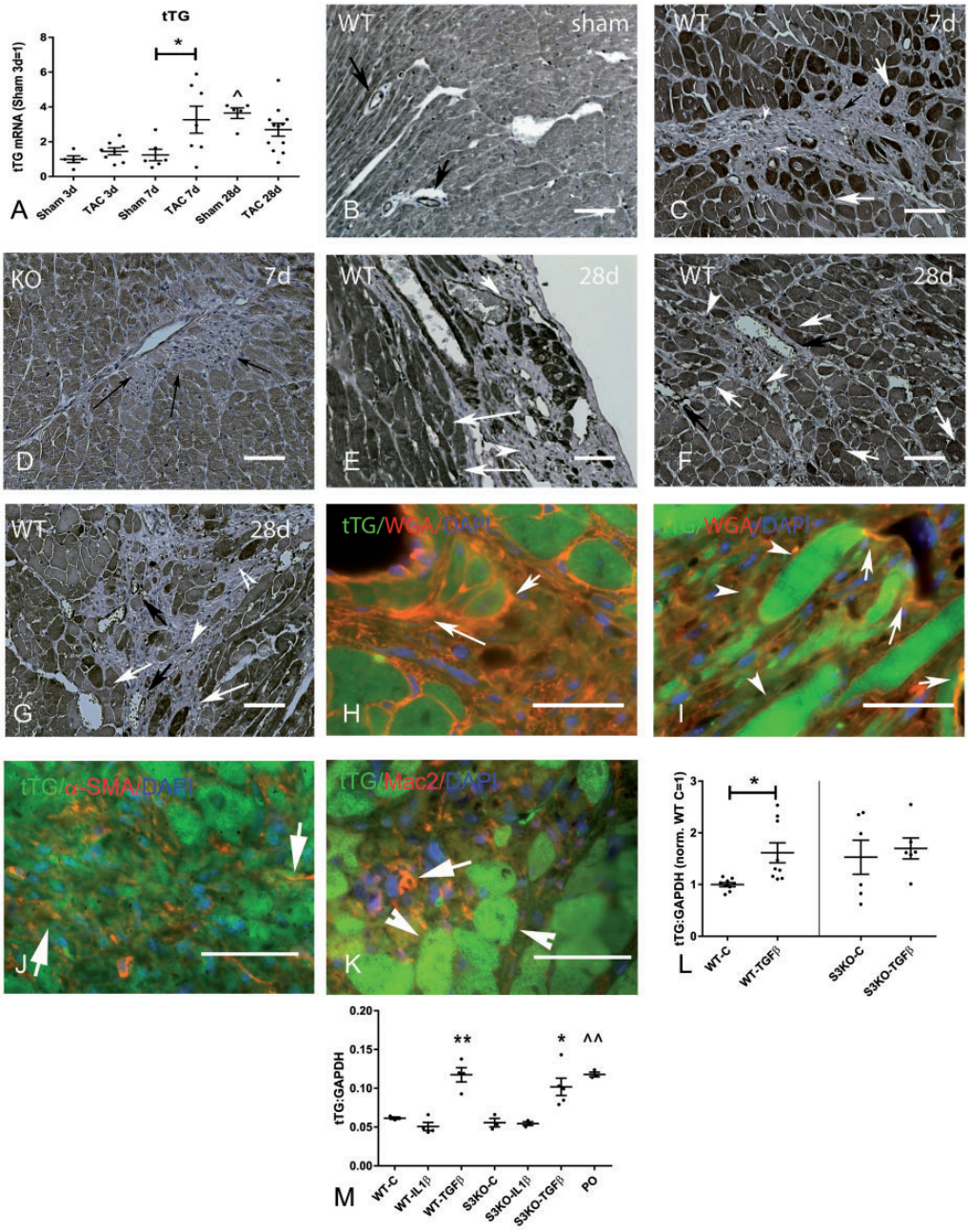

Figure 1 tTG regulation and localization in the pressure-overloaded myocardium. (*A*) qPCR analysis demonstrated marked tTG mRNA upregulation in the pressure-overloaded myocardium after 7 days of TAC (*$P < 0.05$ vs. corresponding sham; ^$P < 0.05$ vs. 3-day sham; $n = 5$–12/group). (*B*–*G*) Immunohistochemical staining demonstrated tTG localization in cardiomyocytes, interstitial matrix, and interstitial cells in the pressure-overloaded heart after 7–28 days of TAC. The specificity of the anti-tTG antibody was validated using tissues from WT and tTG KO animals (see Supplementary material online, *Figure S2*). In sham WT myocardium, tTG was expressed in cardiomyocytes and vascular cells (arrows). In the pressure-overloaded myocardium, tTG was highly expressed in a subset of cardiomyocytes (white arrows), was localized in interstitial cells (arrowheads), and was deposited in the perivascular extracellular matrix (black arrows) after 7–28 days of TAC. Sections from pressure-overloaded tTG KO (*D*) hearts showed minimal immunoreactivity (despite evidence of extensive fibrotic remodelling—arrows) and served as negative controls. Significant heterogeneity in cardiomyocyte tTG expression was noted in the pressure overloaded myocardium with some cells (white arrows, F) exhibiting very high levels of immunoreactivity. (*H* and *I*) Dual immunofluorescence for tTG and WGA localized tTG (green) in cardiomyocytes (arrowheads) and in the WGA-positive interstitial matrix (arrows—orange). (*J*) tTG immunoreactivity was also noted in a subset of infiltrating spindle-shaped myofibroblasts (arrows—orange), identified with α-SMA staining (red). (*K*) A subset of interstitial macrophages (orange—arrows), stained with Mac2 (red) also expressed tTG (green). Please note that cardiomyocytes adjacent to areas of fibrosis are intensely positive for tTG (arrowheads). (*L*) TGF-β stimulation upregulated tTG in cardiac fibroblasts through Smad-dependent signalling. In cardiac fibroblasts harvested from WT hearts, TGF-β1 stimulation (25 ng/ml for 4 h) induced tTG mRNA upregulation (*$P < 0.05$ vs. control, $n = 6$–9). In contrast, no significant tTG upregulation was noted in TGF-β1-stimulated Smad3-/- (S3KO) fibroblasts (P = NS, $n = 6$–9). (*M*) In isolated splenic macrophages, TGF-β1, but not IL-1β induced tTG in both WT and Smad3 KO cells. Macrophages harvested from the pressure-overloaded (PO) myocardium after 7 days of TAC had higher tTG expression levels than control splenic macrophages (*$P < 0.01$, **$P < 0.01$ vs. corresponding controls; ^$P < 0.01$ vs. WT C, $n = 9$–15/group). Scale bar = 40 μm.

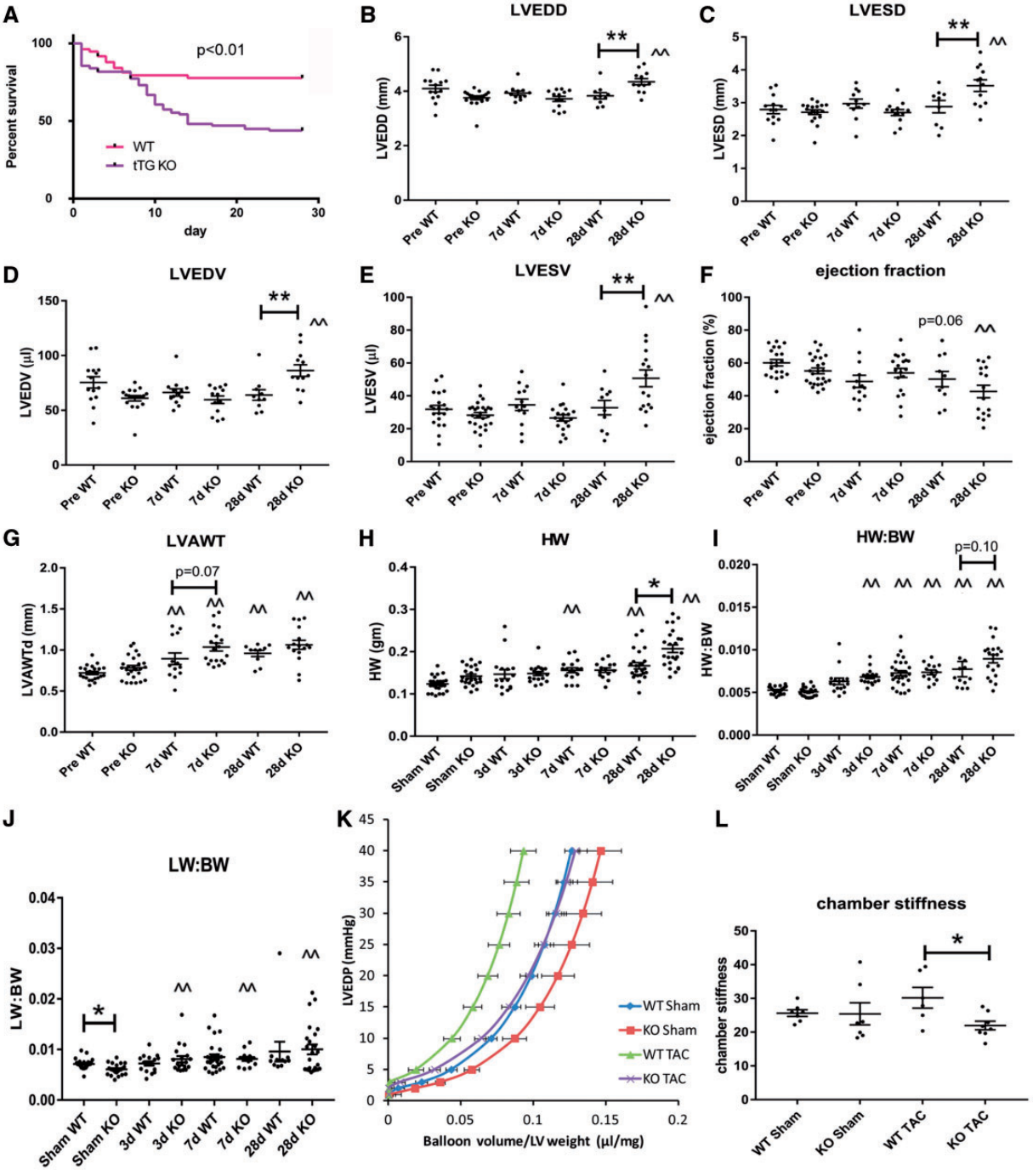

Figure 2 tTG loss increases mortality and dilative ventricular remodelling, but protects from the development of diastolic dysfunction following pressure overload. (*A*) When compared with WT animals, tTG KO mice had increased mortality following pressure overload ($P < 0.01$; WT, $n = 129$; tTG KO, $n = 128$, log-rank test). (B–E) tTG KO mice had increased dilative remodelling after 28 days of TAC, exhibiting significantly higher LVEDD (*B*), LVESD (*C*), LVEDV (*D*) and LVESV (*E*) in comparison to WT animals (**$P < 0.01$ vs. corresponding WT, $n = 13$–18/group, one-way ANOVA followed by Sidak's test). (*F*) tTG KO mice had a trend towards reduced ejection fraction after 28 days of TAC. (*G*) Both WT and tTG KO mice exhibited cardiac hypertrophy following pressure overload (^$P < 0.05$,^^$P < 0.01$ vs. corresponding baseline values, Kruskal–Wallis test). tTG KO mice had trends towards increased anterior wall thickness after 7–28 days of TAC. (*H* and *I*) Both heart weight and heart weight:body weight ratio was increased in both WT and tTG KO animals following pressure overload (^^$P < 0.01$ vs. corresponding sham, Kruskal–Wallis test). KO mice had significantly increased heart weight and a trend towards an increase in HW:BW after 28 days of TAC. (*J*) Lung weight:body weight ratio was also significantly increased in both WT and tTG KO mice after 7–28 days of TAC indicating the development of heart failure (*$P < 0.05$, **$P < 0.01$ vs. sham, $n = 12$–28/group, Kruskal–Wallis test). However, no significant differences in lung weight were noted between WT and tTG KO groups. (K and L) tTG loss attenuated diastolic dysfunction in the pressure overloaded myocardium. (*K*) Pressure:Volume analysis in isolated perfused hearts showed that tTG KO mice had a rightward shift of the curve. (*L*) Following TAC, chamber stiffness was significantly higher in WT animals when compared with tTG KOs (*$P < 0.05$, $n = 6$–8/group, ANOVA followed by Sidak's test).

and LVESV in comparison to WT animals (*Figure 2B–E*). Accentuated dilative remodelling in pressure-overloaded tTG KO mice was not associated with a significant deterioration in systolic function (*Figure 2F*). Both WT and tTG KO mice exhibited marked hypertrophic changes following pressure overload, showing increases in LVAWTd, in heart weight, and in the heart weight: body weight ratio after 7 and 28 days of TAC (*Figure 2G–I*). tTG null mice showed a trend towards increased hypertrophic remodelling after 7 and 28 days of TAC (*Figure 2G–I*). Lung weight:body weight ratio after TAC was comparable between groups (2J). Pressure:volume loop analysis in pressure-overloaded hearts using a Langendorff system showed that after 28 days of TAC, tTG KO hearts were more compliant than corresponding WT hearts, suggested by significantly lower chamber stiffness (*Figure 2K* and *L*). Thus, tTG loss enhanced chamber dilation and systolic dysfunction, but increased ventricular compliance and attenuated diastolic dysfunction following pressure overload.

3.7 tTG loss does not affect cardiomyocyte apoptosis following pressure overload

Next, we examined whether accentuated dilation in pressure-overloaded tTG null hearts was due to increased cardiomyocyte apoptosis. We identified rare apoptotic cells in the pressure-overloaded myocardium. Dual fluorescence combining WGA histochemistry to outline cardiomyocytes and TUNEL showed that the majority of apoptotic cells were interstitial cells. After 3, 7 and 28 days of TAC, tTG null and WT mice had comparable numbers of apoptotic cardiomyocytes and non-cardiomyocytes (see Supplementary material online, *Figure S6*).

3.8 Effects of tTG loss on collagen deposition in the pressure-overloaded myocardium

Alterations in composition of the interstitial matrix critically regulate geometric remodelling of the ventricle. Chamber dilation is often associated with accentuated matrix degradation, whereas deposition of cross-linked collagen in the cardiac interstitium causes diastolic dysfunction. Accordingly, we examined whether the geometric and functional changes in pressure-overloaded tTG null hearts are associated with alterations in collagen deposition and remodelling.

We used light microscopy, polarized microscopy and biochemical analysis to assess collagen deposition and structure in the remodelling myocardium (*Figure 3A–I*). Quantitative analysis of total collagen staining showed no significant effects of tTG loss on the collagen-stained area after 7–28 days of TAC (*Figure 3B* and *C*). Assessment of green and orange-red collagen fibres (reflecting thinner and thicker collagen fibres, respectively) using polarized light showed no significant differences between WT and tTG KO mice (*Figure 3D* and *E*). Biochemical analysis showed that in WT mice, pressure overloaded hearts had markedly higher levels of total collagen, insoluble collagen, and an increased ratio of insoluble:soluble and insoluble:total collagen (*Figure 3F–I*). In contrast, in pressure-overloaded tTG KO hearts, no statistically significant increase in collagen and insoluble collagen levels was noted in comparison to sham hearts.

3.9 tTG absence is associated with increased MMP2 activity and accentuated expression of cross-linking enzymes in the pressure-overloaded myocardium

Zymography demonstrated that tTG null hearts had increased levels of active MMP2 after 28 days of TAC, when compared with WT hearts (*Figure 4A* and *B*). Accentuated MMP activity in tTG null hearts was not due to significantly higher MMP2 mRNA levels (*Figure 4C*). tTG loss was associated with a significant accentuation in expression of the matrix cross-linking enzymes lysyl oxidase-like (LOXL)1, LOXL2 and LOXL4. (**$P < 0.01$ vs. corresponding WT). In contrast, LOX and LOXL3 expression was comparable between WT and tTG KO animals (*Figure 4D–H*).

3.10 Pressure-overloaded tTG null hearts have a higher number of non-cardiomyocytes than WT hearts, exhibiting increased macrophage and myofibroblast density

Hematoxylin/eosin staining demonstrated that tTG KO hearts had a highly cellular interstitium after 7–28 days of pressure overload (see Supplementary material online, *Figure S7*). We compared the cellular composition of the interstitium between pressure-overloaded WT and tTG null hearts using two independent techniques: flow cytometry and immunohistochemistry. Flow cytometric analysis of non-cardiomyocytes harvested from pressure-overloaded hearts (*Figure 5A–F*) demonstrated that after 7 days of TAC, tTG KO mice had higher cellular content (*Figure 5C*), increased number of CD45+ hematopoietic cells (*Figure 5D*), more α-smooth muscle actin (SMA)+/collagen I+ myofibroblasts (*Figure 5E*), but comparable numbers of CD31+ endothelial cells (*Figure 5F*). Flow cytometric findings were supported by immunohistochemical studies: tTG KO hearts had higher numbers of Mac2+ macrophages and α-SMA+ myofibroblasts after 7 and 28 days of TAC (*Figure 6*). Taken together, the quantitative analysis of collagen content (*Figure 3*) and the flow cytometric, histological and immunohistochemical study of the cellular infiltrate (*Figures 5* and *6*; see Supplementary material online, *Figure S7*) supported the notion that tTG loss is associated with a hypercellular interstitium that contains lower amounts of collagen, findings consistent with a matrix-degrading environment.

3.11 Accentuated MMP activity in tTG null hearts is not due to changes in macrophage or fibroblast MMP synthesis

Recently, tTG has been proposed as a specific marker for M2 macrophages that is conserved between species;[29] however, its role in modulation of macrophage phenotype remains unknown. In order to examine whether the effects of tTG on cardiac remodelling are mediated through alterations in macrophage phenotype we harvested myocardial CD11b+ myeloid cells from WT and tTG KO mice undergoing TAC protocols. CD11b+ macrophages isolated from tTG null animals exhibited lower levels of MMP2 and MMP9 expression and comparable MMP3 and TIMP1 expression (see Supplementary material online, *Figure S8*). Moreover, fibroblasts isolated from tTG KO hearts also expressed lower MMP2 mRNA levels than WT cells (see Supplementary material online, *Figure S9*). The findings suggested that the increased MMP2 activity observed in pressure-overloaded tTG null

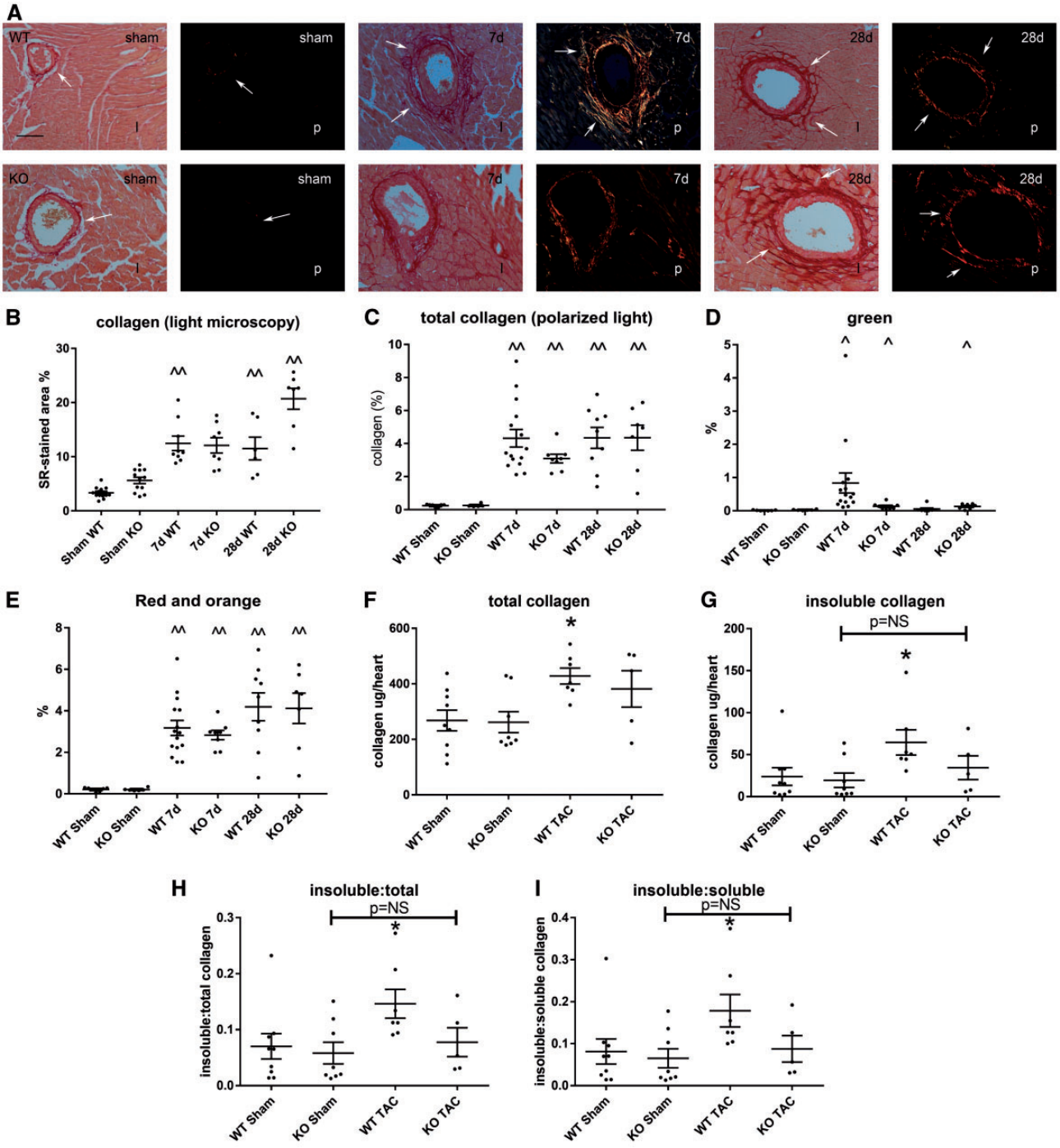

Figure 3 Effects of tTG loss on collagen deposition in the pressure-overloaded myocardium. (*A*) Light microscopy (l) of sirius red-stained sections and polarized light microscopy (p) were used to study the distribution and birefringence of collagen fibres in sham and pressure-overloaded myocardium (arrows). (*B* and *C*) Quantitative analysis showed that in both WT and tTG KO animals, pressure overloaded hearts had significantly increased collagen-stained area (^$P < 0.05$,^^$P < 0.01$ vs. corresponding sham, Kruskal–Wallis test, $n = 6$–14/group) after 7–28 days of TAC. No significant differences were noted in total collagen content (B and C) and in the amount of thinner green (*D*) and thicker orange-red (*E*) collagen fibres between WT and tTG KO groups. (F–I) A hydroxyproline biochemical assay showed that after 28 days of TAC, WT animals exhibited a significant increase in total myocardial collagen content (*F*), insoluble collagen (*G*), insoluble:total collagen (*H*) and insoluble:soluble collagen (*I*) when compared with sham mice (*$P < 0.05$ vs. sham, $n = 6$–9/group, Kruskal–Wallis test). In comparison to corresponding sham animals, tTG KO mice had no significant increase in total collagen content after 28 days of pressure overload and no significant increase in the fraction of insoluble collagen. The findings suggest that tTG loss may impair collagen cross-linking in the pressure-overloaded myocardium.

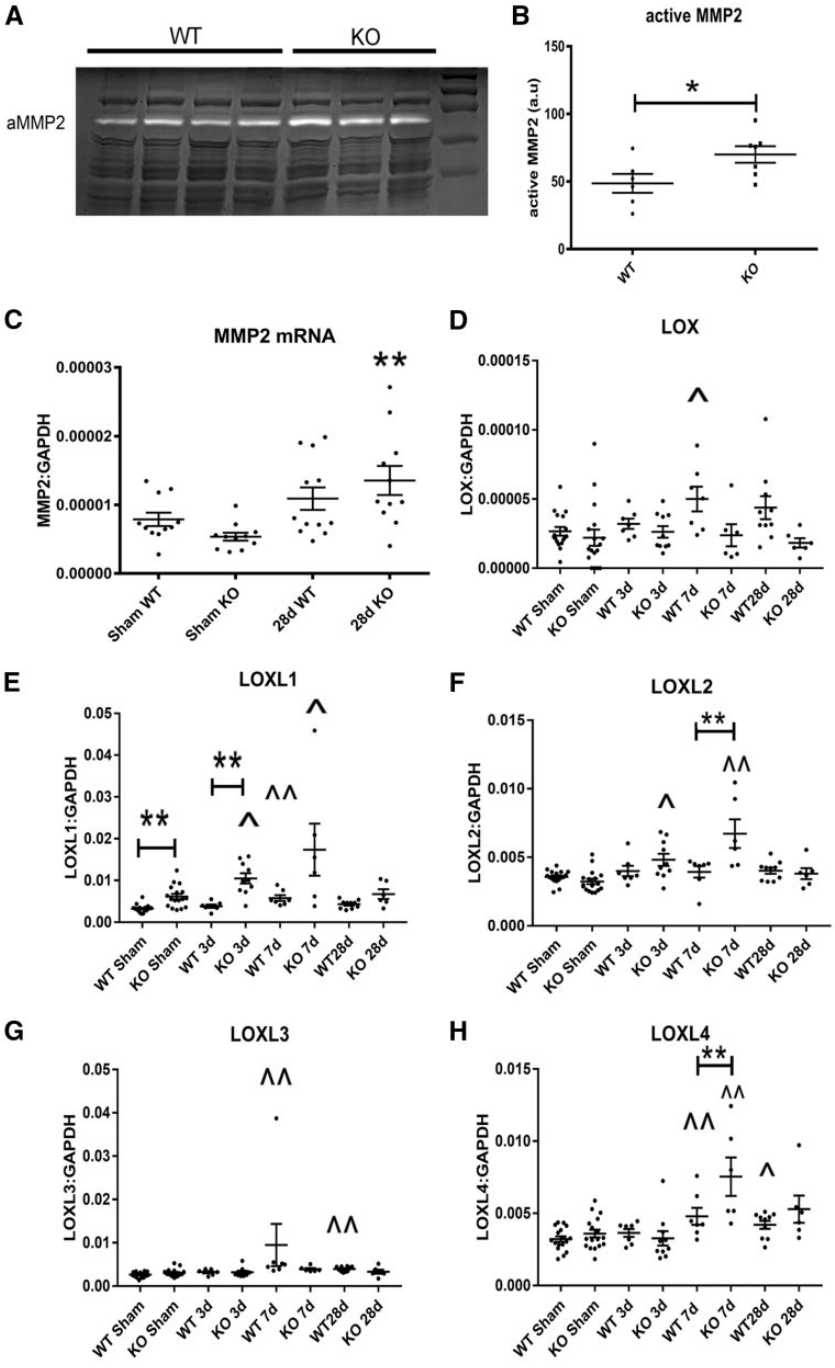

Figure 4 tTG loss increases myocardial MMP2 activity and is associated with accentuated upregulation of LOXL1, LOXL2 and LOXL4 in the pressure-overloaded myocardium. (*A* and *B*) Zymography demonstrated that after 28 days of pressure overload tTG KO animals had increased myocardial MMP2 activity when compared with WT animals (*$P < 0.05$ vs. WT, $n = 6$–7/group, unpaired *t*-test). (*C*) Increased MMP2 activity in tTG null hearts was not due to increased MMP2 transcription. After 28 days of TAC, MMP2 mRNA levels were comparable between WT and tTG KO hearts (**$P < 0.01$ vs. corresponding sham, Kruskal–Wallis test, $n = 6$–12/group). (*D*–*H*) tTG absence had significant effects on expression of matrix cross-linking genes in the pressure overloaded myocardium (^$P < 0.05$, ^^$P < 0.01$ vs. corresponding shams). In comparison to corresponding WT animals, tTG KO mice had significantly increased LOXL1, LOXL2 and LOXL4 mRNA levels after 3–28 days of TAC (*$P < 0.05$, **$P < 0.01$, $n = 6$–17/group, parametric ANOVA followed by Sidak's test or Kruskal–Wallis test).

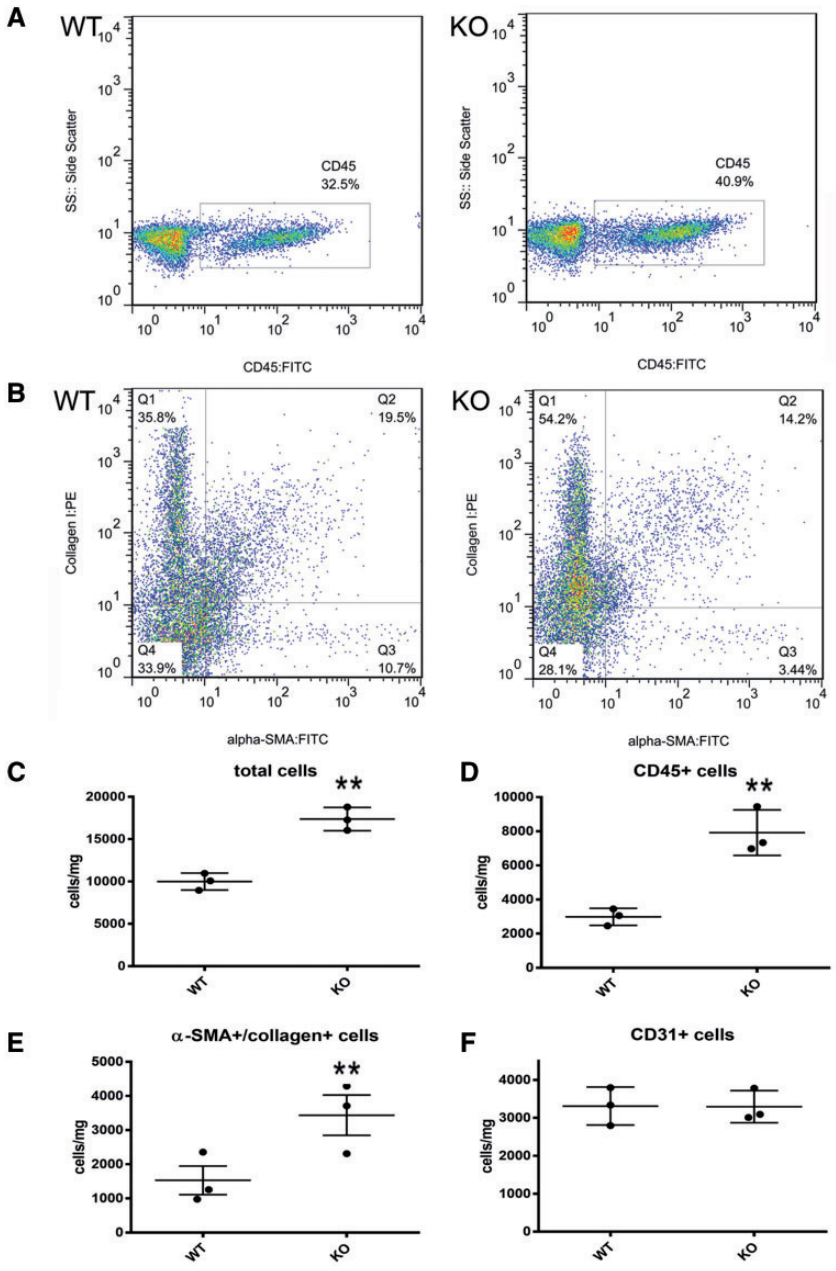

Figure 5 tTG loss is associated with increased infiltration of the remodelling myocardium with non-cardiomyocytes. (A and B) Representative flow cytometry identifying CD45+ hematopoietic cells (*A*) and α-SMA/collagen-expressing myofibroblasts (*B*) in the remodelling myocardium after 7 days of TAC. (C–F) Quantitative analysis of flow cytometry data showed that tTG KO mice had increased numbers of interstitial cells (*C*), CD45+ hematopoietic cells (*D*), α-SMA+/collagen+ myofibroblasts (*E*), but comparable numbers of CD31+ endothelial cells (*F*) after 7 days of pressure overload (**$P < 0.01$ vs. WT, $n = 3$/group, unpaired *t*-test).

hearts was not due to modulation of macrophage or fibroblast MMP2 mRNA synthesis.

3.12 tTG loss does not affect TGF-β-mediated activation of Smad2/3 signalling

tTG has been implicated in TGF-β activation.[30,31] Accordingly, we asked whether tTG loss affects TGF-β-induced Smad2/3 activation. Western blotting experiments demonstrated that WT and tTG KO cardiac fibroblasts had comparable activation of Smad2 signalling (evidenced through a marked increase in Smad2 phosphorylation), upon stimulation with TGF-β1 for 5–30 min. Moreover, in fibroblasts cultured in collagen pads, tTG KO cells and WT cells had comparable p-Smad2 immunoreactivity after 24 h of stimulation with TGF-β1 (see Supplementary material online, *Figure S10*).

3.13 tTG loss is associated with increased fibroblast proliferative activity

Using an *in vitro* proliferation assay, we found that tTG KO fibroblasts had markedly increased proliferative activity upon stimulation with

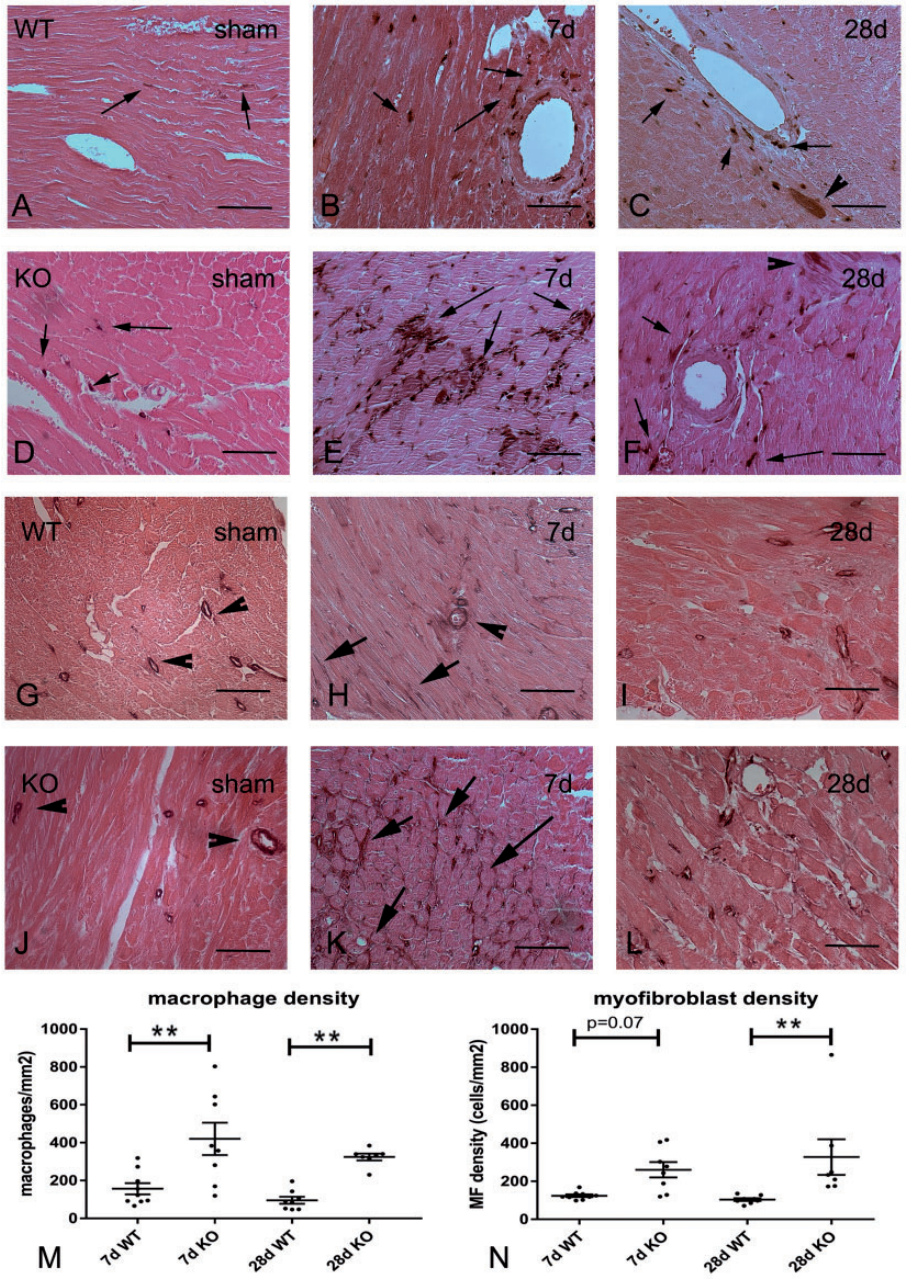

Figure 6 Immunohistochemical staining demonstrates that tTG KO animals have increased macrophage density and enhanced myofibroblast infiltration after 7–28 days of TAC. (A–F) Mac2 immunohistochemistry (black) was used to identify macrophages in the remodelling myocardium of WT (*A–C*) and tTG KO animals (*D–F*) (arrows). WT (*A*) and tTG KO (*D*) sham hearts exhibited small populations of Mac2+ macrophages. Intense infiltration with macrophages was noted in perivascular and interstitial areas after 7–28 days of TAC. tTG KO mice (*E* and *F*) exhibited more intense infiltration than WT animals (*B* and *C*). It should be noted that in the pressure-overloaded myocardium, a subset of cardiomyocytes exhibits Mac2 immunoreactivity[41] (arrowhead). For quantitative analysis, only cells with interstitial localization are identified as macrophages (arrows). (*G–L*) Immunohistochemical staining for α-SMA was used to identify myofibroblasts in the pressure overloaded myocardium of WT (*G–I*) and tTG KO mice (*J–L*) as immunoreactive cells located outside the vascular media. In sham WT (*G*) and tTG KO (*J*) animals α-SMA immunoreactivity was exclusively localized in vascular smooth muscle cells (arrowheads). After 7–28 days of TAC, both WT (*H* and *I*) and tTG KO (*K* and *L*) mice exhibited infiltration with α-SMA+ interstitial myofibroblasts (arrows). Myofibroblast infiltration was more intense in tTG KO animals (*K* and *L*). Quantitative analysis showed that macrophage density (*M*) and myofibroblast density (*N*) was markedly higher in tTG KO animals after 7–28 days of pressure overload (**$P < 0.01$ vs. corresponding WT, $n = 7–9$/group, Kruskal–Wallis test) (Scale bar = 50 μm; counterstained with eosin).

serum (*Figure 7A*). Experiments in fibroblasts cultured in collagen pads (*Figure 7B*) provided further support to the role of intracellular tTG in inhibition of proliferative activity. Collagen pads populated with tTG KO cells had higher fibroblast density upon stimulation with serum (*Figure 7C*).

3.14 Matrix-bound tTG enhances TIMP-1 expression by cardiac fibroblasts through a non-enzymatic pathway

In order to test the hypothesis that extracellular tTG may modulate fibroblast phenotype, we examined the effects of matrix-bound recombinant tTG (rtTG) on gene expression by cardiac fibroblasts populating collagen pads. When incorporated into the matrix, tTG induced TIMP1 mRNA expression in both WT and tTG KO cardiac fibroblasts (*Figure 7D*), suggesting the role of extracellular tTG actions in modulating fibroblast profile. Matrix-bound tTG did not significantly modulate MMP2 mRNA expression in WT, or in tTG KO fibroblasts (*Figure 7D*). Immunofluorescent staining confirmed that rtTG increases TIMP1 immunoreactivity in fibroblasts populating collagen pads (*Figure 7E*). Antibody neutralization experiments demonstrated that the effects of rtTG were independent of β1 integrin activation (*Figure 7F*). Inactive Cys277Ser-mutant recombinant tTG (itTG) with a point mutation in the catalytic centre also increased fibroblast TIMP-1 synthesis, documenting that this effect is transamidase-independent (*Figure 7G*).

4. Discussion

We document for the first time a critical role for endogenous tTG in cardiac remodelling. We demonstrate that tTG is markedly upregulated in the pressure-overloaded myocardium. tTG loss has profound effects on the ventricular response to a pressure load, attenuating diastolic dysfunction, while increasing mortality and accentuating chamber dilation. The effects of tTG absence are not due to actions on cardiomyocyte survival, but reflect activation of a proliferative phenotype in cardiac fibroblasts and modulation of matrix metabolism resulting in overactive matrix-degrading pathways.

Most cell types are capable of producing tTG; vascular cells, fibroblasts and M2 macrophages have been identified as important sources of tTG *in vitro* and *in vivo*.[29,32,33] Neonatal rat cardiomyocytes constitutively express tTG; its expression is upregulated upon stimulation with endothelin-1,[34] or reactive oxygen species.[35] Published evidence suggests that tTG is markedly upregulated in experimental rat models of heart failure due to pressure or volume overload;[17,18] its expression is associated with transition to heart failure. Our experiments show persistent tTG upregulation in the remodelling mouse myocardium after 7–28 days of pressure overload and suggest that tTG is localized in cardiomyocytes, interstitial cells and in the remodelling extracellular matrix (*Figure 1*).

Oxidative stress, growth factors, and cytokines are activated in the remodelling heart,[28] and are capable of inducing tTG transcription in various cell types.[8] TGF-β, a prominent mediator in cardiac remodelling and fibrosis[36] has been shown to exert cell-specific actions on tTG expression, increasing its transcription in fibroblasts and many other cell types, but downregulating tTG synthesis in epithelial cells.[8] Our experiments demonstrate that TGF-β1 induces tTG upregulation in isolated cardiac fibroblasts through activation of Smad3 signalling (*Figure 1L*). In macrophages, TGF-β1, but not the pro-inflammatory cytokine IL-1β stimulated tTG synthesis; however the effects of TGF-β were independent of Smad3 (*Figure 1M*).

In order to explore the role of tTG in cardiac remodelling, we studied the effects of tTG gene disruption on the pressure-overloaded myocardium. Baseline blood pressure, left ventricular geometry, systolic and diastolic function were not affected by tTG loss. However, following pressure overload tTG null animals exhibited significantly increased mortality when compared with WT controls, associated with accentuated chamber dilation (*Figure 2B–E*). Both WT and tTG KO animals had marked increases in heart and lung weight following pressure overload, suggesting comparable severity of heart failure, despite increased dilative remodelling of tTG null hearts. This may reflect the attenuated diastolic dysfunction observed in tTG KO animals (*Figure 2K* and *L*); the adverse effects of tTG loss on cardiac geometry may be counterbalanced by beneficial actions that reduce chamber stiffness.

The effects of tTG on function and remodelling of the pressure-overloaded heart may reflect a wide range of actions on many cell types and effects on the cardiac extracellular matrix. Because tTG has been implicated in the regulation of cellular apoptosis,[37,38] we examined whether worse remodelling in tTG KO hearts is due to loss of pro-survival signalling and subsequent apoptotic death of cardiomyocytes. TUNEL staining demonstrated that apoptotic cardiomyocytes were rare in the pressure-overloaded heart, and their number was not affected by the absence of tTG (see Supplementary material online, *Figure S6*). However, despite comparable loss of cardiomyocytes, tTG KO mice exhibited significant alterations in the cardiac interstitium following pressure overload. We used three different methods to examine the effects of tTG loss on collagen deposition in the remodelling myocardium. Both light microscopy and quantitative analysis of birefringence with polarized light microscopy showed no significant differences in collagen deposition between WT and tTG KO animals (*Figure 3*). Using a biochemical assay we found that pressure overload induced a significant increase in total and insoluble collagen in the remodelling myocardium. In contrast to WT animals, tTG null mice did not exhibit an increase in insoluble collagen content following pressure overload (*Figure 3G–H*), presumably reflecting the loss of the matrix cross-linking effects of tTG. Moreover, zymography showed that tTG absence significantly enhanced MMP2 activation in the remodelling myocardium (*Figure 4A* and *B*). Both flow cytometry and immunohistochemistry demonstrated that tTG KO mice had markedly increased numbers of interstitial myofibroblasts in the remodelling myocardium (*Figures 5* and *6*). tTG absence also increased expression of LOXL1, LOXL2 and LOXL4 in the pressure-overloaded myocardium. Recently published evidence suggested that LOXL2 stimulates cardiac fibroblasts promoting myofibroblast transdifferentiation and migratory activity.[39] Accentuated expression of lysyl oxidases in the absence of tTG may be responsible, at least in part, for the observed expansion of the myofibroblast population in the interstitium of pressure-overloaded tTG KO hearts.

Increased cellularity, impaired matrix cross-linking and enhanced MMP activity may explain the geometric and functional consequences of tTG loss on the remodelling heart. The abundance of interstitial cells, increased matrix-degrading activity, and reduced deposition of cross-linked collagen may on one hand improve compliance and attenuate diastolic dysfunction, while promoting dilative ventricular remodelling.

What is the cell biological basis for the effects of tTG on the remodelling myocardium? Effects of tTG on fibroblast phenotype and function have been previously reported. tTG may affect fibroblast function by modulating growth factor-stimulated signalling cascades. Experiments in human fibroblasts have demonstrated that cell surface tTG facilitates platelet-derived growth factor signalling.[31] Moreover, a role for tTG in activation and induction of the TGF-β response has been suggested.[30,40]

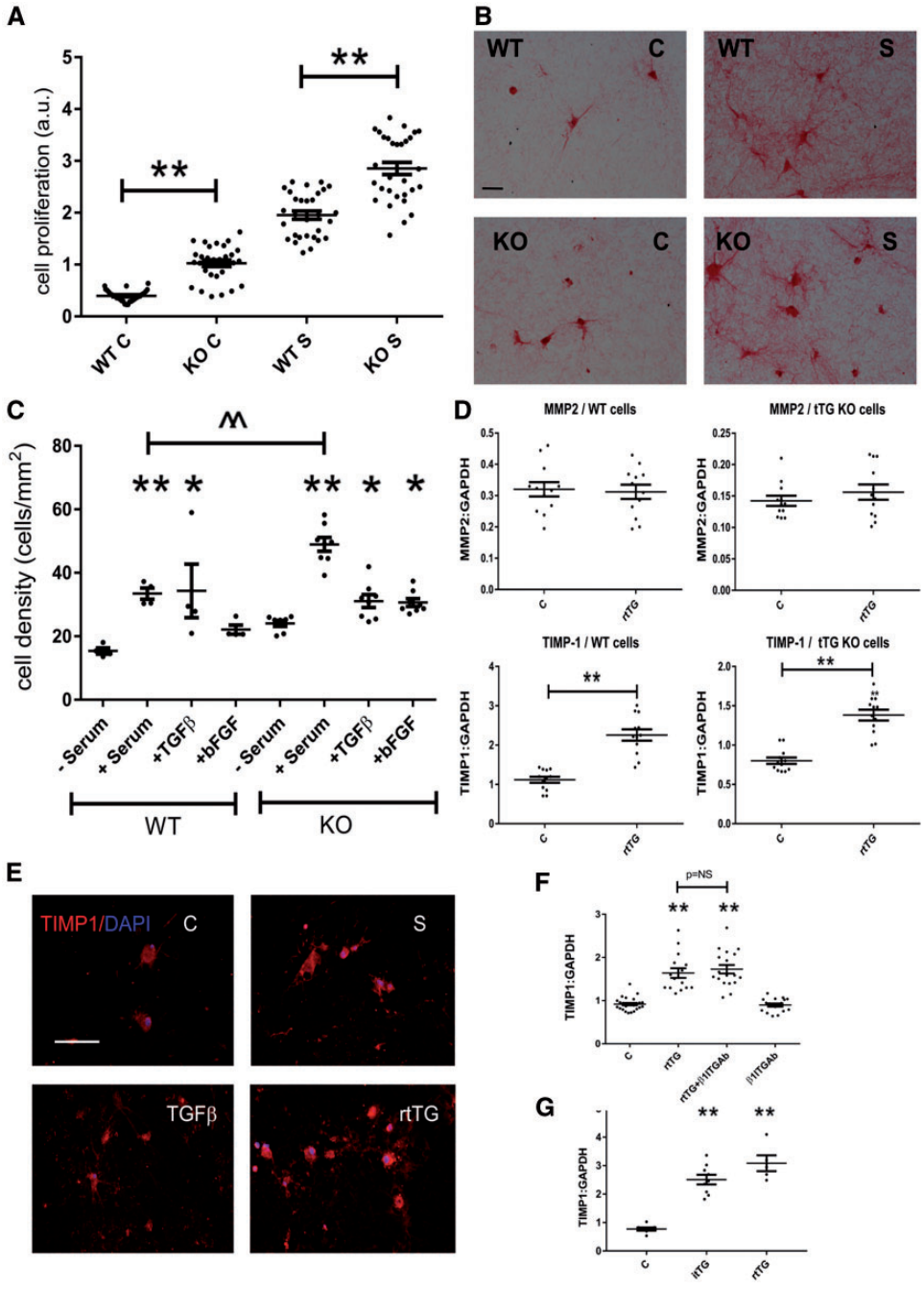

Figure 7 Actions of matrix-bound tTG on cardiac fibroblasts. (*A–C*) Loss of intracellular tTG increases fibroblast proliferative activity. Using a BrdU proliferation assay, we found that tTG KO cardiac fibroblasts had significantly higher proliferative activity than WT cells at baseline and after stimulation with serum (S) (**$P < 0.01$ vs. corresponding WT, $n = 30$, one-way ANOVA followed by Sidak's test). (*B* and *C*) The effects of tTG in suppression of fibroblast proliferation were supported by experiments in fibroblasts populating collagen pads. Fibroblasts were identified using sirius red staining (B, scale bar = 50 μm). Incubation with serum, TGF-β, or bFGF increased cell density in pads populated with WT or tTG KO cells (*$P < 0.05$, **$P < 0.01$ vs. corresponding control, Kruskal–Wallis test). Upon serum stimulation, pads populated with tTG KO cells had markedly higher density than pads stimulated with WT cells ‡$P < 0.01$, $n = 5$, Kruskal–Wallis test). (*D*) Extracellular matrix-bound rtTG induces TIMP-1 synthesis by cardiac fibroblasts through both enzymatic and non-enzymatic actions. To examine the effects of extracellular rtTG on cardiac fibroblasts, we performed 24-h tTG stimulation experiments in fibroblasts populating collagen pads. rtTG did not affect MMP2 synthesis in WT or tTG KO cells. rtTG markedly induced TIMP-1 mRNA expression in both WT and tTG KO cardiac fibroblasts †$P < 0.05$,‡$P < 0.01$ vs. control, $n = 10–12$/group, unpaired *t*-test). (*E*) Immunofluorescent staining showed that serum, TGF-β1, or rtTG stimulation accentuated TIMP1 immunoreactivity in fibroblasts populating collagen pads. (*F*) Incubation with an antibody to β1 integrin (β1ITGAb) demonstrated that the effects of rtTG were independent of β1 integrin signalling. (*G*) Stimulation with inactive tTG with a point mutation in the catalytic site (itTG) also induced TIMP1 in cardiac fibroblasts, suggesting effects independent of transamidase activity (**$P < 0.01$ vs. control, one-way ANOVA followed by Sidak's test).

Our *in vitro* experiments demonstrated that tTG does not play a significant role in regulation of TGF-β responses in cardiac fibroblasts. WT and tTG KO cells had comparable Smad2 phosphorylation upon stimulation with TGF-β1 (see Supplementary material online, *Figure S10*). However, tTG null cells exhibited increased proliferative activity at baseline, and upon stimulation with serum (*Figure 7*). Accentuated proliferation may explain the abundance of interstitial fibroblasts in pressure overloaded tTG KO hearts.

In order to examine the effects of tTG in modulating behaviour of fibroblasts in their matrix environment, we used an *in vitro* model of cardiac fibroblasts cultured in collagen pads enriched with tTG. We found that matrix-bound recombinant tTG exerts potent matrix-preserving actions on cardiac fibroblasts. When incorporated into the collagenous matrix, tTG induced TIMP-1 synthesis in both WT and tTG KO cells (*Figure 7*). The effect of tTG on TIMP1 expression by fibroblasts is not due to enzymatic actions; mutant tTG that lacks transglutaminase activity due to a point mutation in the active catalytic centre had similar effects on cardiac fibroblasts populating collagen pads (*Figure 7G*).

Our observations illustrate the critical role of matrix metabolism in cardiac remodelling. In the pressure-overloaded heart, activation of matrix-preserving signals results in fibrosis and diastolic dysfunction. From a theoretical perspective, inhibition of selected matrix-preserving mechanisms (such as tTG) seems an attractive therapeutic approach to reduce fibrosis and to protect from diastolic heart failure. However, this approach has significant risks. Matrix-preserving signals may exert protective actions by providing much needed mechanical support to the pressure-overloaded ventricle. Thus, overzealous inhibition of pathways involved in preservation of the matrix (such as the complete loss of tTG in mutant mice) may perturb the matrix balance leading to chamber dilation and systolic dysfunction.

Supplementary material

Supplementary material is available at *Cardiovascular Research* online.

Conflict of interest: none declared.

Funding

Supported by grants from the National Institutes of Health (R01 HL76246 and R01 HL85440 to N.G.F.), the Department of Defense (PR151134 and PR151029 to N.G.F.) and the American Heart Association Founders' affiliate (to A.V.S.).

References

1. Frangogiannis NG. Matricellular proteins in cardiac adaptation and disease. *Physiol Rev* 2012;**92**:635–688.
2. Skrbic B, Engebretsen KV, Strand ME, Lunde IG, Herum KM, Marstein HS, Sjaastad I, Lunde PK, Carlson CR, Christensen G, Bjornstad JL Tonnessen T. Lack of collagen VIII reduces fibrosis and promotes early mortality and cardiac dilatation in pressure overload in mice. *Cardiovasc Res* 2015;**106**:32–42.
3. Gonzalez-Santamaria J, Villalba M, Busnadiego O, Lopez-Olaneta MM, Sandoval P, Snabel J, Lopez-Cabrera M, Erler JT, Hanemaaijer R, Lara-Pezzi E Rodriguez-Pascual F. Matrix cross-linking lysyl oxidases are induced in response to myocardial infarction and promote cardiac dysfunction. *Cardiovasc Res* 2016;**109**:67–78.
4. Takawale A, Sakamuri SS Kassiri Z. Extracellular matrix communication and turnover in cardiac physiology and pathology. *Compr Physiol* 2015;**5**:687–719.
5. Goldsmith EC, Bradshaw AD Spinale FG. Cellular mechanisms of tissue fibrosis. 2. Contributory pathways leading to myocardial fibrosis: moving beyond collagen expression. *Am J Physiol Cell Physiol* 2013;**304**:C393–C402.
6. Kong P, Christia P Frangogiannis NG. The pathogenesis of cardiac fibrosis. *Cell Mol Life Sci* 2014;**71**:549–574.
7. Schellings MW, Pinto YM Heymans S. Matricellular proteins in the heart: possible role during stress and remodeling. *Cardiovasc Res* 2004;**64**:24–31.
8. Nurminskaya MV Belkin AM. Cellular functions of tissue transglutaminase. *Int Rev Cell Mol Biol* 2012;**294**:1–97.
9. Wang Z Griffin M. TG2, a novel extracellular protein with multiple functions. *Amino Acids* 2012;**42**:939–949.
10. Iismaa SE, Mearns BM, Lorand L Graham RM. Transglutaminases and disease: lessons from genetically engineered mouse models and inherited disorders. *Physiol Rev* 2009;**89**:991–1023.
11. Facchiano A Facchiano F. Transglutaminases and their substrates in biology and human diseases: 50 years of growing. *Amino Acids* 2009;**36**:599–614.
12. Barsigian C, Fellin FM, Jain A Martinez J. Dissociation of fibrinogen and fibronectin binding from transglutaminase-mediated cross-linking at the hepatocyte surface. *J Biol Chem* 1988;**263**:14015–14022.
13. Aeschlimann D Paulsson M. Cross-linking of laminin-nidogen complexes by tissue transglutaminase. A novel mechanism for basement membrane stabilization. *J Biol Chem* 1991;**266**:15308–15317.
14. Belkin AM. Extracellular TG2: emerging functions and regulation. *FEBS J* 2011;**278**:4704–4716.
15. Stamnaes J, Pinkas DM, Fleckenstein B, Khosla C Sollid LM. Redox regulation of transglutaminase 2 activity. *J Biol Chem* 2010;**285**:25402–25409.
16. Oh K, Park HB, Byoun OJ, Shin DM, Jeong EM, Kim YW, Kim YS, Melino G, Kim IG Lee DS. Epithelial transglutaminase 2 is needed for T cell interleukin-17 production and subsequent pulmonary inflammation and fibrosis in bleomycin-treated mice. *J Exp Med* 2011;**208**:1707–1719.
17. Iwai N, Shimoike H Kinoshita M. Genes up-regulated in hypertrophied ventricle. *Biochem Biophys Res Commun* 1995;**209**:527–534.
18. Petrak J, Pospisilova J, Sedinova M, Jedelsky P, Lorkova L, Vit O, Kolar M, Strnad H, Benes J, Sedmera D, Cervenka L Melenovsky V. Proteomic and transcriptomic analysis of heart failure due to volume overload in a rat aorto-caval fistula model provides support for new potential therapeutic targets – monoamine oxidase A and transglutaminase 2. *Proteome Sci* 2011;**9**:69.
19. Small K, Feng JF, Lorenz J, Donnelly ET, Yu A, Im MJ, Dorn GW, 2nd Liggett SB. Cardiac specific overexpression of transglutaminase II (G(h)) results in a unique hypertrophy phenotype independent of phospholipase C activation. *J Biol Chem* 1999;**274**:21291–21296.
20. De Laurenzi V Melino G. Gene disruption of tissue transglutaminase. *Mol Cell Biol* 2001;**21**:148–155.
21. Xia Y, Dobaczewski M, Gonzalez-Quesada C, Chen W, Biernacka A, Li N, Lee DW Frangogiannis NG. Endogenous thrombospondin 1 protects the pressure-overloaded myocardium by modulating fibroblast phenotype and matrix metabolism. *Hypertension* 2011;**58**:902–911.
22. Hilfiker-Kleiner D, Hilfiker A, Fuchs M, Kaminski K, Schaefer A, Schieffer B, Hillmer A, Schmiedl A, Ding Z, Podewski E, Podewski E, Poli V, Schneider MD, Schulz R, Park JK, Wollert KC Drexler H. Signal transducer and activator of transcription 3 is required for myocardial capillary growth, control of interstitial matrix deposition, and heart protection from ischemic injury. *Circ Res* 2004;**95**:187–195.
23. Biernacka A, Cavalera M, Wang J, Russo I, Shinde A, Kong P, Gonzalez-Quesada C, Rai V, Dobaczewski M, Lee DW, Wang XF Frangogiannis NG. Smad3 signaling promotes fibrosis while preserving cardiac and aortic geometry in obese diabetic mice. *Circ Heart Fail* 2015;**8**:788–798.
24. Mukherjee D Sen S. Collagen phenotypes during development and regression of myocardial hypertrophy in spontaneously hypertensive rats. *Circ Res* 1990;**67**:1474–1480.
25. Dobaczewski M, Bujak M, Li N, Gonzalez-Quesada C, Mendoza LH, Wang XF Frangogiannis NG. Smad3 signaling critically regulates fibroblast phenotype and function in healing myocardial infarction. *Circ Res* 2010;**107**:418–428.
26. Saxena A, Bujak M, Frunza O, Dobaczewski M, Gonzalez-Quesada C, Lu B, Gerard C Frangogiannis NG. CXCR3-independent actions of the CXC chemokine CXCL10 in the infarcted myocardium and in isolated cardiac fibroblasts are mediated through proteoglycans. *Cardiovasc Res* 2014;**103**:217–227.
27. Shinde AV, Humeres C Frangogiannis NG. The role of alpha-smooth muscle actin in fibroblast-mediated matrix contraction and remodeling. *Biochim Biophys Acta* 2017;**1863**:298–309.
28. Xia Y, Lee K, Li N, Corbett D, Mendoza L Frangogiannis NG. Characterization of the inflammatory and fibrotic response in a mouse model of cardiac pressure overload. *Histochem Cell Biol* 2009;**131**:471–481.
29. Martinez FO, Helming L, Milde R, Varin A, Melgert BN, Draijer C, Thomas B, Fabbri M, Crawshaw A, Ho LP, Ten Hacken NH, Cobos Jimenez V, Kootstra NA, Hamann J, Greaves DR, Locati M, Mantovani A Gordon S. Genetic programs expressed in resting and IL-4 alternatively activated mouse and human macrophages: similarities and differences. *Blood* 2013;**121**:e57–e69.
30. Nunes I, Shapiro RL Rifkin DB. Characterization of latent TGF-beta activation by murine peritoneal macrophages. *J Immunol* 1995;**155**:1450–1459.
31. Zemskov EA, Loukinova E, Mikhailenko I, Coleman RA, Strickland DK Belkin AM. Regulation of platelet-derived growth factor receptor function by integrin-associated cell surface transglutaminase. *J Biol Chem* 2009;**284**:16693–16703.
32. Haroon ZA, Hettasch JM, Lai TS, Dewhirst MW Greenberg CS. Tissue transglutaminase is expressed, active, and directly involved in rat dermal wound healing and angiogenesis. *FASEB J* 1999;**13**:1787–1795.

33. Jung SA, Lee HK, Yoon JS, Kim SJ, Kim CY, Song H, Hwang KC, Lee JB Lee JH. Upregulation of TGF-beta-induced tissue transglutaminase expression by PI3K-Akt pathway activation in human subconjunctival fibroblasts. *Invest Ophthalmol Vis Sci* 2007;**48**:1952–1958.
34. Li X, Wei XL, Meng LL, Chi MG, Yan JQ, Ma XY, Jia YS, Liang L, Yan HT Zheng JQ. Involvement of tissue transglutaminase in endothelin 1-induced hypertrophy in cultured neonatal rat cardiomyocytes. *Hypertension* 2009;**54**:839–844.
35. Song H, Kim BK, Chang W, Lim S, Song BW, Cha MJ, Jang Y Hwang KC. Tissue transglutaminase 2 promotes apoptosis of rat neonatal cardiomyocytes under oxidative stress. *J Recept Signal Transduct Res* 2011;**31**:66–74.
36. Dobaczewski M, Chen W Frangogiannis NG. Transforming growth factor (TGF)-beta signaling in cardiac remodeling. *J Mol Cell Cardiol* 2011;**51**:600–606.
37. Fesus L Szondy Z. Transglutaminase 2 in the balance of cell death and survival. *FEBS Lett* 2005;**579**:3297–3302.
38. Verderio EA, Telci D, Okoye A, Melino G Griffin M. A novel RGD-independent cel adhesion pathway mediated by fibronectin-bound tissue transglutaminase rescues cells from anoikis. *J Biol Chem* 2003;**278**:42604–42614.
39. Yang J, Savvatis K, Kang JS, Fan P, Zhong H, Schwartz K, Barry V, Mikels-Vigdal A, Karpinski S, Kornyeyev D, Adamkewicz J, Feng X, Zhou Q, Shang C, Kumar P, Phan D, Kasner M, Lopez B, Diez J, Wright KC, Kovacs RL, Chen PS, Quertermous T, Smith V, Yao L, Tschope C Chang CP. Targeting LOXL2 for cardiac interstitial fibrosis and heart failure treatment. *Nat Commun* 2016;**7**:13710.
40. Telci D, Collighan RJ, Basaga H Griffin M. Increased TG2 expression can result in induction of transforming growth factor beta1, causing increased synthesis and deposition of matrix proteins, which can be regulated by nitric oxide. *J Biol Chem* 2009;**284**:29547–29558.
41. Frunza O, Russo I, Saxena A, Shinde AV, Humeres C, Hanif W, Rai V, Su Y Frangogiannis NG. Myocardial galectin-3 expression is associated with remodeling of the pressure-overloaded heart and may delay the hypertrophic response without affecting survival, dysfunction, and cardiac fibrosis. *Am J Pathol* 2016;**186**:1114–1127.

European Heart Journal
Acute Cardiovascular Care
EUROPEAN SOCIETY OF CARDIOLOGY®

Editorial

European Heart Journal: Acute Cardiovascular Care
1–4

DOI: 10.1177/2048872617707456
journals.sagepub.com/home/acc
SAGE

Activation of the innate immune system in the pathogenesis of acute heart failure

Nikolaos G Frangogiannis

Acute heart failure syndromes account for more than 950,000 annual emergency department visits in the United States[1] and represent a major healthcare burden in western societies.[2,3] Virtually all patients with chronic heart failure will experience at some point an acute exacerbation that requires admission to the hospital.[4] Despite therapeutic advances, acute heart failure remains a life-threatening condition with a mortality rate in most registries ranging from 4% to 7%. The rate of rehospitalisation is also very high; almost 30% of the patients are readmitted within 3 months following discharge.[5] Our limited success in preventing recurrent hospitalisations in patients with heart failure reflects, at least in part, our superficial understanding of the pathophysiological basis for the acute exacerbations. Traditional clinical experience teaches that acute heart failure exacerbations may be triggered by a wide range of precipitating factors, both cardiovascular (such as ischaemia, arrhythmic events, hypertensive crises, etc.) and non-cardiovascular (including infections, anaemia, renal or pulmonary disease and non-compliance with medical treatment or dietary restrictions). Although this perspective remains extremely useful in managing patients with acute heart failure, there is a need to deepen our understanding of the underlying pathophysiological mechanisms, by identifying specific cellular events and molecular signals that may mediate the functional deterioration. Understanding of the mechanistic underpinnings of acute heart failure exacerbations is crucial in order to develop new therapeutic strategies.

Prolonged, excessive or dysregulated activation of the immune system has been implicated in the pathogenesis and progression of chronic heart failure.[6] The innate immune system has evolved to protect multicellular organisms from pathogens and to initiate a reparative response to 'danger signals' following tissue injury. Because the evolutionary pressures that led to the development of innate immune responses were related to protection from pathogenic organisms or traumatic injury, responses to sterile myocardial injury may be excessive for the delicate requirements of the myocardium.[7] Thus, in the heart, immune responses triggered by injurious stimuli may perturb the relation between structure and function, leading to catastrophic consequences such as cardiomyocyte death, inflammation and fibrosis. Both experimental studies in animal models and clinical investigations have suggested an important role for innate immune pathways in chronic heart failure. Activation of Toll-like receptors, the central effectors of the innate immune response has been documented in injured and failing hearts and has been suggested to play an important role in cardiac remodelling.[8] Another vital component of the innate immune response, the complement system, is composed of more than 30 proteins organised into proteolytic cascades, which are activated in response to the recognition of pathogen-associated molecular patterns, antigen–antibody complexes or danger signals released by injured cells.[9] Activation of the complement cascade has been documented in patients with chronic heart failure[10,11] and has been suggested to participate in disease progression. Although experimental evidence suggests that activation of inflammatory and immune responses may contribute to the pathogenesis of chronic heart failure, whether innate immunity mediates acute heart failure exacerbations remains unknown.

In the current issue of the journal, Trendelenburg and coworkers[12] examined the possible link between the activation of innate immunity and acute decompensated heart failure by measuring levels of complement activation products in the peripheral blood of patients admitted with an acute exacerbation of heart failure. The authors found that, when compared with healthy individuals, patients with acute heart failure exhibited increased plasma levels of the complement activation proteins C4d, C3a and sC5b-9. Complement protein levels were significantly higher in individuals with an infectious cause triggering the exacerbation, in comparison

The Wilf Family Cardiovascular Research Institute, Albert Einstein College of Medicine, USA

Corresponding author:
Nikolaos G Frangogiannis, The Wilf Family Cardiovascular Research Institute, Albert Einstein College of Medicine, 1300 Morris Park Avenue Forchheimer G46B Bronx, NY 10461, USA.
Email: nikolaos.frangogiannis@einstein.yu.edu

to individuals with other precipitating factors. Complement activation did not predict mortality within 2 years after the acute event. The study has several major limitations. First, the control group consisted of healthy individuals and was not adjusted for age or gender or the presence of comorbid conditions that could affect complement levels. Thus, the observed differences in complement activation between acute heart failure patients and control individuals may be due to the presence of comorbidities, or may simply reflect the presence of chronic heart failure. An adjusted control group of individuals with chronic heart failure is needed, in order to test whether acute exacerbations activate the complement cascade. Second, complement protein levels in the peripheral blood may not directly reflect myocardial localisation but may be due to activation of the cascade in other tissues. Third, the activation of innate immune signalling and downstream secretion of pro-inflammatory mediators was not systematically studied.

Despite these limitations, the study supports a very attractive concept, suggesting that in some patients with heart failure, activation of innate immune pathways may accompany (and possibly even trigger) an acute exacerbation. Moreover, the findings raise several intriguing questions: Which cellular events are responsible for sudden activation of the innate immune system in patients with chronic heart failure? Does innate immune activation play a causative role, or does it simply represent an epiphenomenon reflecting the systemic consequences of decompensated acute heart failure? If causative links between innate immune activation and acute heart failure do exist, which specific immune-mediated events cause cardiac dysfunction? Does evidence of immune activation identify a subset of patients who may benefit from a brief course of targeted anti-inflammatory intervention?

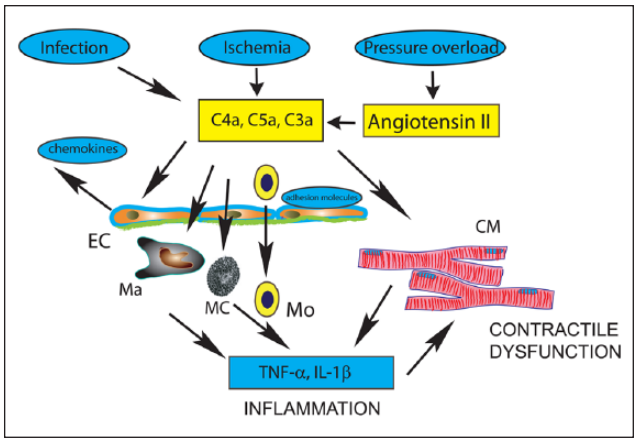

Figure 1. The schematic illustration proposes a cell biological paradigm for the potential involvement of complement activation in acute heart failure. In patients with chronic heart failure precipitating factors such as infection, ischaemia or pressure overload may trigger activation of the complement cascade, contributing to functional decompensation. Activated complement components may stimulate a pro-inflammatory programme in cardiac microvascular endothelial cells (EC), thus promoting inflammatory monocyte (Mo) recruitment, may induce cytokine expression in macrophages (Ma), and may trigger degranulation and cytokine production in cardiac mast cells (MC). C5a stimulation of cardiomyocytes (CM) may suppress contractile function and stimulate the synthesis of pro-inflammatory cytokines. Activation of a pro-inflammatory environment in the myocardium may overwhelm the limited functional reserve of patients with chronic heart failure causing an acute exacerbation. Considering the pathophysiological heterogeneity of acute heart failure, elevated circulating complement activation proteins may identify a patient subpopulation with immune-mediated decompensation who may benefit from brief and targeted anti-inflammatory interventions (such as interleukin (IL)-1 blockade). TNF: tumour necrosis factor.

Possible mechanisms of complement activation in patients with heart failure: links with known precipitating factors

Elevated complement activation proteins in the blood of patients with an acute heart failure exacerbation may reflect myocardial production and activation of complement components in response to injury, or the release of complement proteins due to a systemic condition (such as infection, or systemic inflammatory disease) (Figure 1). Patients with infection as a precipitating factor exhibited the highest levels of complement activation proteins, supporting the potential role of innate immune signalling in this subpopulation. In the myocardium, a wide range of stimuli, including ischaemia and pressure overload may trigger the local synthesis of complement components by cardiomyocytes, vascular endothelial cells or macrophages. Local activation of the complement cascade and deposition of complement components has been documented in the experimental models of myocardial ischaemia.[13] Activation of neurohumoral pathways in response to pressure overload may also activate the complement cascade. C5a levels were found to be increased in hypertensive individuals. Moreover, in a mouse model of angiotensin infusion complement activation mediated inflammatory activation.[14] Thus, in patients with a hypertensive crisis, the stimulation of neurohumoral signalling may activate the complement cascade in the myocardium contributing to decompensation. Microvascular endothelial cells may be an important site of complement activation in the failing heart. Cytokine stimulation of endothelial cells induces complement activation that is not only bound to the cells, but is also deposited in the subendothelial extracellular matrix.[15]

The cellular consequences of complement activation on the failing heart

In host defence, complement actions are mediated through three broad effector limbs: (a) assembly of the membrane

attack complex and subsequent lysis of the targeted pathogen; (b) opsonisation of the target, leading to phagocytosis by macrophages and neutrophils; and (c) activation of pro-inflammatory cascades. In patients with heart failure, complement activation may play an important role in triggering systolic dysfunction by stimulating the secretion of pro-inflammatory cytokines that suppress contractile function, such as tumour necrosis factor (TNF)-α and interleukin (IL)-1β. Complement may stimulate several myocardial cell types, including cardiomyocytes, microvascular endothelial cells, cardiac macrophages and mast cells (Figure 1).[16] In macrophages, C5a is known to induce pro-inflammatory cytokine synthesis.[17] In mast cells, C3a and C5a may trigger degranulation and promote the release of chemokines and TNF-α.[18,19] Endothelial cells respond to C5a by increasing the expression of adhesion molecules, chemokines, cytokines and chemokine receptors;[20] these effects may promote local inflammation. In cardiomyocytes, complement-mediated signalling may stimulate cytokine expression and cause contractile dysfunction.[21] Due to their limited functional reserve, patients with chronic heart failure may be particularly susceptible to modest elevations in activated complement components and may respond with significant suppression of contractile function.

The clinical implications of innate immune activation in patients with acute heart failure

In chronic heart failure, elevations in complement proteins identified a subpopulation with a higher incidence of adverse events.[22] In the current study, complement proteins did not predict death within 2 years, failing to support a role for complement activation as a prognostic biomarker in patients with decompensated heart failure. However, assessment of complement activation may serve as a valuable tool for pathophysiological stratification of heart failure patients, by distinguishing acute episodes of inflammation-driven decompensation, or by identifying patient subpopulations susceptible to recurrent immune-mediated heart failure exacerbations. Such insights may have important therapeutic implications, identifying patients who may benefit from a brief course of targeted anti-inflammatory therapy. A recent study demonstrated that IL-1 blockade with anakinra reduced C-reactive protein levels in patients with acute decompensated heart failure,[23] suggesting effective inhibition of inflammatory signalling. Whether brief inhibition of the innate immune response is beneficial in subsets of patients with acute heart failure has not been tested.

Effective treatment of complex cardiovascular conditions, such as heart failure, is hampered by their pathophysiological heterogeneity.[24] The expanding use of relevant biomarkers and sophisticated imaging strategies will allow us to stratify patients on the basis of underlying pathophysiological perturbations, providing the basis for mechanism-driven therapy.

Conflict of interest

The author declares that there is no conflict of interest.

Funding

The author's laboratory is supported by grants from the National Institutes of Health (R01 HL76246 and R01 HL85440), and the US Department of Defense (PR151134 and PR151029).

References

1. Storrow AB, Jenkins CA, Self WH, et al. The burden of acute heart failure on U.S. emergency departments. *JACC Heart Fail* 2014; 2: 269–277.
2. Abdo AS. Hospital management of acute decompensated heart failure. *Am J Med Sci* 2017; 353: 265–274.
3. Miro O, Peacock FW, McMurray JJ, et al. Acute Heart Failure Study Group of the ESCACCA. European Society of Cardiology – Acute Cardiovascular Care Association position paper on safe discharge of acute heart failure patients from the emergency department. *Eur Heart J Acute Cardiovasc Care*. Epub ahead of print 21 February 2016. DOI: 10.1177/2048872616633853.
4. Weintraub NL, Collins SP, Pang PS, et al. American Heart Association Council on Clinical Cardiology, Council on Cardiopulmonary CCP Resuscitation. Acute heart failure syndromes: emergency department presentation, treatment, and disposition: current approaches and future aims: a scientific statement from the American Heart Association. *Circulation* 2010; 122: 1975–1996.
5. Farmakis D, Parissis J, Lekakis J, et al. Acute heart failure: epidemiology, risk factors, and prevention. *Rev Esp Cardiol (Engl Ed)* 2015; 68: 245–248.
6. Mann DL. The emerging role of innate immunity in the heart and vascular system: for whom the cell tolls. *Circ Res* 2011; 108: 1133–1145.
7. Frangogiannis NG. Regulation of the inflammatory response in cardiac repair. *Circ Res* 2012; 110: 159–173.
8. Frantz S, Kobzik L, Kim YD, et al. Toll4 (TLR4) expression in cardiac myocytes in normal and failing myocardium. *J Clin Invest* 1999; 104: 271–280.
9. Dunkelberger JR and Song WC. Complement and its role in innate and adaptive immune responses. *Cell Res* 2010; 20: 34–50.
10. Aukrust P, Gullestad L, Lappegard KT, et al. Complement activation in patients with congestive heart failure: effect of high-dose intravenous immunoglobulin treatment. *Circulation* 2001; 104: 1494–1500.
11. Shahini N, Michelsen AE, Nilsson PH, et al. The alternative complement pathway is dysregulated in patients with chronic heart failure. *Sci Rep* 2017; 7: 42532.
12. Trendelenburg M, Stallone F, Pershyna K, et al. Complement activation products in acute heart failure: potential role in pathophysiology, responses to treatment and impacts on long term survival. *Eur Heart J Acute Cardiovasc Care*. Epub ahead of print 1 February 2017. DOI: 10.1177/2048872617694674.

13. Yasojima K, Kilgore KS, Washington RA, et al. Complement gene expression by rabbit heart: upregulation by ischemia and reperfusion. *Circ Res* 1998; 82: 1224–1230.
14. Zhang C, Li Y, Wang C, et al. Complement 5a receptor mediates angiotensin II-induced cardiac inflammation and remodeling. *Arterioscler Thromb Vasc Biol* 2014; 34: 1240–1248.
15. Hindmarsh EJ and Marks RM. Complement activation occurs on subendothelial extracellular matrix in vitro and is initiated by retraction or removal of overlying endothelial cells. *J Immunol* 1998; 160: 6128–6136.
16. Frangogiannis NG, Lindsey ML, Michael LH, et al. Resident cardiac mast cells degranulate and release preformed TNF-alpha, initiating the cytokine cascade in experimental canine myocardial ischemia/reperfusion. *Circulation* 1998; 98: 699–710.
17. Cavaillon JM, Fitting C and Haeffner-Cavaillon N. Recombinant C5a enhances interleukin 1 and tumor necrosis factor release by lipopolysaccharide-stimulated monocytes and macrophages. *Eur J Immunol* 1990; 20: 253–257.
18. Pundir P, MacDonald CA and Kulka M. The novel receptor C5aR2 is required for C5a-mediated human mast cell adhesion, migration, and proinflammatory mediator production. *J Immunol* 2015; 195: 2774–2787.
19. Gaudenzio N, Sibilano R, Marichal T, et al. Different activation signals induce distinct mast cell degranulation strategies. *J Clin Invest* 2016; 126: 3981–3998.
20. Albrecht EA, Chinnaiyan AM, Varambally S, et al. C5a-induced gene expression in human umbilical vein endothelial cells. *Am J Pathol* 2004; 164: 849–859.
21. Kalbitz M, Fattahi F, Herron TJ, et al. Complement destabilizes cardiomyocyte function in vivo after polymicrobial sepsis and in vitro. *J Immunol* 2016; 197: 2353–2361.
22. Clark DJ, Cleman MW, Pfau SE, et al. Serum complement activation in congestive heart failure. *Am Heart J* 2001; 141: 684–690.
23. Van Tassell BW, Abouzaki NA, Oddi Erdle C, et al. Interleukin-1 blockade in acute decompensated heart failure: a randomized, double-blinded, placebo-controlled pilot study. *J Cardiovasc Pharmacol* 2016; 67: 544–551.
24. Frangogiannis NG. The inflammatory response in myocardial injury, repair, and remodelling. *Nat Rev Cardiol* 2014; 11: 255–265.

Cardiovascular Research
doi:10.1093/cvr/cvx146

SPOTLIGHT REVIEW

Fibroblasts and the extracellular matrix in right ventricular disease

Nikolaos G. Frangogiannis*

Department of Medicine (Cardiology), The Wilf Family Cardiovascular Research Institute, Albert Einstein College of Medicine, 1300 Morris Park Avenue, Forchheimer G46B Bronx, 10461 NY, USA

Received 20 March 2017; revised 13 June 2017; editorial decision 14 July 2017; accepted 1 August 2017

Abstract

Right ventricular failure predicts adverse outcome in patients with pulmonary hypertension (PH), and in subjects with left ventricular heart failure and is associated with interstitial fibrosis. This review manuscript discusses the cellular effectors and molecular mechanisms implicated in right ventricular fibrosis. The right ventricular interstitium contains vascular cells, fibroblasts, and immune cells, enmeshed in a collagen-based matrix. Right ventricular pressure overload in PH is associated with the expansion of the fibroblast population, myofibroblast activation, and secretion of extracellular matrix proteins. Mechanosensitive transduction of adrenergic signalling and stimulation of the renin–angiotensin–aldosterone cascade trigger the activation of right ventricular fibroblasts. Inflammatory cytokines and chemokines may contribute to expansion and activation of macrophages that may serve as a source of fibrogenic growth factors, such as transforming growth factor (TGF)-β. Endothelin-1, TGF-βs, and matricellular proteins co-operate to activate cardiac myofibroblasts, and promote synthesis of matrix proteins. In comparison with the left ventricle, the RV tolerates well volume overload and ischemia; whether the right ventricular interstitial cells and matrix are implicated in these favourable responses remains unknown. Expansion of fibroblasts and extracellular matrix protein deposition are prominent features of arrhythmogenic right ventricular cardiomyopathies and may be implicated in the pathogenesis of arrhythmic events. Prevailing conceptual paradigms on right ventricular remodelling are based on extrapolation of findings in models of left ventricular injury. Considering the unique embryologic, morphological, and physiologic properties of the RV and the clinical significance of right ventricular failure, there is a need further to dissect RV-specific mechanisms of fibrosis and interstitial remodelling.

Keywords Cardiac fibrosis • Right ventricular failure • Pulmonary hypertension • Extracellular matrix • Arhhythmogenic right ventricular cardiomyopathy

This article is part of the Spotlight Issue on Right Ventricle.

1. Introduction

The right ventricle (RV) is no longer the 'forgotten chamber'.[1] Extensive clinical evidence supports the prognostic significance of right ventricular dysfunction in a wide range of cardiovascular conditions. In myocardial infarction[2] and in heart failure,[3,4] right ventricular dysfunction is associated with adverse outcome and may predict arrhythmic events, marking a high-risk group.[5] In patients with acute pulmonary embolism, persistent depression of right ventricular function is associated with recurrent thromboembolic events.[6] In patients with pulmonary hypertension (PH), right ventricular systolic dysfunction predicts adverse outcome irrespective of changes in pulmonary vascular resistance.[7] Although therapeutic interventions in PH are focused on the pulmonary vasculature, survival is significantly associated with improved right ventricular function, whereas changes in pulmonary vascular resistance have little relationship to outcome.[8] Considering the outstanding clinical significance of right ventricular failure, understanding of the cellular events and molecular signals responsible for adverse remodelling of the RV following injury should be a major priority in cardiovascular research.

Over the past 20 years, cardiovascular investigators have appreciated the role of the cardiac interstitium in myocardial homeostasis and disease. Experimental studies have unravelled the complexity and phenotypic plasticity of cardiac interstitial cells and have challenged the traditional view of the cardiac extracellular matrix as a static structural scaffold. Following injury, the cardiac matrix is enriched through deposition of extracellular macromolecules that do not serve a structural role,

* Corresponding author: Tel: +1 718 430 3546; fax: +1 718 430 8989, E-mail: nikolaos.frangogiannis@einstein.yu.edu

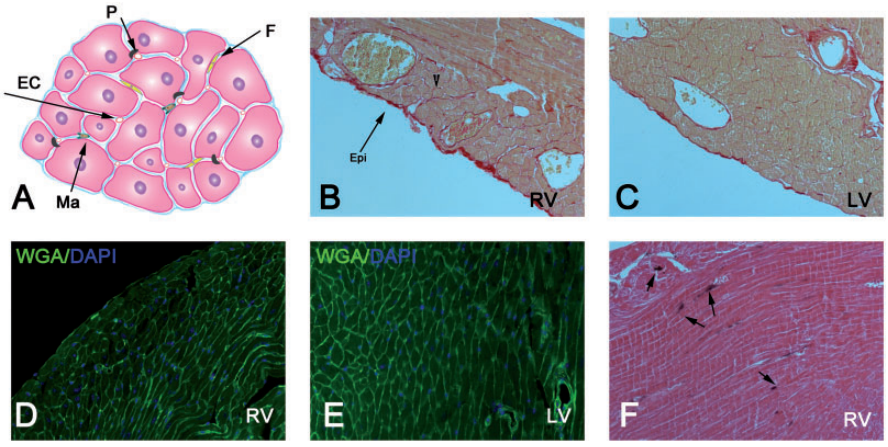

Figure 1 The right ventricular interstitium. (*A*) The adult mammalian myocardium is comprised of cardiomyocytes, abundant microvessels (EC, endothelial cells) and a highly cellular interstitium that contains large numbers of fibroblasts (F), pericytes (P) and smaller populations of macrophages (Ma) and other immune cells, enmeshed into a collagen-based matrix. Although systematic comparison of the cellular composition and matrix content between the right and the left ventricular myocardium has not been performed, the interstitium of the RV and the left ventricle have similar morphological characteristics. (*B* and *C*) Representative images show staining with picrosirius red of sections from the right ventricular free wall (B, RV) and the left ventricular free wall (*C*, LV) in adult mouse hearts, in order to identify the collagen network. The epimysial collagen surrounds the organ (arrow); each cardiomyocyte is associated with a thin rim of endomysial collagen (arrowhead). (*D*, *E*) Dual fluorescence for wheat germ agglutinin outlines the cardiomyocytes in the mouse right ventricle (D, RV) and in the left ventricular free wall (E, LV). Experimental studies in adult rats have suggested that due to the lower baseline pressure load and the smaller size of right ventricular cardiomyocytes, the RV exhibits a higher relative collagen content, when compared with the left ventricle and the interventricular septum.[20] (*F*) Immunohistochemical staining for the macrophage-specific antibody Mac2 identified a resident macrophage population in the right ventricular wall (arrows).

but modulate signalling cascades by regulating growth factor activity and by transducing signals through binding to cell surface receptors. These macromolecules termed 'matricellular proteins',[9,10] drive the cellular responses that mediate repair, remodelling, and fibrosis of the injured myocardium.[11] Although our knowledge on the role of the cardiac interstitium in myocardial repair, remodelling, and fibrosis is derived primarily from studies investigating left ventricular injury, a growing body of evidence suggests a crucial involvement of interstitial changes and matrix remodelling in the pathogenesis and progression of right ventricular disease. The current manuscript discusses the cellular effectors and molecular signals implicated in interstitial remodelling of the RV in a wide range of pathophysiological conditions. Although right ventricular and left ventricular interstitial cells may have similar baseline phenotypic profiles and functional properties, the distinct morphologic, physiologic, and pathophysiological characteristics of the RV create a unique environment, leading to different responses under conditions of stress. Unfortunately, in many cases, prevailing paradigms on the mechanisms of right ventricular fibrosis and on the role of the extracellular matrix in remodelling of the RV are based on extrapolation of experimental observations in models of left ventricular disease.

2. The interstitium in the healthy right ventricle

The adult mammalian heart is composed of cardiomyocytes, a rich microvascular network, and a highly cellular collagen-based interstitium (*Figure 1*) that contains abundant fibroblast-like interstitial cells and smaller populations of macrophages, mast cells and dendritic cells.[12–15] Interstitial cells play an important role in maintaining the cardiac extracellular matrix and may also transduce signals that regulate cardiomyocyte survival and function. Systematic studies comparing the cellular composition and extracellular matrix content of the right and left ventricle have not been performed.

While the left ventricle is derived exclusively from the first heart field, the RV derives in part from the second heart field, which is characterized by increased proliferative activity and differentiation delay.[16] Moreover, the low resistance of the pulmonary vascular territory reduces energy demands on the right ventricular myocardium, leading to thinner walls, a lower muscle mass and increased compliance.[17] To what extent the distinct embryologic origin and the lower pressure load affect the cellular composition and extracellular matrix content of the RV in the absence of injury remains unknown. At birth, right and left ventricles have comparable collagen content; neonatal remodelling of the heart leads to regression in right ventricular myocyte size, resulting in a relative increase of collagen content in the adult right ventricle.[18,19] In normal adult rats, a hydroxyproline assay demonstrated a lower collagen content in the left ventricular free wall, when compared with the right ventricle and the interventricular septum.[20] On the other hand, experiments comparing fibroblasts from different sites suggested no significant differences in transcriptomic profiles between right ventricular and left ventricular cardiac fibroblasts.[21,22] All forms of myocardial injury activate the cardiac interstitium leading to expansion of interstitial cell populations and dynamic alterations in the composition of the extracellular matrix.

3. The right ventricular interstitium in heart disease

The RV tolerates a volume load much better than a pressure load and is more sensitive to changes in afterload than the left ventricle.[23]

Moreover, due to a more favourable supply and demand ratio, the RV is less susceptible to ischemic injury. Thus, in human patients, the most common pathophysiological cause of right ventricular failure is pressure overload due to pulmonary hypertension. The impact of pressure overload on the RV is dependent not only on the magnitude of the pressure increase but also on the underlying aetiology, and on the rate of progression of the changes in pulmonary pressures. A sudden increase in pulmonary pressures following massive acute pulmonary embolism causes a marked elevation in right ventricular end-diastolic volume, as the chamber attempts to compensate in order to maintain stroke volume. Marked acute increases in pulmonary pressures overwhelm the compensatory response, leading to rapid development of right ventricular failure. In contrast, chronic progressive elevations of pulmonary pressures are better tolerated by the RV and lead to extensive remodelling, involving both the cardiomyocytes and the right ventricular interstitium.

3.1 The extracellular matrix in acute right ventricular pressure overload

Descriptive studies in experimental models of acute pulmonary embolism demonstrated rapid infiltration of the right ventricular outflow tract (RVOT) with neutrophils and monocytes, accompanied by local activation of matrix metalloproteinases (MMPs),[24] followed by stimulation of a pro-fibrotic program.[25] Early matrix degradation may contribute to the pathogenesis of acute right ventricular failure, depriving the cardiomyocytes from important pro-survival signals, or abrogating matrix-dependent pathways that preserve cardiomyocyte function. In three studies performed by the same group in rat, canine and ovine models of acute pulmonary embolism pre-treatment with doxycycline, a broad non-selective MMP inhibitor attenuated right ventricular dilation[26–28] and decreased cardiomyocyte injury.[27] Considering the broad effects of doxycycline on inflammatory signalling and oxidative stress,[29] whether the protective actions reflect attenuated matrix degradation remains unknown.

3.2 The extracellular matrix in chronic pressure overload

Chronic right ventricular pressure overload increases wall stress and promotes a hypertrophic response. Right ventricular mass is significantly increased in PH patients[30] and right ventricular hypertrophy is consistently observed in experimental models of PH. However, in human patients, the likelihood of progression to right ventricular failure cannot be explained by differences in right ventricular mass or in pressure load. Despite similar elevations in right ventricular pressures and comparable right ventricular hypertrophy, some patients remain stable for decades, while others rapidly decompensate developing right ventricular failure.[8,31] The aetiology of PH plays a major role in determining the outcome. For example, right ventricular failure is highly prevalent in patients with scleroderma-induced PH.[32] In contrast, patients with right ventricular pressure overload caused through purely mechanical causes (such as pulmonic stenosis) exhibit prolonged concentric hypertrophy without significant contractile depression.[33,31] Animal models recapitulate this heterogeneity, as development of right ventricular dysfunction is dependent not only on the severity of pressure overload but also on the underlying pathophysiological basis.[34] In models of PH due to administration of endothelial toxins (such as monocrotaline), right ventricular failure is more prominent than in models of mechanical pressure overload induced through pulmonary artery banding.[35] Distinct responses of interstitial cells and the extracellular matrix may explain the heterogeneity of the functional responses of the RV to the various pathophysiological conditions causing PH.

3.2.1 Fibrosis in the pressure-overloaded right ventricular myocardium

A growing body of evidence suggests that right ventricular fibrosis, the expansion of the interstitium through deposition of collagenous matrix, may play an important role in the pathogenesis of right ventricular dysfunction and failure following pressure overload. Magnetic resonance imaging (MRI) suggests that many patients with PH exhibit evidence of right ventricular fibrosis.[36] Histological studies have demonstrated increased collagen deposition in the RV from patients with end-stage PH undergoing heart–lung transplantation.[30] In experimental models of right ventricular pressure overload, fibrotic remodelling of the RV is often associated with decompensation and evidence of severe systolic dysfunction.[37] *Ex vivo* studies suggested that the contribution of fibrosis to the increased right ventricular stiffness increases with worsening severity of dysfunction.[38] Increased collagen deposition in the RV following pressure overload is due to new synthesis of collagen protein,[39] and is associated with a disproportionate increase in collagen I secretion,[38] a subtype exhibiting higher tensile strength and reduced elasticity when compared with type III collagen. Perturbation of the collagen I:III ratio may be responsible, at least in part, for the increase in right ventricular stiffness following pressure overload.

In the model of pulmonary artery banding, late increases in the levels of insoluble collagen are noted and are associated with right ventricular diastolic dysfunction.[40] Accumulation of insoluble collagen may reflect cross-linking of the right ventricular interstitial matrix; however, the potential involvement of specific cross-linking enzymes, such as lysyl-oxidases and tissue transglutaminase has not been investigated.

3.2.2 The cellular effectors implicated in right ventricular fibrosis and remodelling

Our current understanding of the cell biological events responsible for fibrotic remodelling of the pressure-overloaded RV is based predominantly on descriptive experiments and on extrapolation of findings from studies investigating left ventricular fibrosis. Thus, the prevailing paradigm (*Figure 2*) assumes similar cellular properties and mechanism of activation for right and left ventricular myocardial cells, and has not been systematically validated by direct experimentation.

3.2.2.1 Fibroblasts. Cardiac fibroblasts are the main effector cells in cardiac fibrosis.[41] Extensive evidence suggests that fibrosis of the pressure-overloaded RV is associated with activation and expansion of fibroblasts, which acquire a myofibroblast phenotype and secrete large amounts of extracellular matrix proteins. In a rabbit model of pulmonary artery constriction, early infiltration of the myocardium with mononuclear cells was noted 2 days after banding and was associated with evidence of cardiomyocyte injury. After 7 days of banding, resolution of the inflammatory infiltrate was accompanied by recruitment of activated myofibroblasts, expressing α-smooth muscle actin. After 14 days, the right ventricular interstitium contained significant amounts of fibrillar collagen.[42] Activated myofibroblasts in the pressure-overloaded RV synthesize large amounts of collagen and secrete matricellular proteins.[40] The time course of these cellular alterations suggests that fibrogenic activation may be dependent on early induction of inflammation in the pressure-overloaded RV, either through direct stimulation of mechanosensitive pro-inflammatory signalling pathways, or secondary to cardiomyocyte necrosis. Direct stimulation of resident cardiac fibroblasts

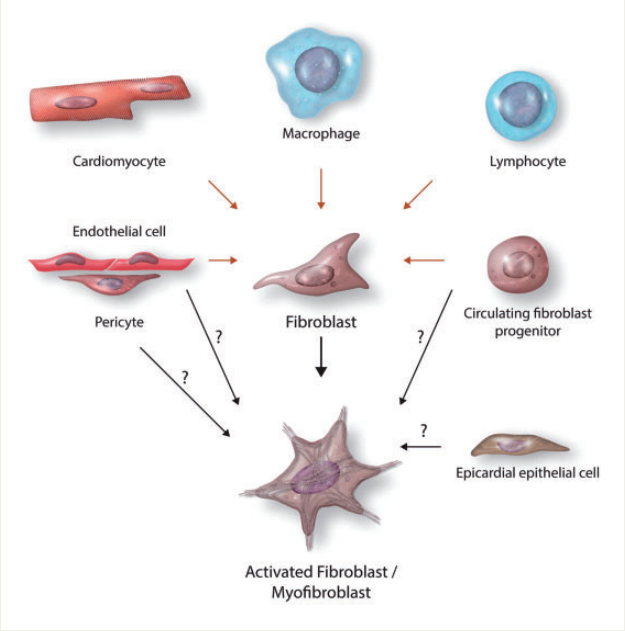

Figure 2 Cell biological effectors of fibrosis in the pressure-overloaded RV. Based on insights from lineage tracing experiments in models of left ventricular pressure overload, activated myofibroblasts are predominantly derived from resident populations. Endothelial cells, pericytes, epicardial epithelial cells, and circulating fibroblast progenitors may also play contributory roles. Vascular cells, stressed cardiomyocytes, resident, and recruited macrophages may play an important role in activation of resident fibroblast population in the pressure-overloaded myocardium.

through activation of neurohumoral or growth factor-mediated pathways may also contribute to the fibrotic response.

The cellular origin of fibroblasts in the remodelling RV has not been systematically investigated. Recent lineage tracing experiments demonstrated that in experimental models of left ventricular pressure overload, resident cardiac fibroblast populations are the main source of activated myofibroblasts.[43,44] Endothelial to mesenchymal transdifferentiation and circulating fibroblast progenitors may also contribute smaller, but potentially important, fibroblast subsets.[45] The distinct embryologic, morphologic and functional characteristics of the RV, and the unique features of the right ventricular response to injury may have an impact on the relative contributions of various cell types in right ventricular fibrosis.

3.2.2.2 Macrophages and lymphocytes. The adult mouse RV contains a sparse population of macrophages.[15] Right ventricular pressure overload is associated with significant expansion of the macrophage population in the right ventricular wall.[46] Moreover, patients with PH exhibit significantly increased macrophage density in the RV.[47] In models of left ventricular pressure overload, cardiac macrophages have been implicated in the activation of a fibrogenic program.[48] Expansion of the macrophage population in the pressure-overloaded myocardium may be triggered through chemokine-dependent mechanisms.[49] Moreover, neurohumoral mediators may activate macrophages towards a pro-fibrotic phenotype characterized by secretion of growth factors and cytokines. Unfortunately, experimental evidence supporting this plausible concept is lacking, as studies investigating the contribution of macrophages in right ventricular fibrosis have not been performed.

A growing body of evidence implicates lymphocytes in the pathogenesis of myocardial fibrosis in experimental models of left ventricular pressure overload.[50] In a model of transverse aortic constriction, CD4+ T cells-mediated fibrosis, decompensation, and transition to heart failure.[51] Although systemic aldosterone infusion leads to recruitment of lymphocytes in the RV,[52] the potential involvement of lymphocyte subpopulations in right ventricular fibrosis has not been investigated.

3.2.2.3 Mast cells. Mast cells have been implicated in the pathogenesis of left ventricular remodelling and fibrosis.[53] Mast cells accumulate in the injured myocardium and degranulate, releasing fibrogenic cytokines and growth factors, and secreting mast cell-specific mediators with fibroblast-activating properties, such as histamine, tryptase, and chymase.[54–56] In rodent models of pulmonary artery banding, significant increases in mast cell density were observed in the right ventricular myocardium.[57,58] Whether mast cell-derived mediators critically regulate the fibrotic response in the RV has not been investigated.

3.2.2.4 Cardiomyocytes. Focal cardiomyocyte necrosis has been documented in experimental models of right ventricular pressure overload[42] and can trigger fibrosis by activating pro-inflammatory signalling. Under conditions of stress, cardiomyocytes are capable of stimulating fibrosis even in the absence of significant necrosis. Mechanical stretch induces expression of renin, angiotensinogen, and ACE in cardiomyocytes[59]; these effects may trigger an angiotensin-driven fibrogenic program following pressure overload. Moreover, stimulated cardiomyocytes may be an important source of transforming growth factor (TGF)-β,[60] a crucial fibrogenic mediator that promotes myofibroblast transdifferentiation and induces extracellular matrix protein synthesis.[61] The potential contribution of pressure-overloaded right ventricular cardiomyocytes in fibrotic remodelling of the RV has not been investigated.

3.2.2.5 Vascular cells. In the pressure-overloaded myocardium, vascular endothelial cells may be an important source of fibrogenic mediators, such as endothelin-1. Right ventricular capillary rarefaction is a consistent characteristic of maladaptive right ventricular hypertrophy in both animal models of pressure overload and in human patients with PH.[8,62,63] Reduced perfusion of the right ventricular wall may exacerbate local ischemia, thus promoting a fibrogenic response. Although capillary loss in the RV may reflect transdifferentiation of vascular endothelial cells or pericytes to fibroblasts, evidence suggesting an important role for vascular cells as a cellular source for activated fibroblasts infiltrating the pressure overloaded RV is lacking.

3.2.3. Molecular signals mediating right ventricular fibrosis

Development of fibrosis in the pressure-overloaded RV involves activation of mechanosensitive signalling pathways that release neurohumoral mediators, stimulate inflammatory responses, and trigger growth factor-mediated cascades (*Table 1* and *Figure 3*).

3.2.3.1 Neurohumoral pathways

Sympathetic stimulation and activation of the renin–angiotensin–aldosterone system (RAAS) are prominent features of PH and are implicated in the pathogenesis of right ventricular dysfunction.[64] In experimental models of PH, the administration of the non-selective β-blocker carvedilol,[65] or the β1 adrenergic receptor (AR) antagonist bisoprolol[66] attenuated right ventricular remodelling and decreased fibrosis of the right ventricular wall without affecting pulmonary pressures. Although

Table 1 Molecular signals implicated in right ventricular fibrosis following pressure overload

Pathway	Likely mechanisms of action	Functional effects	References
Adrenergic stimulation	β-AR signalling stimulates fibroblast proliferation[67,145] and may modulate fibroblast function[146]	AR signalling may contribute to adverse right ventricular remodelling and may promote progression of right-sided heart failure	65,66
Renin–angiotensin–aldosterone system (RAAS)	Angiotensin II-mediated AT-1 activation promotes fibroblast activation, and stimulates extracellular matrix protein synthesis[147] Aldosterone-mediated mineralocorticoid receptor signalling activates fibroblasts[148] and may promote a fibrogenic macrophage phenotype[149] Activation of the RAAS may promote inflammation, thus triggering a fibrotic response[52].	Pharmacologic inhibition experiments have suggested an important role for the RAAS in right ventricular dysfunction following pressure overload in some[70,71] but not all studies[72]	70–72
Endothelin-1	Endothelin-1 stimulates proliferation and matrix synthesis in cardiac fibroblasts[77] Endothelin-1 may promote a pro-fibrotic phenotype in vascular cells[150]	Pharmacological inhibition experiments suggest that endothelin receptor signalling promotes right ventricular remodelling and fibrosis in models of pulmonary hypertension.[78–80] In addition to its role in the pulmonary vasculature, endothelin-1 may also mediate fibrosis of the RV	78–80
Oxidative stress	Mechanosensitive activation of Rho kinase may trigger ROS generation in fibroblasts, thus promoting collagen synthesis Accentuated oxidative stress in the pressure-overloaded RV may be due to defective antioxidant responses	Pharmacologic interventions using antioxidants suggest that ROS generation contributes to right ventricular remodelling fibrosis and dysfunction following pressure overload	81–83
Inflammatory cytokines and chemokines	Neurohumoral pathways and oxidative stress may be responsible for induction of inflammatory cytokines and chemokines in the pressure-overloaded RV. Cytokines may modulate fibroblast activity and may promote a fibrogenic phenotype in macrophages	Although descriptive studies show induction of inflammatory signals in the pressure overloaded RV, studies examining the role of cytokines and chemokines in the pathogenesis of right ventricular fibrosis have not been performed	85
TGF-β	TGF-βs are critical regulators of fibroblast function, but may also mediate fibrosis by promoting fibrogenic actions on other cell types (such as immune and vascular cells)	Although descriptive studies suggest TGF-β1 induction in the remodelling RV, the role of the TGF-β cascade in right ventricular fibrosis has not been systematically studied. Studies in both angio-obliterative and surgical models of right ventricular pressure overload have suggested an important role for the accessory TGF-β receptor endoglin in right ventricular fibrosis and dysfunction[97]	70,91,97
Matricellular proteins	Matricellular proteins (thrombospondins, tenascin-C, periostin, osteopontin, SPARC, CCNs) modulate growth factor signalling and protease activity and have profound effects on phenotype and function of fibroblasts, inflammatory cells and vascular cells	Upregulation of osteopontin, tenascin-C, SPARC and CCN2 in the RV has been demonstrated in models of pulmonary hypertension. However, their role in right ventricular remodelling and fibrosis has not been investigated	40,70,102,103

adrenergic stimulation is known to activate cardiac fibroblasts *in vitro*,[67] whether reduced fibrosis following AR blockade *in vivo* is due to direct actions on the fibroblasts, or represents an epiphenomenon, reflecting effects on cardiomyocytes or vascular cells is unknown. Moreover, the relative significance of attenuated fibrosis and modulation of the matrix environment in mediating the protective actions of β-AR blockade on right ventricular function has not been elucidated.

Local activation of angiotensin II and aldosterone signalling may also be implicated in the pathogenesis of right ventricular fibrosis following pressure overload. *In vitro* studies have demonstrated that mechanical stress induces components of the RAAS in cardiomyocytes.[59,68]. In models of PH, significantly increased expression of angiotensin converting enzyme was noted in the RV and was localized in fibrotic areas.[69] Evidence supporting an important role for the RAAS in mediating right ventricular fibrosis following pressure overload is predominantly derived from pharmacologic inhibition experiments. In a rabbit model of pulmonary artery banding and in a model of monocrotaline-induced pulmonary hypertension, angiotensin type 1 (AT1) receptor blockade attenuated right ventricular fibrosis.[70,71] In contrast, experiments in a rat model of pulmonary artery constriction, combined treatment with an AT1 inhibitor and an aldosterone antagonist had no effects on right ventricular dysfunction, did not significantly affect fibrosis, and did not

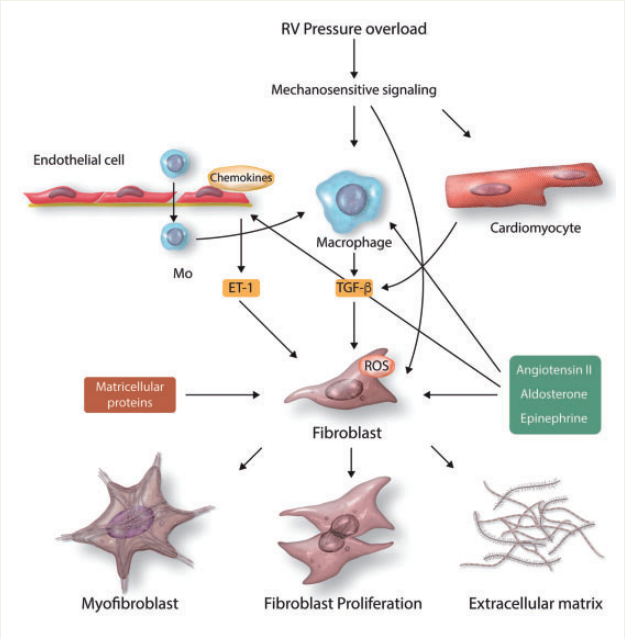

Figure 3 Molecular signals implicated in fibroblast activation in the pressure-overloaded RV. Right ventricular pressure overload transduces mechanosensitive signalling in cardiomyocytes (CM), fibroblasts (F), vascular endothelial cells (EC), and macrophages (Ma), stimulating neurohumoral pathways and activating reactive oxygen species (ROS) generation. Activation of the RAAS pathway, adrenergic signalling, and oxidative stress stimulate fibroblast expansion and triggers synthesis of extracellular matrix proteins. Angiotensin II and aldosterone may also induce an inflammatory and fibrogenic program in endothelial cells, stimulating expression of endothelin-1 (ET-1), and synthesis of chemokines, and triggering recruitment of monocytes (Mo). Activated macrophages secrete transforming growth factor (TGF)-β and other growth factors in the cardiac interstitium. Enrichment of the extracellular matrix though the deposition of matricellular proteins regulates activation of growth factor signalling. TGF-β exerts potent matrix-preserving actions by promoting myofibroblast transdifferentiation, by stimulating synthesis of matrix proteins, and by inducing expression of antiproteases.

attenuate capillary rarefaction.[72] Currently, there is no evidence to support the use of RAAS inhibition strategies in patients with right ventricular dysfunction due to PH.[73]

3.2.3.2 Endothelin-1

Endothelin-1, a powerful vasoconstrictor with potent fibrogenic properties, is critically implicated in the pathogenesis of PH.[74] Endothelin receptor blockade is a safe and effective therapeutic approach for PH patients.[75] A growing body of evidence suggests that, in addition to its actions on the pulmonary vasculature, endothelin-1 may also mediate right ventricular dysfunction and fibrosis. The expression of endothelin and the endothelin type A receptor are significantly upregulated in the RV in experimental models of right ventricular pressure overload and in patients with PH.[76] In the RV, activation of the endothelin-1 axis may promote fibroblast proliferation and stimulate synthesis of extracellular matrix proteins.[77] Endothelin receptor blockade attenuates right ventricular fibrosis in mechanical, angio-obliterative, and hypoxia-induced models of pulmonary hypertension.[78–80] Whether these actions contribute to the beneficial effects of endothelin inhibition in patients with PH remains unknown.

3.2.3.3 Oxidative stress

Generation of reactive oxygen species (ROS) plays an important role in fibroblast activation and in deposition of extracellular matrix proteins in the remodelling myocardium. *In vivo* studies in a model of pulmonary artery constriction demonstrated that right ventricular pressure overload causes a marked increase in oxidative stress in the right ventricular myocardium, and suggested that, when compared to the left ventricle, the RV may exhibit an accentuated oxidative response to a pressure load.[81] Mechanosensitive activation of Rho kinase may play an important role in ROS generation following right ventricular pressure overload.[81] It has been suggested that the exaggerated oxidative response of the RV following stress may be due to defective antioxidant defenses. In a model of NO deficiency induced by L-NAME feeding, the RV exhibited early cardiomyopathic changes, and dilation; in contrast, the left ventricle had only subtle hypertrophic alterations. The selective involvement of the RV in this model was associated with increased oxidative stress and failure to activate antioxidant responses.[82] Treatment with antioxidants attenuated adverse remodelling and dysfunction of the RV, reducing right ventricular fibrosis in the rat monocrotaline model of pulmonary hypertension.[83]

3.2.3.4 Inflammatory signals

Pro-inflammatory cytokines and chemokines play an important role in fibrotic remodelling in many tissues, including the myocardium, both through direct stimulation of fibroblasts and through induction of fibrogenic signals in other cell types (such as macrophages and vascular cells).[84] Our understanding of the role of inflammatory mediators in right ventricular fibrosis is based on descriptive evidence and on known effects of these signals in left ventricular disease. In a mouse model of pulmonary artery constriction, marked upregulation of several members of the chemokine family was noted in the pressure-overloaded RV, including the CC chemokines CCL2 and CCL5, the CXC chemokines CXCL16 and CXCL10, and CX3CL1.[85] Neurohumoral mediators, generation of ROS, and direct activation of mechanosensitive pro-inflammatory signals in cardiomyocytes and macrophages may explain the induction of inflammatory genes in the pressure-overloaded RV. *In vitro* studies suggested that CXCL16, CX3CL1, and CCL5 may increase expression of the small leucine-rich glycoproteins decorin, biglycan, lumican, and fibromodulin, important activators of the fibrotic response.[85] CCL2 may also be implicated in the fibrotic myocardial response by recruiting mononuclear cells that may activate cardiac fibroblasts.[86] On the other hand, induction of the anti-fibrotic chemokine CXCL10[87,88] may serve as an endogenous inhibitory signal that restrains the fibrotic response.

3.2.3.5 The TGF-*β* superfamily

Several members of the TGF-β superfamily have been implicated in regulation of tissue fibrosis and extracellular matrix remodelling. TGF-β1 is critically involved in activation of a pro-fibrotic program, by inducing synthesis of extracellular matrix proteins and by promoting myofibroblast transdifferentiation.[61] On the other hand, members of the bone morphogenetic protein (BMP) subfamily, such as BMP-2 and BMP-7, may attenuate fibrosis by inhibiting TGF-β actions.[45,89,90]. The role of TGF-β signalling pathways in mediating right ventricular dysfunction and fibrosis

following pressure overload is poorly understood. TGF-β1 upregulation has been demonstrated in the RV in models of pulmonary artery constriction and in pulmonary hypertension secondary to left sided heart failure[91]; however, findings on downstream activation of TGF-β signalling cascades are conflicting. In an experimental model of pulmonary artery banding, increased levels of phosphorylated Smad2 (p-Smad2) in the right ventricular myocardium suggested activation of TGF-β signalling.[70] However, in patients with end-stage pulmonary hypertension, p-Smad2 immunoreactivity in the RV was reduced, when compared with controls.[92] The contradictory findings may reflect the dynamic regulation of the TGF-β cascade *in vivo*. Early activation of the pathway in the pressure-overloaded myocardium may be followed by induction of inhibitory signals that restrain TGF-β/Smad signalling.

Dissection of the *in vivo* actions of TGF-β family members is hampered by the wide range of their context-dependent effects that target many different cell types. In models of reparative and interstitial left ventricular fibrosis, both Smad-dependent and Smad-independent actions of TGF-β signalling have been suggested to play important roles in regulation of fibroblast responses[93–96] and in deposition of extracellular matrix proteins. Experiments investigating the *in vivo* role of TGF-β signalling cascades in fibrosis and remodelling of the RV have not been performed. Experimental studies in both angio-obliterative and surgical models of right ventricular pressure overload suggested that endoglin, an accessory receptor for the TGF-β family, may mediate fibrosis and dysfunction of the RV.[97]

3.2.3.6 The matricellular proteins

Matricellular proteins are extracellular macromolecules that do not serve a primary structural role, but are secreted following injury and modulate growth factor and cytokine responses. In the remodelling myocardium, the extracellular matrix is enriched through the deposition of matricellular proteins. Over the last 10–15 years, experimental studies have suggested that several members of the matricellular family (including the thrombospondins, tenascins, osteopontin, SPARC, periostin, and members of the CCN family) are markedly induced in the injured and pressure overloaded left ventricle and play a critical role in regulating inflammatory, fibrotic, and angiogenic responses.[11,98–101] The potential involvement of members of the matricellular proteins in remodelling of the pressure-overloaded RV is suggested almost exclusively by descriptive studies. Right ventricular upregulation of osteopontin, tenascin-C, SPARC, and CCN2 has been documented in experimental models of PH.[40,70,102,103] Induction of matricellular proteins in the pressure-overloaded RV may be mediated through the activation of neurohumoral and inflammatory pathways and may involve activation of TGF-β. Investigations examining the role of matricellular actions in regulating right ventricular fibrosis, matrix remodelling, and dysfunction have not been performed.

3.3. The extracellular matrix in right ventricular volume overload

Pure right ventricular volume overload is generally well tolerated by human patients and experimental animals. Many patients with tetralogy of Fallot develop pulmonary insufficiency that typically has minimal consequences over several decades, but can be the source of late complications including right ventricular dysfunction due to chronic volume overload.[104] In both large animal and rodent models of pulmonary insufficiency, right ventricular volume overload resulted in dilation of the RV, accompanied by diastolic dysfunction, without affecting systolic function.[105,106] In the mouse model, right ventricular volume overload was associated with development of subendocardial fibrosis in the right ventricular wall. Dynamic changes in the expression of matrix remodelling genes were observed: early downregulation of some members of the TGF-β superfamily (such as growth differentiation factor (GDF)-5 and GDF-7) was followed by late induction of cytokines and chemokines, TGF-β1 upregulation and increased transcription of matricellular proteins (including thromsbospondin-1 and periostin).[105] The functional significance of these alterations remains unknown.

3.4. Right ventricular infarction

Although the cellular events and molecular pathways involved in fibrotic repair of the infracted left ventricle have been extensively characterized,[107] much less is known about the response of the RV to infractive injury. In the clinic, right ventricular infarction is quite common; 40–50% of patients with acute inferior myocardial infarction exhibit right ventricular involvement.[108] Experimental animal models and clinical experience suggest that although early functional depression of the RV following infarction may have adverse consequences, the right ventricular myocardium is resistant to infarction and recovers even after prolonged coronary occlusion.[109] In human patients with early right ventricular ischemic dysfunction, the function of the RV returns to normal within 3–12 months.[110] In the dog, persistent occlusion of the right coronary artery does not cause infarction.[111] The more favourable balance between oxygen supply and demand explains the reduced vulnerability of the RV to ischemic injury. The extensive collateralization of the RV provides more reliable blood supply under ischemic conditions, while the lower myocardial mass and the reduced afterload account for the decreased demand, in comparison to the left ventricular myocardium. Moreover, the RV exhibits higher capabilities to extract oxygen under conditions of stress, due to its low oxygen contraction levels at rest. Whether differences in the matrix composition of the cardiac interstitium, or distinct functional properties of right ventricular fibroblasts and immune cells contribute to the unique response of the RV to ischemia is unknown.

3.5. The right ventricular extracellular matrix in arrhythmogenic cardiomyopathies

Myocardial fibrosis perturbs propagation of the electrical impulse and has been implicated in arrhythmia generation. Evidence of right ventricular interstitial or perivascular fibrosis was found in 56% of patients with ventricular arrhythmias in the absence of clinical structural heart disease.[112] Interstitial fibrosis in the RVOT has been detected in patients with sudden cardiac death related to Brugada syndrome.[113] In patients with hypertrophic cardiomyopathy, right ventricular fibrosis predicted arrhythmic events.[114] Individuals with arrhythmogenic right ventricular cardiomyopathy (ARVC) exhibit expansion of right ventricular fibroadipocytes, leading to fibrosis and fatty infiltration.[115–118]

The mechanisms responsible for the marked alterations in myocardial cellular composition in patients with ARVC and other arrhythmogenic cardiomyopathies remain unknown. Genetic studies have identified mutations in genes encoding desmosome proteins as the underlying cause in many patients with ARVC. Mutations in *PKP2*, which encodes plakophilin-2, in desmoplakin, and desmoglein-2 have been identified in many patients with ARVC.[119–121] In mice, loss of desmoplakin in a subset of interstitial cells with fibroadipocyte characteristics promotes adipocyte differentiation through a Wnt-dependent mechanism.[122,123] The cellular link between these mutations and right ventricular fibrosis is less

clear. Fibrosis may reflect cardiomyocyte injury, or primary activation of interstitial cell populations and transition to a fibroblast phenotype.[124] Recent cell biological experiments suggested that plakophilin-2 loss promotes TGF-β1 expression and may activate a fibrogenic program in cardiomyocytes.[125] The significance of these actions in the pathogenesis of fibrosis in ARVC remains unclear.

3.6. Right ventricular fibrosis in response to cancer chemotherapy

Patients treated with anthracyclines as cancer chemotherapy exhibit a high incidence of cardiac complications. Acute anthracycline cardiotoxicity is rare in human patients and is associated with dose-dependent cardiomyocyte injury and secondary inflammation.[126] Chronic cardiotoxicity on the other hand, may occur within 1 year after completion of treatment (early-onset chronic cardiomyopathy), or may affect cancer survivors many years after therapy (late-onset chronic cardiomyopathy).[127] A growing body of evidence suggests that interstitial fibrosis may be an important component of the cardiac pathology in cancer survivors exposed to anthracyclines. Magnetic resonance imaging showed enhanced chronic fibrotic changes in anthracycline-treated patients.[128] Moreover, late development of systolic heart failure, arrhythmias, and sudden death in patients treated with anthracyclines was associated with histological evidence of myocardial fibrosis.[129,130] In animal models of doxorubicin toxicity, a subacute increase in myocardial fibrosis was strongly linked with late mortality.[131] Data on the extent of right ventricular fibrotic remodelling following anthracycline administration are conflicting. In a mouse model, doxorubicin administration significantly increased collagen deposition in both the left and the right ventricle.[132] In contrast, in rabbits treated with daunorubicin fibrotic, changes were reported to be much less severe in the right ventricle.[133] Species-specific effects, differences in the dose of the anthracycline, and in the timing of assessment of fibrosis may explain the conflicting findings. The cellular basis of fibrosis in response to anthracycline treatment has not been systematically studied. Fibrotic changes may represent an epiphenomenon, reflecting activation of a reparative program in response to anthracycline-induced cardiomyocyte death. Direct effects of anthracyclines on fibroblasts should also be considered. A recent study suggested that doxorubicin-induced generation of reactive oxygen species may activate ataxia telangiectasia mutated (ATM) kinase in cardiac fibroblasts promoting a fibrotic response.[134]

3.7. The profibrotic effects of cigarette smoke

A recently published study suggested that cigarette smoke exposure may increase right ventricular collagen content in mice, suppressing right ventricular function, in the absence of any effects on the left ventricle and on the pulmonary vasculature.[135] The profibrotic effects of cigarette smoke were attributed to nicotine-mediated activation of α7 nicotine acetylcholine receptor signalling in cardiac fibroblasts. The basis for the selective involvement of the RV is unknown. Direct profibrotic effects of cigarette smoke may explain the presence of right ventricular dysfunction in some patients with chronic obstructive pulmonary disease, despite the absence of pulmonary hypertension.[136]

3.8. Right ventricular fibrosis in response to left ventricular disease

Although the systemic and the pulmonary circulation are arranged in series, there are several layers of functional integration between the left and the right ventricle. The common pericardium that encircles both chambers, the continuity between the muscle fibres of the left and right ventricular-free wall, the shared interventricular septum, and perfusion by the coronary arterial system generate a physiologic interdependence between the right and the left ventricle. In left ventricular disease, additional mechanisms contribute to structural remodelling and dysfunction of the RV. In an experimental model of left ventricular myocardial infarction, a marked upregulation in right ventricular collagen type I and III mRNA synthesis was reported, peaking 7–14 days after coronary occlusion. Collagen deposition was followed by significantly increased right ventricular stiffness, 56 days after infarction.[137] Moreover, increased right ventricular stiffness is noted in a model of left ventricular pressure overload,[138] and in a model of renovascular hypertension, interstitial fibrosis is noted in both the pressure-overloaded left ventricle and in the RV.[19] Structural remodelling of the extracellular matrix network of the RV in response to left ventricular disease is, at least in part, secondary to the increased right ventricular pressures caused by left ventricular failure, but may also reflect systemic activation of neurohumoral pathways that affect both ventricles.[19]

3.9. The right ventricular interstitium in senescent and diabetic hearts

Aging, obesity, and diabetes are associated with interstitial and perivascular cardiac fibrosis that may contribute to diastolic dysfunction.[139–141] Some studies have reported that in senescent mice, the fibrotic response may be more diffuse in the RV than in the left ventricle, suggesting that these changes may explain the aging-associated increase in the incidence of arrhythmias.[142,143] Moreover, in a rat model of type 1 diabetes, significant RV fibrosis was noted in the absence of hypertrophy or cardiomyocyte apoptosis.[144] Whether these observations are relevant in senescent or diabetic human subjects remains unknown.

4. Does the right ventricular interstitium exhibit unique pathophysiological responses?

Although the importance of right ventricular dysfunction in patients with cardiac and pulmonary disease is widely appreciated, understanding of the pathophysiological underpinnings of right ventricular failure remains limited. This is due, at least in part, to the notion that considering the intense research interest on the cell biological responses to left ventricular injury, relatively little additional information can be derived by investigating interactions between the same cell types in the RV. In the absence of injury, right and left ventricular fibroblasts appear to have similar characteristics; the matrix networks of the left and the right ventricle share common structural properties. However, the right ventricular predilection of certain genetic conditions associated with interstitial remodelling, such as ARVC, suggests unique characteristics of the interstitial cells populating the right ventricular wall. The cellular composition of the RV has not been systematically studied and the molecular links between genetic alterations and right ventricular interstitial remodelling remain unknown.

Moreover, various diseases impose unique pathophysiological challenges to the right ventricular interstitium. In conditions associated with right ventricular pressure overload, the dramatic pressure increases would be expected to transduce potent activating signals in interstitial cells populating the RV. Under hypoxic conditions, the favourable

oxygen supply and demand relations in the RV may result in distinct interstitial cell responses. To what extent the relative resistance of the RV to infarctive injury is dependent on unique properties of the right ventricular interstitium remains unknown. Thus, understanding the pathobiology of right ventricular interstitial cells may provide unique insights into strategies to improve adverse remodelling in left ventricular diseases.

5. Conclusions

A growing body of evidence suggests that phenotypic and functional alterations of interstitial cell populations and changes in the composition of the extracellular matrix network may play an important role in the pathogenesis of right ventricular dysfunction in a wide range of pathologic conditions. Our current understanding of the cell biological mechanisms and molecular signals involved in right ventricular fibrosis is based to a large extent on extrapolation from studies investigating left ventricular remodelling. Although the two ventricles have similarities in cellular composition and share several layers of functional integration, they also exhibit significant differences in embryologic origin, physiologic properties, and pathophysiological responses. Studies dissecting RV-specific cellular responses to injury are needed in order to understand the basis for right ventricular remodelling and dysfunction. Insights into the mechanisms of right ventricular fibrosis are necessary in order to develop novel therapeutic strategies to prevent right ventricular dysfunction in patients with pulmonary hypertension, and to inhibit arrhythmia generation in patients with right ventricular cardiomyopathies.

Funding

Dr Frangogiannis' Laboratory is supported by grants from the National Institutes of Health (R01 HL76246 and R01 HL85440), and the Department of Defense (PR151134 and PR151029).

Conflict of interest. none declared.

References

1. Rigolin VH, Robiolio PA, Wilson JS, Harrison JK, Bashore TM. The forgotten chamber: the importance of the right ventricle. *Cathet Cardiovasc Diagn* 1995;**35**:18–28.
2. Mehta SR, Eikelboom JW, Natarajan MK, Diaz R, Yi C, Gibbons RJ, Yusuf S. Impact of right ventricular involvement on mortality and morbidity in patients with inferior myocardial infarction. *J Am Coll Cardiol* 2001;**37**:37–43.
3. de Groote P, Millaire A, Foucher-Hossein C, Nugue O, Marchandise X, Ducloux G, Lablanche JM. Right ventricular ejection fraction is an independent predictor of survival in patients with moderate heart failure. *J Am Coll Cardiol* 1998;**32**:948–954.
4. Burke MA, Katz DH, Beussink L, Selvaraj S, Gupta DK, Fox J, Chakrabarti S, Sauer AJ, Rich JD, Freed BH, Shah SJ. Prognostic importance of pathophysiologic markers in patients with heart failure and preserved ejection fraction. *Circ Heart Fail* 2014;**7**:288–299.
5. Mikami Y, Jolly U, Heydari B, Peng M, Almehmadi F, Zahrani M, Bokhari M, Stirrat J, Lydell CP, Howarth AG, Yee R, White JA. Right ventricular ejection fraction Is incremental to left ventricular ejection fraction for the prediction of future arrhythmic events in patients with systolic dysfunction. *Circ Arrhythm Electrophysiol* 2017;**10**:e004067.
6. Grifoni S, Vanni S, Magazzini S, Olivotto I, Conti A, Zanobetti M, Polidori G, Pieralli F, Peiman N, Becattini C, Agnelli G. Association of persistent right ventricular dysfunction at hospital discharge after acute pulmonary embolism with recurrent thromboembolic events. *Arch Intern Med* 2006;**166**:2151–2156.
7. van de Veerdonk MC, Kind T, Marcus JT, Mauritz GJ, Heymans MW, Bogaard HJ, Boonstra A, Marques KM, Westerhof N, Vonk-Noordegraaf A. Progressive right ventricular dysfunction in patients with pulmonary arterial hypertension responding to therapy. *J Am Coll Cardiol* 2011;**58**:2511–2519.
8. Ryan JJ, Archer SL. The right ventricle in pulmonary arterial hypertension: disorders of metabolism, angiogenesis and adrenergic signaling in right ventricular failure. *Circ Res* 2014;**115**:176–188.
9. Bornstein P. Matricellular proteins: an overview. *J Cell Commun Signal* 2009;**3**:163–165.
10. Sage EH, Bornstein P. Extracellular proteins that modulate cell–matrix interactions. SPARC, tenascin, and thrombospondin. *J Biol Chem* 1991;**266**:14831–14834.
11. Frangogiannis NG. Matricellular proteins in cardiac adaptation and disease. *Physiol Rev* 2012;**92**:635–688.
12. Pinto AR, Ilinykh A, Ivey MJ, Kuwabara JT, D'antoni ML, Debuque R, Chandran A, Wang L, Arora K, Rosenthal NA, Tallquist MD. Revisiting cardiac cellular composition. *Circ Res* 2016;**118**:400–409.
13. Frangogiannis NG, Burns AR, Michael LH, Entman ML. Histochemical and morphological characteristics of canine cardiac mast cells. *Histochem J* 1999;**31**:221–229.
14. Nag AC. Study of non-muscle cells of the adult mammalian heart: a fine structural analysis and distribution. *Cytobios* 1980;**28**:41–61.
15. Mylonas KJ, Jenkins SJ, Castellan RF, Ruckerl D, McGregor K, Phythian-Adams AT, Hewitson JP, Campbell SM, MacDonald AS, Allen JE, Gray GA. The adult murine heart has a sparse, phagocytically active macrophage population that expands through monocyte recruitment and adopts an 'M2' phenotype in response to Th2 immunologic challenge. *Immunobiology* 2015;**220**:924–933.
16. Buckingham M, Meilhac S, Zaffran S. Building the mammalian heart from two sources of myocardial cells. *Nat Rev Genet* 2005;**6**:826–835.
17. Laks MM, Garner D, Swan HJ. Volumes and compliances measured simultaneously in the right and left ventricles of the dog. *Circ Res* 1967;**20**:565–569.
18. Weber KT, Brilla CG. Pathological hypertrophy and cardiac interstitium. Fibrosis and renin-angiotensin-aldosterone system. *Circulation* 1991;**83**:1849–1865.
19. Brilla CG, Pick R, Tan LB, Janicki JS, Weber KT. Remodeling of the rat right and left ventricles in experimental hypertension. *Circ Res* 1990;**67**:1355–1364.
20. Medugorac I. Collagen content in different areas of normal and hypertrophied rat myocardium. *Cardiovasc Res* 1980;**14**:551–554.
21. Furtado MB, Costa MW, Pranoto EA, Salimova E, Pinto AR, Lam NT, Park A, Snider P, Chandran A, Harvey RP, Boyd R, Conway SJ, Pearson J, Kaye DM, Rosenthal NA. Cardiogenic genes expressed in cardiac fibroblasts contribute to heart development and repair. *Circ Res* 2014;**114**:1422–1434.
22. Furtado MB, Nim HT, Boyd SE, Rosenthal NA. View from the heart: cardiac fibroblasts in development, scarring and regeneration. *Development* 2016;**143**:387–397.
23. Dandel M, Hetzer R. Echocardiographic assessment of the right ventricle: impact of the distinctly load dependency of its size, geometry and performance. *Int J Cardiol* 2016;**221**:1132–1142.
24. Watts JA, Gellar MA, Obraztsova M, Kline JA, Zagorski J. Role of inflammation in right ventricular damage and repair following experimental pulmonary embolism in rats. *Int J Exp Pathol* 2008;**89**:389–399.
25. Zagorski J, Obraztsova M, Gellar MA, Kline JA, Watts JA. Transcriptional changes in right ventricular tissues are enriched in the outflow tract compared with the apex during chronic pulmonary embolism in rats. *Physiol Genomics* 2009;**39**:61–71.
26. Cau SB, Barato RC, Celes MR, Muniz JJ, Rossi MA, Tanus-Santos JE. Doxycycline prevents acute pulmonary embolism-induced mortality and right ventricular deformation in rats. *Cardiovasc Drugs Ther* 2013;**27**:259–267.
27. Neto-Neves EM, Dias-Junior CA, Rizzi E, Castro MM, Sonego F, Gerlach RF, Tanus-Santos JE. Metalloproteinase inhibition protects against cardiomyocyte injury during experimental acute pulmonary thromboembolism. *Crit Care Med* 2011;**39**:349–356.
28. Neto-Neves EM, Sousa-Santos O, Ferraz KC, Rizzi E, Ceron CS, Romano MM, Gali LG, Maciel BC, Schulz R, Gerlach RF, Tanus-Santos JE. Matrix metalloproteinase inhibition attenuates right ventricular dysfunction and improves responses to dobutamine during acute pulmonary thromboembolism. *J Cell Mol Med* 2013;**17**:1588–1597.
29. Griffin MO, Ceballos G, Villarreal FJ. Tetracycline compounds with non-antimicrobial organ protective properties: possible mechanisms of action. *Pharmacol Res* 2011;**63**:102–107.
30. Rain S, Handoko ML, Trip P, Gan CT, Westerhof N, Stienen GJ, Paulus WJ, Ottenheijm CA, Marcus JT, Dorfmuller P, Guignabert C, Humbert M, Macdonald P, Dos Remedios C, Postmus PE, Saripalli C, Hidalgo CG, Granzier HL, Vonk-Noordegraaf A, van der Velden J, de Man FS. Right ventricular diastolic impairment in patients with pulmonary arterial hypertension. *Circulation* 2013;**128**:2016–2025. 2011–2010.
31. Jurcut R, Giusca S, Ticulescu R, Popa E, Amzulescu MS, Ghiorghiu I, Coman IM, Popescu BA, Voigt JU, Ginghina C. Different patterns of adaptation of the right ventricle to pressure overload: a comparison between pulmonary hypertension and pulmonary stenosis. *J Am Soc Echocardiogr* 2011;**24**:1109–1117.
32. Kawut SM, Taichman DB, Archer-Chicko CL, Palevsky HI, Kimmel SE. Hemodynamics and survival in patients with pulmonary arterial hypertension related to systemic sclerosis. *Chest* 2003;**123**:344–350.
33. De Meester P, Buys R, Van De Bruaene A, Gabriels C, Voigt JU, Vanhees L, Herijgers P, Troost E, Budts W. Functional and haemodynamic assessment of mild-to-moderate pulmonary valve stenosis at rest and during exercise. *Heart* 2014;**100**:1354–1359.
34. Guihaire J, Bogaard HJ, Flecher E, Noly PE, Mercier O, Haddad F, Fadel E. Experimental models of right heart failure: a window for translational research in pulmonary hypertension. *Semin Respir Crit Care Med* 2013;**34**:689–699.
35. Sutendra G, Dromparis P, Paulin R, Zervopoulos S, Haromy A, Nagendran J, Michelakis ED. A metabolic remodeling in right ventricular hypertrophy is

associated with decreased angiogenesis and a transition from a compensated to a decompensated state in pulmonary hypertension. *J Mol Med* 2013;**91**:1315–1327.
36. Ozawa K, Funabashi N, Takaoka H, Tanabe N, Tatsumi K, Kobayashi Y. Detection of right ventricular myocardial fibrosis using quantitative CT attenuation of the right ventricular myocardium in the late phase on 320 slice CT in subjects with pulmonary hypertension. *Int J Cardiol* 2017;**228**:165–168.
37. Egemnazarov B, Schmidt A, Crnkovic S, Sydykov A, Nagy BM, Kovacs G, Weissmann N, Olschewski H, Olschewski A, Kwapiszewska G, Marsh LM. Pressure overload creates right ventricular diastolic dysfunction in a mouse model: assessment by echocardiography. *J Am Soc Echocardiogr* 2015;**28**:828–843.
38. Rain S, Andersen S, Najafi A, Gammelgaard Schultz J, da Silva Goncalves Bos D, Handoko ML, Bogaard HJ, Vonk-Noordegraaf A, Andersen A, van der Velden J, Ottenheijm CA, de Man FS. Right ventricular myocardial stiffness in experimental pulmonary arterial hypertension: relative contribution of fibrosis and myofibril stiffness. *Circ Heart Fail* 2016;**9**:e002636.
39. Bonnin CM, Sparrow MP, Taylor RR. Collagen synthesis and content in right ventricular hypertrophy in the dog. *Am J Physiol* 1981;**241**:H708–H713.
40. Baicu CF, Li J, Zhang Y, Kasiganesan H, Cooper G, Zile MR, Bradshaw AD. Time course of right ventricular pressure-overload induced myocardial fibrosis: relationship to changes in fibroblast postsynthetic procollagen processing. *Am J Physiol Heart Circ Physiol* 2012;**303**:H1128–H1134.
41. Kong P, Christia P, Frangogiannis NG. The pathogenesis of cardiac fibrosis. *Cell Mol Life Sci* 2014;**71**:549–574.
42. Leslie KO, Taatjes DJ, Schwarz J, vonTurkovich M, Low RB. Cardiac myofibroblasts express alpha smooth muscle actin during right ventricular pressure overload in the rabbit. *Am J Pathol* 1991;**139**:207–216.
43. Moore-Morris T, Guimaraes-Camboa N, Banerjee I, Zambon AC, Kisseleva T, Velayoudon A, Stallcup WB, Gu Y, Dalton ND, Cedenilla M, Gomez-Amaro R, Zhou B, Brenner DA, Peterson KL, Chen J, Evans SM. Resident fibroblast lineages mediate pressure overload-induced cardiac fibrosis. *J Clin Invest* 2014;**124**:2921–2934.
44. Ali SR, Ranjbarvaziri S, Talkhabi M, Zhao P, Subat A, Hojjat A, Kamran P, Muller AM, Volz KS, Tang Z, Red-Horse K, Ardehali R. Developmental heterogeneity of cardiac fibroblasts does not predict pathological proliferation and activation. *Circ Res* 2014;**115**:625–635.
45. Zeisberg EM, Tarnavski O, Zeisberg M, Dorfman AL, McMullen JR, Gustafsson E, Chandraker A, Yuan X, Pu WT, Roberts AB, Neilson EG, Sayegh MH, Izumo S, Kalluri R. Endothelial-to-mesenchymal transition contributes to cardiac fibrosis. *Nat Med* 2007;**13**:952–961.
46. Dewachter C, Belhaj A, Rondelet B, Vercruyssen M, Schraufnagel DP, Remmelink M, Brimioulle S, Kerbaul F, Naeije R, Dewachter L. Myocardial inflammation in experimental acute right ventricular failure: effects of prostacyclin therapy. *J Heart Lung Transplant* 2015;**34**:1334–1345.
47. Overbeek MJ, Mouchaers KTB, Niessen HM, Hadi AM, Kupreishvili K, Boonstra A, Voskuyl AE, Belien JAM, Smit EF, Dijkmans BC, Vonk-Noordegraaf A, Grünberg K. Characteristics of interstitial fibrosis and inflammatory cell infiltration in right ventricles of systemic sclerosis-associated pulmonary arterial hypertension. *Int J Rheumatol* 2010;**2010**:1.
48. Usher MG, Duan SZ, Ivaschenko CY, Frieler RA, Berger S, Schutz G, Lumeng CN, Mortensen RM. Myeloid mineralocorticoid receptor controls macrophage polarization and cardiovascular hypertrophy and remodeling in mice. *J Clin Invest* 2010;**120**:3350–3364.
49. Shioi T, Matsumori A, Kihara Y, Inoko M, Ono K, Iwanaga Y, Yamada T, Iwasaki A, Matsushima K, Sasayama S. Increased expression of interleukin-1 beta and monocyte chemotactic and activating factor/monocyte chemoattractant protein-1 in the hypertrophied and failing heart with pressure overload. *Circ Res* 1997;**81**:664–671.
50. Nevers T, Salvador AM, Grodecki-Pena A, Knapp A, Velazquez F, Aronovitz M, Kapur NK, Karas RH, Blanton RM, Alcaide P. Left ventricular T-cell recruitment contributes to the pathogenesis of heart failure. *Circ Heart Fail* 2015;**8**:776–787.
51. Laroumanie F, Douin-Echinard V, Pozzo J, Lairez O, Tortosa F, Vinel C, Delage C, Calise D, Dutaur M, Parini A, Pizzinat N. CD4+ T cells promote the transition from hypertrophy to heart failure during chronic pressure overload. *Circulation* 2014;**129**:2111–2124.
52. Sun Y, Zhang J, Lu L, Chen SS, Quinn MT, Weber KT. Aldosterone-induced inflammation in the rat heart: role of oxidative stress. *Am J Pathol* 2002;**161**:1773–1781.
53. Levick SP, Melendez GC, Plante E, McLarty JL, Brower GL, Janicki JS. Cardiac mast cells: the centrepiece in adverse myocardial remodelling. *Cardiovasc Res* 2011;**89**:12–19.
54. Frangogiannis NG, Lindsey ML, Michael LH, Youker KA, Bressler RB, Mendoza LH, Spengler RN, Smith CW, Entman ML. Resident cardiac mast cells degranulate and release preformed TNF-alpha, initiating the cytokine cascade in experimental canine myocardial ischemia/reperfusion. *Circulation* 1998;**98**:699–710.
55. Frangogiannis NG, Perrard JL, Mendoza LH, Burns AR, Lindsey ML, Ballantyne CM, Michael LH, Smith CW, Entman ML. Stem cell factor induction is associated with mast cell accumulation after canine myocardial ischemia and reperfusion. *Circulation* 1998;**98**:687–698.
56. Somasundaram P, Ren G, Nagar H, Kraemer D, Mendoza L, Michael LH, Caughey GH, Entman ML, Frangogiannis NG. Mast cell tryptase may modulate endothelial cell phenotype in healing myocardial infarcts. *J Pathol* 2005;**205**:102–111.
57. Olivetti G, Lagrasta C, Ricci R, Sonnenblick EH, Capasso JM, Anversa P. Long-term pressure-induced cardiac hypertrophy: capillary and mast cell proliferation. *Am J Physiol* 1989;**257**:H1766–H1772.
58. Luitel H, Sydykov A, Schymura Y, Mamazhakypov A, Janssen W, Pradhan K, Wietelmann A, Kosanovic D, Dahal BK, Weissmann N, Seeger W, Grimminger F, Ghofrani HA, Schermuly RT. Pressure overload leads to an increased accumulation and activity of mast cells in the right ventricle. *PHY2* 2017;**5**:e13146.
59. Malhotra R, Sadoshima J, Brosius FC 3rd, Izumo S. Mechanical stretch and angiotensin II differentially upregulate the renin–angiotensin system in cardiac myocytes in vitro. *Circ Res* 1999;**85**:137–146.
60. Takahashi N, Calderone A, Izzo NJ Jr, Maki TM, Marsh JD, Colucci WS. Hypertrophic stimuli induce transforming growth factor-beta 1 expression in rat ventricular myocytes. *J Clin Invest* 1994;**94**:1470–1476.
61. Biernacka A, Dobaczewski M, Frangogiannis NG. TGF-beta signaling in fibrosis. *Growth Factors* 2011;**29**:196–202.
62. Nergui S, Fukumoto Y, Do EZ, Nakajima S, Shimizu T, Ikeda S, Elias-Al-Mamun M, Shimokawa H. Role of endothelial nitric oxide synthase and collagen metabolism in right ventricular remodeling due to pulmonary hypertension. *Circ J* 2014;**78**:1465–1474.
63. Drake JI, Bogaard HJ, Mizuno S, Clifton B, Xie B, Gao Y, Dumur CI, Fawcett P, Voelkel NF, Natarajan R. Molecular signature of a right heart failure program in chronic severe pulmonary hypertension. *Am J Respir Cell Mol Biol* 2011;**45**:1239–1247.
64. Maron BA, Leopold JA. Emerging concepts in the molecular basis of pulmonary arterial hypertension: Part II: neurohormonal signaling contributes to the pulmonary vascular and right ventricular pathophenotype of pulmonary arterial hypertension. *Circulation* 2015;**131**:2079–2091.
65. Bogaard HJ, Natarajan R, Mizuno S, Abbate A, Chang PJ, Chau VQ, Hoke NN, Kraskauskas D, Kasper M, Salloum FN, Voelkel NF. Adrenergic receptor blockade reverses right heart remodeling and dysfunction in pulmonary hypertensive rats. *Am J Respir Crit Care Med* 2010;**182**:652–660.
66. de Man FS, Handoko ML, van Ballegoij JJ, Schalij I, Bogaards SJ, Postmus PE, van der Velden J, Westerhof N, Paulus WJ, Vonk-Noordegraaf A. Bisoprolol delays progression towards right heart failure in experimental pulmonary hypertension. *Circ Heart Fail* 2012;**5**:97–105.
67. Kim J, Eckhart AD, Eguchi S, Koch WJ. Beta-adrenergic receptor-mediated DNA synthesis in cardiac fibroblasts is dependent on transactivation of the epidermal growth factor receptor and subsequent activation of extracellular signal-regulated kinases. *J Biol Chem* 2002;**277**:32116–32123.
68. Zou Y, Akazawa H, Qin Y, Sano M, Takano H, Minamino T, Makita N, Iwanaga K, Zhu W, Kudoh S, Toko H, Tamura K, Kihara M, Nagai T, Fukamizu A, Umemura S, Iiri T, Fujita T, Komuro I. Mechanical stress activates angiotensin II type 1 receptor without the involvement of angiotensin II. *Nat Cell Biol* 2004;**6**:499–506.
69. Morrell NW, Danilov SM, Satyan KB, Morris KG, Stenmark KR. Right ventricular angiotensin converting enzyme activity and expression is increased during hypoxic pulmonary hypertension. *Cardiovasc Res* 1997;**34**:393–403.
70. Friedberg MK, Cho MY, Li J, Assad RS, Sun M, Rohailla S, Honjo O, Apitz C, Redington AN. Adverse biventricular remodeling in isolated right ventricular hypertension is mediated by increased transforming growth factor-beta1 signaling and is abrogated by angiotensin receptor blockade. *Am J Respir Cell Mol Biol* 2013;**49**:1019–1028.
71. Okada M, Harada T, Kikuzuki R, Yamawaki H, Hara Y. Effects of telmisartan on right ventricular remodeling induced by monocrotaline in rats. *J Pharmacol Sci* 2009;**111**:193–200.
72. Borgdorff MA, Bartelds B, Dickinson MG, Steendijk P, Berger RM. A cornerstone of heart failure treatment is not effective in experimental right ventricular failure. *Int J Cardiol* 2013;**169**:183–189.
73. Ameri P, Bertero E, Meliota G, Cheli M, Canepa M, Brunelli C, Balbi M. Neurohormonal activation and pharmacological inhibition in pulmonary arterial hypertension and related right ventricular failure. *Heart Fail Rev* 2016;**21**:539–547.
74. Giaid A, Yanagisawa M, Langleben D, Michel RP, Levy R, Shennib H, Kimura S, Masaki T, Duguid WP, Stewart DJ. Expression of endothelin-1 in the lungs of patients with pulmonary hypertension. *N Engl J Med* 1993;**328**:1732–1739.
75. Rubin LJ, Badesch DB, Barst RJ, Galie N, Black CM, Keogh A, Pulido T, Frost A, Roux S, Leconte I, Landzberg M, Simonneau G. Bosentan therapy for pulmonary arterial hypertension. *N Engl J Med* 2002;**346**:896–903.
76. Nagendran J, Sutendra G, Paterson I, Champion HC, Webster L, Chiu B, Haromy A, Rebeyka IM, Ross DB, Michelakis ED. Endothelin axis is upregulated in human and rat right ventricular hypertrophy. *Circ Res* 2013;**112**:347–354.
77. Piacentini L, Gray M, Honbo NY, Chentoufi J, Bergman M, Karliner JS. Endothelin-1 stimulates cardiac fibroblast proliferation through activation of protein kinase C. *J Mol Cell Cardiol* 2000;**32**:565–576.
78. Mouchaers KT, Schalij I, Versteilen AM, Hadi AM, van Nieuw Amerongen GP, van Hinsbergh VW, Postmus PE, van der Laarse WJ, Vonk-Noordegraaf A. Endothelin receptor blockade combined with phosphodiesterase-5 inhibition increases right ventricular mitochondrial capacity in pulmonary arterial hypertension. *Am J Physiol Heart Circ Physiol* 2009;**297**:H200–H207.
79. Choudhary G, Troncales F, Martin D, Harrington EO, Klinger JR. Bosentan attenuates right ventricular hypertrophy and fibrosis in normobaric hypoxia model of pulmonary hypertension. *J Heart Lung Transplant* 2011;**30**:827–833.

80. Nielsen EA, Sun M, Honjo O, Hjortdal VE, Redington AN, Friedberg MK, Gonzalez GE. Dual endothelin receptor blockade abrogates right ventricular remodeling and biventricular fibrosis in isolated elevated right ventricular afterload. *PLoS One* 2016; **11**:e0146767.
81. Ikeda S, Satoh K, Kikuchi N, Miyata S, Suzuki K, Omura J, Shimizu T, Kobayashi K, Kobayashi K, Fukumoto Y, Sakata Y, Shimokawa H. Crucial role of rho-kinase in pressure overload-induced right ventricular hypertrophy and dysfunction in mice. *Arterioscler Thromb Vasc Biol* 2014;**34**:1260–1271.
82. Schreckenberg R, Rebelo M, Deten A, Weber M, Rohrbach S, Pipicz M, Csonka C, Ferdinandy P, Schulz R, Schluter KD. Specific mechanisms underlying right heart failure: the missing upregulation of superoxide dismutase-2 and its decisive role in antioxidative defense. *Antioxid Redox Signal* 2015;**23**:1220–1232.
83. Redout EM, van der Toorn A, Zuidwijk MJ, van de Kolk CW, van Echteld CJ, Musters RJ, van Hardeveld C, Paulus WJ, Simonides WS. Antioxidant treatment attenuates pulmonary arterial hypertension-induced heart failure. *Am J Physiol Heart Circ Physiol* 2010;**298**:H1038–H1047.
84. Dobaczewski M, Frangogiannis NG. Chemokines and cardiac fibrosis. *Front Biosci (Schol Ed)* 2009;**1**:391–405.
85. Waehre A, Vistnes M, Sjaastad I, Nygard S, Husberg C, Lunde IG, Aukrust P, Yndestad A, Vinge LE, Behmen D, Neukamm C, Brun H, Thaulow E, Christensen G. Chemokines regulate small leucine-rich proteoglycans in the extracellular matrix of the pressure-overloaded right ventricle. *J Appl Physiol (1985)* 2012;**112**:1372–1382.
86. Frangogiannis NG, Dewald O, Xia Y, Ren G, Haudek S, Leucker T, Kraemer D, Taffet G, Rollins BJ, Entman ML. Critical role of monocyte chemoattractant protein-1/CC chemokine ligand 2 in the pathogenesis of ischemic cardiomyopathy. *Circulation* 2007;**115**:584–592.
87. Bujak M, Dobaczewski M, Gonzalez-Quesada C, Xia Y, Leucker T, Zymek P, Veeranna V, Tager AM, Luster AD, Frangogiannis NG. Induction of the CXC chemokine interferon-gamma-inducible protein 10 regulates the reparative response following myocardial infarction. *Circ Res* 2009;**105**:973–983.
88. Saxena A, Bujak M, Frunza O, Dobaczewski M, Gonzalez-Quesada C, Lu B, Gerard C, Frangogiannis NG. CXCR3-independent actions of the CXC chemokine CXCL10 in the infarcted myocardium and in isolated cardiac fibroblasts are mediated through proteoglycans. *Cardiovasc Res* 2014;**103**:217–227.
89. Wang S, Sun A, Li L, Zhao G, Jia J, Wang K, Ge J, Zou Y. Up-regulation of BMP-2 antagonizes TGF-beta1/ROCK-enhanced cardiac fibrotic signalling through activation of Smurf1/Smad6 complex. *J Cell Mol Med* 2012;**16**:2301–2310.
90. Merino D, Villar AV, Garcia R, Tramullas M, Ruiz L, Ribas C, Cabezudo S, Nistal JF, Hurle MA. BMP-7 attenuates left ventricular remodelling under pressure overload and facilitates reverse remodelling and functional recovery. *Cardiovasc Res* 2016;**110**: 331–345.
91. Kapur NK, Paruchuri V, Aronovitz MJ, Qiao X, Mackey EE, Daly GH, Ughreja K, Levine J, Blanton R, Hill NS, Karas RH. Biventricular remodeling in murine models of right ventricular pressure overload. *PLoS One* 2013;**8**:e70802.
92. van der Bruggen CE, Happe CM, Dorfmuller P, Trip P, Spruijt OA, Rol N, Hoevenaars FP, Houweling AC, Girerd B, Marcus JT, Mercier O, Humbert M, Handoko ML, van der Velden J, Vonk Noordegraaf A, Bogaard HJ, Goumans MJ, de Man FS. Bone morphogenetic protein receptor type 2 mutation in pulmonary arterial hypertension: a view on the right ventricle. *Circulation* 2016;**133**:1747–1760.
93. Bujak M, Ren G, Kweon HJ, Dobaczewski M, Reddy A, Taffet G, Wang XF, Frangogiannis NG. Essential role of Smad3 in infarct healing and in the pathogenesis of cardiac remodeling. *Circulation* 2007;**116**:2127–2138.
94. Dobaczewski M, Bujak M, Li N, Gonzalez-Quesada C, Mendoza LH, Wang XF, Frangogiannis NG. Smad3 signaling critically regulates fibroblast phenotype and function in healing myocardial infarction. *Circ Res* 2010;**107**:418–428.
95. Koitabashi N, Danner T, Zaiman AL, Pinto YM, Rowell J, Mankowski J, Zhang D, Nakamura T, Takimoto E, Kass DA. Pivotal role of cardiomyocyte TGF-beta signaling in the murine pathological response to sustained pressure overload. *J Clin Invest* 2011;**121**:2301–2312.
96. Biernacka A, Cavalera M, Wang J, Russo I, Shinde A, Kong P, Gonzalez-Quesada C, Rai V, Dobaczewski M, Lee DW, Wang XF, Frangogiannis NG. Smad3 signaling promotes fibrosis while preserving cardiac and aortic geometry in obese diabetic mice. *Circ Heart Fail* 2015;**8**:788–798.
97. Kapur NK, Qiao X, Paruchuri V, Mackey EE, Daly GH, Ughreja K, Morine KJ, Levine J, Aronovitz MJ, Hill NS, Jaffe IZ, Letarte M, Karas RH. Reducing endoglin activity limits calcineurin and TRPC-6 expression and improves survival in a mouse model of right ventricular pressure overload. *J Am Heart Assoc* 2014;**3**:e000965.
98. Xia Y, Dobaczewski M, Gonzalez-Quesada C, Li N, Tian Q, Mendoza L, Frangogiannis NG. Endogenous TSP-1 modulates the hypertrophic and fibrotic response in the pressure-overloaded heart. *Circulation* 2010;**122**:A16231. abstract).
99. Schellings MW, Vanhoutte D, Swinnen M, Cleutjens JP, Debets J, van Leeuwen RE, D'hooge J, Van de Werf F, Carmeliet P, Pinto YM, Sage EH, Heymans S. Absence of SPARC results in increased cardiac rupture and dysfunction after acute myocardial infarction. *J Exp Med* 2009;**206**:113–123.
100. Bradshaw AD, Baicu CF, Rentz TJ, Van Laer AO, Boggs J, Lacy JM, Zile MR. Pressure overload-induced alterations in fibrillar collagen content and myocardial diastolic function: role of secreted protein acidic and rich in cysteine (SPARC) in post-synthetic procollagen processing. *Circulation* 2009;**119**:269–280.
101. Frangogiannis NG. The extracellular matrix in myocardial injury, repair, and remodeling. *J Clin Invest* 2017;**127**:1600–1612.
102. Nadadur RD, Umar S, Wong G, Eghbali M, Iorga A, Matori H, Partow-Navid R, Eghbali M. Reverse right ventricular structural and extracellular matrix remodeling by estrogen in severe pulmonary hypertension. *J Appl Physiol (1985)* 2012;**113**: 149–158.
103. Hessel M, Steendijk P, den Adel B, Schutte C, van der Laarse A. Pressure overload-induced right ventricular failure is associated with re-expression of myocardial tenascin-C and elevated plasma tenascin-C levels. *Cell Physiol Biochem* 2009;**24**: 201–210.
104. Gregg D, Foster E. Pulmonary insufficiency is the nexus of late complications in tetralogy of Fallot. *Curr Cardiol Rep* 2007;**9**:315–322.
105. Reddy S, Zhao M, Hu DQ, Fajardo G, Katznelson E, Punn R, Spin JM, Chan FP, Bernstein D. Physiologic and molecular characterization of a murine model of right ventricular volume overload. *Am J Physiol Heart Circ Physiol* 2013;**304**:H1314–H1327.
106. Agger P, Hyldebrandt JA, Nielsen EA, Hjortdal V, Smerup M. A novel porcine model for right ventricular dilatation by external suture plication of the pulmonary valve leaflets – practical and reproducible. *Interact CardioVasc Thoracic Surg* 2010;**10**: 962–966.
107. Frangogiannis NG. Pathophysiology of myocardial infarction. *Compr Physiol* 2015;**5**: 1841–1875.
108. Goldstein JA. Pathophysiology and management of right heart ischemia. *J Am Coll Cardiol* 2002;**40**:841–853.
109. Goldstein JA. Acute right ventricular infarction: insights for the interventional era. *Curr Probl Cardiol* 2012;**37**:533–557.
110. Yasuda T, Okada RD, Leinbach RC, Gold HK, Phillips H, McKusick KA, Glover DK, Boucher CA, Strauss HW. Serial evaluation of right ventricular dysfunction associated with acute inferior myocardial infarction. *Am Heart J* 1990;**119**:816–822.
111. Laster SB, Shelton TJ, Barzilai B, Goldstein JA. Determinants of the recovery of right ventricular performance following experimental chronic right coronary artery occlusion. *Circulation* 1993;**88**:696–708.
112. d'Amati G, Factor SM. Endomyocardial biopsy findings in patients with ventricular arrhythmias of unknown origin. *Cardiovasc Pathol* 1996;**5**:139–144.
113. Nademanee K, Raju H, de Noronha SV, Papadakis M, Robinson L, Rothery S, Makita N, Kowase S, Boonmee N, Vitayakritsirikul V, Ratanarapee S, Sharma S, van der Wal AC, Christiansen M, Tan HL, Wilde AA, Nogami A, Sheppard MN, Veerakul G, Behr ER. Fibrosis, Connexin-43, and conduction abnormalities in the Brugada syndrome. *J Am Coll Cardiol* 2015;**66**:1976–1986.
114. Wada Y, Aiba T, Matsuyama T-A, Nakajima I, Ishibashi K, Miyamoto K, Yamada Y, Okamura H, Noda T, Satomi K, Morita Y, Kanzaki H, Kusano K, Anzai T, Kamakura S, Ishibashi-Ueda H, Shimizu W, Horie M, Yasuda S, Ogawa H. Clinical and pathological impact of tissue fibrosis on lethal arrhythmic events in hypertrophic cardiomyopathy patients with impaired systolic function. *Circ J* 2015;**79**:1733–1741.
115. Fornes P, Ratel S, Lecomte D. Pathology of arrhythmogenic right ventricular cardiomyopathy/dysplasia–an autopsy study of 20 forensic cases. *J Forensic Sci* 1998;**43**: 777–783.
116. Burke AP, Farb A, Tashko G, Virmani R. Arrhythmogenic right ventricular cardiomyopathy and fatty replacement of the right ventricular myocardium: are they different diseases? *Circulation* 1998;**97**:1571–1580.
117. Hamilton RM. Arrhythmogenic right ventricular cardiomyopathy. 2009;**32**:S44–S51.
118. Tandri H, Saranathan M, Rodriguez ER, Martinez C, Bomma C, Nasir K, Rosen B, Lima JA, Calkins H, Bluemke DA. Noninvasive detection of myocardial fibrosis in arrhythmogenic right ventricular cardiomyopathy using delayed-enhancement magnetic resonance imaging. *J Am Coll Cardiol* 2005;**45**:98–103.
119. Yang Z, Bowles NE, Scherer SE, Taylor MD, Kearney DL, Ge S, Nadvoretskiy VV, DeFreitas G, Carabello B, Brandon LI, Godsel LM, Green KJ, Saffitz JE, Li H, Danieli GA, Calkins H, Marcus F, Towbin JA. Desmosomal dysfunction due to mutations in desmoplakin causes arrhythmogenic right ventricular dysplasia/cardiomyopathy. *Circ Res* 2006;**99**:646–655.
120. Gerull B, Heuser A, Wichter T, Paul M, Basson CT, McDermott DA, Lerman BB, Markowitz SM, Ellinor PT, MacRae CA, Peters S, Grossmann KS, Drenckhahn J, Michely B, Sasse-Klaassen S, Birchmeier W, Dietz R, Breithardt G, Schulze-Bahr E, Thierfelder L. Mutations in the desmosomal protein plakophilin-2 are common in arrhythmogenic right ventricular cardiomyopathy. *Nat Genet* 2004;**36**:1162–1164.
121. Pilichou K, Nava A, Basso C, Beffagna G, Bauce B, Lorenzon A, Frigo G, Vettori A, Valente M, Towbin J, Thiene G, Danieli GA, Rampazzo A. Mutations in desmoglein-2 gene are associated with arrhythmogenic right ventricular cardiomyopathy. *Circulation* 2006;**113**:1171–1179.
122. Lombardi R, Chen SN, Ruggiero A, Gurha P, Czernuszewicz GZ, Willerson JT, Marian AJ. Cardiac fibro-adipocyte progenitors express desmosome proteins and preferentially differentiate to adipocytes upon deletion of the Desmoplakin gene. *Circ Res* 2016;**119**:41–54.
123. Lombardi R, Dong J, Rodriguez G, Bell A, Leung TK, Schwartz RJ, Willerson JT, Brugada R, Marian AJ. Genetic fate mapping identifies second heart field progenitor cells as a source of adipocytes in arrhythmogenic right ventricular cardiomyopathy. *Circ Res* 2009;**104**:1076–1084.
124. Garcia-Gras E, Lombardi R, Giocondo MJ, Willerson JT, Schneider MD, Khoury DS, Marian AJ. Suppression of canonical Wnt/beta-catenin signaling by nuclear

plakoglobin recapitulates phenotype of arrhythmogenic right ventricular cardiomyopathy. *J Clin Invest* 2006;**116**:2012–2021.
125. Dubash AD, Kam CY, Aguado BA, Patel DM, Delmar M, Shea LD, Green KJ. Plakophilin-2 loss promotes TGF-beta1/p38 MAPK-dependent fibrotic gene expression in cardiomyocytes. *J Cell Biol* 2016;**212**:425–438.
126. Bristow MR, Mason JW, Billingham ME, Daniels JR. Doxorubicin cardiomyopathy: evaluation by phonocardiography, endomyocardial biopsy, and cardiac catheterization. *Ann Intern Med* 1978;**88**:168–175.
127. Volkova M, Russell R 3rd. Anthracycline cardiotoxicity: prevalence, pathogenesis and treatment. *Curr Cardiol Rev* 2011;**7**:214–220.
128. Neilan TG, Coelho-Filho OR, Shah RV, Feng JH, Pena-Herrera D, Mandry D, Pierre-Mongeon F, Heydari B, Francis SA, Moslehi J, Kwong RY, Jerosch-Herold M. Myocardial extracellular volume by cardiac magnetic resonance imaging in patients treated with anthracycline-based chemotherapy. *Am J Cardiol* 2013;**111**:717–722.
129. Steinherz LJ, Steinherz PG, Tan CT, Heller G, Murphy ML. Cardiac toxicity 4 to 20 years after completing anthracycline therapy. *JAMA* 1991;**266**:1672–1677.
130. Steinherz LJ, Steinherz PG, Tan C. Cardiac failure and dysrhythmias 6–19 years after anthracycline therapy: a series of 15 patients. *Med Pediatr Oncol* 1995;**24**:352–361.
131. Farhad H, Staziaki PV, Addison D, Coelho-Filho OR, Shah RV, Mitchell RN, Szilveszter B, Abbasi SA, Kwong RY, Scherrer-Crosbie M, Hoffmann U, Jerosch-Herold M, Neilan TG. Characterization of the changes in cardiac structure and function in mice treated with anthracyclines using serial cardiac magnetic resonance imaging. *Circ Cardiovasc Imaging* 2016;**9**:e003584.
132. Milano G, Raucci A, Scopece A, Daniele R, Guerrini U, Sironi L, Cardinale D, Capogrossi MC, Pompilio G. Doxorubicin and trastuzumab regimen induces biventricular failure in mice. *J Am Soc Echocardiogr* 2014;**27**:568–579.
133. Lencova-Popelova O, Jirkovsky E, Mazurova Y, Lenco J, Adamcova M, Simunek T, Gersl V, Sterba M. Molecular remodeling of left and right ventricular myocardium in chronic anthracycline cardiotoxicity and post-treatment follow up. *PLoS One* 2014;**9**:e96055.
134. Zhan H, Aizawa K, Sun J, Tomida S, Otsu K, Conway SJ, McKinnon PJ, Manabe I, Komuro I, Miyagawa K, Nagai R, Suzuki T. Ataxia telangiectasia mutated in cardiac fibroblasts regulates doxorubicin-induced cardiotoxicity. *Cardiovasc Res* 2016;**110**:85–95.
135. Vang A, Clements RT, Chichger H, Kue N, Allawzi A, O'connell K, Jeong E-M, Dudley SC, Sakhatskyy P, Lu Q, Zhang P, Rounds S, Choudhary G. Effect of alpha7 nicotinic acetylcholine receptor activation on cardiac fibroblasts: a mechanism underlying RV fibrosis associated with cigarette smoke exposure. *Am J Physiol Lung Cell Mol Physiol* 2017;**312**:L748–L759.
136. Hilde JM, Skjorten I, Grotta OJ, Hansteen V, Melsom MN, Hisdal J, Humerfelt S, Steine K. Right ventricular dysfunction and remodeling in chronic obstructive pulmonary disease without pulmonary hypertension. *J Am Coll Cardiol* 2013;**62**:1103–1111.
137. Dixon IM, Ju H, Jassal DS, Peterson DJ. Effect of ramipril and losartan on collagen expression in right and left heart after myocardial infarction. *Mol Cell Biochem* 1996;**165**:31–45.
138. Gonçalves N, Gomes-Ferreira C, Moura C, Roncon-Albuquerque R, Leite-Moreira AF, Falcão-Pires I. Worse cardiac remodeling in response to pressure overload in type 2 diabetes mellitus. *Int J Cardiol* 2016;**217**:195–204.
139. Biernacka A, Frangogiannis NG. Aging and cardiac fibrosis. *Aging Dis* 2011;**2**:158–173.
140. Russo I, Frangogiannis NG. Diabetes-associated cardiac fibrosis: cellular effectors, molecular mechanisms and therapeutic opportunities. *J Mol Cell Cardiol* 2016;**90**:84–93.
141. Cavalera M, Wang J, Frangogiannis NG. Obesity, metabolic dysfunction, and cardiac fibrosis: pathophysiological pathways, molecular mechanisms, and therapeutic opportunities. *Transl Res* 2014;**164**:323–335.
142. Spadaccio C, Rainer A, Mozetic P, Trombetta M, Dion RA, Barbato R, Nappi F, Chello M. The role of extracellular matrix in age-related conduction disorders: a forgotten player? *J Geriatr Cardiol* 2015;**12**:76–82.
143. Stein M, Noorman M, van Veen TA, Herold E, Engelen MA, Boulaksil M, Antoons G, Jansen JA, van Oosterhout MF, Hauer RN, de Bakker JM, van Rijen HV. Dominant arrhythmia vulnerability of the right ventricle in senescent mice. *Heart Rhythm* 2008;**5**:438–448.
144. Hao PP, Yang JM, Zhang MX, Zhang K, Chen YG, Zhang C, Zhang Y. Angiotensin-(1-7) treatment mitigates right ventricular fibrosis as a distinctive feature of diabetic cardiomyopathy. *Am J Physiol Heart Circ Physiol* 2015;**308**:H1007–H1019.
145. Turner NA, Porter KE, Smith WH, White HL, Ball SG, Balmforth AJ. Chronic beta2-adrenergic receptor stimulation increases proliferation of human cardiac fibroblasts via an autocrine mechanism. *Cardiovasc Res* 2003;**57**:784–792.
146. Sun M, Yu H, Zhang Y, Li Z, Gao W. MicroRNA-214 mediates isoproterenol-induced proliferation and collagen synthesis in cardiac fibroblasts. *Sci Rep* 2016;**5**:18351.
147. Hafizi S, Wharton J, Chester AH, Yacoub MH. Profibrotic effects of endothelin-1 via the ETA receptor in cultured human cardiac fibroblasts. *Cell Physiol Biochem* 2004;**14**:285–292.
148. Brilla CG, Zhou G, Matsubara L, Weber KT. Collagen metabolism in cultured adult rat cardiac fibroblasts: response to angiotensin II and aldosterone. *J Mol Cell Cardiol* 1994;**26**:809–820.
149. Rickard AJ, Morgan J, Tesch G, Funder JW, Fuller PJ, Young MJ. Deletion of mineralocorticoid receptors from macrophages protects against deoxycorticosterone/salt-induced cardiac fibrosis and increased blood pressure. *Hypertension* 2009;**54**:537–543.
150. Widyantoro B, Emoto N, Nakayama K, Anggrahini DW, Adiarto S, Iwasa N, Yagi K, Miyagawa K, Rikitake Y, Suzuki T, Kisanuki YY, Yanagisawa M, Hirata K. Endothelial cell-derived endothelin-1 promotes cardiac fibrosis in diabetic hearts through stimulation of endothelial-to-mesenchymal transition. *Circulation* 2010;**121**:2407–2418.

Curr Pathobiol Rep (2017) 5:145–152
DOI 10.1007/s40139-017-0132-z

ACTIVATED MYOFIBROBLASTS AND FIBROSIS IN VARIOUS ORGANS (T KISSELEVA AND Y LIU, SECTION EDITORS)

Mechanisms of Fibroblast Activation in the Remodeling Myocardium

Arti V. Shinde[1] · **Nikolaos G. Frangogiannis**[1,2]

Published online: 22 April 2017

Abstract
Purpose of Review Activated fibroblasts are critically implicated in repair and remodeling of the injured heart. This manuscript discusses recent progress in the cell biology of fibroblasts in the infarcted and remodeling myocardium, highlighting advances in understanding the origin, function, and mechanisms of activation of these cells.
Recent Findings Following myocardial injury, fibroblasts undergo activation and myofibroblast transdifferentiation. Recently published studies have suggested that most activated myofibroblasts in the infarcted and pressure-overloaded hearts are derived from resident fibroblast populations. In the healing infarct, fibroblasts undergo dynamic phenotypic alterations in response to changes in the cytokine milieu and in the composition of the extracellular matrix. Fibroblasts do not simply serve as matrix-producing cells, but may also regulate inflammation, modulate cardiomyocyte survival and function, mediate angiogenesis, and contribute to phagocytosis of dead cells.
Summary In the injured myocardium, fibroblasts are derived predominantly from resident populations and serve a wide range of functions.

This article is part of the Topical Collection on *Activated Myofibroblasts and Fibrosis in Various Organs*

✉ Nikolaos G. Frangogiannis
nikolaos.frangogiannis@einstein.yu.edu

[1] The Wilf Family Cardiovascular Research Institute, Department of Medicine, Division of Cardiology, Albert Einstein College of Medicine, Bronx, NY, USA

[2] Division of Cardiology, the Wilf Cardiovascular Research Institute, Albert Einstein College of Medicine, 1300 Morris Park Avenue Forchheimer G46B, Bronx, NY 10461, USA

Keywords Fibroblast · Myofibroblast · Myocardial infarction · Cardiac remodeling · Cytokine

Introduction

Heart failure is a major cause of morbidity and mortality in western societies [1]. Despite extensive research in the field, prognosis for patients with heart failure remains poor, reflecting our limited understanding of the pathophysiology of the disease and the challenges in development and implementation of new therapeutic strategies [2]. Cardiac fibrosis is one of the major pathophysiologic underpinnings of heart failure [3]. Expansion of the cardiac interstitium and deposition of extracellular matrix proteins are consistently noted in experimental models of heart failure and in human patients with cardiomyopathic conditions, regardless of etiology. In the injured heart, fibrosis is an important part of the reparative response. Cardiomyocytes have very limited regenerative capacity; as a result, sudden loss of significant amounts of cardiac muscle in myocardial infarction activates a fibrotic response that preserves the structural integrity of the heart, preventing catastrophic events, such as cardiac rupture. The reparative function of cardiac fibrosis is dependent on timely activation and suppression of signals that mediate matrix deposition. Excessive or prolonged fibrogenic activation following myocardial injury increases chamber stiffness causing diastolic dysfunction. Moreover, perturbations of the myocardial architecture in fibrotic hearts can also trigger systolic dysfunction [4].

Fibroblasts are the central cellular effectors of fibrosis. Following myocardial injury, fibroblasts undergo dramatic phenotypic changes in response to microenvironmental alterations in the cytokine milieu and in the composition of the extracellular matrix [5–8]. Traditional concepts paint a

unidimensional picture of cardiac fibroblasts, as the main cellular source of extracellular matrix proteins in the injured myocardium [9]. However, a growing body of evidence suggests that fibroblasts are functionally and phenotypically heterogeneous, and may play diverse roles in cardiac homeostasis and disease [10••, 11–13]. The current review manuscript discusses recent advances in our understanding of the biology of fibroblasts in cardiac remodeling. We will focus on the cellular origin and function of activated fibroblasts in infarcted and remodeling hearts, and we will discuss key molecular signals implicated in fibroblast activation.

Fibroblasts in Normal Myocardium

Extensive experimental evidence suggests that the adult mammalian heart contains a large population of interstitial cells; many of these cells exhibit fibroblast-like characteristics. Early reports using transmission electron microscopy suggested that fibroblasts may be the most abundant myocardial cells [14]. More recent studies using combinations of markers for cell labeling suggested that in adult mouse hearts, less than 20% of non-cardiomyocytes can be identified as fibroblasts [15•]. The relative abundance of myocardial fibroblasts reported in different studies varies depending on the species, gender, and age of experimental subjects and on the markers used for cell identification. The absence of specific markers is a major limitation for definitive identification of fibroblast populations in both normal and injured hearts.

The role of fibroblasts in cardiac homeostasis remains poorly understood. In vitro studies have suggested that embryonic cardiac fibroblasts stimulate cardiomyocyte proliferation, whereas adult cells promote hypertrophy [16]. In the absence of injury, resident cardiac fibroblasts may serve to maintain the cardiac extracellular matrix network. Because of their abundance and their close interactions with cardiomyocytes and vascular cells, fibroblasts may also play an important role in regulating baseline cardiac function. However, in vivo experiments testing this intriguing hypothesis have not been performed.

Fibroblasts in the Infarcted Myocardium

The adult mammalian heart has limited regenerative capacity; as a result, sudden death of a large number of cardiomyocytes following infarction triggers a reparative response, forming a collagen-based scar that preserves the structural integrity of the ventricle [17]. Cardiac repair following myocardial infarction can be divided in three distinct but overlapping phases: the inflammatory, proliferative, and maturation phase [18]. In response to the dramatic changes in the cytokine milieu and to the alterations in composition of the surrounding extracellular matrix following infarction, cardiac fibroblasts exhibit dynamic phenotypic changes during the three phases of cardiac repair [5, 19, 20].

The Fibroblasts during the Inflammatory Phase of Infarct Healing

In the infarcted myocardium, necrosis of cardiomyocytes activates innate immune signaling pathways triggering an intense inflammatory reaction [21, 22], associated with marked upregulation of pro-inflammatory cytokines and chemokines [23]. Upon stimulation with interleukin (IL)-1 or tumor necrosis factor (TNF)-α, cardiac fibroblasts are capable of secreting large amounts of pro-inflammatory mediators and proteases [13, 24, 25]. Considering their relative abundance and their strategic location in close proximity to vessels and cardiomyocytes, fibroblasts may be important cellular effectors of the post-infarction inflammatory response. Although in vivo experiments testing this hypothesis have not been performed, a growing body of evidence suggests that resident cardiac fibroblasts may promote early post-ischemic dysfunction, at least in part, through activation of a pro-inflammatory program [11, 12].

The Fibroblasts during the Proliferative Phase: Myofibroblast Transdifferentiation

Activation of endogenous pathways that inhibit innate immune signaling and suppress pro-inflammatory activation [26] marks the transition from the inflammatory to the proliferative phase of infarct healing. As the neutrophil infiltrate is cleared by macrophages, fibroblasts expand and undergo myofibroblast transdifferentiation [13], expressing contractile proteins, such as α-smooth muscle actin (αSMA) (Fig. 1 a-d), and secreting large amounts of extracellular matrix proteins [27, 28]. Activated fibroblasts play a critical role in preservation of the structural integrity of the infarcted ventricle [10••]; however, excessive or prolonged activation of fibroblast populations may reduce ventricular compliance, promote adverse remodeling, and precipitate heart failure [29]. In addition to their established role in matrix synthesis, injury-associated myofibroblasts (or specific subsets of these cells) may serve a wide range of additional roles. In the infarcted myocardium, activated fibroblasts have been implicated in phagocytosis of dead cells [30]. Moreover, activated fibroblasts may modulate cardiomyocyte survival, hypertrophy, and function under conditions of stress [31••]. Recent evidence has suggested that following injury, myocardial fibroblasts exhibit remarkable phenotypic plasticity and may generate endothelial cells contributing to neovascularization [32•].

Although the heart contains abundant resident cardiac fibroblasts that can respond to activating signals, several other potential cellular sources have been proposed to explain the expanding myofibroblast population in the infarcted and

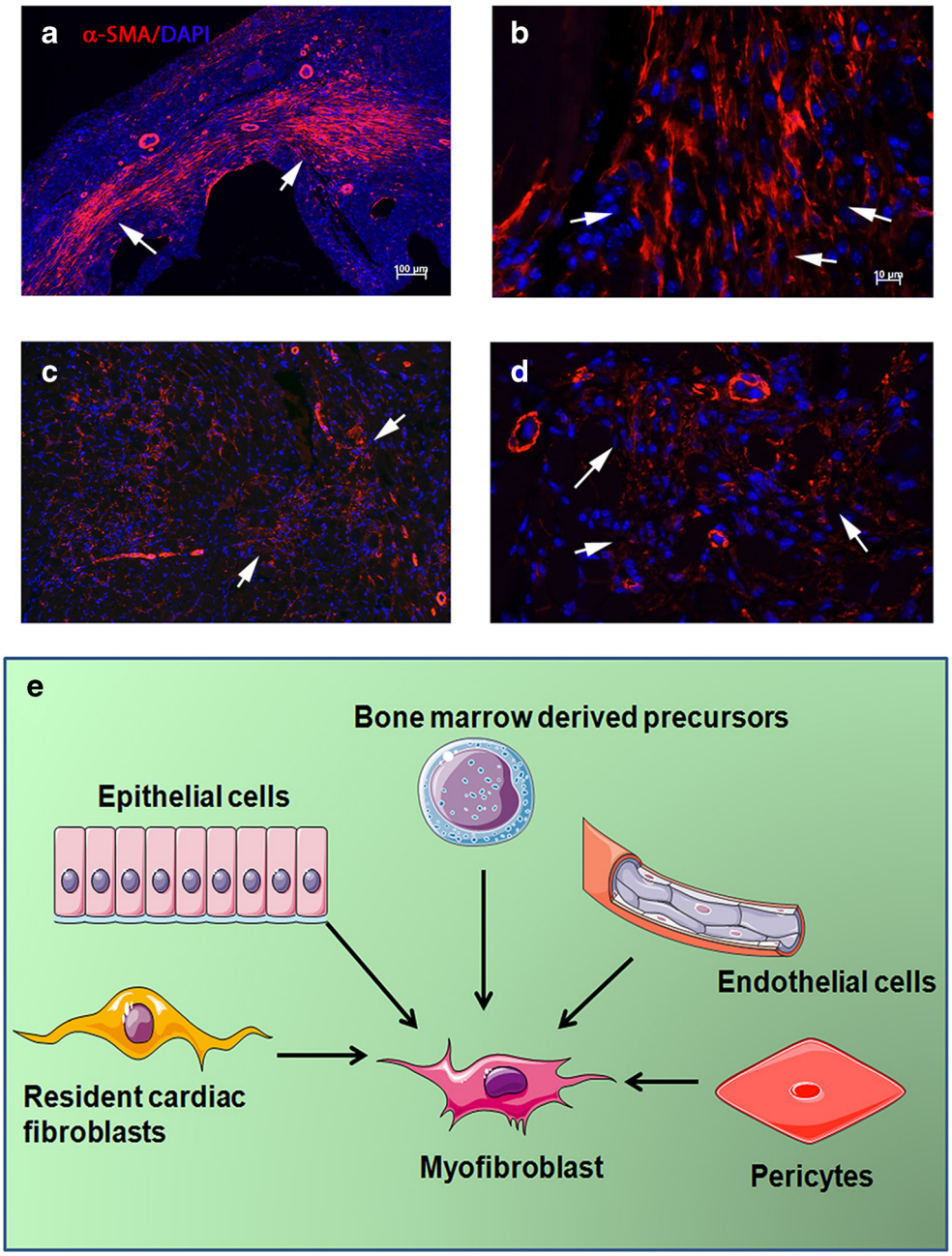

Fig. 1 Myofibroblasts in the infarcted and remodeling myocardium. αSMA immunofluorescence identifies abundant myofibroblasts (*arrows*) in infarcted mouse hearts (after 7 days of coronary occlusion) (**a**, **b**) and in pressure-overloaded hearts after 7 days of transverse aortic constriction (**c**, **d**). **e** Myofibroblasts in injured hearts may originate from a variety of sources, including epicardial epithelial cells, endothelium (through EndMT), vascular pericytes, bone marrow-derived precursors, and resident cardiac fibroblasts. Recently published studies in mouse models using lineage tracing approaches suggest that resident cardiac fibroblast populations may be the most important source of activated myofibroblasts in infarcted and pressure-overloaded hearts

remodeling myocardium. Endothelial cells, hematopoietic fibroblast progenitors, pericytes and vascular smooth muscle cells, and epicardial epithelial cells have been proposed as important contributors to myocardial fibrotic responses (Fig. 1e) [33]. Over the last 10 years, several investigative groups have combined bone marrow transplantation experiments, parabiosis and lineage tracing strategies to investigate the cellular origin of fibroblasts in the infarcted and remodeling myocardium [10••, 34–38]. Interpretation of the findings is inherently challenging because of the functional and phenotypic heterogeneity of fibroblast populations and the lack of specific molecular markers to identify fibroblasts [39]. Moreover, it should be emphasized that the relative contributions of various cell types may depend on the type of myocardial injury. In pathophysiologic conditions associated with extensive cardiomyocyte necrosis (such as myocardial infarction), intense upregulation of chemokines may drive recruitment of non-resident populations that may significantly contribute to the activated fibroblast populations. Table 1 provides an overview of recently published investigations examining the cellular origin of activated fibroblasts in infarcted and pressure-overloaded hearts. Although earlier studies have suggested important contributions of endothelial cells [34, 35] and hematopoietic progenitors [36], recent investigations

Table 1 Overview of the studies identifying the cellular sources of activated fibroblasts in the infarcted and remodeling myocardium

Reference	Cellular source(s) of activated fibroblasts	Species	Model of cardiac remodeling	Strategies used to identify the cellular origins of fibroblasts	Markers used for fibroblast labeling
Kanisicak et al. [10••]	Activated fibroblasts in infarcted and remodeling hearts are derived from Tcf21+ tissue-resident fibroblasts. Endothelial cells, myeloid cells and smooth muscle cells do not significantly contribute to the activated fibroblast population	Mouse	Myocardial infarction. Pressure overload induced through Transverse aortic constriction (TAC)	Lineage tracing using Periostin^{MCM}, Tcf21^{MCM} (to label resident fibroblasts), LysM-Cre (to label myeloid cells), Cdh5Cre (for endothelial cells) and Myh11Cre^{ERT2} (for smooth muscle cells)	Vimentin, PDGFRα, αSMA
Ruiz-Villalba et al. [40]	Epicardial-derived resident mesenchymal cells (Wt1Cre-eYFP+/CD31−/CD90+/αSM-A low/−) (major contribution) and bone marrow-derived cells (Lin/cKit+/Sca1+/Flk2+/CD34) (minor contribution), mobilized in response to chemotactic stromal cell–derived factor (SDF)-1α gradient	Mouse	Myocardial infarction Pressure overload induced through angiotensin infusion	Permanent genetic tracing of epicardium-derived cell and bone marrow-derived blood cell lineages using Wt1/IRES/GFP-Cre (Wt1Cre) mice crossed with Rosa26R-eYFP activating permanent reporter enhanced yellow fluorescent protein (eYFP+) expression in the Wt1+ cell lineage (Wt1Cre-YFP+)	Collagen I, FSP1, DDR2, CD90, αSMA
Aisaghboni et al. [34]	A significant proportion of activated fibroblasts (35–40%) is derived from endothelial cells	Mouse	Myocardial infarction	Cell lineage tracing using TOPGAL reporter transgenic mouse line, which carries the lacZ gene under the control of three tandem β-catenin-responsive consensus TCF/LEF-binding motifs upstream of a minimal fos promoter and double transgenic line carrying the inducible Cre recombinase under the endothelial-specific enhancer of the stem cell leukemia (SCL) gene and the R26RstoplacZ locus	αSMA, snail, FSP1, vimentin, and collagen I
Zhou et al. [41]	Epicardium-derived cells differentiate into fibroblasts in the infarcted myocardium	Mouse	Myocardial infarction	Genetic lineage tracing strategy using tamoxifen induced Cre allele, Wt1CreERT2/+, with epicardium-restricted cardiac activity, crossed with Rosa26mTmG/+ reporter line, which switches from mRFP to mGFP expression following Cre catalyzed recombination	FSP1, procollagen I, collagen III, fibronectin, α-SMA
Van Amerongen et al. [42]	Bone marrow-derived cells contribute to the myofibroblast population in the infarcted myocardium (approximately 24% of myofibroblasts are bone marrow-derived)	Mouse	Myocardial infarction	Myocardial infarction induced in C57BL/6 mice reconstituted with bone marrow transgenic for EGFP, as a reporter molecule, or with bone marrow cells that express two reporter genes (luciferase and β-galactosidase) under the control of the promoter and enhancer elements of the collagen I (α2 chain) gene	α-SMA+ cells with spindle shaped morphology
Fujita et al. [43]	Blood-derived cells contributed to the myofibroblast population	Mouse	Myocardial infarction	Whole bone marrow or single hematopoietic cell transplantation from GFP transgenic mice	CD45low/− elongated cells expressing vimentin and αSMA
Mollmann et al. [36]	A large population of infarct fibroblasts is derived from bone marrow cells (57% on day 7 after infarction, 32% on day 21)	Mouse	Myocardial infarction	Bone marrow transplantation from enhanced green fluorescent protein (eGFP)-transgenic mice	Vimentin, αSMA, SMemb
Yano et al. [44]	Circulating bone marrow cells do not contribute to the myofibroblast population	Rat	Myocardial infarction	Bone marrow transplantation from green fluorescent protein (GFP) + transgenic mice into nude rats	Vimentin, αSMA
Ali et al. [37]	The majority of cardiac fibroblasts in the pressure-overloaded myocardium are derived from epicardial populations, a minority from endothelial cells, and a small fraction from Pax3-expressing cells	Mouse	Pressure overload through TAC	Fate-mapping models using Pax3Cre/+, Tie2Cre/+, Wt1CreERT2/+, Myh11cre/+-GFP, Vav1Cre/+, Tbx18Cre transgenic mice, Myh6-GFP and R26RmT/mG mice, bone marrow transplantation and parabiosis, global- and fibroblast-specific gene expression analysis	Collagen I, DDR2, PDGFRα, vimentin, αSMA, CD90 exclusion criteria for hematopoietic cells, macrophages and endothelial cells
Moore-Morris et al. [38]	Activated fibroblasts in the pressure-overloaded myocardium are derived from two resident fibroblast populations, and not from hematopoietic cells, endothelial cells or epithelial cells	Mouse	Pressure overload through TAC	Genetic lineage tracing using transgenic GFP reporter mouse line driven by a collagen1a1 enhancer crossed with Wt1-Cre, Tie2-Cre, Vav-Cre, VE-cadherin-Cre^{ERT2}, Tbx18-Cre, Wt1-Cre^{ERT2}, Nfatc1-Cre, and Rosa-tdT-Cre	Vimentin, PDGFRα, Thy1, DDR2

Table 1 (continued)

Reference	Cellular source(s) of activated fibroblasts	Species	Model of cardiac remodeling	Strategies used to identify the cellular origins of fibroblasts	Markers used for fibroblast labeling
Zeisberg et al. [35]	Activated fibroblasts in the pressure-overloaded myocardium are derived from endothelial cells through endothelial-mesenchymal transition (EndMT) (27–35% of all fibroblasts) either FSP1+ or αSMA+), and from bone marrow-derived cells (13.4% of FSP1+ cells and 21.1% of α-SMA+ cells)	Mouse	Pressure overload through TAC	Lineage tracing using Tie1Cre;R26RstoplacZ mice, in which cells of endothelial origin are irrevocably marked by lacZ expression, and FSP1-GFP transgenic mice, in which green fluorescent protein (GFP) is expressed under the control of the promoter of fibroblast-specific protein 1 (FSP1), bone marrow transplantation of WT mice with Tie1Cre;R26RstoplacZ bone marrow	FSP-1, αSMA, DDR2, type I collagen α1
Krammann et al. [45•]	Gli-1+ pericytes contribute to the myofibroblast population in the remodeling pressure-overloaded myocardium (approximately 60% of activated fibroblasts are derived from Gli1+ cells)	Mouse	Pressure overload induced through angiotensin infusion or ascending aortic constriction	Lineage tracing using $Gli1Cre^{ERT2}$ mice	Collagen I, PDGFRα, αSMA

combining lineage tracing approaches with several distinct Cre drivers suggested that subpopulations of resident cardiac fibroblasts are the main source for activated myofibroblasts in infarcted and remodeling hearts [10••, 37••, 38••].

Signals Mediating Myofibroblast Activation in the Remodeling Myocardium

Myofibroblast activation in the infarcted and remodeling myocardium requires the cooperation of growth factors and specialized matrix proteins, which signal through cell surface receptors to activate transcription of extracellular matrix proteins. Macrophages, mast cells and lymphocytes infiltrating the remodeling heart play an important role in fibroblast activation by secreting a wide range of bioactive mediators, including cytokines (such as transforming growth factor (TGF)-β and IL-10) and matricellular proteins [46–50]. Stimulated cardiomyocytes and vascular cells in the area of injury may also activate molecular cascades that modulate fibroblast behavior [51].

Activation of the renin-angiotensin-aldosterone system signaling plays an important role in fibroblast proliferation and activation in the infarcted and remodeling myocardium. Experimental studies have demonstrated that angiotensin type 1 receptor (AT1) and aldosterone signaling activate fibroblasts in healing myocardial infarcts [52, 53]. Clinical studies in human patients with acute infarction support this concept demonstrating that administration of an aldosterone antagonist reduces the levels of circulating markers of collagen synthesis [54]. Moreover, in patients with hypertensive heart disease, AT1 blockade significantly reduced indicators associated with myocardial fibrosis [55].

The pleiotropic mediator TGF-β also plays a crucial role in activation of fibroblasts in the remodeling myocardium. TGF-β isoforms are markedly upregulated in the infarcted and remodeling myocardium and are secreted by macrophages, fibroblasts, platelets, vascular cells, and cardiomyocytes in a latent form [56, 57]. Activation of TGF-β in the cardiac interstitium requires protease actions and an interaction with the matricellular protein thrombospondin-1 [58, 59]. Following activation, the TGF-β dimer binds to a heterodimeric complex of TGF-β receptors I and II activating canonical signaling cascades that involve the intracellular effectors Smad2 and Smad3, and triggering Smad-independent pathways. Smad3 signaling appears to play an important role in fibroblast-mediated matrix synthesis and αSMA expression [60, 61]. Although effects of Smad-independent pathways have been documented in hypertrophic remodeling and dysfunction of cardiomyocytes in the pressure-overloaded myocardium [62], the in vivo role of non-Smad signaling in cardiac fibroblast function has not been documented.

Recent studies have revealed that profibrotic mediators, such as angiotensin II or TGF-β act by activating the transient receptor potential (TRP) channel-calcineurin axis. In fibroblasts, TRPC6 is induced through TGF-β-mediated Smad-independent signaling and is implicated in cardiac myofibroblast transdifferentiation by activating a calcineurin-nuclear factor of activated T cells (NFAT) cascade [63, 64••]. Experiments in atrial fibroblasts suggested that TRPM7 is implicated in TGF-β-induced calcium signaling and in myofibroblast transdifferentiation [65] TRPV4 is also involved in cardiac myofibroblast activation by integrating signals from secreted growth factors (such as TGF-β) and mechanosensitive stimuli [66].

Fibroblast Deactivation, Quiescence, and Apoptosis in the Infarcted and Remodeling Myocardium

As the healing scar matures, myofibroblasts become quiescent, reducing synthesis of extracellular matrix proteins. Many myofibroblasts in the infarct border zone may undergo apoptosis. Despite their potential importance in protecting the infarcted and remodeling myocardium from overactive fibrosis and dysfunction, the inhibitory signals responsible for myofibroblast deactivation in the healing scar are poorly understood. Our experimental work has suggested that at all stages of repair, fibroblasts are exposed to inhibitory mediators, such as the CXC chemokine interferon-γ-inducible protein (IP)-10/CXCL10 that may serve to prevent excessive fibrosis [67, 68]. However, the role of specific endogenous inhibitory pathways in negative regulation of TGF-β and angiotensin-mediated responses following infarction has not been investigated.

Conclusions and Future Directions

Cardiac fibroblasts play a crucial role in repair of the infarcted myocardium, but are also implicated in the pathogenesis of adverse remodeling and heart failure following cardiac injury. Despite the recent expansion of our knowledge on the cellular origins of fibroblasts in infarcted and remodeling hearts, our understanding of the molecular signals implicated in fibroblast activation following myocardial injury remains limited. Future research needs to focus on in vivo experiments to identify functionally distinct fibroblast subsets in injured and remodeling hearts, and on studies dissecting the molecular pathways mediating specific fibroblast responses. Moreover, study of endogenous inhibitory signals that inhibit fibroblast activity is crucial in order to design novel strategies protecting from adverse remodeling and heart failure.

Compliance with Ethical Standards

Conflict of Interest Arti Shinde and Nikolaos Frangogiannis declare that they have no conflicts of interest.

Human and Animal Rights and Informed Consent This article does not contain any studies with human or animal subjects performed by any of the authors.

Sources of Funding Supported by grants from the National Institutes of Health (R01 HL76246 and R01 HL85440 to N.G.F.), the Department of Defense (PR151134 and PR151029 to N.G.F.) and a post-doctoral award by the American Heart Association Founders' affiliate (to A.V.S.).

References

Papers of particular interest, published recently, have been highlighted as:
- • Of importance
- •• Of major importance

1. Christiansen MN, Kober L, Weeke P, Vasan RS, Jeppesen JL, Smith JG et al (2017) Age-specific trends in incidence, mortality and comorbidities of heart failure in Denmark 1995-2012. Circulation. doi:10.1161/CIRCULATIONAHA.116.025941
2. Chen J, Hsieh AF, Dharmarajan K, Masoudi FA, Krumholz HM (2013) National trends in heart failure hospitalization after acute myocardial infarction for Medicare beneficiaries: 1998-2010. Circulation 128(24):2577–2584. doi:10.1161/CIRCULATIONAHA.113.003668
3. Kong P, Christia P, Frangogiannis NG (2014) The pathogenesis of cardiac fibrosis. Cell Mol Life Sci 71(4):549–574
4. Berk BC, Fujiwara K, Lehoux S (2007) ECM remodeling in hypertensive heart disease. J Clin Invest 117(3):568–575
5. Shinde AV, Frangogiannis NG (2014) Fibroblasts in myocardial infarction: a role in inflammation and repair. J Mol Cell Cardiol 70C:74–82
6. Souders CA, Bowers SL, Baudino TA (2009) Cardiac fibroblast: the renaissance cell. Circ Res 105(12):1164–1176
7. Turner NA, Porter KE (2013) Function and fate of myofibroblasts after myocardial infarction. Fibrogenesis Tissue Repair 6(1):5. doi:10.1186/1755-1536-6-5
8. Dobaczewski M, de Haan JJ, Frangogiannis NG (2012) The extracellular matrix modulates fibroblast phenotype and function in the infarcted myocardium. J Cardiovasc Transl Res 5(6):837–847
9. Cleutjens JP, Verluyten MJ, Smiths JF, Daemen MJ (1995) Collagen remodeling after myocardial infarction in the rat heart. Am J Pathol 147(2):325–338
10. •• Kanisicak O, Khalil H, Ivey MJ, Karch J, Maliken BD, Correll RN et al (2016) Genetic lineage tracing defines myofibroblast origin and function in the injured heart. Nat Commun 7:12260. doi:10.1038/ncomms12260 **This study used a wide range of lineage tracing experiments to investigate the cellular origin of activated myofibroblasts in healing myocardial infarction.**
11. Frangogiannis NG (2016) The functional pluralism of fibroblasts in the infarcted myocardium. Circ Res 119(10):1049–1051. doi:10.1161/CIRCRESAHA.116.309926
12. Woodall MC, Woodall BP, Gao E, Yuan A, Koch WJ (2016) Cardiac fibroblast GRK2 deletion enhances contractility and remodeling following ischemia/reperfusion injury. Circ Res 119(10):1116–1127. doi:10.1161/CIRCRESAHA.116.309538
13. Saxena A, Chen W, Su Y, Rai V, Uche OU, Li N et al (2013) IL-1 induces Proinflammatory leukocyte infiltration and regulates fibroblast phenotype in the infarcted myocardium. J Immunol 191(9):4838–4848
14. Nag AC (1980) Study of non-muscle cells of the adult mammalian heart: a fine structural analysis and distribution. Cytobios 28(109):41–61
15. • Pinto AR, Ilinykh A, Ivey MJ, Kuwabara JT, D'Antoni ML, Debuque R et al (2016) Revisiting cardiac cellular composition. Circ Res 118(3):400–409. doi:10.1161/CIRCRESAHA.115.307778 **A robust and systematic characterization of the cellular composition of the adult mouse heart.**
16. Ieda M, Tsuchihashi T, Ivey KN, Ross RS, Hong TT, Shaw RM et al (2009) Cardiac fibroblasts regulate myocardial proliferation through beta1 integrin signaling. Dev Cell 16(2):233–244
17. Frangogiannis NG (2015) Pathophysiology of myocardial infarction. Compr Physiol 5(4):1841–1875. doi:10.1002/cphy.c150006

18. Frangogiannis NG (2012) Regulation of the inflammatory response in cardiac repair. Circ Res 110(1):159–173
19. Chen W, Frangogiannis NG (2013) Fibroblasts in post-infarction inflammation and cardiac repair. Biochim Biophys Acta 1833(4): 945–953
20. Frangogiannis NG (2016) Fibroblast-extracellular matrix interactions in tissue fibrosis. Curr Pathobiol Rep 4(1):11–18. doi:10.1007/s40139-016-0099-1
21. Prabhu SD, Frangogiannis NG (2016) The biological basis for cardiac repair after myocardial infarction: from inflammation to fibrosis. Circ Res 119(1):91–112. doi:10.1161/CIRCRESAHA.116.303577
22. Epelman S, Liu PP, Mann DL (2015) Role of innate and adaptive immune mechanisms in cardiac injury and repair. Nat Rev Immunol 15(2):117–129. doi:10.1038/nri3800
23. Dewald O, Zymek P, Winkelmann K, Koerting A, Ren G, Abou-Khamis T et al (2005) CCL2/monocyte chemoattractant protein-1 regulates inflammatory responses critical to healing myocardial infarcts. Circ Res 96(8):881–889
24. van Nieuwenhoven FA, Hemmings KE, Porter KE, Turner NA (2013) Combined effects of interleukin-1alpha and transforming growth factor-beta1 on modulation of human cardiac fibroblast function. Matrix Biol 32(7–8):399–406. doi:10.1016/j.matbio.2013.03.008
25. Zymek P, Nah DY, Bujak M, Ren G, Koerting A, Leucker T et al (2007) Interleukin-10 is not a critical regulator of infarct healing and left ventricular remodeling. Cardiovasc Res 74(2):313–322
26. Chen W, Saxena A, Li N, Sun J, Gupta A, Lee DW et al (2012) Endogenous IRAK-M attenuates postinfarction remodeling through effects on macrophages and fibroblasts. Arterioscler Thromb Vasc Biol 32(11):2598–2608
27. Shinde AV, Humeres C, Frangogiannis NG (2017) The role of alpha-smooth muscle actin in fibroblast-mediated matrix contraction and remodeling. Biochim Biophys Acta 1863(1):298–309. doi:10.1016/j.bbadis.2016.11.006
28. Frangogiannis NG, Michael LH, Entman ML (2000) Myofibroblasts in reperfused myocardial infarcts express the embryonic form of smooth muscle myosin heavy chain (SMemb). Cardiovasc Res 48(1):89–100
29. Kaur H, Takefuji M, Ngai CY, Carvalho J, Bayer J, Wietelmann A et al (2016) Targeted ablation of Periostin-expressing activated fibroblasts prevents adverse cardiac remodeling in mice. Circ Res 118(12):1906–1917. doi:10.1161/CIRCRESAHA.116.308643
30. Nakaya M, Watari K, Tajima M, Nakaya T, Matsuda S, Ohara H et al (2017) Cardiac myofibroblast engulfment of dead cells facilitates recovery after myocardial infarction. J Clin Invest 127(1):383–401. doi:10.1172/JCI83822
31.•• Bang C, Batkai S, Dangwal S, Gupta SK, Foinquinos A, Holzmann A et al (2014) Cardiac fibroblast-derived microRNA passenger strand-enriched exosomes mediate cardiomyocyte hypertrophy. J Clin Invest 124(5):2136–2146. doi:10.1172/JCI70577 **The study documents effects of fibroblasts in regulation of cardiomyocyte hypertrophy, mediated through secretion of miRNA-rich exosomes.**
32.• Ubil E, Duan J, Pillai IC, Rosa-Garrido M, Wu Y, Bargiacchi F et al (2014) Mesenchymal-endothelial transition contributes to cardiac neovascularization. Nature 514(7524):585–590. doi:10.1038/nature13839 **This study suggests that fibroblasts exhibit remarkable plasticity and may generate endothelial cells contributing to neovessel formation.**
33. Krenning G, Zeisberg EM, Kalluri R (2010) The origin of fibroblasts and mechanism of cardiac fibrosis. J Cell Physiol 225(3): 631–637. doi:10.1002/jcp.22322
34. Aisagbonhi O, Rai M, Ryzhov S, Atria N, Feoktistov I, Hatzopoulos AK (2011) Experimental myocardial infarction triggers canonical Wnt signaling and endothelial-to-mesenchymal transition. Dis Model Mech 4(4):469–483. doi:10.1242/dmm.006510
35. Zeisberg EM, Tarnavski O, Zeisberg M, Dorfman AL, McMullen JR, Gustafsson E et al (2007) Endothelial-to-mesenchymal transition contributes to cardiac fibrosis. Nat Med 13(8):952–961
36. Mollmann H, Nef HM, Kostin S, von Kalle C, Pilz I, Weber M et al (2006) Bone marrow-derived cells contribute to infarct remodelling. Cardiovasc Res 71(4):661–671
37.•• Ali SR, Ranjbarvaziri S, Talkhabi M, Zhao P, Subat A, Hojjat A et al (2014) Developmental heterogeneity of cardiac fibroblasts does not predict pathological proliferation and activation. Circ Res 115(7):625–635. doi:10.1161/CIRCRESAHA.115.303794 **A systematic and well-documented investigation on the cellular origins of activated fibroblasts in remodeling pressure-overloaded hearts.**
38.•• Moore-Morris T, Guimaraes-Camboa N, Banerjee I, Zambon AC, Kisseleva T, Velayoudon A et al (2014) Resident fibroblast lineages mediate pressure overload-induced cardiac fibrosis. J Clin Invest 124(7):2921–2934. doi:10.1172/JCI74783 **This study identified resident fibroblast populations as the main cellular source of activated fibroblasts in the remodeling pressure-overloaded myocardium.**
39. Kong P, Christia P, Saxena A, Su Y, Frangogiannis NG (2013) Lack of specificity of fibroblast-specific protein 1 in cardiac remodeling and fibrosis. Am J Physiol Heart Circ Physiol 305(9):H1363–H1372
40. Ruiz-Villalba A, Simon AM, Pogontke C, Castillo MI, Abizanda G, Pelacho B et al (2015) Interacting resident epicardium-derived fibroblasts and recruited bone marrow cells form myocardial infarction scar. J Am Coll Cardiol 65(19):2057–2066. doi:10.1016/j.jacc.2015.03.520
41. Zhou B, Honor LB, He H, Ma Q, Oh JH, Butterfield C et al (2011) Adult mouse epicardium modulates myocardial injury by secreting paracrine factors. J Clin Invest 121(5):1894–1904. doi:10.1172/JCI45529
42. van Amerongen MJ, Bou-Gharios G, Popa E, van Ark J, Petersen AH, van Dam GM et al (2008) Bone marrow-derived myofibroblasts contribute functionally to scar formation after myocardial infarction. J Pathol 214(3):377–386
43. Fujita J, Mori M, Kawada H, Ieda Y, Tsuma M, Matsuzaki Y et al (2007) Administration of granulocyte colony-stimulating factor after myocardial infarction enhances the recruitment of hematopoietic stem cell-derived myofibroblasts and contributes to cardiac repair. Stem Cells 25(11):2750–2759. doi:10.1634/stemcells.2007-0275
44. Yano T, Miura T, Ikeda Y, Matsuda E, Saito K, Miki T et al (2005) Intracardiac fibroblasts, but not bone marrow derived cells, are the origin of myofibroblasts in myocardial infarct repair. Cardiovasc Pathol 14(5):241–246
45.• Kramann R, Schneider RK, DiRocco DP, Machado F, Fleig S, Bondzie PA et al (2015) Perivascular Gli1+ progenitors are key contributors to injury-induced organ fibrosis. Cell Stem Cell 16(1):51–66. doi:10.1016/j.stem.2014.11.004 **This study documents the contribution of Gli1+ pericytes as a source of activated myofibroblasts in the injured myocardium and in other fibrotic tissues.**
46. Carlson S, Helterline D, Asbe L, Dupras S, Minami E, Farris S et al (2016) Cardiac macrophages adopt profibrotic/M2 phenotype in infarcted hearts: role of urokinase plasminogen activator. J Mol Cell Cardiol. doi:10.1016/j.yjmcc.2016.05.016
47. Nevers T, Salvador AM, Grodecki-Pena A, Knapp A, Velazquez F, Aronovitz M et al (2015) Left ventricular T-cell recruitment contributes to the pathogenesis of heart failure. Circ Heart Fail 8(4): 776–787. doi:10.1161/CIRCHEARTFAILURE.115.002225
48. Saxena A, Dobaczewski M, Rai V, Haque Z, Chen W, Li N et al (2014) Regulatory T cells are recruited in the infarcted mouse myocardium and may modulate fibroblast phenotype and function. Am

J Physiol Heart Circ Physiol 307(8):H1233–H1242. doi:10.1152/ajpheart.00328.2014
49. Shiraishi M, Shintani Y, Shintani Y, Ishida H, Saba R, Yamaguchi A et al (2016) Alternatively activated macrophages determine repair of the infarcted adult murine heart. J Clin Invest 126(6):2151–2166. doi:10.1172/JCI85782
50. Frangogiannis NG (2012) Matricellular proteins in cardiac adaptation and disease. Physiol Rev 92(2):635–688
51. Sassi Y, Ahles A, Truong DJ, Baqi Y, Lee SY, Husse B et al (2014) Cardiac myocyte-secreted cAMP exerts paracrine action via adenosine receptor activation. J Clin Invest 124(12):5385–5397. doi:10.1172/JCI74349
52. Ju H, Zhao S, Jassal DS, Dixon IM (1997) Effect of AT1 receptor blockade on cardiac collagen remodeling after myocardial infarction. Cardiovasc Res 35(2):223–232
53. van den Borne SW, Isobe S, Zandbergen HR, Li P, Petrov A, Wong ND et al (2009) Molecular imaging for efficacy of pharmacologic intervention in myocardial remodeling. JACC Cardiovasc Imaging 2(2):187–198. doi:10.1016/j.jcmg.2008.11.011
54. Hayashi M, Tsutamoto T, Wada A, Tsutsui T, Ishii C, Ohno K et al (2003) Immediate administration of mineralocorticoid receptor antagonist spironolactone prevents post-infarct left ventricular remodeling associated with suppression of a marker of myocardial collagen synthesis in patients with first anterior acute myocardial infarction. Circulation 107(20):2559–2565
55. Ciulla MM, Paliotti R, Esposito A, Diez J, Lopez B, Dahlof B et al (2004) Different effects of antihypertensive therapies based on losartan or atenolol on ultrasound and biochemical markers of myocardial fibrosis: results of a randomized trial. Circulation 110(5):552–557. doi:10.1161/01.CIR.0000137118.47943.5C
56. Dobaczewski M, Chen W, Frangogiannis NG (2011) Transforming growth factor (TGF)-beta signaling in cardiac remodeling. J Mol Cell Cardiol 51(4):600–606
57. Dewald O, Ren G, Duerr GD, Zoerlein M, Klemm C, Gersch C et al (2004) Of mice and dogs: species-specific differences in the inflammatory response following myocardial infarction. Am J Pathol 164(2):665–677
58. Xia Y, Dobaczewski M, Gonzalez-Quesada C, Chen W, Biernacka A, Li N et al (2011) Endogenous thrombospondin 1 protects the pressure-overloaded myocardium by modulating fibroblast phenotype and matrix metabolism. Hypertension 58(5):902–911
59. Frangogiannis NG, Ren G, Dewald O, Zymek P, Haudek S, Koerting A et al (2005) The critical role of endogenous thrombospondin (TSP)-1 in preventing expansion of healing myocardial infarcts. Circulation 111(22):2935–2942
60. Bujak M, Ren G, Kweon HJ, Dobaczewski M, Reddy A, Taffet G et al (2007) Essential role of Smad3 in infarct healing and in the pathogenesis of cardiac remodeling. Circulation 116:2127–2138
61. Dobaczewski M, Bujak M, Li N, Gonzalez-Quesada C, Mendoza LH, Wang XF et al (2010) Smad3 signaling critically regulates fibroblast phenotype and function in healing myocardial infarction. Circ Res 107(3):418–428
62. Koitabashi N, Danner T, Zaiman AL, Pinto YM, Rowell J, Mankowski J et al (2011) Pivotal role of cardiomyocyte TGF-beta signaling in the murine pathological response to sustained pressure overload. J Clin Invest 121(6):2301–2312
63. Nishida M, Onohara N, Sato Y, Suda R, Ogushi M, Tanabe S et al (2007) Galpha12/13-mediated up-regulation of TRPC6 negatively regulates endothelin-1-induced cardiac myofibroblast formation and collagen synthesis through nuclear factor of activated T cells activation. J Biol Chem 282(32):23117–23128. doi:10.1074/jbc.M611780200
64.•• Davis J, Burr AR, Davis GF, Birnbaumer L, Molkentin JD (2012) A TRPC6-dependent pathway for myofibroblast transdifferentiation and wound healing in vivo. Dev Cell 23(4):705–715 **This study provides the first in vivo demonstration of an important role for TRPC6 in myofibroblast activation in healing wounds.**
65. Du J, Xie J, Zhang Z, Tsujikawa H, Fusco D, Silverman D et al (2010) TRPM7-mediated Ca2+ signals confer fibrogenesis in human atrial fibrillation. Circ Res 106(5):992–1003. doi:10.1161/CIRCRESAHA.109.206771
66. Adapala RK, Thoppil RJ, Luther DJ, Paruchuri S, Meszaros JG, Chilian WM et al (2013) TRPV4 channels mediate cardiac fibroblast differentiation by integrating mechanical and soluble signals. J Mol Cell Cardiol 54:45–52. doi:10.1016/j.yjmcc.2012.10.016
67. Saxena A, Bujak M, Frunza O, Dobaczewski M, Gonzalez-Quesada C, Lu B et al (2014) CXCR3-independent actions of the CXC chemokine CXCL10 in the infarcted myocardium and in isolated cardiac fibroblasts are mediated through proteoglycans. Cardiovasc Res 103(2):217–227. doi:10.1093/cvr/cvu138
68. Bujak M, Dobaczewski M, Gonzalez-Quesada C, Xia Y, Leucker T, Zymek P et al (2009) Induction of the CXC chemokine interferon-gamma-inducible protein 10 regulates the reparative response following myocardial infarction. Circ Res 105(10):973–983